

Fri. Jun 4, 2021

[E] Poster | U (Union) : Union

5:15 PM - 6:30 PM JST | 8:15 AM - 9:30 AM UTC | Ch.01_1

[U-08] Advancing SDGs through inclusive partnerships I: Strategic leadership

convener: Vincent Tong (University College London), Hidenroi Nakamura (Toyama Prefectural University), Mika Shimizu (Kyoto University), Fumiko Noguchi (United Nations University, Institute for the Advanced Study of Sustainability)

[U08-P01] A few points to be considered when we engaging with a local community for research and practice for sustainability

★Invited Papers

*Fumiko Noguchi¹ (1. United Nations University, Institute for the Advanced Study of Sustainability)

[U08-P02] Citizen dialogue-led environmental governance: Toward inclusiveness and culture of dialogue in post-Fukushima Japan

★Invited Papers

*Hidenroi Nakamura¹ (1. Toyama Prefectural University)

[E] Poster | U (Union) : Union

5:15 PM - 6:30 PM JST | 8:15 AM - 9:30 AM UTC | Ch.01_2

[U-10] What is the true value of Knowledge Creation? The Ideal and Reality of Research Evaluation.

convener: Michiyo SHIMAMURA (Japan Agency for Marine-Earth Science and Technology), Brooks Hanson (American Geophysical Union), Yasuhiro Yamanaka (Faculty of Environmental Earth Science, Hokkaido University), Kiyoshi Suyehiro (Japan Agency for Marine-Earth Science and Technology)

[U10-P01] Researchers' perceptions of research and its evaluation: A comparison between the JpGU and AGU communities

*Yasuhiro Yamanaka¹, Michiyo SHIMAMURA², Kiyoshi Suyehiro², Brooks Hanson³ (1. Faculty of Environmental Earth Science, Hokkaido University, 2. Japan Agency Marine-Earth Science and Technology, 3. American Geophysical Union)

[E] Poster | U (Union) : Union

5:15 PM - 6:30 PM JST | 8:15 AM - 9:30 AM UTC | Ch.01_3

[U-11] Diversity and equality - Where do we stand on gender equality or equity in the geosciences?

convener: Rie Hori, S. (Department of Earth Science, Faculty of Science, Ehime University), Chiaki T. Oguchi (Institute for Environmental Science and Technology, Graduate School of Science and Engineering, Saitama University), Claudia Jesus-Rydin (European Research Council), Eiichi Tajika (Department of Earth and Planetary Science, Graduate School of Science, The University of Tokyo)

[U11-P01] **An action guideline and the activity of the Women for One Ocean, Japan**

*Natsue Abe^{1,2}, Kaoru Kubokawa³, Women for One Ocean (1. Mantle Drilling Promotion Office, MarE3, Japan Agency for Marine-Earth Science and Technology, 2. Graduate School of Natural Science & Technology, Kanazawa University, 3. Teikyo University)

[E] Poster | U (Union) : Union

5:15 PM - 6:30 PM JST | 8:15 AM - 9:30 AM UTC | Ch.01_4

[U-12] From Hazard to Resilience

convener:Naoshi Hirata(National Research Institute for Earth Science and Disaster Resilience), Keiko Tamura(Risk Management Office, Niigata University), Matt Gerstenberger(GNS Science), Danijel Schorlemmer(GFZ German Research Centre for Geosciences)

[U12-P01] Interdisciplinary and industry-academia collaboration research for resilient society in the Tokyo metropolitan area, DEKATSU Activity

*Takashi Furuya¹, Keiko Tamura², Danijel Schorlemmer³, Naoshi Hirata¹ (1.National Research Institute for Earth Science and Disaster Resilience, 2.Niigata University, Risk Management Office, 3.GFZ German Research Center for Geosciences)

[E] Poster | P (Space and Planetary Sciences) : P-PS Planetary Sciences

5:15 PM - 6:30 PM JST | 8:15 AM - 9:30 AM UTC | Ch.02_1

[P-PS01] Outer Solar System Exploration Today, and Tomorrow

convener: Jun Kimura (Osaka University), M. Kunio Sayanagi (Hampton University), Fuminori Tsuchiya (Planetary Plasma and Atmospheric Research Center, Graduate School of Science, Tohoku University), Cindy Young (NASA Langley Research Center)

[PPS01-P01] Estimation of apparent areas of Earth-orbiting UV telescope required to detect water plumes on icy moons

*Ryoichi Koga¹, Fuminori Tsuchiya², Go Murakami³, Shotaro Sakai² (1.Nagoya University, 2.Tohoku University, 3.ISAS/JAXA)

[PPS01-P02] Quantitative analysis of hot electron density variation during transient brightening in the Io plasma torus observed by Hisaki/EXCEED

*Kento Furukawa¹, Fuminori Tsuchiya¹, Kazuo Yoshioka², Reina Hikida³, Tomoki Kimura¹, Masato Kagitani¹, Go Murakami³, Atsushi Yamazaki³, Hajime Kita⁴, Ichiro Yoshikawa² (1.Tohoku University, 2.the University of Tokyo, 3.JAXA, 4.Tohoku Institute of Technology)

[PPS01-P03] Expected source regions of Jupiter's hectometric radio components viewed from their polarization characteristics

*Hiroaki Misawa¹, Fuminori Tsuchiya¹, Atsushi Kumamoto², Yoshiya Kasahara³, Yoshizumi Miyoshi⁴, Masahiro Kitahara⁴, Satoko Nakamura⁴ (1.PPARC, Graduate School of Science, Tohoku University, 2.Department of Geophysics, Graduate School of Science, Tohoku University, 3.ARC-SAT, Kanazawa University, 4.ISEE, Nagoya University)

[PPS01-P04] New magnetic field and current sheet models of the night-side Jovian magnetosphere and their long-term variations

*Naoya Momoki¹, Hiroaki TOH² (1.Division of Earth and Planetary Sciences, Graduate School of Science, Kyoto University, 2.Data Analysis Center for Geomagnetism and Space Magnetism, Graduate School of Science, Kyoto University)

[PPS01-P05] Exploring the roof of Jovian atmosphere by large and small groundbased telescopes in visible and infrared light

*Yasumasa Kasaba¹, Takeshi Sakanoi¹, Masato Kagitani¹, Hajime Kita² (1.Planetary Plasma and Atmospheric Research Center, Tohoku University, 2.Tohoku Institute of Technology)

[PPS01-P06] Jupiter Icy Moons Explorer JUICE: Science perspectives from planetary formation and geochemistry of the JUICE Japan team

*Yasuhito Sekine¹, Yoshifumi Saito², Kazushi Asamura², Keigo Enya², YASUKO KASAI⁴, Yasumasa Kasaba³, Junichi Haruyama², Ayako Matsuoka⁵ (1.Earth-Life Science Institute, Tokyo Institute of Technology, 2.ISAS, JAXA, 3.Tohoku University, 4.NICT, 5.Kyoto University)

[PPS01-P07] Numerical simulation of the passive subsurface radar for Jupiter's icy moons

*Tomoki Kimura¹, Rikuto Yasuda¹, Fuminori Tsuchiya¹, Atsushi Kumamoto¹, Hiroaki Misawa¹, Yasumasa Kasaba¹ (1.Tohoku U.)

[PPS01-P08] Numerical radar simulation for the explorations of the ionosphere and plume at Jupiter's icy moons

*Rikuto Yasuda¹, Tomoki Kimura¹, Hiroaki Misawa¹, Fuminori Tsuchiya¹, Atsushi Kumamoto¹, Yasumasa Kasaba¹ (1.TOHOKU UNIVERSITY)

[PPS01-P09] Performance, Operation and their Feasibilities for Jupiter and Icy Moons: High Frequency Receiver of Radio & Plasma Wave Investigation (RPWI) aboard JUICE during the Flight Model Test campaign

*Yasumasa Kasaba¹, Hiroaki Misawa¹, Fuminori Tsuchiya¹, Tomoki Kimura¹, Hajime Kita², Atsushi Kumamoto¹, Yuto Katoh¹, Yoshizumi Miyoshi³, Yoshiya Kasahara⁴, Satoshi Yagitani⁴, Hirotsugu Kojima⁵, Baptiste Cecconi⁶ (1.Tohoku University, 2.Tohoku Institute of Technology, 3.Nagoya University, 4.Kanazawa University, 5.Kyoto University, 6.Obs. de Paris)

[E] Poster | P (Space and Planetary Sciences) : P-EM Solar-Terrestrial Sciences, Space Electromagnetism & Space Environment

5:15 PM - 6:30 PM JST | 8:15 AM - 9:30 AM UTC | Ch.04_1

[P-EM11] Coupling Processes in the Atmosphere-Ionosphere System

convener:Huixin Liu(Earth and Planetary Science Division, Kyushu University SERC, Kyushu University), Loren Chang(Institute of Space Science, National Central University), Yuichi Otsuka(Institute for Space-Earth Environmental Research, Nagoya University), Yue Deng(University of Texas at Arlington)

[PEM11-P01] Year-to-year variation in polar mesospheric clouds observed by geostationary earth orbit satellite, Himawari

*Beng Aun Peh¹, Takuo T. Tsuda¹, Hidehiko Suzuki², Yuta Hozumi¹, Yoshiaki Ando¹, Keisuke Hosokawa¹, Takuji Nakamura³, Ken T. Murata⁴ (1.The University of Electro-Communications, 2.Meiji University, 3.National Institute of Polar Research, 4.National Institute of Information and Communications Technology)

[PEM11-P02] Analysis of vertical profiles of ionospheric disturbances caused by the tsunami associated with the Tohoku earthquake using GPS occultation observation

*Ryosuke Fushimi¹, Hiroyuki Nakata², Hiroyo Ohya² (1.Graduate School of Science and Engineering, Chiba University, 2.Graduate School of Engineering, Chiba University)

[PEM11-P03] Imaging observation of Ionospheric Field Aligned Irregularities by the PANSY radar at Antarctic Syowa Station

*Daisuke Kagawa¹, Taishi Hashimoto², Akinori Saito¹, Koji Nishimura², Masaki Tsutsumi², Toru Sato³, Kaoru Sato⁴ (1.Graduate School of Science, Kyoto University, 2.National Institute of Polar Research, 3.Graduate School of Informatics, Kyoto University, 4.Graduate School of Science, Tokyo University)

[PEM11-P04] Two-dimensional distributions of GPS-TEC disturbances associated with Sakurajima eruptions

*Yuki Nishiyama¹, Hiroyuki Nakata¹, Hiroyo Ohya¹, Takuya Tsugawa², Michi Nishioka² (1.Graduate School of Science and Engineering, Chiba University, 2.National Institute of Information and Communications Technology)

[PEM11-P05] Atomic Oxygen Ion-Neutral Collision Frequency Models at Ionospheric Temperatures

*Akimasa Ieda¹ (1.Institute for Space-Earth Environmental Research, Nagoya University)

[PEM11-P06] Effects of auroral Ionosphere on atmospheric electricity

*Osuke Saka¹ (1.Office Geophysik)

[PEM11-P07] Data processing and quality-control of the ISS-IMAP mission data

*Akinori Saito¹, Takeshi Sakanoi², Yuta Hozumi³ (1.Department of Geophysics, Graduate School of Science, Kyoto University, 2.Planetary Plasma and Atmospheric Research Center, Graduate School of Science, Tohoku University, 3.University of Electro-Communications)

[PEM11-P08] Polar cap patches, GPS TEC variations, and atmospheric gravity waves

*Paul Prikryl¹, Robert G. Gillies², David R. Themens^{1,3}, Bharat S. R. Kunduri⁴, Evan G. Thomas⁵, Roger Varney⁶, James M. Weygand⁷ (1.Physics Department, University of New Brunswick, 2.Department of Physics and Astronomy, University of Calgary, 3.School of Engineering, University of Birmingham, 4.Bradley Department of Electrical and Computer Engineering, Virginia Tech, 5.Thayer School of Engineering, Dartmouth College, 6.Center for Geospace Studies, SRI International, 7.Earth Planetary and Space Sciences, University of California)

[PEM11-P09] Development and accuracy evaluation of the image processing system for Stabilized High-sensitive Imager on Shirase

*Saki Yamashina¹, Akinori Saito¹, Takeshi Sakanoi², Takuo T. Tsuda³, Yuta Hozumi³, Takeshi Aoki³, Mitsumu K. Ejiri⁴, Takanori Nishiyama⁴, Takahiro Naoi⁵, Masato Nagahara⁵ (1.Graduate School of Science, Kyoto University, 2.Planetary Plasma and Atmospheric Research Center, Graduate School of Science, Tohoku University, 3.Graduate School of Informatics and Engineering, The University of Electro-Communications, 4.National Institute of Polar Research, 5.National Institute of Information and Communications Technology)

[PEM11-P10] Statistical analysis of local time dependence of MSTID characteristics using the SuperDARN pair of radars

*Wataru Hazeyama¹, Nozomu Nishitani¹, Tomoaki Hori¹ (1.Institute for Space-Earth Environmental Research)

[PEM11-P11] The nature of large off-vertical MF radar echoes over Syowa station, Antarctica

*Masaki Tsutsumi¹ (1.National Institute of Polar Research)

[PEM11-P12] ICON satellite observations of thermospheric winds

*Yusuke Ioka¹, Huixin Liu¹ (1.Earth and Planetary Science Division, Kyushu University SERC, Kyushu University)

[PEM11-P13] **The relation between *hmF2* and radio occultation scintillation amplitude index RO-S4 index observed using FORMOSAT-7/COSMIC-2**

*YI DUANN^{1,2}, Loren Chang^{1,2}, Chi-Kuang Chao^{1,2}, Jann-Yenq Liu^{1,2}, Tung-Yuan Hsiao³, Shih-Ping Chen⁴
(1.Department of Space Science and Engineering, National Central University, Taoyuan City, Taiwan, 2.Center for Astronautical Physics and Engineering, National Central University, Taoyuan City, Taiwan, 3.Nuclear Science and Technology Development Center, National Tsing Hua University, Hsinchu City, Taiwan, 4.Department of Earth Sciences, National Cheng Kung University, Tainan City, Taiwan)

[PEM11-P14] Simultaneous observations of plasma bubbles with an HF Doppler sounding system in Taiwan and an all-sky imager in Ishigaki Island

*Hiromi Sejima¹, Keisuke Hosokawa¹, Jaroslav Chum², Hiroyuki Nakata³, Jun Sakai⁴, Susumu Saito⁵ (1.Department of Communication Engineering and Informatics, University of Electro-Communications, 2.Institute of Atmospheric Physics of the Czech Academy of Sciences, 3.Graduate School of Engineering, Chiba University, 4.Center for Space Science and Radio Engineering, University of Electro-communications, 5.Electronic Navigation Research Institute, National Institute of Maritime, Port, and Aviation Technology)

[PEM11-P15] Automated detection of mid-latitude sporadic E using GPS-TEC ROTI data

*Masahiro Takahi¹, Keisuke Hosokawa¹, Jun Sakai², Susumu Saito³ (1.Department of Communication Engineering and Informatics, University of Electro-Communications, 2.Center for Space Science and Radio Engineering, University of Electro-communications, 3.Electronic Navigation Research Institute, National Institute of Maritime, Port, and Aviation Technology)

[PEM11-P16] Research about the thermospheric structure and variations by comparing the simultaneous data of GOCE and CHAMP

*Nakayama Sayuka¹, Liu Huixin¹ (1.Kyushu university)

[PEM11-P17] Effects of static electric fields and Alfvén waves on Joule heating in the cusp

*Tomokazu Oigawa¹, Hiroyuki Shinagawa², Satoshi Taguchi¹ (1.Department of Geophysics, Graduate School of Science, Kyoto University, 2.National Institute of Information and Communications Technology)

[PEM11-P18] The impact of FORMOSAT-7/COSMIC-2 in-situ plasma drift observations on the space weather forecasting system

*Chia-Hung Chen¹, Charles Lin¹, Tomoko Matsuo², Ching-Hua Shen¹ (1.Department of Earth Sciences, National Cheng Kung University, 2.Ann and H. J. Smead Department of Aerospace Engineering Sciences, University of Colorado, Boulder, CO 80309-0429, USA)

[PEM11-P19] Scintillation Drift Velocity Observed by Closely-Spaced GPS Receivers in Indonesia

*Yuichi Otsuka¹, Prayitno Abadi² (1.Institute for Space-Earth Environmental Research, Nagoya University, 2.LAPAN, Indonesia)

[PEM11-P20] The ionospheric disturbances associated with Typhoons observed by HF Doppler, Infrasound, and GPS occultation observations

*Hiroyuki Nakata¹, Ryota Yagihashi², Hiroyo Ohya¹, Keisuke Hosokawa³, Masa-yuki Yamamoto⁴ (1.Graduate School of Engineering, Chiba University, 2.Graduate School of Science and Engineering, Chiba University, 3.School of Informatics and Engineering, The University of Electro-Communications, 4.School of Systems Engineering, Kochi University of Tecnology)

[PEM11-P21] Calcium ion thin layer observed with a resonance scattering lidar at Syowa, Antarctic

*Mitsumu K. Ejiri^{1,2}, Takanori Nishiyama^{1,2}, Takuo T. Tsuda³, Katsuhiko Tsuno⁴, Masaki Tsutsumi^{1,2}, Makoto Abo⁵, Takuya Kawahara⁶, Takayo Ogawa⁴, Satoshi Wada⁴, Takuji Nakamura^{1,2} (1.National Institute of Polar Research, 2.The Graduate University for Advanced Studies, SOKENDAI, 3.The University of Electro-Communications, 4.RIKEN,RAP, 5.Tokyo Metropolitan Univ., 6.Shinshu Univ.)

[PEM11-P22] Relationship between energetic particle precipitations and an intensity of OH airglow over Syowa Station.

*Satoshi Ishii¹, Hidehiko Suzuki¹, Masaki Tsutsumi^{2,4}, Makoto Taguchi³, Mitsumu K. Ejiri^{2,4}, Takanori Nishiyama^{2,4}
(1.Meiji University, 2.National Institute of Polar Research, 3.Rikkyo University, 4.SOKENDAI)

[PEM11-P23] Variations in the D-region ionosphere observed in fireballs occurred using VLF/LF transmitter signals

*Takeru Suzuki¹, Hiroyo Ohya², Fuminori Tsuchiya³, Kazuo Shiokawa⁴, Hiroyuki Nakata² (1.Graduate School of Science Engineering, Chiba University, 2.Graduate School of Engineering, Chiba University, 3.Planetary Plasma and Atmospheric Research Center, Graduate School of Science, Tohoku University, 4.Institute for Space-Earth Environmental Research, Nagoya University)

[PEM11-P24] Sporadic Fe layer event associated with vertical ion drift based on wind shear theory: simultaneous observation of Fe density and wind at Syowa station (69.0°S, 39.6°E) and simulation

*Takanori Nishiyama^{1,2}, Mitsumu K. Ejiri^{1,2}, Takuo T. Tsuda³, Takuji Nakamura^{1,2}, Katsuhiko Tsuno⁴, Masaki Tsutsumi^{1,2}, Takuya Kawahara⁵, Makoto Abo⁶, Takayo Ogawa⁴, Satoshi Wada⁴ (1.National Institute of Polar Research, 2.Department of Polar Science, The Graduate University for Advanced Studies, SOKENDAI, 3.The University of Electro- Communications, 4.RIKEN, 5.Shinshu University, 6.Tokyo Metropolitan University)

[E] Poster | P (Space and Planetary Sciences) : P-EM Solar-Terrestrial Sciences, Space Electromagnetism & Space Environment

5:15 PM - 6:30 PM JST | 8:15 AM - 9:30 AM UTC | Ch.05_1

[P-EM13] Study of coupling processes in solar-terrestrial system

convener: Mamoru Yamamoto (Research Institute for Sustainable Humanosphere, Kyoto University), Yasunobu Ogawa (National Institute of Polar Research), Satonori Nozawa (Institute for Space-Earth Environmental Research, Nagoya University), Akimasa Yoshikawa (Department of Earth and Planetary Sciences, Kyushu University)

[PEM13-P01] Status of Equatorial MU Radar project in 2021

*Mamoru Yamamoto¹, Hiroyuki Hashiguchi¹, Tatsuhiro Yokoyama¹, Toshitaka Tsuda¹ (1. Research Institute for Sustainable Humanosphere, Kyoto University)

[PEM13-P02] Development of instruments for dual-band beacon (DBB) experiment of total electron content (TEC)

*Mamoru Yamamoto¹ (1. Research Institute for Sustainable Humanosphere, Kyoto University)

[PEM13-P03] Development of multi-scale numerical simulation model for the study on ionospheric disturbances

*Tatsuhiro Yokoyama¹, Taichi Komoto¹ (1. Research Institute for Sustainable Humanosphere, Kyoto University)

[PEM13-P04] Study on adaptive clutter rejection system using external receiving antennas for the MU radar

*Ryo Yabuki¹, Hiroyuki Hashiguchi¹, Issei Terada¹, Mamoru Yamamoto¹ (1. Research Institute for Sustainable Humanosphere, Kyoto University)

[PEM13-P05] Volume Scatter Simulation for 3D Wind Vector Estimation using Radar Inversion

*Ryosuke Tamura¹, Koji Nishimura¹, Hiroyuki Hashiguchi¹ (1. Research Institute for Sustainable Humanosphere)

[PEM13-P06] Multiple equatorial ionospheric observation project based on FMCW radar combining MAGDAS/SDR-based scintillation detector

*Akiko Fujimoto¹, Shuji Abe², Toru Mikura¹, Akihiro Ikeda³, Akimasa Yoshikawa² (1. Kyushu Institute of Technology, 2. Kyushu University, 3. National Institute of Technology, Kagoshima College)

[PEM13-P07] **Development of an Autonomous Method for Equatorial Spread-F (ESF) Detection of SEALION Ionosonde Data**

*Septi Perwitasari¹, Kornyanat Hozumi¹ (1. National Institute of Information and Communications Technology)

[PEM13-P08] Progress of atmospheric coupling studies with the EISCAT_3D radar system

*Hitoshi Fujiwara¹, Satonori Nozawa², Yasunobu Ogawa³, Yasunobu Miyoshi⁴ (1. Education and Research Center for Sustainable Development/Faculty of Science and Technology, Seikei University, 2. Institute for Space-Earth Environmental Research, Nagoya University, 3. National Institute of Polar Research, 4. Department of Earth and Planetary Sciences, Faculty of Sciences, Kyushu University)

[PEM13-P09] Optical calibration system of NIPR for aurora and airglow observations

*Yasunobu Ogawa^{1,2,3}, Akira Kadokura^{1,2,3}, Mitsumu K. Ejiri^{1,2} (1. National Institute of Polar Research, 2. The Graduate University for Advanced Studies, SOKENDAI, 3. Joint Support-Center for Data Science Research, Research Organization of Information and Systems)

[PEM13-P10] Spectroscopic and imaging observations for short-wavelength infrared aurora and airglow at Longyearbyen (78.2°N, 15.6°E) coordinated with EISCAT Svalbard radar and VLF/LF radio wave receivers.

*Takanori Nishiyama^{1,2}, Masato Kagitani³, Yasunobu Ogawa^{1,2,4}, Fuminori Tsuchiya³, Keisuke Hosokawa⁵, Takeshi Sakanoi³ (1. National Institute of Polar Research, 2. Department of Polar Science, The Graduate University for Advanced Studies, SOKENDAI, 3. Planetary Plasma and Atmospheric Research Center, Tohoku University, 4. Joint Support-Center for Data Science Research, Research Organization of Information and Systems, 5. The University of Electro-Communications)

[PEM13-P11] **Study of 8 hr and 6 hr atmospheric waves in the polar upper mesosphere and lower thermosphere by using sodium LIDAR data**

*Chiaki Morikawa¹, Satonori Nozawa¹, Takuo T. Tsuda², Takuya Kawahara³, Norihito Saito⁴, Satoshi Wada⁴, Toru Takahashi⁵, Tetsuya Kawabata¹, Chris Hall⁶ (1.ISEE, Nagoya University, 2.Department of Communication Engineering and Informatics, The University of Electro-Communications, 3.Faculty of Engineering, Shinshu University, 4.RIKEN Center for Advanced Photonics, RIKEN, 5.Electronic Navigation Research Institute, 6.UiT The Arctic University of Norway)

[PEM13-P12] Research on the Analysis of Nitric Oxide Molecular Spectral Data with Millimeter-wave Spectroscopic Observations in Tromsø, Norway

*Hirofumi Goto¹, Akira Mizuno¹, Tomoo Nagahama¹, Tac Nakajima¹, Satonori Nozawa¹, Yasusuke Kojima¹, Tetsuya Kawabata¹, Ryuji Fujimori¹, Kazuji Suzuki¹, Yasunobu Ogawa² (1.Institute for Space Earth Environmental Research, Nagoya University, 2.National Institute of Polar Research)

[PEM13-P13] Aurora and airglow observations by an optical spectrograph at Tromsø, Norway

*Takuo T. Tsuda¹, Keisuke Hosokawa¹, Satonori Nozawa², Tetsuya Kawabata², Akira Mizuno², Shin-ichiro Oyama², Junichi Kurihara³, Kim Nielsen⁴ (1.University of Electro-Communications, 2.Nagoya University, 3.Hokkaido University, 4.Utah Valley University)

[PEM13-P14] Statistical investigation on thermospheric Na based on Na lidar observations at Tromsø

*Hatsumi Hyodo¹, Takuo T. Tsuda¹, Satonori Nozawa², Takuya Kawahara³, Norihito Saito⁴, Tetsuya Kawabata² (1.The University of Electro-Communications, 2.Nagoya University, 3.Shinshu University, 4.RIKEN)

[PEM13-P15] Automated detection system of aurora using deep learning: real-time operation in Tromsø, Norway

*Sota Nanjo¹, Keisuke Hosokawa¹, Satonori Nozawa² (1.The University of Electro-Communications, 2.Nagoya University)

[PEM13-P16] Observational evaluation of temperature/wind perturbations associated with small-scale AGWs : Parameterisation and validation of wave structures

*Shin Suzuki¹, Satonori Nozawa², Shin-ichiro Oyama², Kazuo Shiokawa² (1.Faculty of Regional Policy, Aichi University, 2.Institute for Space-Earth Environmental Research, Nagoya University)

[E] Poster | P (Space and Planetary Sciences) : P-CG Complex & General

5:15 PM - 6:30 PM JST | 8:15 AM - 9:30 AM UTC | Ch.06_1

[P-CG17] Future missions and instrumentation for space and planetary science

convener:Kazunori Ogawa(Japan Aerospace Exploration Agency), Mitsunori Ozaki(Faculty of Electrical and Computer Engineering, Institute of Science and Engineering, Kanazawa University), Naoya Sakatani(Department of Physics, Rikkyo University), Kazuo Yoshioka(Graduate School of frontier Science, The University of Tokyo)

[PCG17-P01] Challenges for ion measurements in a comet mission

*Satoshi Kasahara¹, Shoichiro Yokota², Kazushi Asamura³, Yoshifumi Saito³, Masafumi Hirahara⁴ (1.The University of Tokyo, 2.Osaka University, 3.ISAS, 4.Nagoya University)

[PCG17-P02] Miniaturization of energetic electron sensor for future planetary explorations using ASIC

*Shin Sugo¹, Satoshi Kasahara¹, Ikeda Hirokazu², Hirotsugu Kojima³, Motoyuki Kikukawa³, Takahiro Zushi⁴ (1.The University of Tokyo, 2.Institute of Space and Astronautical Science, 3.Research Institute for Sustainable Humanosphere, Kyoto University, 4.National Institute of Technology, Nara College)

[PCG17-P03] Development of a miniature ion-trap Fourier-transform mass spectrometer for future space missions

*Oya Kawashima¹, Satoshi Kasahara¹, Yoshifumi Saito², Shoichiro Yokota³, Masafumi Hirahara⁴, Seiji Sugita¹ (1.The university of tokyo, 2.ISAS/JAXA, 3.Osaka univ., 4.Nagoya Univ.)

[PCG17-P04] Development of the bread board model of the Life-signature Detection Microscope (LDM)

*Yoshitaka Yoshimura¹, Akihiko Yamagishi², Atsuo Miyakawa², Eiichi Imai³, Satoshi Sasaki⁴, Mita Hajime⁵, Kensei Kobayashi⁶, Yoko Kebukawa⁶, Naoto Sato⁷, Takehiko Satoh⁸, Keigo Enya⁸, Kazuhisa Fujita⁸, Tomohiro Usui⁸ (1.Tamagawa University, 2.Tokyo University of Pharmacy and Life Science, 3.Nagaoka University of Technology, 4.Tokyo University of Technology, 5.Fukuoka Institute of Technology, 6.Yokohama National University, 7.Meiji University, 8.Japan Aerospace Exploration Agency)

[PCG17-P05] Investigation of the response of an all-sky electrostatic analyzer

Tzu-Fang Chang¹, *SHENG-CHENG TSAI¹, Chih-Yu Johnson Chiang¹ (1.Institute of Space and Plasma Sciences, National Cheng Kung University, tainan, taiwan)

[PCG17-P06] Radar experiments for sounding internal structures of the asteroids using scale-down model

*Atsushi Kumamoto¹, Hideaki Miyamoto², Toshiyuki Nishibori³, Fuminori Tsuchiya¹, Ken Ishiyama⁴ (1.Graduate School of Science, Tohoku University, 2.Graduate School of Engineering, The University of Tokyo, 3.Japan Aerospace Exploration Agency, 4.National Institute of Technology, Tsukuba College)

[PCG17-P07] Development and Integration of the High-Speed Current Detection Circuits in Particle Sensors

*Motoyuki Kikukawa¹, Hirotsugu Kojima¹, Yoshifumi Saito², Kazushi Asamura² (1.Research Institute for Sustainable Humanosphere, Kyoto University, 2.Institute of Space and Astronautical Science)

[PCG17-P08] The new type of plasma wave instruments capable of both waveform and spectrum observation

*Takahiro Zushi¹, Hirotsugu Kojima² (1.National Institute of Technology, Nara College, 2.Research Institute for Sustainable Humanosphere, Kyoto University)

[PCG17-P09] S Band and UHF Band Communication Systems for Kanazawa-SAT3 Microsatellite

*Mayuko Tachiya¹, Sota Yamamoto¹, Koyo Ina¹, Tomohiko Imachi¹, Satoshi Yagitani¹, Daisuke Yonetoku¹, Yoshiya Kasahara¹, Tatsuya Sawano¹, Makoto Arimoto¹ (1.Kanazawa University)

[PCG17-P10] Attitude Control System for Kanazawa-SAT3 Microsatellite

*Kohei Fujiki¹, Shinsaku Suzukawa¹, Yuki Yasuda¹, Tomohiko Imachi¹, Satoshi Yagitani¹, Yoshiya Kasahara¹, Daisuke Yonetoku¹, Tatsuya Sawano¹, Makoto Arimoto¹ (1.Kanazawa University)

[PCG17-P11] Developing software for Kanazawa-SAT3

*Yuta Inoue¹, Akane Sasaoka¹, Yasuhiro Kishino¹, Tomohiko Imachi¹, Yoshiya Kasahara¹, Tatsuya Sawano¹, Satoshi Yagitani¹, Daisuke Yonetoku¹, Makoto Arimoto¹ (1.Kanazawa University Graduate School)

[PCG17-P12] Development of mid-IR heterodyne spectrometer with hollow optical fiber for solar system exploration

*Satoki Tsukada¹, Hiromu Nakagawa¹, Isao Murata¹, Yasuhiro Hirahara², Yasumasa Kasaba¹, Takashi Katagiri³, Yuji Matsuura⁴, Akiho Miyamoto¹, Atsushi Yamazaki⁵ (1.Science, Tohoku Univ., 2.Environmental Studies, Nagoya Univ., 3.Science and Engineering for Education, Toyama Univ., 4.Biomedical Engineering, Tohoku Univ., 5.Institute of Space and Astronautical Science, Japan Aerospace Exploration Agency)

[PCG17-P13] Investigation of potential candidates for a sample return mission

*Yuri Shimaki¹, Shigeru Wakita^{2,3}, Seitaro Urakawa⁴, Peng Hong⁵, Fumihiko Usui¹, Moe Matsuoka¹, Naoya Sakatani⁶, Satoshi Tanaka¹, Sunao Hasegawa¹, Daisuke Kuroda⁷ (1.Institute of Space and Astronautical Science, Japan Aerospace Exploration Agency, 2.Massachusetts Institute of Technology, 3.Purdue University, 4.Japan Spaceguard Association, 5.Planetary Exploration Research Center, Chiba Institute of Technology, 6.Rikkyo University, 7.Kyoto University)

[PCG17-P14] Observation Plans and Development Status of MIRS: MMX Infrared Spectrometer on the MMX Spacecraft

*Takahiro Iwata¹, Hiromu Nakagawa², Fuminori Tsuchiya², Tomoki Nakamura², Maria Antonietta Barucci³, Jean-Michel Reess³, Pernelle Bernardi³, Alain Doressoundiram³, Sonia Fornasier³, Michel Le Du⁴, Eric Sawyer⁴ (1.Institute of Space and Astronautical Science, Japan Aerospace Exploration Agency, 2.Tohoku University, 3.LESIA, Observatoire de Paris, 4.CNES)

[E] Poster | A (Atmospheric and Hydrospheric Sciences) : A-AS Atmospheric Sciences, Meteorology & Atmospheric Environment

5:15 PM - 6:30 PM JST | 8:15 AM - 9:30 AM UTC | Ch.07_1

[A-AS01] Large-scale moisture and organized cloud systems

convener:Satoru Yokoi(Japan Agency for Marine-Earth Science and Technology), Hiroaki Miura(The University of Tokyo), Atsushi Hamada(University of Toyama), Masaki Satoh(Atmosphere and Ocean Research Institute, The University of Tokyo)

[AAS01-P01] Intraseasonal variability in the initialization of a seasonal prediction system simulated by a new convection scheme

★Invited Papers

*Yuya Baba¹ (1.JAMSTEC Japan Agency for Marine-Earth Science and Technology)

[AAS01-P02] The Different Pathways to self-aggregation between SCALE and VVM

★Invited Papers

*Ching-Shu Hung¹, Hiroaki Miura¹, Jin-De Huang², Chien-Ming Wu² (1.The University of Tokyo, 2.National Taiwan University)

[AAS01-P03] A Numerical Study on the Diurnal Variation of Precipitation Bands Observed around the West Coast of Sumatra Island

*Mamiko Terada¹, Hiroaki Miura¹, Satoru Yokoi² (1. The University of Tokyo Department of Earth and Planetary Science, 2.Japan Agency for Marine-Earth Science and Technology)

[AAS01-P04] A conservative and consistent remapping of moisture on the icosahedral mesh

*Hiroaki Miura¹ (1.The University of Tokyo)

[AAS01-P05] Observational study on boundary-layer moist static energy budget over the tropical Indo-Pacific warm pool domain

*Satoru Yokoi¹ (1.Japan Agency for Marine-Earth Science and Technology)

[E] Poster | A (Atmospheric and Hydrospheric Sciences) : A-AS Atmospheric Sciences, Meteorology & Atmospheric Environment

5:15 PM - 6:30 PM JST | 8:15 AM - 9:30 AM UTC | Ch.07_2

[A-AS04] Machine Learning Techniques in Weather, Climate, Hydrology and Disease Predictions

convener: Venkata Ratnam Jayanthi (Application Laboratory, JAMSTEC), Rajib Maity (Indian Institute of Technology Kharagpur), Swadhin Behera (Application Laboratory, JAMSTEC, 3173-25 Showa-machi, Yokohama 236-0001), Takeshi Doi (JAMSTEC)

[AAS04-P01] 3D Precipitation Nowcasting: RESNet applied to Highly Dense PAWR Data

*Maha Mdini¹, Takemasa Miyoshi¹, Shigenori Otsuka¹ (1. RIKEN Center for Computational Science)

[AAS04-P02] **A reservoir inflow forecasting model using a Wavelet transformed - deep learning algorithm**

Trung Duc Tran¹, *Jongho Kim¹ (1. University of Ulsan)

[AAS04-P03] Development of an integrated NWP-DA-AI system for 30-second-update 3D precipitation prediction

*Shigenori Otsuka¹, Yasumitsu Maejima¹, Pierre Tandeo², Takemasa Miyoshi¹ (1. RIKEN Center for Computational Science, 2. IMT Atlantique)

[E] Poster | A (Atmospheric and Hydrospheric Sciences) : A-HW Hydrology & Water Environment

5:15 PM - 6:30 PM JST | 8:15 AM - 9:30 AM UTC | Ch.09_1

[A-HW22] Material transportation and cycling in watershed ecosystems; from headwaters to coastal areas

convener: Morihiro Maeda (Okayama University), Tomohisa Irino (Faculty of Environmental Earth Science, Hokkaido University), Shin-ichi Onodera (Graduate School of Advanced Science and Engineering, Hiroshima University), Adina Paytan (University of California Santa Cruz)

[AHW22-P01] Distribution of sea ice rafted detritus yielded from the sediments of Okhotsk coast of Hokkaido, northern Japan

*Tomohisa Irino¹, Ryuki Saijo², Koji Suzuki¹, Jun Nishioka³, Tomohiro Nakamura³ (1. Faculty of Environmental Earth Science, Hokkaido University, 2. Graduate School of Environmental Science, Hokkaido University, 3. Institute of Low Temperature Science, Hokkaido University)

[AHW22-P02] Effect of stream water from nitrogen-saturated forests in the Koise River Basin on nitrogen concentrations in the main river

*Masahiro Kobayashi¹, Yuko Itoh¹ (1. Forestry and Forest Products Research Institute)

[AHW22-P03] **Hydro-geographical Study on the Water Environment of Asakawa River in Tamagawa River System**

*Masato ODA¹, Koji KODERA² (1. Under Graduate Student, Hosei Univ., 2. Department of Geography, Hosei Univ.)

[AHW22-P04] Impact of COVID-19 on air pollutants influx into forest ecosystems in Japan

*Yuko Itoh¹, Toru Okamoto¹, Keiji Takase², Sakae Horisawa³ (1. Forestry and Forest Products Research Institute, Japan, 2. Ishikawa Prefectural University, 3. Kochi University of Technology)

[AHW22-P05] Long-term trends in zooplankton production and ecological transfer efficiency over four decades in Lake Biwa, Japan

*Xin Liu¹, Naoshige Goto¹, Syuhei Ban¹ (1. The University of Shiga Prefecture)

[AHW22-P06] High resolution monitoring for subsidiary nutrient loadings and phytoplankton production in north basin of Lake Biwa

*Syuhei Ban¹, Xin Liu¹, Ken'ichi Osaka¹, Naoshige Goto¹, John Wells² (1. The University of Shiga Prefecture, 2. Ritsumeikan University)

[AHW22-P07] Hydrological controls on phosphorus export from diffuse source in Lake Biwa basin, central Japan.

*Ken'ichi Osaka¹, Haruto Tanabe¹, Syuhei Ban¹ (1. Department of ecosystem study, University of Shiga Prefecture)

[AHW22-P08] **The influence of vertical water mixing on inter-annual nitrogen dynamics in Lake Biwa**

*Takaaki Ishibashi¹, Ken'ichi Osaka², Keisuke Koba³, Kei Nishida⁴, Takashi Nakamura⁴ (1. Graduate School of Environmental Science, University of Shiga Prefecture, 2. Department of ecosystem study, University of Shiga Prefecture, 3. Center for Ecological Research, Kyoto University, 4. Interdisciplinary Centre for River Basin Environment, Interdisciplinary Graduate School, University of Yamanashi)

[AHW22-P09] Detection of Dissolved Methylphosphonate in Freshwater of Lake Biwa by pre-concentration with Iron(III) hydroxide coprecipitation

Tomoki Yamamoto¹, Kazuma Tsuji³, Yuki Yamanaka³, *Masahiro Maruo¹, Hajime Obata² (1. Department of Ecosystem Studies, School of Environmental Science, The University of Shiga Prefecture, 2. Atmosphere and Ocean Research Institute, The University of Tokyo, 3. Graduate School of Environmental Science, The University of Shiga Prefecture)

[AHW22-P10] **Estimation of groundwater and lake water interaction in the deeper zone of Lake Biwa, using ¹⁸O and D in pore water and groundwater**

*Shin-ichi Onodera¹, Mitsuyo Saito², Yusuke Tomozawa¹, Takuya Ishida¹, Syuhei Ban³, Noboru Okuda⁴ (1. Graduate School of Advanced Science and Engineering, Hiroshima University, 2. Okayama University, 3. The University of Shiga Prefecture, 4. Kobe University)

[AHW22-P11] Identification of enriched phosphate in groundwater: insights from distribution of phosphate oxygen isotope ratio in aquifer sediments

*Takuya Ishida¹, Yusuke Tomozawa¹, Xin Liu², Mitsuyo Saito³, Shin-ichi Onodera¹, Noboru Okuda⁴, Syuhei Ban² (1.Hiroshima University, 2.The University of Shiga Prefecture, 3.Okayama University, 4.Kobe University)

[AHW22-P12] Long-term Estimation on Phosphorus flux in a Coastal Catchment Influenced by the Anthropogenic Land Use Change

*Kunyang Wang¹, Shin-ichi Onodera¹, Mitsuyo Saito², Yuta Shimizu³ (1.Graduate School of Integrated Arts and Science, Hiroshima University, 2.Faculty of Environmental Science and Technology, Okayama University, 3. National Agriculture and Food Research Organization)

[AHW22-P13] Analysis for the characteristics of water and nutrient discharge in a sub-basin of Osaka Bay catchment

*Shuta Ishihara¹, Kunyang Wang², Mitsuyo Saito³, Shin-ichi Onodera⁴ (1.Faculty of Environmental Science and Technology, Okayama University, 2.Graduate School of Integrated Arts and Sciences, Hiroshima University, 3.Graduate School of Environmental and Life Science, Okayama University, 4.Graduate School of Advanced Science and Engineering, Hiroshima University)

[AHW22-P14] Estimation of groundwater flow and a river water contribution to it in an alluvial plain of western Japan, using tracer methods

*Yusuke Tomozawa¹, Toru Takeuchi², Shin-ichi Onodera¹, Mitsuyo Saito³, Shotaro Fujioka⁴ (1.Graduate School of Advanced Science and Engineering Hiroshima University, 2.Fujita Geology Co., Ltd, , 3.Graduate School of Environmental and Life Science, Okayama University, 4.River fishermen)

[AHW22-P15] Estimation of Landuse Change Impact on Water Budget in Higashihiroshima Catchment using SWAT

*Sharon Bih Kimbi¹, Kunyang Wang¹, Shin-ichi Onodera², Ichirow Kaihotsu¹, Shingo Nozaki², Yusuke Tomozawa² (1.Graduate School of Integrate Arts and Sciences, Hiroshima University, 2.Graduate School of Advanced Science and Engineering, Hiroshima University)

[AHW22-P16] Flood Impact on water quality in a Small Catchment Area: Preliminary Study

*Sharon Bih Kimbi¹, Shin-ichi Onodera², Shingo Nozaki², Yusuke Tomozawa² (1.Graduate School of Integrate Arts and Sciences, Hiroshima University, 2.Graduate School of Advanced Science and Engineering, Hiroshima University)

[AHW22-P17] Process of spatio-temporal variation in seagrass-seaweed meadows in intertidal areas of Seto Inland Sea, western Japan

*Mitsuyo Saito¹, Shin-ichi Onodera², Natsushi Soga³, Yuto Ideishi³, Shingo Nozaki², Yusuke Tomozawa² (1.Graduate School of Environmental and Life Science, Okayama University, 2.Graduate School of Advanced Science and Engineering, Hiroshima University, 3.Faculty of Environmental Science and Technology, Okayama University)

[AHW22-P18] Analysis of coastal seagrass bed distribution using UAV and near-infrared camera data

*Toru Iwata¹, Akimitsu Shiraishi¹, Mitsuyo Saito¹, Shin-ichi Onodera² (1.Graduate School of Environmental and Life Science, Okayama University, 2.Graduate School of Integrated and Arts Sciences, Hiroshima University)

[AHW22-P19] **Physically Based Groundwater Flow Simulation using Tracer-aided model in Kumamoto Region, Japan**

*A T M Sakiur Rahman¹, Takahiro Hosono^{2,3}, Yasuhiro Tawara⁴, Youichi Fukuoka⁴, Aurelien Hazart, Jun Shimada³ (1.Postdoctotal researcher, Kumamoto University, 2.Faculty of Advanced Science and Technology, Kumamoto University, 3.International Research Organization for Advanced Science and Technology, Kumamoto University, 4.Geosphere Environmental Technology Corporation, NCO Kanda, Awajicho Building 3F, 2-1 Kanda, Awajicho, Chiyoda-ku, Tokyo 101-0063, Japan)

[AHW22-P20] Quantitative evaluation of groundwater pollution at Ryukyu limestone area in southern Okinawa Island: Trial application of boron isotope

*KE-HAN SONG¹, Yumi Moromizato², Ryuichi Shinjo², Jun Yasumoto³, Kazuko Sawada⁴ (1.Graduate School of Engineering and Science, University of the Ryukyus, Senbaru 1, Nishihara, Okinawa 903-0213, Japan, 2.Department of Physics and Earth Sciences, Faculty of Science, University of the Ryukyus, Senbaru 1, Nishihara, Okinawa 903-0213, Japan, 3.Department of Regional Agricultural Engineering, Faculty of Agriculture, University of the Ryukyus, Senbaru 1, Nishihara, Okinawa 903-0213, Japan, 4.Center for Strategic Research Projects, University of the Ryukyus, Senbaru 1, Nishihara, Okinawa 903-0213, Japan)

[AHW22-P21] Metagenomic analysis on the groundwater in the Ryukyu Limestone area

*Maruyama Rio¹, Nanami Mizusawa¹, Jun Yasumoto², Mariko Iijima³, Yasumoto Ko¹, Mina Hirose⁴, Akira Iguchi³, Mitsuru Jimbo¹, Shugo Watabe¹ (1.School of Marine Biosciences, Kitasto University, 2.Faculty of Agriculture, University of the Ryukyus, 3.National Institute of Advanced Industrial Science and Technology, 4.Tropical Technology Plus)

[AHW22-P22] The effects of groundwater runoff on the coastal bacterial communities near the Ryukyu Limestone area

*Nanami Mizusawa¹, Akira Iguchi², Mariko Iijima², Rio Maruyama¹, Jun Yasumoto³, Ko Yasumoto¹, Mina Hirose⁴, Shugo Watabe¹ (1.Kitasato University School of Marine Biosciences, 2.National Institute of Advanced Industrial Science and Technology, 3.Faculty of Agriculture, University of the Ryukyus, 4.Tropical Technology Plus)

[AHW22-P23] Water environment issues in Chinese megacity delta-Sewage impacts on Peral river coastal area

*Guangzhe Jin¹, Shin-ichi Onodera², Mitsuyo Saito³, Yuta Shimizu⁴, Jianyao Chen⁵ (1.College of Ocean and Meteorology, Guangdong Ocean University, 2.Graduate School of Integrated and Arts Sciences, Hiroshima University, 3.Graduate school of Environmental and Life Science, Okayama University, 4.Western Region Agricultural Research Center, National Agriculture and Food Research Organization., 5.The School of Geography and Planning, Sun Yat-sen University)

[AHW22-P24] Assessment of drought trends in the Dakbla watershed, Vietnam

*Tram Ngoc Quynh Vo¹, Hiroaki Somura¹ (1.Graduate School of Environmental and Life Science, Okayama University)

[AHW22-P25] Hydrogeochemical evolution mechanisms of groundwater in the Semarang Coastal Zone, Java Island, Indonesia

*Rizka Maria Maria^{1,6}, Anna Fadiah Rusydi^{2,6}, Shin-ichi Onodera³, Mitsuyo Saito⁴, Seiichiro Ioka⁵, Robert Muhammad Delinom⁶, Wahyu Purwoko⁶, Dadi Sukmayadi⁶, Hendarmawan Hendarmawan¹ (1.Faculty of Geological Engineering, Padjadjaran University, Indonesia, 2.Graduate School of Integrated Arts and Sciences, Hiroshima University, Japan, 3.Graduate School of Advance Science and Engineering, Hiroshima University, Japan, 4.Graduate School of Environmental and Life Science, Okayama University, Japan, 5.Research Institute for Sustainable Energy, Hirosaki University, Japan, 6.Research Center for Geotechnology, Indonesian Institute of Sciences, Indonesia)

[AHW22-P26] A comparative analysis in modeling surface runoff under climate and land use change in two catchments in Iran and Indonesia

*Sharif Joorabian Shoostari¹, Shin-ichi Onodera², Yuta Shimizu³ (1.Department of Nature Engineering, Agricultural Sciences and Natural Resources University of Khuzestan, Mollasani, Iran, 2.Graduate School of Advanced Science and Engineering, Hiroshima University, 3.Western Region Agricultural Research Center, National Agriculture and Food Research Organization)

[AHW22-P27] Effects of different NH₄⁺-N contents on N₂O and CO₂ emissions from manure compost-amended soil

*Thanuja Deepani Panangala Liyanage¹, Morihiro Maeda¹, Hiroaki Somura¹ (1.Okayama University)

[E] Poster | A (Atmospheric and Hydrospheric Sciences) : A-CG Complex & General

5:15 PM - 6:30 PM JST | 8:15 AM - 9:30 AM UTC | Ch.10_1

[A-CG29] Extratropical oceans and atmosphere

convener: Toyama Katsuya (Meteorological Research Institute), Youichi Kamae (Faculty of Life and Environmental Sciences, University of Tsukuba), Shoichiro Kido (JAMSTEC Application Lab), Shion Sekizawa (Research Center for Advanced Science and Technology, University of Tokyo)

[ACG29-P01] East-Asian atmospheric rivers bring more frequent and intense extreme rainfall under global warming

*Youichi Kamae¹, Yukiko Imada², Hiroaki Kawase², Wei Mei³ (1. Faculty of Life and Environmental Sciences, University of Tsukuba, 2. Meteorological Research Institute, Japan Meteorological Agency, 3. University of North Carolina at Chapel Hill)

[ACG29-P02] AGCM experiments for winters of 2017/18 and 2019/20

*Kazuaki Nishii¹, Bunmei Taguchi², Hisashi Nakamura³ (1. Graduate School of Bioresources, Mie University, 2. Faculty of Sustainable Design, University of Toyama, 3. RCAST, The University of Tokyo)

[ACG29-P03] A breakdown of the diabatic genesis/loss of polar cold air masses and its relationship with air-sea interactions

*Yuki Kanno¹, Toshiki Iwasaki² (1. Central Research Institute of Electric Power Industry, 2. Department of Geophysics, Graduate School of Science, Tohoku University)

[ACG29-P04] Year-to-year variations of the extratropical direct circulation associated with the Aleutian-Icelandic lows

*Masaya Kuramochi¹, Hiroaki Ueda² (1. Graduate School of Science and Technology, University of Tsukuba, 2. Faculty of Life and Environmental Sciences, University of Tsukuba)

[ACG29-P05] Impact of recent warming in East Asian marginal seas on the torrential rainfall event occurred in Kyushu Island, Japan in July 2017

*ATSUYOSHI MANDA¹ (1. Mie University)

[ACG29-P06] **Mechanism of the warming of the North Pacific subtropical mode water from 1901 to 2010 in a regional ocean model**

*Yoshi N Sasaki¹, Tomoya Nakamura¹ (1. Hokkaido University)

[ACG29-P07] Interannual and decadal surface velocity variations in the Kuroshio and Kuroshio Extension System

*YUXIANG QIAO¹, Hirohiko Nakamura¹, Shinichiro Kako¹, Ayako Nishina¹, Tomohiko Tomita² (1. Kagoshima University, 2. Kumamoto University)

[ACG29-P08] Late-winter glider observation of upper ocean responses to weather disturbances in the western subtropical North Pacific

*Toyama Katsuya¹ (1. Meteorological Research Institute)

[E] Poster | A (Atmospheric and Hydrospheric Sciences) : A-CG Complex & General

5:15 PM - 6:30 PM JST | 8:15 AM - 9:30 AM UTC | Ch.10_2

[A-CG32] Land-Atmosphere interactions and Asian monsoon precipitation (LAMos)

convener:G. Hiroshi Takahashi(Department of Geography, Tokyo Metropolitan University), Shiori Sugimoto(JAMSTEC Japan Agency for Marine-Earth Science and Technology), Hatsuki Fujinami(Nagoya University), Hirokazu Endo(Meteorological Research Institute, Japan Meteorological Agency)

[ACG32-P01] Links between torrential rainfall and urban land use in Jakarta, Indonesia using Geographically Weighted Regression

*Asteria Satyaning Handayani^{1,2}, Yuzuru Isoda¹ (1.Earth Science Department, Graduate School of Science, Tohoku University, Japan, 2.Agency for Meteorology Climatology and Geophysics (BMKG), Indonesia)

[ACG32-P02] The simulation for the nocturnal precipitation over the Himalayas

*Shiori Sugimoto¹, Kenichi Ueno², Hatsuki Fujinami³, Tomoe Nasuno¹, Tomonori Sato⁴, Hiroshi G. Takahashi⁵ (1.JAMSTEC Japan Agency for Marine-Earth Science and Technology, 2.University of Tsukuba, 3.Nagoya University, 4.Hokkaido University, 5.Tokyo Metropolitan University)

[ACG32-P03] **Simulated precipitation characteristics over the tropical Asian monsoon regions** by high-resolution climate models

*Hiroshi G. Takahashi¹, Rakesh Teja Konduru¹, Nozomi Kamizawa¹, Moeka Yamaji¹ (1.Department of Geography, Tokyo Metropolitan University)

[E] Poster | A (Atmospheric and Hydrospheric Sciences) : A-CG Complex & General

5:15 PM - 6:30 PM JST | 8:15 AM - 9:30 AM UTC | Ch.10_3

[A-CG35] Projection and detection of global environmental change

convener:Michio Kawamiya(Japan Agency for Marine-Earth Science and Technology), Kaoru Tachiiri(Japan Agency for Marine-Earth Science and Technology), Hiroaki Tatebe(Japan Agency for Marine-Earth Science and Technology), V Ramaswamy(NOAA GFDL)

[ACG35-P01] Future directions of Earth system modeling: outcome of the discussion forum under TOUGOU program

*Michio Kawamiya¹, Kaoru Tachiiri^{1,2}, Tomohiro Hajima¹, Tokuta Yokohata², Junichi Tsutsui³, Takashi Arakawa⁴, Takahiro Inoue^{1,5} (1.Japan Agency for Marine-Earth Science and Technology, 2.National Institute for Environmental Studies, 3.Central Research Institute of Electric Power Industry, 4.Research organization for Information Science and Technology, 5.Remote Sensing Technology Center of Japan)

[ACG35-P02] Development of a coupled Earth and socio-economic system model

*Kaoru Tachiiri^{1,3}, Xuanming Su¹, Ken'ichi Matsumoto^{2,1}, Tomohiro Hajima¹, Tokuta Yokohata³ (1.Japan Agency for Marine-Earth Science and Technology, 2.Nagasaki University, 3.National Institute for Environmental Studies)

[ACG35-P03] **Quantifying committed warming from individual climate forcers based on the Simple Climate Model for Optimization (SCM4OPT)**

*Xuanming Su¹, Katsumasa Tanaka^{2,3}, Kaoru Tachiiri¹, Michio Watanabe¹, Michio Kawamiya¹ (1.Japan Agency for Marine-Earth Science and Technology, 2.Laboratoire des Sciences du Climat et de l'Environnement, 3.National Institute for Environmental Studies)

[ACG35-P04] Simulated impact of the 1815 Tambora eruption on global climate with MIROC-ES2L

*Manabu Abe¹, Tomohiro Hajima¹ (1.Japan Agency for Marine-Earth Science and Technology)

[ACG35-P05] Millennium time-scale experiments with doubled CO2 concentration by Earth system models

*Tomohiro Hajima¹, Akitomo Yamamoto¹, Michio Kawamiya¹, Xuaming Su¹, Michio Watanabe¹, Rumi Ohgaito¹, Hiroaki Tatebe¹ (1.Japan Agency for Marine-Earth Science and Technology)

[ACG35-P06] Climate impact of reducing CO2 and other emissions from the COVID-19 pandemic

*Rumi Ohgaito¹, Manabu Abe¹, Tomohiro Hajima¹, Kaoru Tachiiri¹, Michio Kawamiya¹ (1.Japan Agency for Marine-Earth Science and Technology)

[E] Poster | H (Human Geosciences) : H-TT Technology & Techniques

5:15 PM - 6:30 PM JST | 8:15 AM - 9:30 AM UTC | Ch.12_3

[H-TT30] GEOMORPHOLOGICAL APPLICATIONS OF HIGH-DEFINITION TOPOGRAPHY AND GEOPHYSICAL DATA IN THE ANTHROPOCENE

convener:Yuichi S. Hayakawa(Faculty of Environmental Earth Science, Hokkaido University), Tsuyoshi Hattanji(Faculty of Life and Environmental Sciences, University of Tsukuba), Shigekazu Kusumoto(Institute for Geothermal Sciences, Graduate School of Science, Kyoto University), A Christopher Gomez(Kobe University Faculty of Maritime Sciences Volcanic Risk at Sea Research Group), Masayuki Seto(Fukushima Future Center for Regional Revitalization, Fukushima University)

[HTT30-P01] Comparison of high resolution multispectral orthoimages with physiological activities of deciduous conifer trees

*Masuto Ebina¹, Wataru Ishizuka¹ (1.Forestry Research Institute, Hokkaido Research Organization)

[HTT30-P02] Subsurface structure of dolines on the Akiyoshi-dai Plateau, Japan: An approach from electrical resistivity tomography

Naoya Hiramoto¹, *Tsuyoshi Hattanji² (1.Graduate School of Life and Environmental Sciences, University of Tsukuba, 2.Faculty of Life and Environmental Sciences, University of Tsukuba)

[HTT30-P03] **Ground-Penetrating-Radar Investigation of drifted wood trapped in river-sand – Laboratory Experiments**

*Christopher A Gomez¹, Norifumi Hotta² (1.Kobe University Faculty of Maritime Sciences Volcanic Risk at Sea Research Group, 2.Graduate School of Agricultural and Life Sciences, The University of Tokyo)

[HTT30-P04] Drainage density and relative relief for the Kitakami Mountains, Japan

*Takashi Oguchi¹ (1.Center for Spatial Information Science, The University of Tokyo)

[E] Poster | S (Solid Earth Sciences) : S-SS Seismology

5:15 PM - 6:30 PM JST | 8:15 AM - 9:30 AM UTC | Ch.13_2

[S-SS02] Seismological advances in the ocean

convener:Takeshi Akuhara(Earthquake Research Institute, University of Tokyo), Takashi Tonegawa(Research and Development center for Earthquake and Tsunami, Japan Agency for Marine-Earth Science and Technology), Tatsuya Kubota(National Research Institute for Earth Science and Disaster Resilience)

[SSS02-P01] Improving the constraint of the 2016 Off-Fukushima shallow normal-faulting earthquake with the high-coverage tsunami data from the S-net wide network: implication on the crustal stress in the overriding plate

*Tatsuya Kubota¹, Hisahiko Kubo¹, Naotaka Yamamoto Chikasada¹, Keisuke Yoshida², Wataru Suzuki¹, Takeshi Nakamura³ (1.National Research Institute for Earth Science and Disaster Resilience, 2.Graduate School of Science, Tohoku University, 3.Central Research Institute of Electric Power Industry)

[SSS02-P02] Receiver function imaging of the amphibious NE Japan subduction zone - effects of low-velocity sediment layer-

*HyeJeong Kim¹, Hitoshi Kawakatsu¹, Takeshi Akuhara¹, Masanao Shinohara¹, Hajime Shiobara¹, Hiroko Sugioka², Ryota Takagi³ (1.Earthquake Research Institute, University of Tokyo, 2.Department of Planetology, Kobe University, 3.Research Center for Prediction of Earthquakes and Volcanic Eruptions, Graduate School of Science, Tohoku University)

[SSS02-P03] Transversely isotropic velocity structure of marine sedimentary layers estimated by Rayleigh wave ellipticity of ambient noise

*Shun Fukushima¹, Kiyoshi Yomogida¹ (1.Hokkaido University,Graduate school of Science,Department of Natural History Sciences,Seismology Laboratory)

[SSS02-P04] **Very broadband strain-rate measurements along a submarine fiber-optic cable off Cape Muroto, Nankai subduction zone, Japan**

*Satoshi Ide¹, Eiichiro Araki², Hiroyuki Matsumoto² (1.Department of Earth and Planetary Science, University of Tokyo, 2.Japan Agency for Marine-Earth Science and Technology)

[SSS02-P05] **The lithosphere–asthenosphere boundary beneath the Sea of Japan back-arc basin**

*Takeshi Akuhara¹, Kazuo Nakahigashi², Masanao Shinohara¹, Tomoaki Yamada³, Yusuke Yamashita⁴, Hajime Shiobara¹, Kimihiro Mochizuki¹ (1.Earthquake Research Institute, University of Tokyo, 2.Tokyo University of Marine Science and Technology, 3.Japan Meteorological Agency, 4.Disaster Prevention Research Institute, Kyoto University)

[SSS02-P06] **Surface wave envelope fitting for S wave velocity structure of the oceanic upper mantle**

*Haruka Nagai¹, Nozomu Takeuchi¹, Hitoshi Kawakatsu¹, Hajime Shiobara¹, Takehi Isse¹, Hiroko Sugioka², Aki Ito³, Hisashi Utada¹ (1.Earthquake Research Institute, The University of Tokyo, 2.Kobe University, 3.Japan Agency for Marine-Earth Science and Technology)

[SSS02-P07] Application of the wavefield decomposition for the Oldest-1 array data

*Hitoshi Kawakatsu¹, Takehi Isse¹, Nozomu Takeuchi¹, Hajime Shiobara¹, Hiroko Sugioka², YoungHee Kim³, Hisashi Utada¹, Sang-Mook Lee³ (1.Earthquake Research Institute, The University of Tokyo, 2.Kobe University, 3.Seoul National University)

[E] Poster | S (Solid Earth Sciences) : S-IT Science of the Earth's Interior & Tectonophysics

5:15 PM - 6:30 PM JST | 8:15 AM - 9:30 AM UTC | Ch.15_2

[S-IT15] Study of the Earth's Deep Interior - Interaction and Coevolution of the Core and Mantle

convener:Kenji Kawai(Department of Earth and Planetary Science, School of Science, University of Tokyo), Tsuyoshi Iizuka(University of Tokyo), Kenji Ohta(Department of Earth and Planetary Sciences, Tokyo Institute of Technology), Taku Tsuchiya(Geodynamics Research Center, Ehime University)

[SIT15-P01] First-principles study on the thermal transport properties of the subducting slab

*Haruhiko Dekura¹ (1.Geodynamics Research Center, Ehime University)

[SIT15-P02] A constraint to thermal conductivity of Earth's core and CMB heat flow by assessment on a stable region of Earth's core

*Takashi Nakagawa^{1,2}, Shin-ichi Takehiro³, Youhei SASAKI⁴ (1.Kobe University, 2.Hiroshima University, 3.Kyoto University, 4.Setsunan University)

[SIT15-P03] Self-diffusion of hcp-iron at high pressure

*Daisuke Yamazaki¹, Naoya Sakamoto², Hisayoshi Yurimoto² (1.Institute for Planetary Materials, Okayama University, 2.Hokkaido University)

[SIT15-P04] Inner core differential rotation inferred from antipodal seismic observations

*Seiji Tsuboi¹, Rhett Butler² (1.JAMSTEC, Center for Earth Information Science and Technology, 2.University of Hawaii at Manoa)

[E] Poster | S (Solid Earth Sciences) : S-IT Science of the Earth's Interior & Tectonophysics

5:15 PM - 6:30 PM JST | 8:15 AM - 9:30 AM UTC | Ch.15_3

[S-IT16] Structure and Dynamics of Earth and Planetary Mantles

convener:Takashi Nakagawa(University of Leeds), Takashi Yoshino(Institute for Planetary Materials, Okayama University), Dapeng Zhao(Department of Geophysics, Tohoku University)

[SIT16-P01] *None could explore* Origin of Plate Tectonics and Driving Force.

Abduction with Evolution explained and *verified all of them*, *Formation Mechanism of Deep Ocean Floor (Plate)*, and *Cause of Sudden Changes in Plate Movement Direction*.

*Akira Taneko¹ (1.SEED SCIENCE Lab.)

[SIT16-P02] High-temperature deformation properties of Li-doped polycrystalline olivine

*Bunrin Natsui¹, Takehiko Hiraga¹ (1.Earthquake Research Institute, University of Tokyo)

[SIT16-P03] Lattice preferred orientation of akimotoite and its implication to seismic anisotropy in the Earth's mantle

*Longli Guan¹, Daisuke Yamazaki¹, Noriyoshi Tsujino¹, Yoshinori Tange², Yuji Higo² (1.Institute for Planetary Materials, Okayama University, Misasa, Japan, 2.Japan Synchrotron Radiation Research Institute, 1-1-1 Kouto, Sayo, Hyogo 679-5198, Japan.)

[E] Poster | M (Multidisciplinary and Interdisciplinary) : M-GI General Geosciences, Information Geosciences & Simulations

5:15 PM - 6:30 PM JST | 8:15 AM - 9:30 AM UTC | Ch.20_2

[M-GI30] Near Surface Investigation and Modeling for Groundwater Resources Assessment and Conservation

convener:Jui-Pin Tsai(National Taiwan University, Taiwan), Makoto Taniguchi(Research Institute for Humanity and Nature), Ping-Yu Chang(National Central University)

[MGI30-P01] Multiple-point geostatistics for Simulation of Lithological Classification

*TING-AN LIN¹, Hwa-Lung Yu¹ (1.National Taiwan University)

[E] Poster | M (Multidisciplinary and Interdisciplinary) : M-SD Space Development & Earth Observation from Space

5:15 PM - 6:30 PM JST | 8:15 AM - 9:30 AM UTC | Ch.19_3

[M-SD39] Micro-satellite and its constellation in remote sensing

convener:Yukihiro Takahashi(Department of CosmoSciences, Graduate School of Science, Hokkaido University)

[MSD39-P01] Status of International Micro-satellite Consortium

*Yukihiro Takahashi¹ (1.Department of CosmoSciences, Graduate School of Science, Hokkaido University)

[MSD39-P02] Preliminary design and case study of Satellite Operation Management System for constellations and ground station network

*Yuji Sakamoto¹, Shinya Fujita¹, Naoya Shiraishi¹, Toshinori Kuwahara¹, Junichi Kurihara² (1.Department of Aerospace Engineering, Graduate School of Engineering, Tohoku University, 2.Faculty of Science, Hokkaido University)

[MSD39-P03] Development of a Miniature Ku-band RF Transceiver for Airborne Remote Sensing

*VOON CHET KOO¹, How Hsin William Hii², Yee Kit Chan¹ (1.Multimedia University, 2.iRadar Sdn Bhd)

[MSD39-P04] Myanmar Earth Observation Micro-Satellite Development and its Applications

*Hline Htet Win¹, San Lin Phyo¹, Ye Min Htay¹, Junichi Kurihara¹ (1.Hokkaido University)

[MSD39-P05] Extreme weather monitoring in Indonesia using TIS camera onboard on LAPAN A4

*Purwadi Purwadi¹, Yukihiro Takahashi², Findy Renggono¹, Halda Aditya Belgaman¹, Arif Saefudin³ (1.Agency for Assessment and Application for Technology, Jakarta 10340, Indonesia, 2.Faculty of Science, Hokkaido University, Sapporo 0600810, Japan, 3.National Institute of Aeronautics and Space of Indonesia, Jakarta 13220, Indonesia)

[MSD39-P06] Determination of Water Contaminant Concentration using Band Ratio and Statistical Method

*Ahmad Shaqeer Mohamed Thaheer¹, Yukihiro Takahashi¹ (1.Hokkaido University)

[MSD39-P07] Method for improving the exhaust speed and thrust of storage type Regolith Thruster

*Noruji MUTO¹, Necmi Cihan ORGER¹, Jose Rodrigo CORDOVA-ALARCON¹, Kazuhiro TOYODA¹, Mengu CHO¹ (1.Graduate school of Kyushu Institute of Technology)

[MSD39-P08] Lunar Observations with a Multispectral Sensor Onboard RISESAT Microsatellite and its Radiometric Calibration

*Masataka Imai^{1,2}, Junichi Kurihara³, Toru Kouyama^{1,2}, Toshinori Kuwahara⁴, Shinya Fujita⁴, Yuji Sakamoto⁴, Sei-ichi Saitoh⁵, Takafumi Hirata⁵, Hirokazu YAMAMOTO⁶, Yuji Sato⁴, Yukihiro Takahashi³ (1.Artificial Intelligence Research Center, National Institute of Advanced Industrial Science and Technology (AIST)), 2.AIST-UTokyo Advanced Operand-Measurement Technology Open Innovation Laboratory (OPERAN-DO-OIL), AIST, 3.Faculty of Science, Hokkaido University, 4.Department of Aerospace Engineering, Tohoku University, 5.Arctic Research Center, Hokkaido University, 6.Geological Survey of Japan, AIST)

[E] Poster | U (Union) : Union

📅 Fri. Jun 4, 2021 5:15 PM - 6:30 PM JST | Fri. Jun 4, 2021 8:15 AM - 9:30 AM UTC | 🏠 Ch.01_1

[U-08] Advancing SDGs through inclusive partnerships I: Strategic leadership

convener: Vincent Tong (University College London), Hidenroi Nakamura (Toyama Prefectural University), Mika Shimizu (Kyoto University), Fumiko Noguchi (United Nations University, Institute for the Advanced Study of Sustainability)



Sustainable Development Goals (SDGs) provide a comprehensive framework underpinning a wide range of interdisciplinary initiatives in Earth Sciences. With interconnected objectives and impact across natural, social and human sciences, partnerships between academics, students, citizens, industry, businesses and other stakeholders are critical to the success of these initiatives. How equity, diversity and inclusion (EDI) are valued and embedded in these partnerships therefore warrants reflection and critical examination - for empowering and benefiting all stakeholders. These considerations are all the more important given that many education and research initiatives on SDGs have strong values-driven elements. In this session, we examine the diverse forms of partnerships in the design, implementation and impact of SDGs initiatives. We invite presentations and discussions on how inclusion has played a part in developing and sustaining such partnerships - with a focus on the strategic and international leadership. We particularly welcome reflections on values-driven initiatives in different cultural contexts.

[U08-P01] A few points to be considered when we engaging with a local community for research and practice for sustainability

★Invited Papers

*Fumiko Noguchi¹ (1. United Nations University, Institute for the Advanced Study of Sustainability)

[U08-P02] Citizen dialogue-led environmental governance: Toward inclusiveness and culture of dialogue in post-Fukushima Japan

★Invited Papers

*Hidenroi Nakamura¹ (1. Toyama Prefectural University)

A few points to be considered when we engaging with a local community for research and practice for sustainability

*Fumiko Noguchi¹

1. United Nations University, Institute for the Advanced Study of Sustainability

Local community-based and multi-stakeholder approach are considered as essential in a research and practice for achieving sustainable development. This is because governmental policies and conference declarations can create the frame but local community is the only place where we can actually work on and change the things (Fien and Tilbury 2002). Also, many sustainability challenges root in multiple causes, which even are complexly twined. Diversity is required in search for the solution at local community level. People from different fields, sectors, generations, cultural and socio-economic and educational backgrounds should participate in search for the solution of challenges. They share their knowledges and experiences in that process, so that they co-create a new knowledge for making their community sustainable.

Then, how can be multi-stakeholder participation realised truly –not in a tokenism way but in a really inclusive way where everyone, including, the marginalised, has ownership, is empowered and controls over the decision making process? And what role should we, researchers, take there? In my presentation, I would like to look at a few examples of local community practice and discuss the key factors to make community engagement successful and a potential epistemological pitfall of ‘participatory approach’ when everybody is fully believing that they are taking a participatory approach.

Education for Sustainable Development (ESD), which is addressed in SDGs Target 4.7, is the interplay between the empowerment and participation of multi-stakeholders and their active collaboration and action for social transformation (UN, 2015). The role of ESD in SDGs is neither just one of the 17 Goals nor one of the 169 Targets. As clearly stated in ESD for 2030, which will be launched in 2021 and led by the United Nations Educational, Scientific and Cultural Organization (UNESCO), ESD is “an integral element of the SDGs on quality education and a key enabler of all the other SDGs” (UNESCO, 2019). ESD provides the framework for developing critical and contextualized understanding of the efforts for sustainable community development by raising questions on the inter-linkages and tensions among different SDGs (UNESCO, 2017).

ESD perspectives helps everyone including practitioner/researcher inside/outside education field to effectively articulate and tackle the sustainability problem, when they work with local community. At the same time, it is important for them to share their own ESD experience in diverse fields and sectors with the policy makers so that more supportive and effective policy can be developed for ESD beyond education field. Doing so is important, particularly now, when a national platform expected to be prepared by respective UNESCO Member State. Diverse voices to be heard and reflected in the policy making process for ESD for 2030.

Fien, J., and Tilbury, D. (2002). *The global challenge of sustainability*. In D. Tilbury, R. Stevenson, J. Fien, & D. Schreuder (Eds.), *Education and Sustainability - Responding to the Global Challenge*, IUCN, Switzerland and Cambridge. p.p.1-12.

UN. (2015). *Transforming our world: the 2030 Agenda for Sustainable Development (A/RES/70/1)*. United Nations.

UNESCO. (2017). *Education for Sustainable Development Goals: Learning Objectives*. Paris, France: UNESCO

UNESCO. (2019). *Framework for the Implementation of Education for Sustainable Development (ESD) beyond 2019 (40 C/23)*. Paris, France: UNESCO

Keywords: Multi-stakeholder partnership, Community empowerment and participation, Education for Sustainable Development (ESD)

Citizen dialogue-led environmental governance: Toward inclusiveness and culture of dialogue in post-Fukushima Japan

*Hidenroi Nakamura¹

1. Toyama Prefectural University

To promote inclusive environmental governance that is relevant to geoscience community, the author argues that institutionalization of citizen dialogue is a key. Based on an exploratory case study using the methods for polyphonic dialogue among citizens, and between citizens and experts, participatory deliberate policy process that leads to quality collective action was sought. Citizens are not necessarily the last, and experts are not necessarily the first, in collective decision making.

A random sampling-based citizen dialogue was held in Fukushima, Japan, regarding radioactive waste disposal and involving experts and citizens. Three proposed methods were manner of dialogue, evidence-based and position-explicit presentations by experts with differing views, and experts reflecting in tandem with citizens engaged in dialogue. Attitudes toward dialogue with others holding different views, as well as better internal self-deliberation, or dialogue within oneself, were measured.

Acknowledgement: This work was supported by the Collaboration Research Program of IDEAS, Chubu University (IDEAS202005).

References:

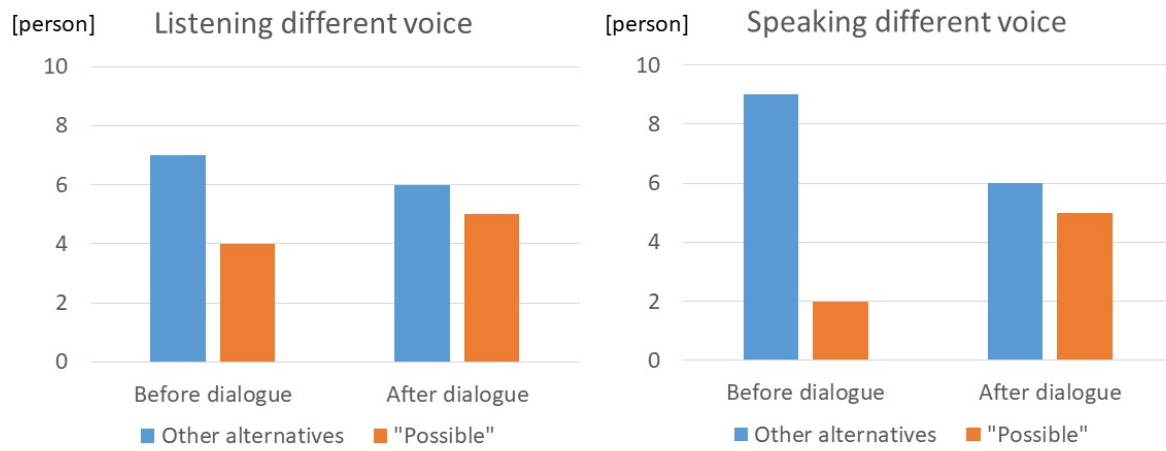
Nakamura, H., Ueno, F., Higashihara, H. *et al.* Toward Citizen Dialogue-led Environmental Governance: An Exploratory Case Study in Post-Fukushima Japan. *Environmental Management* (2021).
<https://doi.org/10.1007/s00267-021-01433-6> Available at: <https://rdcu.be/ce8aq>

Keywords: SDGs, deliberation, participation

Attitude for dialogue before and after participating in citizen dialogue event

(1) **Listening** to others with a view different from mine regarding social, national, or local issues, without denying it, if not accepting it.

(2) **Conveying** my own ideas to others who may have different ideas from mine, regarding social, national, or local issues.



Alternatives other than "Possible": "Difficult," "Difficult, if any," "Hard to say," and "Possible, if any"

[E] Poster | U (Union) : Union

📅 Fri. Jun 4, 2021 5:15 PM - 6:30 PM JST | Fri. Jun 4, 2021 8:15 AM - 9:30 AM UTC | 🏠 Ch.01_2

[U-10] What is the true value of Knowledge Creation? The Ideal and Reality of Research Evaluation.

convener: Michiyo SHIMAMURA (Japan Agency for Marine-Earth Science and Technology), Brooks Hanson (American Geophysical Union), Yasuhiro Yamanaka (Faculty of Environmental Earth Science, Hokkaido University), Kiyoshi Suyehiro (Japan Agency for Marine-Earth Science and Technology)



There is a wide range of research, from "research that responds to the obligations of society" to "research that responds to the intellectual curiosity of humankind," but in recent years, researchers have been required to be more accountable to society. How are the research community and funding agencies accountable for "social mandates"?

Amid growing social interest in climate variability and natural disasters, in 2020, the Japan Geoscience Union signed an international joint declaration on "the importance of geoscientific knowledge to address the challenges of global society." At the time of the JpGU2020 conference, convenors conducted a questionnaire to the JpGU members, and the interest in "research that responds to the mandate of society" stated in this declaration is less than the interest in "research that responds to the intellectual curiosity of humankind."

In this session, we invite the members of the geoscience research community to discuss "the connection between ideal science and our own community and society", and would like to promote mutual understanding of our diversity. Also, we would like to consider together about how researchers themselves can evaluate their research activities and create a culture that fulfills their accountability to society. To that end, it will consist of discussions by panelists based on reports of overseas cases and questionnaires.

[U10-P01] Researchers' perceptions of research and its evaluation: A comparison between the JpGU and AGU communities

*Yasuhiro Yamanaka¹, Michiyo SHIMAMURA², Kiyoshi Suyehiro², Brooks Hanson³ (1. Faculty of Environmental Earth Science, Hokkaido University, 2. Japan Agency Marine-Earth Science and Technology, 3. American Geophysical Union)

Researchers' perceptions of research and its evaluation: A comparison between the JpGU and AGU communities

*Yasuhiro Yamanaka¹, Michiyo SHIMAMURA², Kiyoshi Suyehiro², Brooks Hanson³

1. Faculty of Environmental Earth Science, Hokkaido University, 2. Japan Agency Marine-Earth Science and Technology, 3. American Geophysical Union

We could answer naive questions such as "What kind of research do you think is good?" and "Why do you get research funding?" based on our personal experiences. But we could not answer these questions based on the data as our research community's opinion. We have easily used quantifiable indicators such as the number of citations and journal impact factors (JIF) as evaluation indices, without any researchers' ideal and discussions. As a result, our own evaluation has been distorted. A situation is emerging where we can believe that if we were researchers who had papers with high evaluation indexes and our organization had many such researchers, the organizations and researchers would obtain more research funds allocated by the government (we call it "*the worship of papers*"). However, does such a situation equals contribution to society? Starting by questioning researchers' fundamental perceptions, the research community itself will need to create indicators to evaluate its own activities based on its own perceptions (creating Indicators of researchers for researchers by researchers) and to fulfill its accountability to society.

As a first step, to clarify the perceptions of the members of the earth science community, we notified about 6,000 JpGU members via the JpGU mailing list on June 11 and 28, 2020, and about 38,000 AGU members via the AGU mailing list on November 15 and 20, 2020, and received 292 (4.9%) and 883 (2.3%) valid responses, respectively. The results for the JpGU community were reported in the latest *Japan Geoscience Letters* (Yamanaka, 2021).

We asked respondents to rank the order in which they thought it was important for knowledge creation, for six items related to science in general, not just earth science, which consist of three sets of trade-offs: discovering vs. elaborating/systematizing (Set A), answering the intellectual curiosity of humanity vs. responding to the responsibilities of society (Set B), and emphasizing perfection vs. emphasizing timeliness (Set C) (Table 1). The JpGU and AGU communities are the same in terms of ranking 1 and 2 for discovery and curiosity and 5 and 6 for timeliness and perfection. But the JpGU community ranks lower in social responsibility than the AGU community in Set B and a similar ranking of timeliness and perfection in Set C.

Six questions were asked to contribute to the creation of knowledge in the earth sciences. These are the two commonly known items, "Elucidating the origin of the earth and planets" and "understanding the current state of the earth and planets," and the four items picked up from "Declaration of the Significance of Geoscience Expertise to Meet Global Societal Challenges," which JpGU signed on May 4, 2020, together with the European Geosciences Union (EGU), the American Geophysical Union (AGU), and others (Table 2). The JpGU community did not regard the four items mentioned in the Joint Declaration as contributing to knowledge creation as the two items, while the AGU community thought them to be about the same as the two items. In particular, in these four items, the significant difference is that 1/2 to 2/3 of the AGU community's doctoral degree recipients after 2015 and graduate students answered, "Strongly Agree," while 1/4 to 1/3 of the same age group in the JpGU community answered, "Strongly Agree."

However, when asked if they refer to the JIF during selecting papers to be included in the application of the research proposal, 40% of respondents in the JpGU community were concerned about it. In comparison, only 12% of respondents in the AGU community were worried about it. This may reflect differences in the quality and quantity of research applications.

Keywords: Institutional Research (IR), Impact Factor (IF), the worship of papers, creation of knowledge, ideals of science and researchers

Table 1

(2-1) Please put in order you think is "important" for the scientific knowledge creation

Rank	Set A		Set B		Set C	
	L	R	L	R	L	R
	Discovery	Elaboration / Synthesis	Responding to the responsibilities of society	Answering the intellectual curiosity of humanity	Timeliness	Perfection
AGU (n=883)						
1 st	464	88	138	171	4	10
2 nd	196	232	172	203	47	25
3 rd	118	228	177	193	109	50
4 th	60	191	209	145	195	75
5 th	26	101	117	117	388	126
6 th	11	35	62	46	132	589
JpGU (n=292)						
1 st	171	36	16	67	2	0
2 nd	68	88	32	85	6	13
3 rd	30	93	57	74	19	19
4 th	12	51	102	33	42	52
5 th	10	20	46	21	102	93
6 th	1	4	39	12	121	115

Table 2

(2-2) Do you think the following items are "Contributions of Earth and Planetary science" for the creation of scientific knowledge?

Picked up from "Declaration of the Significance of Geoscience Expertise To Meet Global Societal Challenges" signed by the EGU, AGU, JpGU with others on May 4, 2020.

	Elucidating the origin of the Earth and Planets	Understanding the current status of the Earth and Planets	Contributions of Earth and Planetary science			
			Promote interdisciplinary research in collaboration with other disciplines	Understanding, preserving and restoring the Earth and ecosystems	Devising strategies for sustainability of the Earth and humankind	Increasing social trust in science and returning knowledge to society
AGU (n=883)						
Strongly Agree	486	647	396	494	416	382
Agree	247	197	288	234	262	255
Somewhat Agree	110	33	168	106	130	178
Somewhat Disagree	23	4	17	32	40	31
Disagree	10	2	11	8	18	19
Strongly Disagree	7	0	3	9	17	18
JpGU (n=292)						
Strongly Agree	172	197	76	93	83	78
Agree	91	78	110	99	91	119
Somewhat Agree	20	14	85	72	76	74
Somewhat Disagree	3	0	12	20	31	14
Disagree	3	1	5	3	6	1
Strongly Disagree	3	2	4	5	5	6

[E] Poster | U (Union) : Union

📅 Fri. Jun 4, 2021 5:15 PM - 6:30 PM JST | Fri. Jun 4, 2021 8:15 AM - 9:30 AM UTC | 🏠 Ch.01_3

[U-11] Diversity and equality - Where do we stand on gender equality or equity in the geosciences?

convener: Rie Hori, S. (Department of Earth Science, Faculty of Science, Ehime University), Chiaki T. Oguchi (Institute for Environmental Science and Technology, Graduate School of Science and Engineering, Saitama University), Claudia Jesus-Rydin (European Research Council), Eiichi Tajika (Department of Earth and Planetary Science, Graduate School of Science, The University of Tokyo)



In the last decades efforts have been made to raise awareness on the underrepresentation of women in the geosciences. Numerous actions were initiated and supported by geosciences societies across the world, such as AGU, EGU and JpGU. Despite this, the progress is slow and the barriers complex, and the underrepresentation of women remains a reality.

Gender equality is not only a fundamental human right, but a necessary foundation for our society that must tap the potential of every talented mind to develop solutions for a sustainable future. The existence of under-representation of different groups (cultural, national, and gender) remains a reality and a threat to getting maximal value from research investment across STEM fields around the world, including the geosciences.

Professional societies have a privileged position to catalyse change by setting the tone and leading by example. Promoting fairness and inclusion, in a safe environment, to all members are common goals, which require effective concerted actions. In this session, speakers will present and discuss data showing the evolution of women representation retrospectively. Furthermore, concrete examples of successful actions and future initiatives to bridge the gender gap in the geosciences are presented.

[U11-P01] An action guideline and the activity of the Women for One Ocean, Japan

*Natsue Abe^{1,2}, Kaoru Kubokawa³, Women for One Ocean (1. Mantle Drilling Promotion Office, MarE3, Japan Agency for Marine-Earth Science and Technology, 2. Graduate School of Natural Science & Technology, Kanazawa University, 3. Teikyo University)

An action guideline and the activity of the Women for One Ocean, Japan

*Natsue Abe^{1,2}, Kaoru Kubokawa³, Women for One Ocean

1. Mantle Drilling Promotion Office, MarE3, Japan Agency for Marine-Earth Science and Technology, 2. Graduate School of Natural Science & Technology, Kanazawa University, 3. Teikyo University

Women for One Ocean is a networking mechanism based on the Ocean Alliance Initiative, University of Tokyo, which was a research project for the development of a network of women in Ocean-related research and industries. The purpose of our activities is; 1) Increase the proportion of women in the ocean-related research and industries, and women in managerial positions, 2) Develop policy recommendations. Since April 2018, we have been holding a video meeting once a month to exchange information before COVID-19 became pandemic. This style makes it easy for people to join in from home or in remote locations around the world. We also disseminate opinions via booklets, homepage and SNS, have class visits, science schools, and local communities, progress SDGs achievements (eg., 5 and 14). In 2021, the UN Decade of Marine Science for Sustainable Development will begin. As mentioned in the SDGs, sustainable development requires diverse perspectives. It is expected that women will play an increasingly important role in the area of ocean science.

We are aiming for realizing a sustainable society and the marine environment. We are going to set up our action goals in the extended meeting in March 2020 in Tokyo. The action goals will include; 1) the ratio of women, 2) female leaders, 3) continuation of career, support towards child care and education, 4) research collaboration in ocean sciences, 5) policy recommendation for ocean policy, and more active roles of women in the society. In order to continue the network, we need to consider members' needs of support, taking turns to MC the monthly web meetings, build experience in voicing opinions, making recommendations, drafting public documents, taking turns to rapporteur the web meetings. We also encourage students' participation and independent activities and exchange with international networks.

Keywords: Women for One Ocean, the UN Decade of Marine Science for Sustainable Development, SDGs

[E] Poster | U (Union) : Union

📅 Fri. Jun 4, 2021 5:15 PM - 6:30 PM JST | Fri. Jun 4, 2021 8:15 AM - 9:30 AM UTC | 🏠 Ch.01_4

[U-12] From Hazard to Resilience

convener:Naoshi Hirata(National Research Institute for Earth Science and Disaster Resilience), Keiko Tamura(Risk Management Office, Niigata University), Matt Gerstenberger(GNS Science), Danijel Schorlemmer(GFZ German Research Centre for Geosciences)

Natural hazards continue to be a challenge to societies around the world with many impacted by multiple types of hazards. To reduce the impact of these hazards we must not only quantify the hazard and risk associated with multi-hazard events, but we must also understand the associated uncertainty(e.g., ISO 31000 defines risk as the effect of uncertainty on objectives). Resilience can only be improved by considering all of these factors. Multi-hazard and risk modeling approaches are receiving increasing attention globally, however, the challenges of assessing uncertainty in both single- and multi-hazard risks are considerable. Without a clear understanding of the risks and their uncertainties, difficult decisions related to risk mitigation and increasing resilience are incompletely informed.

In this session we will discuss research at the confluence of hazard and risk assessment and their societal uptake. This includes hazard/risk modeling, methods for their use in decision making, and their communication. We solicit presentations on a wide range of topics related to questions such as: What are the latest developments in single- and multi- hazard and risk models? What uncertainties are the most critical for decision making? How can they be identified, quantified and reduced? How can hazards, risks and their uncertainties be communicated to the public and stakeholders in a comprehensible, trustworthy and actionable way? Can artificial intelligence and machine learning fill the uncertainty gap? What is the role of smart cities in helping mitigate risks? What are recent experiences in bringing hazard and risk information into policy and decision making?

We hope for stimulating discussions highlighting the international diversity in approaches. We invite scientists from physical science, engineering and social science, communicators, governmental decision makers, practitioners, and stakeholders to join this session.

[U12-P01] Interdisciplinary and industry-academia collaboration research for resilient society in the Tokyo metropolitan area, DEKATSU Activity

*Takashi Furuya¹, Keiko Tamura², Danijel Schorlemmer³, Naoshi Hirata¹ (1.National Research Institute for Earth Science and Disaster Resilience, 2.Niigata University, Risk Management Office, 3.GFZ German Research Center for Geosciences)

Interdisciplinary and industry–academia collaboration research for resilient society in the Tokyo metropolitan area, DEKATSU Activity

*Takashi Furuya¹, Keiko Tamura², Danijel Schorlemmer³, Naoshi Hirata¹

1. National Research Institute for Earth Science and Disaster Resilience, 2. Niigata University, Risk Management Office, 3. GFZ German Research Center for Geosciences

In 2007, we initiated a 5-year-research project named the “Tokyo Metropolitan Resilience Project.” This project is intended to improve the resilience to natural disasters, particularly earthquakes, in the Tokyo metropolitan area. For this purpose, we have organized multi-disciplinary research including social sciences, natural sciences such as seismology, and civil engineering, with a focus on earthquake engineering. In addition, we facilitate mutual communication between industry and academia. We established the “Data Use and Application Council for Resilience” (Japanese abbreviation: DEKATSU) to organize private and public stakeholders. The DEKATSU council consists of four sectors: industry, government, NPO/NGOs, and academia. To date, 73 organizational members and 15 personal members have joined, and the targeted idea is becoming accepted but not fully implemented in society. We have organized seven thematic panels to discuss specific problems in-depth by organizing closed meetings of the DEKATSU member companies and academic researchers. We need a long-term collaboration system for creating shared values in society for social resilience to disasters.

Keywords: Disaster Resilience, integrated multi-disciplinary research, Data Use and Application Council for Resilience (“DEKATSU”), Industry-Government-Academia-Private Linkage, Tokyo Metropolitan area

[E] Poster | P (Space and Planetary Sciences) : P-PS Planetary Sciences

📅 Fri. Jun 4, 2021 5:15 PM - 6:30 PM JST | Fri. Jun 4, 2021 8:15 AM - 9:30 AM UTC | 🏠 Ch.02_1

[P-PS01] Outer Solar System Exploration Today, and Tomorrow

convener: Jun Kimura (Osaka University), M. Kunio Sayanagi (Hampton University), Fuminori Tsuchiya (Planetary Plasma and Atmospheric Research Center, Graduate School of Science, Tohoku University), Cindy Young (NASA Langley Research Center)



The giant planets provide many keys to understanding planetary processes. They play an important role in shaping our solar system, and the physical and chemical processes they harbor also provide a unique opportunity to study the phenomena relevant for studying Earth and other planets, including exoplanetary systems. In this session, we discuss a wide range of topics encompassing the giant planets and their moons, including their origins, interiors, atmospheres, compositions, surface features, and electromagnetic fields. To advocate for current and future outer planets exploration (Juno, New Horizons, JUICE, Europa Clipper, Dragonfly and beyond), we also call for discussions on future missions to explore giant planet systems, including how to develop better international cooperation. Discussion in this latter category will include progress in developing a solar sail mission concept for observing the Jupiter system and its Trojan asteroids.

[PPS01-P01] Estimation of apparent areas of Earth-orbiting UV telescope required to detect water plumes on icy moons

*Ryoichi Koga¹, Fuminori Tsuchiya², Go Murakami³, Shotaro Sakai² (1.Nagoya University, 2.Tohoku University, 3.ISAS/JAXA)

[PPS01-P02] Quantitative analysis of hot electron density variation during transient brightening in the Io plasma torus observed by Hisaki/EXCEED

*Kento Furukawa¹, Fuminori Tsuchiya¹, Kazuo Yoshioka², Reina Hikida³, Tomoki Kimura¹, Masato Kagitani¹, Go Murakami³, Atsushi Yamazaki³, Hajime Kita⁴, Ichiro Yoshikawa² (1.Tohoku University, 2.the University of Tokyo, 3.JAXA, 4.Tohoku Institute of Technology)

[PPS01-P03] Expected source regions of Jupiter's hectometric radio components viewed from their polarization characteristics

*Hiroaki Misawa¹, Fuminori Tsuchiya¹, Atsushi Kumamoto², Yoshiya Kasahara³, Yoshizumi Miyoshi⁴, Masahiro Kitahara⁴, Satoko Nakamura⁴ (1.PPARC, Graduate School of Science, Tohoku University, 2.Department of Geophysics, Graduate School of Science, Tohoku University, 3.ARC-SAT, Kanazawa University, 4.ISEE, Nagoya University)

[PPS01-P04] New magnetic field and current sheet models of the night-side Jovian magnetosphere and their long-term variations

*Naoya Momoki¹, Hiroaki TOH² (1.Division of Earth and Planetary Sciences, Graduate School of Science, Kyoto University, 2.Data Analysis Center for Geomagnetism and Space Magnetism, Graduate School of Science, Kyoto University)

[PPS01-P05] Exploring the roof of Jovian atmosphere by large and small groundbased telescopes in visible and infrared light

*Yasumasa Kasaba¹, Takeshi Sakanoi¹, Masato Kagitani¹, Hajime Kita² (1.Planetary Plasma and Atmospheric Research Center, Tohoku University, 2.Tohoku Institute of Technology)

[PPS01-P06] Jupiter Icy Moons Explorer JUICE: Science perspectives from planetary formation and geochemistry of the JUICE Japan team

*Yasuhito Sekine¹, Yoshifumi Saito², Kazushi Asamura², Keigo Enya², YASUKO KASAI⁴, Yasumasa Kasaba³, Junichi Haruyama², Ayako Matsuoka⁵ (1.Earth-Life Science Institute, Tokyo Institute of Technology, 2.ISAS, JAXA, 3.Tohoku University, 4.NICT, 5.Kyoto University)

[PPS01-P07] Numerical simulation of the passive subsurface radar for Jupiter's icy moons

*Tomoki Kimura¹, Rikuto Yasuda¹, Fuminori Tsuchiya¹, Atsushi Kumamoto¹, Hiroaki Misawa¹, Yasumasa Kasaba¹ (1.Tohoku U.)

[PPS01-P08] Numerical radar simulation for the explorations of the ionosphere and plume at Jupiter's icy moons

*Rikuto Yasuda¹, Tomoki Kimura¹, Hiroaki Misawa¹, Fuminori Tsuchiya¹, Atsushi Kumamoto¹, Yasumasa Kasaba¹ (1.TOHOKU UNIVERSITY)

[PPS01-P09] Performance, Operation and their Feasibilities for Jupiter and Icy Moons: High Frequency Receiver of Radio & Plasma Wave Investigation (RPWI) aboard JUICE during the Flight Model Test campaign

*Yasumasa Kasaba¹, Hiroaki Misawa¹, Fuminori Tsuchiya¹, Tomoki Kimura¹, Hajime Kita², Atsushi Kumamoto¹, Yuto Katoh¹, Yoshizumi Miyoshi³, Yoshiya Kasahara⁴, Satoshi Yagitani⁴, Hirotsugu Kojima⁵, Baptiste Cecconi⁶ (1.Tohoku University, 2.Tohoku Institute of Technology, 3.Nagoya University, 4.Kanazawa University, 5.Kyoto University, 6.Obs. de Paris)

Estimation of apparent areas of Earth-orbiting UV telescope required to detect water plumes on icy moons

*Ryoichi Koga¹, Fuminori Tsuchiya², Go Murakami³, Shotaro Sakai²

1. Nagoya University, 2. Tohoku University, 3. ISAS/JAXA

In this study, we estimated the apparent areas of Earth-orbiting UV space telescope, which can detect OI and HI emissions ejected from plumes on icy moons. Hubble Space Telescope observed the enhancement of HI 121.6 nm and OI 130.4 nm emissions near the Europa South Pole (Roth et al., 2014). They considered the electron impact of H₂O in the plume yields HI and OI UV emissions. However, frequency and geological conditions of ejecting gasses from Europa plumes are not understood. LOPYUTA (Life-environmentology, Astronomy, and Planetary Ultraviolet Telescope Assembly) is the future Earth-orbiting UV telescope project. One of the main goals of LOPYUTA is to observe icy moon's atmosphere continuously with high spatial resolution (~ 0.1 arcsec) and apparent area (~ 350 cm²), and confine conditions under which the plume eruptions occur.

To validate science feasibility of LOPYUTA, we considered the demand to detect the Europa plume by UV space telescope with integration time of 10 hours. We calculated the signal counts of OI 130.4 nm and HI 121.6 nm from Europa plume, and the noise from Europa atmosphere, solar reflection, Earth geocorona and interplanetary medium. The emission due to solar reflection at the limb is estimated to be several percentages of that at the center of the disk. Therefore, the setting of the plume position in this study is near the limb. The satellite should orbit under $\sim 1,000$ km or over $\sim 36,000$ km from the Earth ground to avoid the noise from the radiation belt. To detect both OI 130.4 nm and HI 121.6 nm emissions, requested apparent areas are ~ 350 cm² when the altitude of the satellite is about 1,000 km, and ~ 160 cm² when the altitude is 36,000 km, which meet the demand of the project. This presentation will also discuss the detectability of plumes of icy moons such as Enceladus.

Keywords: Europa, UV

Quantitative analysis of hot electron density variation during transient brightening in the Io plasma torus observed by Hisaki/EXCEED

*Kento Furukawa¹, Fuminori Tsuchiya¹, Kazuo Yoshioka², Reina Hikida³, Tomoki Kimura¹, Masato Kagitani¹, Go Murakami³, Atsushi Yamazaki³, Hajime Kita⁴, Ichiro Yoshikawa²

1. Tohoku University, 2. the University of Tokyo, 3. JAXA, 4. Tohoku Institute of Technology

The Hisaki satellite observed transient increases in the extreme ultraviolet (EUV) emission from Io Plasma Torus (IPT) by ~10% over a period of ~10 hours, a few hours after a transient variation in Jupiter's UV auroral emission. It has been assumed that it is difficult to transport energy in radial direction with the short time scale since plasma co-rotation in the azimuth direction is dominant in the Jupiter magnetosphere. The transient brightening of the IPT and the aurora suggests that the effects of transient energy release in the magnetosphere which causes auroral brightening could extend to the IPT on a time scale of ~10 hours. Considering that the relaxation time of hot electrons with energy of several hundred eV in the IPT (electron density of about 2000/cc, electron temperature of about 5 eV) due to Coulomb collisions is comparable to the time scale of the brightening, previous studies interpreted the cause of brightening as the influx of hot electrons into the IPT from outside the Jupiter magnetosphere.^{[1][2]} On the other hand, the increase of hot electron density in the IPT has not been quantitatively investigated during the IPT brightening. The purpose of this study is to determine the time variation of hot electron density in the IPT quantitatively from EUV spectra during the brightening, and to clarify the contribution of hot electrons to the energy transport process in Jupiter's inner magnetosphere. To derive variations in electron temperature, electron density, and ion mixing ratio in the IPT from the UV spectra observed by Hisaki/EXCEED, we applied plasma diagnosis analysis^{[3][4]} to the EUV spectral data of IPT observed with the 140 arcsec slit. Sulfur and oxygen ions in the IPT emit ultraviolet emission by electron collision excitation. Plasma diagnosis is a method to derive electron temperature, electron density, and ion composition from spectral data containing several sulfur and oxygen ion emission lines. To analyze the strong IPT brightening events occurred on DOY 66 and 87 in 2015, we chose the data from the period DOY 65-90 in 2015. In this presentation, we will derive plasma fluctuations at 3-hour intervals to capture the variations in the IPT during the transient brightening and discuss quantitative results of the increase in hot electrons during the IPT brightening and the contribution of hot electrons to the energy transport process.

[1] Yoshikawa et al.(2017). Earth, Planets and Space, 69(1), 110.

<https://doi.org/10.1186/s40623-017-0700-9>

[2] Suzuki et al. (2018). J. Geophys. Res.: Space Physics, 123, 9420-9429.

[3] Yoshioka et al. (2014). Science, 345(6204), 1581-1584. <https://doi.org/10.1126/science.1256259>

[4] Hikida et al. (2020). J. Geophys. Res.: Space Physi, 125, e2019JA027100.

<https://doi.org/10.1029/2019JA027100>

Keywords: Jupiter, Io plasma torus, Hisaki satellite

Expected source regions of Jupiter's hectometric radio components viewed from their polarization characteristics

*Hiroaki Misawa¹, Fuminori Tsuchiya¹, Atsushi Kumamoto², Yoshiya Kasahara³, Yoshizumi Miyoshi⁴, Masahiro Kitahara⁴, Satoko Nakamura⁴

1. PPARC, Graduate School of Science, Tohoku University, 2. Department of Geophysics, Graduate School of Science, Tohoku University, 3. ARC-SAT, Kanazawa University, 4. ISEE, Nagoya University

It has been known that Jupiter's auroral radio emission in the hectometric wave range (HOM) is roughly classified into two type occurrence components. One is a component relating to solar wind variations (sw(solar wind)-HOM) appearing around CML (Central Meridian Longitude of an observer) ~ 180 deg when solar wind pressure enhances. The other one is generally more intense than sw-HOM and has no or weak relation with solar wind variations (nsw(non sw)-HOM) appearing around CML ~ 110 deg and ~ 280 deg (the 1st and 2nd nsw-HOM, respectively) when De (Jovicentric declination of an observer) ~ -1 deg (Nakagawa et al., 2000; Nakagawa, 2003). Recently, we found one more nsw-HOM component appearing around CML ~ 340 deg (the 3rd nsw-HOM), which highly correlates occurrence of magnetic reconnection events in Jupiter's magnetotail region (Misawa et al., 2018). This component is an important role for the studies of global magnetospheric dynamics of Jupiter since it is a possible remote marker of the reconnection events occurring in Jupiter's magnetosphere. However, due to difficulty in precise direction finding in the hectometric wave range, the radio source of this component (and also those of the other components), that is, location of transported energy input should be originated from the tail region, has been still unrevealed.

In order to investigate source location of each HOM component we have made their polarization analyses using the data provided by High Frequency Analyzer (HFA) which is a subsystem of Plasma Wave Experiment (PWE) onboard the Arase (ERG) spacecraft. Preliminary analyses show that the 3rd nsw-HOM is left-handed circular polarization. The result suggests that the 3rd nsw-HOM is radiated from the southern hemisphere by taking account of Jupiter's magnetic polarity. In the presentation, we will discuss possible sources of the 3rd nsw-HOM based the polarization analyses by comparing the expected observable rays calculated from Jupiter's magnetic field models, and will also show polarization characteristics and expected source regions of the other HOM components.

Keywords: Jupiter, hectometric radiation, polarization, source region

New magnetic field and current sheet models of the night-side Jovian magnetosphere and their long-term variations

*Naoya Momoki¹, Hiroaki TOH²

1. Division of Earth and Planetary Sciences, Graduate School of Science, Kyoto University, 2. Data Analysis Center for Geomagnetism and Space Magnetism, Graduate School of Science, Kyoto University

In the night side of the Jovian magnetosphere, there exists a sheet-like plasma-rich region, so-called the current sheet (CS), and its shape is variable with the oscillation of the Jovian intrinsic magnetic field, solar wind conditions, and so on. The CS generates a magnetic field by the currents flowing within itself, which is comparable with the Jovian internal field and dominant in the night-side magnetosphere.

The shape of CS and the magnetic field have been modeled since Pioneer 10 observed the Jovian magnetosphere for the first time. However, those models have not sufficiently been updated with newly added data by Galileo and Juno. In this study, we focused on a CS shape model by Khurana (1992) and a magnetic field model by Khurana (1997) and updated these models with new data and methods. Furthermore, we estimated the errors of parameters of the magnetic field model and found that several parameters show significant long-term variations exceeding the error estimates.

The shape of CS is represented as an oscillating surface according to Jovian rotation with the following characteristics: (i) westward bendbacks of magnetic lines of force originating from the finite velocity of the oscillation propagation, and (ii) hinge (saturation of CS height) stemming from the solar wind dynamic pressure. As results of the model updates by this study, we found the weak bendback in the Galileo model, which implies that the average Alfvén velocity in the magnetosphere was strengthened in the Galileo mission period. We also found the weakened hinge effect in the Juno model. This is possibly related to the weakened solar wind dynamic pressure during the solar minimum.

The model of the magnetic field by the CS is expressed with two scalars called Euler potentials and depend on the shape of CS. Our updated Euler potential models explained the observed magnetic field well and we found that the values of the model parameters are dependent on the used data. In addition, we estimated the errors of the Euler potential parameters using resolutions of the magnetic measurements as threshold and found that several parameters changed significantly over decades beyond the error bars. It is possible that the major causes of the changes in the Jovian magnetospheric magnetic field are either solar activity or the amount of electric current in the CS. Comparison among the updated models implied the long-term variation related to the former, with no clear evidence of the latter. Namely, the amount of electric current in the CS significantly decreased in the Galileo mission period.

Our updated models enable us to predict the magnetic field that the forthcoming spacecrafts will observe, to calculate the current density by the CS, and to estimate the time-varying magnetic field at each Galilean satellite. The surfaces of Europa, Ganymede and Calisto are all covered with ice and thought to have subsurface oceans. Our methods and results are expected to be utilized when the new data by Europa Clipper and JUICE are analyzed to detect the subsurface oceans by electromagnetic induction methods.

Keywords: Jupiter, magnetospheric magnetic field, current sheet, long-term variation

Exploring the roof of Jovian atmosphere by large and small groundbased telescopes in visible and infrared light

*Yasumasa Kasaba¹, Takeshi Sakanoi¹, Masato Kagitani¹, Hajime Kita²

1. Planetary Plasma and Atmospheric Research Center, Tohoku University, 2. Tohoku Institute of Technology

Planets do not have their roofs. Their atmospheres are unstable area connected to outer space. This report summarizes our recent observations of this region on Jupiter, by large-sized (8-m class) telescopes and our Tohoku University small-sized telescopes in visible and infrared. There are several targets, (1) the emission from the stratosphere seen in mid-infrared, (2) the emission from the thermosphere and ionosphere seen in near-infrared, and (3) the emission from the magnetosphere filled with Io materials seen in visible light. Those have provided the support activity combined with the Juno orbiter and JAXA Hisaki UV/EUV telescope, linked to the vertical couplings by diffusions, atmospheric waves, and magnetic field.

For (1), variation of hydrocarbons in the stratosphere is seen. High-energy particles that produce H₂ emission in the polar cap can penetrate into the stratosphere. Up to this region, CH₄ rises from the lower layer, and high-energy particles create more complex hydrocarbon molecules. These C_xH_y molecules have a lot of absorption and emission in the mid IR. This range has been covered by Subaru COMICS mid-infrared imaging spectrometer, which was closed at the end of July 2020.

For (2), Jupiter's intense magnetic field captures electrons and ions with orders of magnitude and energy higher than Earth. These enter into the thermosphere (altitude: ~200-1000s km), hit and heat the dilute atmosphere, producing strong aurora emissions. On the dayside seen from the earth, this emission is buried in the cloud reflection light. However, in UV and near IR light, the reflection light is suppressed by the CH₄ absorption in the stratosphere (altitude: <~200 km), and thermospheric emission can be seen. In near IR, H₃⁺ emission is evident. This range has been covered by Subaru IRCS near-infrared imaging spectrometer and mid-large sized telescopes. Metallic ions can also contribute to the conductivity in this region, and it could be the next target for this wavelength range.

For (3), with UV/EUV range observed by Hisaki, Tohoku University's 40-cm (T40) and 60-cm (T60) telescopes at Mt. Haleakala (Hawaii) have provided the support information in the visible range. It can provide the Na neutral cloud which is from the Io volcanic activities. It is not trapped by magnetic field, and distributed in very wide places. It is suitable to be monitored by small-sized telescopes and we have used this data as the index of Io volcanic activities. Sulfic ion lines are confined in the Io torus region and can provide the energetic information with Hisaki.

In 2021 and later, we have plan to modify our Haleakala telescopes. (a) To closure of T-40 and to shift this function to T-60, and (b) To start the near-infrared observation by T-60. The construction activity of the 1.8-m PLANETS telescope (a collaborated project of Tohoku University with Nagoya and Kyoto Universities in Japan, University of Hawaii, Germany, and Brasil) will also be reported.

Keywords: Jupiter, Infrared, Visible

Jupiter Icy Moons Explorer JUICE: Science perspectives from planetary formation and geochemistry of the JUICE Japan team

*Yasuhito Sekine¹, Yoshifumi Saito², Kazushi Asamura², Keigo Enya², YASUKO KASAI⁴, Yasumasa Kasaba³, Junichi Haruyama², Ayako Matsuoka⁵

1. Earth-Life Science Institute, Tokyo Institute of Technology, 2. ISAS, JAXA, 3. Tohoku University, 4. NICT, 5. Kyoto University

Jupiter ICy moons Explorer JUICE is ESA's first L-class mission to explore Jupiter and its satellites. Japan will also participate as a junior partner. In this paper, we discuss the roles of the JUICE-Japan science team in the whole of the JUICE mission. In particular, we focus on collaborative studies with researchers who study planetary formation theory and planetary geochemistry in Japan. The aim of this paper is to share the importances of the future observations by JUICE and potential issues for the interdisciplinary collaborations.

Keywords: Jupiter, icy moons, planetary exploration

Numerical simulation of the passive subsurface radar for Jupiter's icy moons

*Tomoki Kimura¹, Rikuto Yasuda¹, Fuminori Tsuchiya¹, Atsushi Kumamoto¹, Hiroaki Misawa¹, Yasumasa Kasaba¹

1. Tohoku U.

The subsurface ocean at icy bodies in our solar system is one of the most likely habitable environments except for Earth. While the subsurface ocean of Enceladus at Saturn has been already demonstrated with the Cassini explorer, it is still unclear that Europa and Ganymede at Jupiter have it although they are theoretically predicted to have greater amount of liquid water than Earth. The highest priority is placed on detections of the subsurface ocean and related water plume activities at Jupiter's icy moons in the Jupiter Icy Moon Exploration mission JUICE, which is going to start exploration in early 2030s. Here we numerically simulate the passive subsurface radar PSSR for the icy moon's ocean that is going to be observationally made by receiving Jupiter's auroral radio emissions with the radio and plasma wave instrument RPWI onboard JUICE. Based on the ray tracing method, we simulate propagation of Jupiter's radio emission in the icy moon's water plume, tenuous ionosphere, and interior assuming the plasma density and dielectric constant structures. The simulation indicated that some of the structures are clearly detectable by PSSR if the incident radio emission forms chirpy waveform packets at HF frequencies.

Keywords: icy moon, jupiter, radar, subsurface ocean

Numerical radar simulation for the explorations of the ionosphere and plume at Jupiter's icy moons

*Rikuto Yasuda¹, Tomoki Kimura¹, Hiroaki Misawa¹, Fuminori Tsuchiya¹, Atsushi Kumamoto¹, Yasumasa Kasaba¹

1. TOHOKU UNIVERSITY

Jupiter's icy moons such as Europa and Ganymede may harbor subsurface liquid water oceans and have ionospheres and plumes created from the water oceanic materials. While only Earth has the ocean on the surface in our solar system, multiple icy bodies like the icy moons of giant planets have subsurface oceans. The icy body's ocean is potentially more universal habitable environment than the Earth-type surface ocean. Evolution of the subsurface ocean is the most important problem for understanding of the universality of habitable environment. Current structures of the ocean, ionosphere, and plume of the icy moon are essential information for the evolution. In-situ observation of surface and interior with landers is the most effective method for estimation of the structures. However, the structures have been unknown because the lander exploration is still in the technically conceptual level at present. Here we are going to uncover the structures of the oceans, ionospheres, and plumes of Jupiter's icy moons by the radar exploration with the Radio & Plasma Wave Investigation (RPWI) and the Radar for Icy Moon Exploration (RIME) onboard the JUpiter ICy moons Explorer (JUICE) launched in 2022. We are now developing the numerical simulation code for the radar explorations with RPWI and RIME that model propagation of electromagnetic (EM) wave in the ionospheres and plumes of the icy moons. From our preliminary simulations, we confirmed that rays of the EM wave are significantly refracted in the ionosphere and plume with dependences on their frequencies. This result demonstrates that the structures of ionospheres and plumes are detectable with the JUICE instruments. We are going to simulate reflection and transmission of the EM waves in the ice crust and underlying ocean to explore their structures. After completion of this study, we will be able to estimate the structures of icy moons by combining our model with the JUICE radar explorations. The combination will constrain pressure and temperature of the subsurface ocean as well as the structures, which finally lead to deep understanding of the icy moon's habitability.

Keywords: icy moon, Jupiter, radar, JUICE

Performance, Operation and their Feasibilities for Jupiter and Icy Moons: High Frequency Receiver of Radio & Plasma Wave Investigation (RPWI) aboard JUICE during the Flight Model Test campaign

*Yasumasa Kasaba¹, Hiroaki Misawa¹, Fuminori Tsuchiya¹, Tomoki Kimura¹, Hajime Kita², Atsushi Kumamoto¹, Yuto Katoh¹, Yoshizumi Miyoshi³, Yoshiya Kasahara⁴, Satoshi Yagitani⁴, Hirotsugu Kojima⁵, Baptiste Cecconi⁶

1. Tohoku University, 2. Tohoku Institute of Technology, 3. Nagoya University, 4. Kanazawa University, 5. Kyoto University, 6. Obs. de Paris

Flight models of Radio & Plasma Wave Investigation (RPWI) aboard the ESA JUICE mission were joined to the flight model test going in Europe, and is going toward the launch in mid 2022. RPWI provides an elaborate suite for electromagnetic fields and plasma environment around Jupiter and icy moons, with 4 Langmuir probes (LP-PWI; 3-axis E-field up to 1.6 MHz, and cold plasmas), a search coil magnetometer (SCM; 3-axis B-field up to 20 kHz), and a tri-dipole antenna system (RWI; 3-axis E-field 0.08-45 MHz, 2.5-m tip-to-tip length).

In the final test campaign, we have confirmed that RWI with High Frequency (HF) Receiver have enough sensitivity reaching the galactic background for the highly-resolved Jovian radio emissions from magnetosphere (aurora etc.), atmosphere (lightning), and icy moons. Its direction and polarization capabilities enable us to identify the source locations and characteristics. Their developments are under the collaboration of Japan, France, Poland and Sweden.

In this paper, we provide the performance and operation concepts with their feasibilities, including the test and emulation results on the ground, planned activities in commissioning and cruise phases, and the full observations around Jupiter and icy moon system. One of the most key parts is the sensing of the ionospheres, surface, and subsurface of icy moons during the flybys and on the orbit around Ganymede. The ionospheres under the spacecraft can be remotely sensed by the occultation (and reflection) of Jovian radio signals, which has a capability to detect the highest ionospheric density in usual status and expected plume ejection events. The surface and subsurfaces are challenging topics. It is based on the passive subsurface radar (PSSR) concept which sounds the icy crusts of Galilean satellites by the reflections of Jovian radio emissions (HOM/DAM). We are looking forward to see real data and support the JUICE studies with RPWI and other payload team members.

In this paper, we will show the recent performance evaluations and operation plans which are rapidly going in the team and JUICE Science Working Team.

Keywords: Jupiter, JUICE, Radio & Plasma Wave Investigation (RPWI)

[E] Poster | P (Space and Planetary Sciences) : P-EM Solar-Terrestrial Sciences, Space Electromagnetism & Space Environment

📅 Fri. Jun 4, 2021 5:15 PM - 6:30 PM JST | Fri. Jun 4, 2021 8:15 AM - 9:30 AM UTC | 🏠 Ch.04_1

[P-EM11] Coupling Processes in the Atmosphere-Ionosphere System

convener:Huixin Liu(Earth and Planetary Science Division, Kyushu University SERC, Kyushu University), Loren Chang(Institute of Space Science, National Central University), Yuichi Otsuka(Institute for Space-Earth Environmental Research, Nagoya University), Yue Deng(University of Texas at Arlington)

The Atmosphere-Ionosphere (A-I) system forms the so-called near-Earth space. Recent rapidly expanding use of satellite constellations in Low-Earth Orbit (LEO) drives a high demand for better understanding and accurate forecast of the global A-I system for scientific and operational purposes. This session aims to provide a forum for research advances and frontiers related to these aspects, and we invite presentations on global A-I coupling at all temporal and spatial scales. This includes but is not limited to: A-I coupling via atmospheric waves (tides, gravity waves, planetary waves) and trace gases (CO₂, O₃, H₂O), A-I response to Space Weather events (solar flares, CMEs, CIRs), polar-equatorial or inter-hemispheric coupling via TADs/TIDs/disturbance dynamo/penetration electric field, ionospheric plasma irregularities, ionospheric currents, etc. Observations, theoretical studies, model simulations, data assimilation, instruments development are all highly welcome.

[PEM11-P01] Year-to-year variation in polar mesospheric clouds observed by geostationary earth orbit satellite, Himawari

*Beng Aun Peh¹, Takuo T. Tsuda¹, Hidehiko Suzuki², Yuta Hozumi¹, Yoshiaki Ando¹, Keisuke Hosokawa¹, Takuji Nakamura³, Ken T. Murata⁴ (1.The University of Electro-Communications, 2.Meiji University, 3.National Institute of Polar Research, 4.National Institute of Information and Communications Technology)

[PEM11-P02] Analysis of vertical profiles of ionospheric disturbances caused by the tsunami associated with the Tohoku earthquake using GPS occultation observation

*Ryosuke Fushimi¹, Hiroyuki Nakata², Hiroyo Ohya² (1.Graduate School of Science and Engineering, Chiba University, 2.Graduate School of Engineering, Chiba University)

[PEM11-P03] Imaging observation of Ionospheric Field Aligned Irregularities by the PANSY radar at Antarctic Syowa Station

*Daisuke Kagawa¹, Taishi Hashimoto², Akinori Saito¹, Koji Nishimura², Masaki Tsutsumi², Toru Sato³, Kaoru Sato⁴ (1.Graduate School of Science, Kyoto University, 2.National Institute of Polar Research, 3.Graduate School of Informatics, Kyoto University, 4.Graduate School of Science, Tokyo University)

[PEM11-P04] Two-dimensional distributions of GPS-TEC disturbances associated with Sakurajima eruptions

*Yuki Nishiyama¹, Hiroyuki Nakata¹, Hiroyo Ohya¹, Takuya Tsugawa², Michi Nishioka² (1.Graduate School of Science and Engineering, Chiba University, 2.National Institute of Information and Communications Technology)

[PEM11-P05] Atomic Oxygen Ion-Neutral Collision Frequency Models at Ionospheric Temperatures

*Akimasa Ieda¹ (1.Institute for Space-Earth Environmental Research, Nagoya University)

[PEM11-P06] Effects of auroral Ionosphere on atmospheric electricity

*Osuke Saka¹ (1.Office Geophysik)

[PEM11-P07] Data processing and quality-control of the ISS-IMAP mission data

*Akinori Saito¹, Takeshi Sakanoi², Yuta Hozumi³ (1.Department of Geophysics, Graduate School of Science, Kyoto University, 2.Planetary Plasma and Atmospheric Research Center, Graduate School of Science, Tohoku University, 3.University of Electro-Communications)

[PEM11-P08] **Polar cap patches, GPS TEC variations, and atmospheric gravity waves**

*Paul Prikryl¹, Robert G. Gillies², David R. Themens^{1,3}, Bharat S. R. Kunduri⁴, Evan G. Thomas⁵, Roger Varney⁶, James M. Weygand⁷ (1.Physics Department, University of New Brunswick, 2.Department of Physics and Astronomy, University of Calgary, 3.School of Engineering, University of Birmingham, 4.Bradley Department of Electrical and Computer Engineering, Virginia Tech, 5.Thayer School of Engineering, Dartmouth College, 6.Center for Geospace Studies, SRI International, 7.Earth Planetary and Space Sciences, University of California)

[PEM11-P09] Development and accuracy evaluation of the image processing system for Stabilized High-sensitive Imager on Shirase

*Saki Yamashina¹, Akinori Saito¹, Takeshi Sakanoi², Takuo T. Tsuda³, Yuta Hozumi³, Takeshi Aoki³, Mitsumu K. Ejiri⁴, Takanori Nishiyama⁴, Takahiro Naoi⁵, Masato Nagahara⁵ (1.Graduate School of Science, Kyoto University, 2.Planetary Plasma and Atmospheric Research Center, Graduate School of Science, Tohoku University, 3.Graduate School of Informatics and Engineering, The University of Electro-Communications, 4.National Institute of Polar Research, 5.National Institute of Information and Communications Technology)

[PEM11-P10] Statistical analysis of local time dependence of MSTID characteristics using the SuperDARN pair of radars

*Wataru Hazeyama¹, Nozomu Nishitani¹, Tomoaki Hori¹ (1.Institute for Space-Earth Environmental Research)

[PEM11-P11] The nature of large off-vertical MF radar echoes over Syowa station, Antarctica

*Masaki Tsutsumi¹ (1.National Institute of Polar Research)

[PEM11-P12] ICON satellite observations of thermospheric winds

*Yusuke Ioka¹, Huixin Liu¹ (1.Earth and Planetary Science Division, Kyushu University SERC, Kyushu University)

[PEM11-P13] **The relation between *hmF2* and radio occultation scintillation amplitude index RO-S4 index observed using FORMOSAT-7/COSMIC-2**

*YI DUANN^{1,2}, Loren Chang^{1,2}, Chi-Kuang Chao^{1,2}, Jann-Yenq Liu^{1,2}, Tung-Yuan Hsiao³, Shih-Ping Chen⁴ (1.Department of Space Science and Engineering, National Central University, Taoyuan City, Taiwan, 2.Center for Astronautical Physics and Engineering, National Central University, Taoyuan City, Taiwan, 3.Nuclear Science and Technology Development Center, National Tsing Hua University, Hsinchu City, Taiwan, 4.Department of Earth Sciences, National Cheng Kung University, Tainan City, Taiwan)

[PEM11-P14] Simultaneous observations of plasma bubbles with an HF Doppler sounding system in Taiwan and an all-sky imager in Ishigaki Island

*Hiromi Sejima¹, Keisuke Hosokawa¹, Jaroslav Chum², Hiroyuki Nakata³, Jun Sakai⁴, Susumu Saito⁵ (1.Department of Communication Engineering and Informatics, University of Electro-Communications, 2.Institute of Atmospheric Physics of the Czech Academy of Sciences, 3.Graduate School of Engineering, Chiba University, 4.Center for Space Science and Radio Engineering, University of Electro-communications, 5.Electronic Navigation Research Institute, National Institute of Maritime, Port, and Aviation Technology)

[PEM11-P15] Automated detection of mid-latitude sporadic E using GPS-TEC ROTI data

*Masahiro Takahi¹, Keisuke Hosokawa¹, Jun Sakai², Susumu Saito³ (1.Department of Communication Engineering and Informatics, University of Electro-Communications, 2.Center for Space Science and

Radio Engineering, University of Electro-communications, 3.Electronic Navigation Research Institute, National Institute of Maritime, Port, and Aviation Technology)

[PEM11-P16] Research about the thermospheric structure and variations by comparing the simultaneous data of GOCE and CHAMP

*Nakayama Sayuka¹, Liu Huixin¹ (1.Kyushu university)

[PEM11-P17] Effects of static electric fields and Alfvén waves on Joule heating in the cusp

*Tomokazu Oigawa¹, Hiroyuki Shinagawa², Satoshi Taguchi¹ (1.Department of Geophysics, Graduate School of Science, Kyoto University, 2.National Institute of Information and Communications Technology)

[PEM11-P18] The impact of FORMOSAT-7/COSMIC-2 in-situ plasma drift observations on the space weather forecasting system

*Chia-Hung Chen¹, Charles Lin¹, Tomoko Matsuo², Ching-Hua Shen¹ (1.Department of Earth Sciences, National Cheng Kung University, 2.Ann and H. J. Smead Department of Aerospace Engineering Sciences, University of Colorado, Boulder, CO 80309-0429, USA)

[PEM11-P19] Scintillation Drift Velocity Observed by Closely-Spaced GPS Receivers in Indonesia

*Yuichi Otsuka¹, Prayitno Abadi² (1.Institute for Space-Earth Environmental Research, Nagoya University, 2.LAPAN, Indonesia)

[PEM11-P20] The ionospheric disturbances associated with Typhoons observed by HF Doppler, Infrasound, and GPS occultation observations

*Hiroyuki Nakata¹, Ryota Yagihashi², Hiroyo Ohya¹, Keisuke Hosokawa³, Masa-yuki Yamamoto⁴ (1.Graduate School of Engineering, Chiba University, 2.Graduate School of Science and Engineering, Chiba University, 3.School of Informatics and Engineering, The University of Electro-Communications, 4.School of Systems Engineering, Kochi University of Tecnology)

[PEM11-P21] Calcium ion thin layer observed with a resonance scattering lidar at Syowa, Antarctic

*Mitsumu K. Ejiri^{1,2}, Takanori Nishiyama^{1,2}, Takuo T. Tsuda³, Katsuhiko Tsuno⁴, Masaki Tsutsumi^{1,2}, Makoto Abo⁵, Takuya Kawahara⁶, Takayo Ogawa⁴, Satoshi Wada⁴, Takuji Nakamura^{1,2} (1.National Institute of Polar Research, 2.The Graduate University for Advanced Studies, SOKENDAI, 3.The University of Electro-Communications, 4.RIKEN,RAP, 5.Tokyo Metropolitan Univ., 6.Shinshu Univ.)

[PEM11-P22] Relationship between energetic particle precipitations and an intensity of OH airglow over Syowa Station.

*Satoshi Ishii¹, Hidehiko Suzuki¹, Masaki Tsutsumi^{2,4}, Makoto Taguchi³, Mitsumu K. Ejiri^{2,4}, Takanori Nishiyama^{2,4} (1.Meiji University, 2.National Institute of Polar Research, 3.Rikkyo University, 4.SOKENDAI)

[PEM11-P23] Variations in the D-region ionosphere observed in fireballs occurred using VLF/LF transmitter signals

*Takeru Suzuki¹, Hiroyo Ohya², Fuminori Tsuchiya³, Kazuo Shiokawa⁴, Hiroyuki Nakata² (1.Graduate School of Science Engineering, Chiba University, 2.Graduate School of Engineering, Chiba University, 3.Planetary Plasma and Atmospheric Research Center, Graduate School of Science, Tohoku University, 4.Institute for Space-Earth Environmental Research, Nagoya University)

[PEM11-P24] Sporadic Fe layer event associated with vertical ion drift based on wind shear theory: simultaneous observation of Fe density and wind at Syowa station (69.0°S, 39.6°E) and simulation

*Takanori Nishiyama^{1,2}, Mitsumu K. Ejiri^{1,2}, Takuo T. Tsuda³, Takuji Nakamura^{1,2}, Katsuhiko Tsuno⁴, Masaki Tsutsumi^{1,2}, Takuya Kawahara⁵, Makoto Abo⁶, Takayo Ogawa⁴, Satoshi Wada⁴ (1.National Institute of Polar Research, 2.Department of Polar Science, The Graduate University for Advanced Studies, SOKENDAI, 3.The University of Electro- Communications, 4.RIKEN, 5.Shinshu University, 6.Tokyo Metropolitan University)

Year-to-year variation in polar mesospheric clouds observed by geostationary earth orbit satellite, Himawari

*Beng Aun Peh¹, Takuo T. Tsuda¹, Hidehiko Suzuki², Yuta Hozumi¹, Yoshiaki Ando¹, Keisuke Hosokawa¹, Takuji Nakamura³, Ken T. Murata⁴

1. The University of Electro-Communications, 2. Meiji University, 3. National Institute of Polar Research, 4. National Institute of Information and Communications Technology

Polar mesospheric clouds (PMCs) or noctilucent clouds (NLCs) consist of water-ice particles, which can be produced in summer at the mesopause region, mainly at high latitudes. It is considered that the formation of the water-ice particles is sensitive to mesospheric conditions which are the atmospheric temperature, the mixing ratio of water vapor (H_2O), etc. Thus, observations of the PMCs can be a useful diagnosis to understand dynamics as well as chemistry in the mesosphere. For example, the long-term PMC activity may be related to the global change, because the water-ice particle production can be enhanced by CO_2 radiative cooling and H_2O increase which may be induced by greenhouse gases such as CO_2 and CH_4 .

Since the first report on PMCs in 1885, various methods have been used to perform PMC observations. Optical observations by ground-based cameras, imagers, or lidars are often limited by weather conditions because a clear sky is required for such observations. Hence, satellite observations from space are also valuable for more continuous observations, which enable significant systematic data coverage. PMC observations by low-earth-orbit (LEO) satellites have a long history. By contrast, there are only a few reports of PMC observations by geostationary-earth-orbit (GEO) satellites, which include Meteosat First Generation (MFG), Meteosat Second Generation (MSG), and Himawari-8. This kind of GEO satellite can produce full-disk images including the Earth's limb, which would provide valuable opportunities for PMC observations by continuous limb-viewing from its almost fixed location relative to the Earth.

Recently, we developed a near real-time PMC monitoring system by utilizing full-disk imaging of Himawari-8. Based on its PMC data obtained from 2015 to 2021, in this study, we have investigated PMC variations in the most recent years. We have derived the PMC occurrence rates from the near real-time and continuous PMC data, which are provided by the Himawari-8 PMC monitoring system. Concerning to year-to-year variation in the Northern hemisphere, it seems that the PMC occurrence rates tended to gradually increase during 2015-2020, and the occurrence rate was highest in summer 2020. These results may imply a relation to the fact that NLCs were observed over Hokkaido, Japan, during 12-14 June 2020. On the other hand, the PMC occurrence rates in the Southern hemisphere showed more complex features. For example, the PMC occurrence rate was not high in summer 2020-2021, compared with those in the other years. In the presentation, we will show these results, and discuss the observed PMC variations, together with the mesospheric temperature and H_2O mixing ratio data obtained by Aura/Microwave Limb Sounder (Aura/MLS). Furthermore, to extend data coverage, we plan to examine a possibility of PMC observations by Himawari-6/7 in 2005-2015.

Keywords: Polar mesospheric clouds, Noctilucent clouds, Geostationary earth orbit satellite, Himawari

Analysis of vertical profiles of ionospheric disturbances caused by the tsunami associated with the Tohoku earthquake using GPS occultation observation

*Ryosuke Fushimi¹, Hiroyuki Nakata², Hiroyo Ohya²

1. Graduate School of Science and Engineering, Chiba University, 2. Graduate School of Engineering, Chiba University

It is reported that ionospheric disturbances are caused by large earthquakes. One of the causes is the infrasound wave excited by surface waves and/or tsunamis. The characteristics of the ionospheric disturbances horizontally propagating after large earthquakes have been examined by using a network of ground-based GPS receivers. On the other hand, the vertical propagation of ionospheric disturbances, especially due to tsunamis, is rarely reported. In this study, to examine the vertical propagation of the ionospheric disturbances due to tsunamis, we have examined electron density profiles observed by GPS radio occultation measurements of FORMOSAT-3/COSMIC satellites. The data is provided by CDAAC (COSMIC Data Analysis and Archive Center). We analyzed the ionospheric disturbances caused by a tsunami associated with Tohoku Earthquake (M9.0) occurred at 5:46:18 on 11th March 2011 (UTC). We analyzed density profiles observed within 3 hours after the passage of the tsunami. Extracting the fluctuation components from observed height profiles of ionospheric electron densities using the Chapman model, short-wavelength fluctuations of 10-30 km were confirmed in data points observed in the northeast direction from the epicenter. On the other hand, there was no such short-wavelength fluctuation in the data observed in the southeast direction from the epicenter. In addition, we analyzed the data observed about 8 hours after the passage of the tsunami. Short-wavelength fluctuation was still confirmed in the data observed in the northeast direction from the epicenter. The results showed that the fluctuations continued for a long time after the arrival of the tsunami. The tsunami observation data using DART (Deep-ocean Assessment and Reporting of Tsunami) system provided by NOAA (National Oceanic and Atmospheric Administration) shows that the sea surface was continuously disturbed for a long time after the passage of the tsunami. This may be related to the fact that the ionospheric disturbance appeared for a long time in this analysis.

Keywords: ionospheric disturbance, occultation observation

Imaging observation of Ionospheric Field Aligned Irregularities by the PANSY radar at Antarctic Syowa Station

*Daisuke Kagawa¹, Taishi Hashimoto², Akinori Saito¹, Koji Nishimura², Masaki Tsutsumi², Toru Sato³, Kaoru Sato⁴

1. Graduate School of Science, Kyoto University, 2. National Institute of Polar Research, 3. Graduate School of Informatics, Kyoto University, 4. Graduate School of Science, Tokyo University

Program of the Antarctic Syowa Mesosphere-Stratosphere-Troposphere/Incoherent Scatter (PANSY) radar is a large atmospheric and VHF-band radar located at the Antarctic Syowa Station. This radar has a 47 MHz frequency, so it is capable of observing the coherent echoes from 3-m-scale field aligned irregularities (FAIs) in E-region. In this study, we observed them using the PANSY radar, and estimated the 2-dimensional spatial distribution of FAI echoes by the radar imaging. However, the imaging using the Fourier or Capon methods suffers the "ghosts" and the uncertainty of estimating the spatial distribution of FAI because of the beam pattern of the FAI array. On the other hand, the CLEAN method has the capability of estimating the spatial distribution of FAI echoes by removing the its effect, because it iteratively subtracts a scaled beam pattern centered on the location of the significant point on the obtained image. In April and December 2017, E-region FAI observation was operated by the PANSY radar. FAI echoes were detected on 6 observations out of 8, and periodic fluctuations of the echo intensity were shown in all of them. Furthermore, they were classed in two patterns according to their range structure, wide one and narrow one. In wide range echoes, quasi-periodic (QP) patterns with about 7-minute-period were shown. Applying the CLEAN method to one period of the QP echoes, we found the change of the range of the QP-FAI echoes. It was also figure out that the FAIs have the wave front aligned about -60 degrees azimuth angle and propagate from about northeast to southwest with a velocity of about 260 m/s. Furthermore, comparing with data of ionospheric electron density, these FAIs were considered to be produced by gradient-drift instability which were driven by the increases of electron density in ionospheric E-region. On the other hand, we found out that the time variations of narrow range echoes are correlated with Pc5 pulsation comparing with data of the variations of magnetic field on the ground at the Syowa station. The Pc5 pulsation shows the variations of H-component and D-component, so the plasma instability is driven by the strong electrojet with east and north component, and these FAIs are considered to be produced. The CLEAN method also showed little movement of these FAIs.

Keywords: PANSY radar, Field Aligned Irregularities, CLEAN, QP echoes, Pc5 pulsation

Two-dimensional distributions of GPS-TEC disturbances associated with Sakurajima eruptions

*Yuki Nishiyama¹, Hiroyuki Nakata¹, Hiroyo Ohya¹, Takuya Tsugawa², Michi Nishioka²

1. Graduate School of Science and Engineering, Chiba University, 2. National Institute of Information and Communications Technology

We analyzed the disturbances total electron content (TEC) in association with Sakurajima eruptions. The TEC data were derived from the GNSS Earth Observation Network (GEONET) of the Geospatial Information Authority of Japan (GSI). The intersection of the line of sight connecting each GPS satellite and GPS receiver at an altitude of 300 km is defined as the Ionospheric Pierce Point (IPP). The relationship between the position of the IPP and the two-dimensional distribution of TEC disturbances were examined. We analyzed five cases of volcanic eruptions during 2007 ~ 2014. The magnitudes of the eruptions were evaluated by the maximum value observed by the infrasound meter at Higashikourimoto.

In the eruption occurred on 2009/10/3, clear TEC fluctuations were observed. In the other events, the fluctuations were not observed although the magnitudes of some events were larger than the eruption on 2009/10/3. From the distribution of the TEC fluctuations, it is found that the fluctuations were observed in the south of the volcano after about 12 minutes.

This is because the geomagnetic field in Japan directs north-downward. Since the plasma moves along the direction of the geomagnetic field and the acoustic waves due to the eruption propagate almost parallel to the magnetic field (Otsuka et al. 2006). In order to estimate this effect, we calculated the angle α between the propagation direction of the wave and the geomagnetic field. As a result, TEC fluctuations were observed in the region where $|\cos \alpha| > 0.9$.

Since the acoustic waves are compressional, and TEC is the integral of the electron density in the line-of-sight direction, the magnitude of the TEC fluctuations depends on the direction of the acoustic waves and lines of sight between satellites and receivers (Heki, 2006). To estimate the effect of this relation, we also calculated the angle β between the propagation direction of the waves and the line of sight. As a result, TEC fluctuation was observed in the region of $|\cos \alpha| > 0.9$ and $|\sin \beta| > 0.8$.

TEC fluctuations are observed in the area where the influence of the geomagnetic field is sufficiently large and the angle between the propagation direction of the atmospheric wave and the line of sight of the observation is close to a right angle. It is possible to observe fluctuations that are not visible in the TEC data as they are by making corrections for these factors.

Keywords: Sakurajima, TEC fluctuations

Atomic Oxygen Ion–Neutral Collision Frequency Models at Ionospheric Temperatures

*Akimasa Ieda¹

1. Institute for Space-Earth Environmental Research, Nagoya University

The collision between atomic oxygen and its first positive ion plays a major role in Earth's F region ionosphere. An accurate corresponding collision frequency model is necessary to quantitatively understand the ionosphere. However, the widely used classic Banks theoretical model typically provides a collision frequency that is 30% lower than the expectation from ionospheric observations. Accordingly, the classic collision frequency is often adjusted by multiplying it by a constant known as the Burnside factor. This correction-factor model adopted the classic model as its basis due to a misunderstanding that the classic model was based on a laboratory experiment; that is, the correction factor was originally meant to compensate for laboratory contamination.

In this study, a collision frequency model is constructed based on the laboratory experiment, and the resultant laboratory-based model is found to be consistent with ionospheric observations. In this construction, the impact of laboratory contamination is determined to be small (7%) and is mostly canceled by a misinterpretation regarding the conventional definitions of energy. Thus, the 30% difference is mainly caused by a theoretical error in the classic model itself. This error is energy-dependent and corrected by the later wide-energy theoretical model. Thus, the classic model cannot be corrected by a temperature-independent constant and should be replaced by the later model.

Ieda (JGR, 2021): <https://doi.org/10.1029/2020JA028441>

Keywords: Burnside factor, ionospheric conductivity, collision frequency, charge-exchange collision, F region, oxygen

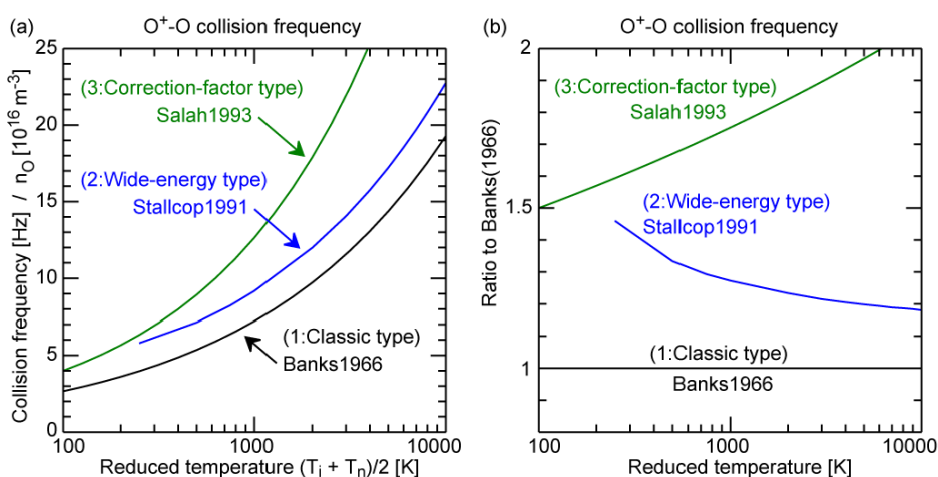


Figure 1. (a) Existing models of O^+ -O momentum-transfer collision frequency. They are for the unit number density of atomic oxygen and are a function of the ion-neutral reduced temperature $(T_i+T_n)/2$. A representative model of each of the three types of models is shown: (1) classic high-energy theory type (Banks, 1966), (2) later wide-energy theory type (Stallcop et al., 1991), and (3) correction-factor type (Salah, 1993). (b) The ratio of (a) to the Banks model, known as the Burnside factor, for each of the representative models.

Effects of auroral Ionosphere on atmospheric electricity

*Osuke Saka¹

1. Office Geophysik

A unique and comprehensible event of atmospheric electricity was observed on 6-7 September 2007 at Syowa station, Antarctica [Minamoto and Kadokura, 2011] (referred to as MK event). Comparing ionospheric sounding data at Syowa station with the MK event, we propose possible scenario of ionospheric effects on the atmospheric electricity.

[Minamoto, Y., and Kadokura, A., 2011: Extracting fair-weather data from atmospheric electric-field observations at Syowa Station, Antarctica, *Polar Science*, 5, 313-318]

The global circuit of atmospheric electricity is generally considered a huge current circuit in the ionosphere-atmosphere-earth system. The currents in this circuit are generated in the atmosphere by charge separation processes in tropical convective storms. Nevertheless, we report here that the current intensity flowing in this current circuit was influenced by the ionospheric conditions at the topside boundary of the atmosphere. Ionospheric influences inferred from the MK event are summarized as follows: (1) currents in the global circuit were suppressed/amplified intermittently by the temporal decrease/increase of ionospheric potentials, (2) currents were intensified by decreasing capacitance of the ionosphere in association with a loss of ionospheric F-Layer.

We emphasize that the global circuit can be regarded as an atmospheric current probe useful for monitoring the ionosphere and magnetosphere.

Keywords: Atmospheric electricity, Auroral ionosphere, Electromagnetic coupling

Data processing and quality-control of the ISS-IMAP mission data

*Akinori Saito¹, Takeshi Sakanoi², Yuta Hozumi³

1. Department of Geophysics, Graduate School of Science, Kyoto University, 2. Planetary Plasma and Atmospheric Research Center, Graduate School of Science, Tohoku University, 3. University of Electro-Communications

Data processing and quality-control of the ISS-IMAP (Ionosphere, Mesosphere, upper Atmosphere, and Plasmasphere mapping) mission has been carried out to improve the data quality and reliability. Two ISS-IMAP instruments, Visible-light and Infrared Spectrum Imager (VISI) and Extreme UltraViolet Imager (EUVI), made observation of the Earth's upper atmosphere from the Exposed Facility of Japanese Experiment Module of the ISS between August 2012 and August 2015. VISI made imaging observations of the airglow and aurora from 500 nm to 900 nm of wavelength in the nadir direction. The airglow of 730 nm (OH, Alt. 85km), 762 nm (O₂, Alt. 95km), and 630 nm (O, Alt. 250km) were mainly observed besides the other airglow, such as 589nm (Na) and 557 (O). There are several observational mode in VISI, such as peak mode, calibration mode, and spectrum mode. The calibration of the pixel sensitivity has been made based on both of pre-flight experiment data and on-orbit data. Error of the measurement is also estimated. Several types of noises, such as city-light, moon light scattering from tropospheric clouds, cosmic rays, and reflection from the solar panel of ISS, are identified to improve the quality of data especially for the statistical analysis. Data is stored in NetCDF file format. EUVI made imaging observation of the resonant scattering from ions, He⁺ in 30.4 nm, and O⁺ in 83.4 nm in the limb direction. In the presentation, the quality and reliability of ISS-IMAP data will be discussed.

Keywords: airglow, resonant scattering, aurora, mesosphere, ionosphere, ISS

Polar cap patches, GPS TEC variations, and atmospheric gravity waves

*Paul Prikryl¹, Robert G. Gillies², David R. Themens^{1,3}, Bharat S. R. Kunduri⁴, Evan G. Thomas⁵, Roger Varney⁶, James M. Weygand⁷

1. Physics Department, University of New Brunswick, 2. Department of Physics and Astronomy, University of Calgary, 3. School of Engineering, University of Birmingham, 4. Bradley Department of Electrical and Computer Engineering, Virginia Tech, 5. Thayer School of Engineering, Dartmouth College, 6. Center for Geospace Studies, SRI International, 7. Earth Planetary and Space Sciences, University of California

The southward pointing field of view of the Canadian component of the Resolute Bay Incoherent Scatter Radar (RISR-C) is well suited for observing the ionospheric signatures of flux transfer events and subsequent polar patch formation in the cusp [1]. The fast azimuthally oriented flows and associated density depletions often show an enhanced ion temperature from Joule heating caused by the sudden change in plasma flow direction. The newly formed polar patches are then observed as they propagate through the field-of-views of both RISR-C and RISR-N. In the ionosphere, the electron density gradients imposed in the cusp, and small-scale irregularities resulting from gradient-drift instability, particularly in the trailing edges of patches, cause GPS TEC and phase variations, and sometimes amplitude scintillation. A byproduct of the coupling process forming polar cap patches are traveling ionospheric irregularities (TIDs) [2]. Pulses of ionospheric currents in the cusp are a source of Joule heating launch atmospheric gravity waves (AGWs) causing medium- and large-scale TIDs propagating equatorward and upward, where they are observed by mid-latitude SuperDARN radars, as well as in the detrended GPS TEC maps. However, the AGWs propagate globally, both upward and downward from the lower thermosphere [3]. The downward propagating AGW packets can impact the lower atmosphere, including the troposphere. Despite significantly reduced wave amplitudes, these AGWs, subject to amplification upon over-reflection in the upper troposphere, can trigger/release existing moist instabilities, initiating convection and latent heat release, the energy leading to intensification of storms [4].

[1] Lockwood, M., and H. C. Carlson, Jr., *Geophys. Res. Lett.*, 19, 1731–1734, 1992.

[2] Prikryl P., et al., *Ann. Geophys.*, 23, 401–417, 2005.

[3] Mayr H.G., et al., *J. Geophys. Res.*, 89, 10929–10959, 1984.

[4] Prikryl P., et al., 2009, *Ann. Geophys.*, 27, 31–57

Keywords: Solar wind - magnetosphere - ionosphere - atmosphere coupling, Polar and auroral ionosphere, Ionospheric irregularities, Ionospheric currents, Atmospheric gravity waves

Development and accuracy evaluation of the image processing system for Stabilized High-sensitive Imager on Shirase

*Saki Yamashina¹, Akinori Saito¹, Takeshi Sakanoi², Takuo T. Tsuda³, Yuta Hozumi³, Takeshi Aoki³, Mitsumu K. Ejiri⁴, Takanori Nishiyama⁴, Takahiro Naoi⁵, Masato Nagahara⁵

1. Graduate School of Science, Kyoto University, 2. Planetary Plasma and Atmospheric Research Center, Graduate School of Science, Tohoku University, 3. Graduate School of Informatics and Engineering, The University of Electro-Communications, 4. National Institute of Polar Research, 5. National Institute of Information and Communications Technology

Ionospheric phenomena such as aurora and airglow are mainly observed by ground-based all-sky imagers, so there are observational gaps over the ocean, especially in the southern hemisphere, where the ocean occupies a large proportion. If these gaps are solved, it will be possible to compare phenomena between the northern and southern hemispheres to evaluate differences, and to observe phenomena with a structure too large to be observed only on the ground. In addition, it will be possible to compare phenomena over the ocean and over the ground, and to evaluate the effect of the ocean-ground distribution on the variability of the upper atmosphere. In order to conduct these observations and evaluations, it is necessary to enable optical observations over the ocean and to solve the gaps. In the case of optical observations from the ocean, the vibration of the ship must be taken account of, unlike on the ground. The imager posture changes during the exposure time due to the vibration of the ship, and the position and orientation of the imager change for each observation data as the ship moves. The purpose of this study is to solve these ship-specific problems and to grasp the structure of airglow and aurora. We installed an all-sky imager on the Antarctic research vessel "Shirase" and conducted optical observations during the 61st Japanese Antarctic Research Expedition from November 2019 to March 2020. Shirase's route is suitable for observing aurora because it sails under the southern auroral zone for a long time. It is also suitable for observing airglow, as it passes through the equatorial anomaly zone. The imager was mounted on a 3-axis attitude stabilized gimbal, which cancels out the vessel's vibration, and was equipped with the bandpass interference filter, whose center wavelength is 630.0nm, and the fisheye lens. The observation system was constructed to capture the light emission at an altitude of 250 km without being affected by vessel motion. The imager's exposure time was set to 20s, and the images were automatically taken every day between sunset and the rising of the moon. For the analysis, I used the position and attitude data of the Shirase, such as latitude, longitude, and ship speed data every second, and azimuth angle data every quarter second. In addition to these data, during the 62nd Japanese Antarctic Research Expedition from 2020 to 2021, we do not only capture the new 670nm wavelength emission with two imagers, but we also installed a GNSS receiver to obtain ionospheric total electron content data. The shooting direction of the imager changes with each shot due to the vibration and movement of the vessel. Therefore, the relative azimuth angle of the shooting direction to the vessel was obtained by automatically detecting the structure of the vessel in the image, and then combined with the position and attitude data of the Shirase, the shooting direction was automatically detected. The accuracy of this direction estimation was evaluated by comparing it with the shooting direction obtained from the position of the stars in the image, and the maximum error was 2 degrees. This error corresponds to a few tens of kilometers on the horizontal scale at an altitude of 250 km, and it is small enough to be compared with the horizontal scale of aurorae and airglow. Other corrections for optical sensitivity were also made. We successfully observed the equatorial anomaly zone with 630.0 nm airglow at low latitudes on November 22 and 23, 2019, and the aurora at high latitudes on several nights from late February to early March 2020. I evaluate the accuracy of the observation system by comparing these phenomena with

other observation data from OMTI. The results of this study will be used to develop and improve the observation system for the 63rd Japanese Antarctic Research Expedition, which will be conducted this year, and will also be used to develop observation systems for other ships in the future.

Keywords: aurora, airglow, ionosphere observation

Statistical analysis of local time dependence of MSTID characteristics using the SuperDARN pair of radars

*Wataru Hazeyama¹, Nozomu Nishitani¹, Tomoaki Hori¹

1. Institute for Space-Earth Environmental Research

We conduct a statistical analysis on medium-scale traveling ionospheric disturbances (MSTIDs) using the Super Dual Auroral Radar Network (SuperDARN) Hokkaido East (43.53°N, 143.61°E) high-frequency (HF) radar data from 2009 to 2019 and the SuperDARN Hokkaido West (43.54°N, 143.61°E) high-frequency (HF) radar data from 2016 to 2019. We applied a three-dimensional fast Fourier transform (3-D FFT) method developed by Matsuda et al. (2014) to the dataset to deduce wave characteristics of the observed MSTIDs. This study focuses on the local time and solar activity dependence of the MSTIDs. We find that the propagation direction of MSTIDs gradually rotates clockwise as time advances during both daytime and nighttime. These changes can be explained by their respective generation mechanisms. We also find a clear negative correlation between the yearly-averaged power spectral density of nighttime MSTIDs and the F10.7 solar flux index. We consider that the relationship between the linear growth rate of the Perkins instability and solar activity causes this negative correlation.

Keywords: MSTID

The nature of large off-vertical MF radar echoes over Syowa station, Antarctica

*Masaki Tsutsumi¹

1. National Institute of Polar Research

MF (Middle Frequency) radars have been used to measure wind velocity in mesosphere and lower thermosphere. The radars need ionization and refractive index fluctuations to receive echoes from the region. The nature of the echoes has been studied to better understand that of the ionized media and also to better estimate wind velocity.

Tsutsumi et al. [2017] compared mesosphere echoes of PANSY radar (47 MHz) and MF radar (2.4 MHz) collocated at Syowa station (69S), and showed lots of similarity in these two radar echoes suggesting a common generation mechanism of the echoes despite a large difference in the radar operating frequency. Summer time echoes are almost always aspect sensitive while winter time echoes are less aspect sensitive.

Winter time MF radar echoes is highly variable in strength and angle-of-arrival. These echoes are quite often very low aspect sensitive coming back from off-vertical zenith angles as large as some tens of degrees. Meteor echoes are partly responsible for this low aspect sensitivity [Tsutsumi and Aso, 2005]. The nature of these off-vertical echoes is discussed in details, and the horizontal structure information of wind velocity is tried to be deduced from these widely distributed targets.

References

Tsutsumi, M., and T. Aso, 2005: MF radar observations of meteors and meteor-derived winds at Syowa (69S, 39E), Antarctica: A comparison with simultaneous spaced antenna winds., *J. Geophys. Res.*, 110, D24111, doi:10.1029/2005JD005849.

Tsutsumi, M., K. Sato, T. Sato, M. Kohma, T. Nakamura, K. Nishimura, and Y. Tomikawa, Characteristics of mesosphere echoes over Antarctica obtained using PANSY and MF radars, *SOLA*, 13A, 19–23, doi:10.2151/sola.13A-004, 2017.

Keywords: mesosphere and lower thermosphere, Antarctic, MF radar

ICON satellite observations of thermospheric winds

*Yusuke Ioka¹, Huixin Liu¹

1. Earth and Planetary Science Division, Kyushu University SERC, Kyushu University

ICON is a NASA scientific satellite launched in 2019. It utilizes the Michelson interferometer, called MIGHTI, to observe airglow at two wavelengths: red at 630.0 nm and green at 557.7 nm. Line-of-sight wind speed can be obtained from these airglow emissions. The horizontal wind vector is then obtained using two MIGHTIs observing the same volume from two directions 90 degree apart (with 5-8 min time delay). The green airglow covers the altitude range of 90-300 km, while the red covers 150-300 km. Large observation errors occur near the day-night boundary and the equatorial ionization anomaly. Observation errors in other regions are generally less than 10 m/s.

Using MIGHTI observations during January –December 2020, we examine the local time and seasonal variation of the thermosphere wind and compare it to climatology previously obtained by CHAMP satellite. Initial results clearly reveal a dominant diurnal variation of winds at 250 km, and semi-diurnal variation at 100 km. Detailed results will be presented in the poster.

The relation between *hmF2* and radio occultation scintillation amplitude index RO-S4 index observed using FORMOSAT-7/COSMIC-2

*YI DUANN^{1,2}, Loren Chang^{1,2}, Chi-Kuang Chao^{1,2}, Jann-Yenq Liu^{1,2}, Tung-Yuan Hsiao³, Shih-Ping Chen⁴

1. Department of Space Science and Engineering, National Central University, Taoyuan City, Taiwan, 2. Center for Astronautical Physics and Engineering, National Central University, Taoyuan City, Taiwan, 3. Nuclear Science and Technology Development Center, National Tsing Hua University, Hsinchu City, Taiwan, 4. Department of Earth Sciences, National Cheng Kung University, Tainan City, Taiwan

Six FORMOSAT-7/COSMIC-2 (F7/C2) satellites were launched into 24 degrees inclination low Earth orbit on June 25th 2019, The data from the primary Tri-GNSS Radio occultation System (TGRS) space weather products: relative total electron content (TEC), scintillation amplitude index (S4), and electron density (Ne) profile have been released. This study focuses on the comparison of F7/C2 radio occultation scintillation amplitude (RO-S4) index and Ne profiles acquired within a time difference of 30 minutes and spatial difference of 110 km (1 degree of longitude and latitude). These nearly collocated observations are examined to clarify, the relation between S4 index and the height of peak electron density in *F2* layer (*hmF2*), and how S4 index and *hmF2* play roles in the occurrences and growth rate of equatorial plasma bubbles (EPBs) due to plasma uplift. The S4 observations at low latitudes derived from the F7/C2 radio occultation experiment are compared with range-time-intensity (RTI) maps of the 50 MHz radar near Jicamarca and the Global scale Observations of the Limb and Disk (GOLD) mission observed 135.6 nm airglow depletions by *Chen et al. (2020)*, and the results show that RO-S4 intensities can be utilized to identify EPBs of specific scales. On the other hand, the longitudinal and seasonal distributions of the *hmF2* observed by FORMOSAT-3/COSMIC during the growth phase of EPBs from 2008 to 2013 by *Chou et al. (2020)* indicates that the casual relationship of EPBs and the *hmF2* should be examined in more detail. *Ghosh et al. (2020)* presents that the *hmF2* elevated to higher altitudes by prereversal enhancement (PRE) around evening terminator due to eastward electric field at the magnetic equator, while Ne in the *F* region shows negative correlation with peak PREs that could be driven by fountain effect. The comparison of different local time periods and locations is analyzed and discussed in this study as well, in order to improve our understanding of the relation between ionospheric structure and the generation mechanism of plasma irregularities.

Keywords: S4 index, *hmF2*, Equatorial plasma bubbles (EPBs), FORMOSAT-7/COSMIC-2 (F7/C2)

Simultaneous observations of plasma bubbles with an HF Doppler sounding system in Taiwan and an all-sky imager in Ishigaki Island

*Hiromi Sejima¹, Keisuke Hosokawa¹, Jaroslav Chum², Hiroyuki Nakata³, Jun Sakai⁴, Susumu Saito⁵

1. Department of Communication Engineering and Informatics, University of Electro-Communications, 2. Institute of Atmospheric Physics of the Czech Academy of Sciences, 3. Graduate School of Engineering, Chiba University, 4. Center for Space Science and Radio Engineering, University of Electro-communications, 5. Electronic Navigation Research Institute, National Institute of Maritime, Port, and Aviation Technology

Plasma bubbles are regions of electron density depletion in the equatorial ionosphere appearing at altitudes above 200 km. Plasma bubbles, that develop to higher altitudes near the magnetic equator, are observed at low latitude regions 10-20 degrees away from the magnetic equator. Plasma bubbles are known to cause disruptions of global navigation satellite systems and/or degradations of their positioning accuracy. For this reason, plasma bubbles are still being actively investigated by using various observation methods. Chum et al. (2016) conducted a statistical study of Doppler spectrograms obtained from HF Doppler sounding systems at low-latitudes, and suggested that plasma bubbles can be detected as oblique spreading traces in the Doppler spectrograms. However, it has not yet been confirmed if the oblique spreading traces are really the manifestations of plasma bubbles in the HF Doppler observations.

In this study, we examined an interval of simultaneous observations of plasma bubbles with an HF Doppler sounding in Taiwan and an all-sky imager in Ishigaki Island, Japan, which occurred on February 14, 2015. By comparing the radio and optical data, we aimed at demonstrating that the oblique spread structures in the Doppler spectrogram are indeed caused by plasma bubbles. In addition, from the intercomparison of the radio and optical data, we also intended to show the relationship between the size of the oblique spread structures in the Doppler spectrograms and the actual spatial extent of plasma bubbles seen in the optical data. The comparison also enabled us to evaluate the accuracy of methods for estimating the propagation velocity of the plasma bubbles using the HF Doppler observations.

During the simultaneous observations, the arrival of the airglow signatures of plasma bubbles at the reflection point of the HF Doppler system well coincided with the start time of the oblique spread structures in the Doppler spectrogram. This strongly implies that the oblique spread structures in the Doppler spectrogram was surely associated with the passage of plasma bubbles. We also found that there is a strong relationship between the size of the oblique spread structures in the Doppler spectrograms and the spatial extent of the airglow signatures of plasma bubbles, which will allow us to monitor the scale size of plasma bubbles by using the HF Doppler sounding system in Taiwan before arriving in the longitudes of Japan. By comparing the radio and optical observations, it was found that, when we determine the propagation velocity of the plasma bubbles from the Doppler spectrogram, the time-delay method using multiple HF Doppler stations is more accurate than the tilt method using single station data. This finding would be useful when estimating the time-lag between the observation of plasma bubbles in Taiwan and their subsequent arrival in the longitudes of Japan. The knowledge obtained from the current simultaneous observations is of particular importance for the detection, monitoring and prediction of plasma bubbles in Japan.

Automated detection of mid-latitude sporadic E using GPS-TEC ROTI data

*Masahiro Takahi¹, Keisuke Hosokawa¹, Jun Sakai², Susumu Saito³

1. Department of Communication Engineering and Informatics, University of Electro-Communications, 2. Center for Space Science and Radio Engineering, University of Electro-communications, 3. Electronic Navigation Research Institute, National Institute of Maritime, Port, and Aviation Technology

The sporadic E (Es) layer is a thin layer having dense electron density that appears at altitudes around 100 km. Es mainly appears at mid-latitudes during summer months. When the Es layer appears, radio waves in HF and VHF frequencies, sometimes above 100 MHz, propagate for a long distance through reflection by the Es layer. Because of such an abnormal reflection, the Es layer leads to anomalous propagation of radio waves and then causes interference on radio systems such as FM broadcast and aeronautical navigation systems. Therefore, the Es layer have been studied by using a number of observational techniques for a long time.

Recently, Global Positioning System Total Electron Content (GPS-TEC) mapping has been used to observe the Es layer. Recent studies of the Es layer using GPS-TEC maps demonstrated that Es has a frontal structure extending roughly along the east-west direction in daytime. More recently, GPS-TEC Rate Of TEC Index (ROTI) mapping was proposed to detect fluctuations of TEC associated with the Es layer. This method also indicated that the Es layer has a frontal structure roughly elongating in the east-west direction. As mentioned above, it is possible to identify the appearance of the Es layer visually by using either GPS-TEC or GPS-TEC ROTI data. However, it is still difficult to extract such Es layer events automatically from a large amount of data in real time. To solve these problems, it is necessary to establish a method for automated detection of Es.

Recently, it has been demonstrated that applying the Hough transform, which can extract lines from images to ROTI maps is effective to detect the Es layer with a frontal structure. In this paper, we propose a method to detect automatically the spatial structure of the Es layer as a segment by applying the Hough transform. We also tried to estimate the length and motion of the frontal structure of the Es layer. We applied the Hough transform to GPS-TEC ROTI maps obtained during an Es layer event in daytime on May 30, 2020 (01:00-02:55 UT) and succeeded in extracting the frontal structure of the Es layer automatically. On the other hand, if the Es layer does not have a linear frontal structure, the extracted lines did not represent the location or the scale of the Es layer correctly. Furthermore, we calculated the moving velocity of the Es structure from horizontal displacement of lines in consecutive ROTI maps. As a result, it was found that the speed ranged from 40 to 100 m/s, the average being 83m/s, and the structure moved northward. These characteristics are roughly consistent with those of previous researches confirming the feasibility of the current method for extracting the dynamical characteristics of the Es layer.

Keywords: Sporadic E, GPS, TEC, ROTI

Research about the thermospheric structure and variations by comparing the simultaneous data of GOCE and CHAMP

*Nakayama Sayuka¹, Liu Huixin¹

1. Kyushu university

Research about the thermospheric structure and variations by comparing the simultaneous data of GOCE and CHAMP

Sayuka Nakayama, Huixin Liu

Earth and planetary science division, Kyushu university, Japan

We examined zonal wind and thermospheric density by using GOCE and CHAMP. GOCE

flighted about 260km, and CHAMP did about 300km. Therefore, comparing those two data will lead to finding the thermosphere structure and variations.

We analyzed zonal wind and thermospheric density for latitude and longitude distributions in 2010/1,5,6. The result shows that zonal wind and thermospheric density are the same latitude distributions on both GOCE and CHAMP in the case of taking the longitude average. We further examined zonal wind's latitude distributions by taking the longitude average. For GOCE, wind direction is same with all latitude. (For example,

If wind direction in 30° north latitude is eastward, all wind direction is eastward.) On the other hand, for CHAMP, wind direction has changed from eastward wind to westward wind. (For instance, in 2010/5 on dusk side, wind direction is eastward south of 10° north latitude, and north of it wind directed westward.) Moreover, we see the daily variations of zonal wind. The zonal wind has been divided into three categories, which are 30° north latitude, equator, and 30° south latitude. There are large variations on some day. The day is similar to the date of SSW. We are analyzing zonal wind and density, and we are highly motivated to find the thermospheric structure and variations.

Keywords: zonal wind, atmospheric density

Effects of static electric fields and Alfvén waves on Joule heating in the cusp

*Tomokazu Oigawa¹, Hiroyuki Shinagawa², Satoshi Taguchi¹

1. Department of Geophysics, Graduate School of Science, Kyoto University, 2. National Institute of Information and Communications Technology

Remarkable enhancements of the thermospheric mass density around the 400-km altitude in the cusp region have been observed by the CHALLENGING Minisatellite Payload (CHAMP) satellite. Many modeling studies have been conducted to reproduce the mass density anomaly. Under geomagnetically disturbed conditions, previous studies have partially been successful in reproducing the mass density anomaly, while still facing difficulties in reproducing sufficient mass density enhancements under quiet conditions. In this study, we first employed a high-resolution two-dimensional local model to gain insights into what extent the static electric field and electron precipitation can explain the mass density enhancements. We found that the calculated mass density enhancement is 10% at most, which is significantly smaller than the observations by the CHAMP satellite (33% on average). The results also showed that the neutral-ion drag process suppresses Joule heating and neutral mass density enhancements, as well as the chemical reaction process. In contrast to the previous modeling studies, the model calculation imposing only the static electric field and electron precipitation cannot explain the mass density anomaly. The discrepancy between our modeling result and the satellite observation suggests the existence of additional energy sources. Recent studies have reported that electric field variability by Alfvén waves can play an important role in the neutral response in the auroral region. Alfvén waves are reflected between the *E* layer and the sharp slope of the Alfvén velocity above the *F* layer, and some are finally absorbed. This process is known as the ionospheric Alfvén resonator (IAR). Joule heating rates generated by Alfvén waves are maximized at *F* layer altitudes, with the altitude profile depending on wavelength and frequency. In contrast, static electric fields maximize Joule heating rates at *E* layer altitudes. In this study, we include Alfvén waves in our numerical model, and the impacts on Joule heating are evaluated. We will report the effects of both static electric fields and Alfvén waves on Joule heating using model calculations.

Keywords: mass density anomaly, cusp, Joule heating, Alfvén wave, ionospheric Alfvén resonator, numerical model

The impact of FORMOSAT-7/COSMIC-2 in-situ plasma drift observations on the space weather forecasting system

*Chia-Hung Chen¹, Charles Lin¹, Tomoko Matsuo², Ching-Hua Shen¹

1. Department of Earth Sciences, National Cheng Kung University, 2. Ann and H. J. Smead Department of Aerospace Engineering Sciences, University of Colorado, Boulder, CO 80309-0429, USA

FORMOSAT-7/COSMIC-2 mission provides the in-situ ionospheric observations, such as the plasma density and the plasma drift velocity around 550 km altitude, which are very important for the accuracy of ionospheric forecasting. The model boundary condition is a bit issue for the current ionospheric data assimilation model. Although the model forecast results can be well modified by assimilating the ionospheric observations, the accuracy of forecasting get worse at the higher altitude region due to the fixed boundary condition in the model. In this study, we use the DART/TIEGCM model which is an ionospheric forecasting system. We try to modify the upper boundary of TIEGCM and further getting the better forecasting results by assimilating the in-situ FORMOSAT-7/COSMIC-2 ionospheric observations and further evaluate its improvement by employing the method of Observation System Simulation Experiment (OSSE).

Keywords: FORMOSAT-7/COSMIC-2, Data assimilation, in-situ ionospheric observations

Scintillation Drift Velocity Observed by Closely-Spaced GPS Receivers in Indonesia

*Yuichi Otsuka¹, Prayitno Abadi²

1. Institute for Space-Earth Environmental Research, Nagoya University, 2. LAPAN, Indonesia

To investigate zonal drift velocities of a few hundred meter-scale irregularities associated with equatorial plasma bubbles, we have operated three single-frequency GPS receivers at the Equatorial Atmosphere Radar (EAR) site at Kototabang, West Sumatra, Indonesia (0.20°S, 100.32°E; geomagnetic latitude 10.6° S) since January 2003. The GPS receivers sampled GPS signal intensity at a rate of 20 Hz. Distances between the receivers were 116, 127, and 152 m. Drift velocities of irregularities were measured using cross-correlation analysis with the time series of the GPS signal intensity obtained from the three receivers. By analyzing the drift velocity data, equinoctial asymmetry of the zonal drift velocity is found. The eastward drift velocity is higher in March Equinox than in September equinox (Otsuka et al. 2006, Abadi et al., 2017). By analyzing the drift velocity data obtained during a period from 2003 to 2021, in this study, we investigate seasonal and solar activity and magnetic activity dependence of the drift velocity.

Keywords: equatorial ionosphere, GPS, plasma bubble

The ionospheric disturbances associated with Typhoons observed by HF Doppler, Infrasound, and GPS occultation observations

*Hiroyuki Nakata¹, Ryota Yagihashi², Hiroyo Ohya¹, Keisuke Hosokawa³, Masa-yuki Yamamoto⁴

1. Graduate School of Engineering, Chiba University, 2. Graduate School of Science and Engineering, Chiba University, 3. School of Informatics and Engineering, The University of Electro-Communications, 4. School of Systems Engineering, Kochi University of Technology

Ionospheric disturbances are excited by the atmospheric waves due to extreme weather events, such as typhoons and tornados. However, there are very few studies on these kinds of topics, especially on the altitude distributions of these disturbances. In this study, we have examined ionospheric disturbances associated with typhoons using electron density profiles obtained by GPS radio occultation measurements. GPS radio occultation measurement was performed by FORMOSAT-3/COSMIC satellites, which is located at an altitude of about 800 km and viewed from a GPS satellite. Derivation of electron density profiles by receiving and analyzing slightly refracted and delayed radio waves grazing the atmosphere. The electron density fluctuations were extracted by comparing the GPS occultation data with the Chapman model. In addition to the GPS occultation data, HF Doppler sounding data and infrasound data were also examined. Infrasound is a sound wave whose frequency is lower than 20 Hz, the lower limit of human audible frequency. Using HF Doppler sounding, the vertical disturbance in the ionosphere can be observed.

Typhoons No.21 in 2017 (LAN) formed on 15 October 2017 and hit Japan on 22 October 2017. It was a quite strong typhoon with a minimum pressure of 915 hPa recorded just before the hit of Japan. In HFD data, the Doppler-shift fluctuation in the frequency increased, especially in the frequency higher than five mHz as the typhoon approached. On the other hand, the disturbances in the infrasound data increased during the period when the typhoon hit on Japan.

Although the observation points of GPS radio occultation measurements were not the same distance from the typhoon, the enhancement of the electron density fluctuations was observed in the height of 150-400 km. The wavelength of the disturbances about several tens kilometers, and the maximum of the disturbance was about 6000 el/cm³. Since the wavelength of these disturbances corresponds to the acoustic mode of the acoustic gravity wave, it is found that the ionospheric disturbances in association with typhoons are caused by the acoustic mode wave generated by typhoons.

Keywords: Typhoon, HF Doppler, Infrasound, occultation

Calcium ion thin layer observed with a resonance scattering lidar at Syowa, Antarctic

*Mitsumu K. Ejiri^{1,2}, Takanori Nishiyama^{1,2}, Takuo T. Tsuda³, Katsuhiko Tsuno⁴, Masaki Tsutsumi^{1,2}, Makoto Abo⁵, Takuya Kawahara⁶, Takayo Ogawa⁴, Satoshi Wada⁴, Takuji Nakamura^{1,2}

1. National Institute of Polar Research, 2. The Graduate University for Advanced Studies, SOKENDAI, 3. The University of Electro-Communications, 4. RIKEN,RAP, 5. Tokyo Metropolitan Univ., 6. Shinshu Univ.

Layers of metal ions in the mesosphere and lower-thermosphere (MLT) are produced by meteoric ablation. The meteoric metal ions have relatively long chemical lifetime in the MLT region and behave as plasma affected by neutral atmosphere dynamics. In the mid-latitude, the meteoric metal ions in the MLT region are generally accepted as key species for generation of sporadic E (E_s) layer in the wind shear theory. The close link between the E_s layer and calcium ion (Ca^+), one of meteoric metal ions, layer has been also clearly shown by radar and lidar observations [Raizada et al., 2012; Ejiri et al., 2019]. On the other hand, ion convergence at high latitude by the wind shear theory is expected less efficient than mid latitude because of large inclination angle of magnetic field line [e.g., Shinagawa et al., 2017]. A resonance scattering lidar developed by the National Institute of Polar Research (NIPR) was installed at Syowa (69S, 40E), Antarctic in 2017 and obtained Ca^+ density profiles 6 nights in total in Spring in 2017 and 2018. Ca^+ thin layers with high densities were observed on October 6 - 7 in 2018. That night was quiet of the geomagnetic activity ($K_p = 0$), therefore, effects of electric field to generation of the Ca^+ thin and dense layer were probably negligible. Vertical Ca^+ velocity induced by the neutral wind can be calculated using background wind measured by MF radar at Syowa. A comparison in temporal variation between Ca^+ density and gradient of vertical Ca^+ velocity profiles shows that the Ca^+ thin and dense layer was located at the altitude that the gradient was $0 \text{ ms}^{-1} \text{ km}^{-1}$. We will discuss a possible generation process of the observed Ca^+ thin and dense layer.

Keywords: mesospheric Ca^+ layer, Lidar observation, Antarctic, thin layer

Relationship between energetic particle precipitations and an intensity of OH airglow over Syowa Station.

*Satoshi Ishii¹, Hidehiko Suzuki¹, Masaki Tsutsumi^{2,4}, Makoto Taguchi³, Mitsumu K. Ejiri^{2,4}, Takanori Nishiyama^{2,4}

1. Meiji University, 2. National Institute of Polar Research, 3. Rikkyo University, 4. SOKENDAI

OH airglow is luminous phenomena in upper mesosphere which has a thin layer with a peak altitude of ~ 85 km. Origin of OH airglow is an emission from Meinel vibration-rotation band of OH molecule excited by an exothermic reaction between ozone molecule and atomic hydrogen. Rotational temperature, which is believed to be equivalent with neutral temperature of background atmosphere in the mesosphere, can be estimated by observing intensity ratio among rotational lines in the band spectrum. Intensity of OH airglow highly depends on dynamics and photochemical reactions involving minor species in upper mesosphere region. Thus, remote sensing of OH airglow is an effective method to monitor the upper mesosphere and widely carried out by many observers. We have conducted OH airglow observation in Syowa Station, Antarctic during winter season (From an end of Feb to middle of Oct) of 2008-2019 by using an OH spectrometer. The OH spectrometer can measure the OH spectrum even under the moderate aurora condition since it is designed to suppress the contamination from aurora emissions. In this study, we show variations of the intensity of OH airglow which are likely related with auroral activity over Syowa Station. We focused on a sudden enhancement of intensity of OH airglow with a time scale from several ten minutes to several days. Such events do not show sinusoidal oscillations which are frequently caused by atmospheric gravity waves. These events are considered to be a result of an enhancement of vertical transport of [O]-rich air to the airglow layers. We discuss the effect on the OH intensity caused by combination of auroral precipitation which modulates a vertical profile of [O] and dynamical effects which enhance a vertical transportation of [O].

Keywords: OH airglow, Aurora, Mesopause, Lower thermosphere

Variations in the D-region ionosphere observed in fireballs occurred using VLF/LF transmitter signals

*Takeru Suzuki¹, Hiroyo Ohya², Fuminori Tsuchiya³, Kazuo Shiokawa⁴, Hiroyuki Nakata²

1. Graduate School of Science Engineering, Chiba University, 2. Graduate School of Engineering, Chiba University, 3. Planetary Plasma and Atmospheric Research Center, Graduate School of Science, Tohoku University, 4. Institute for Space-Earth Environmental Research, Nagoya University

Meteors and fireballs are known to ionize the D-region and lower E-region ionospheres at 80-120 km heights [Davies, 1966]. The fireballs are meteors that the magnitude of brightness is larger than -4 based on the IAU (International Astronomy Union) definition. TID (traveling ionospheric disturbance) associated with the Chelyabinsk meteoroid in Russia was reported based on GPS-TEC (total electron content) observations [Perevalova et al., 2015]. The amplitude of the TEC variations was 0.07-0.5 TECU, and the period was 10 minutes. The epicenter of the TID was airburst point at 20-30 km heights of the meteoroid, and the velocities were 250-660 m/s. However, few quantitative studies for the D-region ionosphere associated with meteors and fireballs have been reported. In this study, we investigate the variations in the D-region ionosphere during a fireball occurred in Hokkaido at 11:55:55 UT on 18 October, 2018, using VLF (very low frequency, 3-30 kHz) / LF (low frequency, 30-300 kHz) transmitter signals. The VLF/LF transmitter signals are reflected in the D-region ionosphere and are sensitive for variations in electron density in the lower ionosphere. The transmitters used in this study were JJY40kHz (Fukushima, Japan, 37.37 N, 140.85 E), JJY60kHz (Saga, Japan, 33.47 N, 130.18 E), and JJI (Miyazaki, Japan, 22.2 kHz, 32.05 N, 130.82 E). The receiver was located at RKB (Rikubetsu, Hokkaido, Japan, 43.45 N, 143.77 E). Periodic variations of 100-200 s were identified by a wavelet transformation of the signal intensities for the JJY40kHz-RKB, JJY60kHz-RKB, and JJI-RKB paths at about five minutes (12:01 UT) after the fireball. We consider that these variations of intensity were caused by the D-region variations due to acoustic waves in the atmosphere excited by the fireball. If the acoustic waves were excited at the luminous point (118 km altitude) or vanishing end point (25 km altitude) of the fireball, the propagation times of the acoustic waves from the excited point to the LF reflection point at 90 km height over RKB were calculated to be 138 s or 311 s, respectively. The arrival time (311 s) of the acoustic waves excited from the vanishing point roughly matched with the onset of the VLF/LF variations. From the onset of the VLF/LF variations, we estimated the location where the variations in the VLF/LF intensity along the paths. The estimated location was close to the RKB. The VLF/LF variations would be caused by acoustic waves excited at the vanishing end point. The acoustic waves obliquely propagated from the vanishing end point (25 km altitude) upto the D-region height (90 km altitude) at the south point of the RKB receiver.

Sporadic Fe layer event associated with vertical ion drift based on wind shear theory: simultaneous observation of Fe density and wind at Syowa station (69.0°S, 39.6°E) and simulation

*Takanori Nishiyama^{1,2}, Mitsumu K. Ejiri^{1,2}, Takuo T. Tsuda³, Takuji Nakamura^{1,2}, Katsuhiko Tsuno⁴, Masaki Tsutsumi^{1,2}, Takuya Kawahara⁵, Makoto Abo⁶, Takayo Ogawa⁴, Satoshi Wada⁴

1. National Institute of Polar Research, 2. Department of Polar Science, The Graduate University for Advanced Studies, SOKENDAI, 3. The University of Electro- Communications, 4. RIKEN, 5. Shinshu University, 6. Tokyo Metropolitan University

Metallic layers, which ablate from meteoroids, are known to be formed between 80 and 105 km in the terrestrial mesopause region. Meteoric species such as Fe, Mg, and Na exist as atoms in the layers and their dynamical and chemical variability have been investigated by resonance scattering lidars [Plane et al., 2015 and references therein] and satellite-borne measurements. Sporadic E layer, Es layer, is characterized as a thin layer with enhanced electron density and mainly observed by incoherent scatter radars and ionosondes. Mg⁺ and Fe⁺ ions are regarded as dominant ion components in Es layers due to their long lifetime, and therefore sporadic metallic layers are believed to play important roles in forming Es layers. Suggested generation mechanisms of sporadic metallic layers in polar regions are mainly as follows: vertical ion converge and neutralization due to wind shear [e.g., Nygrén et al., 1984] and ionospheric electric field [e.g., Kirkwood and von Zahn, 1991].

We identified sporadic Fe, hereafter FeS, event on June 5, 2018 at Syowa station (69.0°S, 39.6°E), Antarctic, that was observed by a resonance scattering lidar. This FeS event can be summarized as follows: a center altitude and FWHM of the FeS layer are 90 km and 5 km, respectively. Duration was about 3 hours. Geomagnetic activity was quiet during this event and co-located ionosonde demonstrated intermittent Es activity. Apparent growth rate is 1.5 %/min implying that development of the FeS is quite slow. During the FeS event, neutral wind data with from an MF radar at Syowa is available. Meridional and zonal wind profiles at the moment of FeS peak density show strong horizontal wind shear (du/dz is positive and dv/dz is negative), which is consistent with Es layer forming in the southern hemisphere. We tried to explain the observed FeS by wind shear theory since ionospheric electric field (less than 10 mV/m) during the FeS can be neglected. Ion-neutral collision frequency for Fe⁺ was estimated by an empirical model of Voiculescu and Ignat [2002], NRLMSISE-00, and IGRF-13. In addition, vertical ion velocity and its temporal variations were calculated in consideration of magnetic declination [Yu et al., 2019]. Magnetic declination angle at Syowa station is -51° and therefore should be taken into account. Estimated vertical ion velocity, w_i , and vertical ion divergence, dw_i/dz , were both negative near 12 UT. In particular, dw_i/dz reached at -0.010 m/s/km, that is comparable to simulation result of Yu et al. [2019]. It is also consistent with strong Es ($f_oE_s \sim 5$ MHz) observed by ionosonde at the moment. However, near 17 UT when FeS peak density was observed, both w_i and dw_i/dz were positive and favorable for vertical ion divergence. This implies that FeS peak was not caused by vertical ion velocity shear at this moment. Our analysis suggests that Fe⁺ converge associated with negative dw_i/dz might take place about 4 hours earlier than FeS appearance and subsequently neutralization of Fe⁺ led to the observed FeS forming. Above 90 km Fe⁺ lifetime ranges from a few minutes to 10^5 s with altitudes [e.g., Plane et al., 2015]. It seems to be roughly consistent with the delayed appearance of FeS. In addition, we plan to discuss the observed results based on numerical calculations in Fe/Fe+ chemical reactions with vertical ion transportation.

Keywords: Mesosphere and Lower Thermosphere, Metallic atom layer, Sporadic layer, Resonance scattering lidar

[E] Poster | P (Space and Planetary Sciences) : P-EM Solar-Terrestrial Sciences, Space Electromagnetism & Space Environment

📅 Fri. Jun 4, 2021 5:15 PM - 6:30 PM JST | Fri. Jun 4, 2021 8:15 AM - 9:30 AM UTC | 🏠 Ch.05_1

[P-EM13] Study of coupling processes in solar-terrestrial system

convener: Mamoru Yamamoto (Research Institute for Sustainable Humanosphere, Kyoto University), Yasunobu Ogawa (National Institute of Polar Research), Satonori Nozawa (Institute for Space-Earth Environmental Research, Nagoya University), Akimasa Yoshikawa (Department of Earth and Planetary Sciences, Kyushu University)

The Earth accepts vast input of energy and material from the Sun. The Earth's environment is maintained by the balance between their inputs and outputs. It is therefore important to study energy and mass transport on the Earth. This is an international session that discusses studies of the coupling processes in the Sun-Earth system based on the project "Study of coupling processes in solar-terrestrial system" that was constantly approved by the Master Plan 2014/2017/2020 of Science Council of Japan. The facilities and networks included are Equatorial MU Radar (EMU) in Indonesia to study the whole equatorial atmosphere, the EISCAT_3D radar system in northern Scandinavia to study detailed structures and elementary processes of the magnetosphere-ionosphere coupling in the polar region, and global networks of various ground-based instruments and observation data. We will show the current status of the project and discuss sciences by soliciting variety papers. This session is open to the world, and we strongly encourage submission of papers related to other facilities and projects, i.e., atmospheric or incoherent scatter radars, observation networks, satellites, and simulation or theoretical studies, etc.

[PEM13-P01] Status of Equatorial MU Radar project in 2021

*Mamoru Yamamoto¹, Hiroyuki Hashiguchi¹, Tatsuhiro Yokoyama¹, Toshitaka Tsuda¹ (1. Research Institute for Sustainable Humanosphere, Kyoto University)

[PEM13-P02] Development of instruments for dual-band beacon (DBB) experiment of total electron content (TEC)

*Mamoru Yamamoto¹ (1. Research Institute for Sustainable Humanosphere, Kyoto University)

[PEM13-P03] Development of multi-scale numerical simulation model for the study on ionospheric disturbances

*Tatsuhiro Yokoyama¹, Taichi Komoto¹ (1. Research Institute for Sustainable Humanosphere, Kyoto University)

[PEM13-P04] Study on adaptive clutter rejection system using external receiving antennas for the MU radar

*Ryo Yabuki¹, Hiroyuki Hashiguchi¹, Issei Terada¹, Mamoru Yamamoto¹ (1. Research Institute for Sustainable Humanosphere, Kyoto University)

[PEM13-P05] Volume Scatter Simulation for 3D Wind Vector Estimation using Radar Inversion

*Ryosuke Tamura¹, Koji Nishimura¹, Hiroyuki Hashiguchi¹ (1. Research Institute for Sustainable Humanosphere)

[PEM13-P06] Multiple equatorial ionospheric observation project based on FMCW radar combining MAGDAS/SDR-based scintillation detector

*Akiko Fujimoto¹, Shuji Abe², Toru Mikura¹, Akihiro Ikeda³, Akimasa Yoshikawa² (1. Kyushu Institute of Technology, 2. Kyushu University, 3. National Institute of Technology, Kagoshima College)

[PEM13-P07] Development of an Autonomous Method for Equatorial Spread-F (ESF) Detection of SEALION Ionosonde Data

*Septi Perwitasari¹, Kornyanat Hozumi¹ (1. National Institute of Information and Communications Technology)

[PEM13-P08] Progress of atmospheric coupling studies with the EISCAT_3D radar system

*Hitoshi Fujiwara¹, Satonori Nozawa², Yasunobu Ogawa³, Yasunobu Miyoshi⁴ (1.Education and Research Center for Sustainable Development/Faculty of Science and Technology, Seikei University, 2.Institute for Space-Earth Environmental Research, Nagoya University, 3.National Institute of Polar Research, 4.Department of Earth and Planetary Sciences, Faculty of Sciences, Kyushu University)

[PEM13-P09] Optical calibration system of NIPR for aurora and airglow observations

*Yasunobu Ogawa^{1,2,3}, Akira Kadokura^{1,2,3}, Mitsumu K. Ejiri^{1,2} (1.National Institute of Polar Research, 2.The Graduate University for Advanced Studies, SOKENDAI, 3.Joint Support-Center for Data Science Research, Research Organization of Information and Systems)

[PEM13-P10] Spectroscopic and imaging observations for short-wavelength infrared aurora and airglow at Longyearbyen (78.2°N, 15.6°E) coordinated with EISCAT Svalbard radar and VLF/LF radio wave receivers.

*Takanori Nishiyama^{1,2}, Masato Kagitani³, Yasunobu Ogawa^{1,2,4}, Fuminori Tsuchiya³, Keisuke Hosokawa⁵, Takeshi Sakano³ (1.National Institute of Polar Research, 2.Department of Polar Science, The Graduate University for Advanced Studies, SOKENDAI, 3.Planetary Plasma and Atmospheric Research Center, Tohoku University, 4.Joint Support-Center for Data Science Research, Research Organization of Information and Systems, 5.The University of Electro- Communications)

[PEM13-P11] **Study of 8 hr and 6 hr atmospheric waves in the polar upper mesosphere and lower thermosphere by using sodium LIDAR data**

*Chiaki Morikawa¹, Satonori Nozawa¹, Takuo T. Tsuda², Takuya Kawahara³, Norihito Saito⁴, Satoshi Wada⁴, Toru Takahashi⁵, Tetsuya Kawabata¹, Chris Hall⁶ (1.ISEE, Nagoya University, 2.Department of Communication Engineering and Informatics, The University of Electro-Communications, 3.Faculty of Engineering, Shinshu University, 4.RIKEN Center for Advanced Photonics, RIKEN, 5.Electronic Navigation Research Institute, 6.UiT The Arctic University of Norway)

[PEM13-P12] Research on the Analysis of Nitric Oxide Molecular Spectral Data with Millimeter-wave Spectroscopic Observations in Tromsø, Norway

*Hiroyuki Goto¹, Akira Mizuno¹, Tomoo Nagahama¹, Tac Nakajima¹, Satonori Nozawa¹, Yasusuke Kojima¹, Tetsuya Kawabata¹, Ryuji Fujimori¹, Kazuji Suzuki¹, Yasunobu Ogawa² (1.Institute for Space Earth Environmental Research, Nagoya University, 2.National Institute of Polar Research)

[PEM13-P13] Aurora and airglow observations by an optical spectrograph at Tromsø, Norway

*Takuo T. Tsuda¹, Keisuke Hosokawa¹, Satonori Nozawa², Tetsuya Kawabata², Akira Mizuno², Shin-ichiro Oyama², Junichi Kurihara³, Kim Nielsen⁴ (1.University of Electro-Communications, 2.Nagoya University, 3.Hokkaido University, 4.Utah Valley University)

[PEM13-P14] Statistical investigation on thermospheric Na based on Na lidar observations at Tromsø

*Hatsumi Hyodo¹, Takuo T. Tsuda¹, Satonori Nozawa², Takuya Kawahara³, Norihito Saito⁴, Tetsuya Kawabata² (1.The University of Electro-Communications, 2.Nagoya University, 3.Shinshu University, 4.RIKEN)

[PEM13-P15] Automated detection system of aurora using deep learning: real-time operation in Tromsø, Norway

*Sota Nanjo¹, Keisuke Hosokawa¹, Satonori Nozawa² (1.The University of Electro-Communications, 2.Nagoya University)

[PEM13-P16] Observational evaluation of temperature/wind perturbations associated with small-scale AGWs : Parameterisation and validation of wave structures

*Shin Suzuki¹, Satonori Nozawa², Shin-ichiro Oyama², Kazuo Shiokawa² (1.Faculty of Regional Policy, Aichi University, 2.Institute for Space-Earth Environmental Research, Nagoya University)

Status of Equatorial MU Radar project in 2021

*Mamoru Yamamoto¹, Hiroyuki Hashiguchi¹, Tatsuhiro Yokoyama¹, Toshitaka Tsuda¹

1. Research Institute for Sustainable Humanosphere, Kyoto University

Research Institute for Sustainable Humanosphere, Kyoto University (RISH) has been studying the atmosphere and ionosphere by using radars. The first big facility was the MU (Middle and Upper atmosphere) radar installed in Shiga, Japan in 1984. This is one of the most powerful and multi-functional radar, and is successful of revealing importance of atmospheric waves for the dynamical vertical coupling processes. The next big radar was the Equatorial Atmosphere Radar (EAR) installed at Kototabang, West Sumatra, Indonesia in 2001. The EAR was operated under close collaboration with LAPAN (Indonesia National Institute for Aeronautics and Space), and conducted the long-term continuous observations of the equatorial atmosphere/ionosphere. The EAR, however, had a limited sensitivity to the MU radar as the total output power is just 1/10 to the MU radar. Our new project is to establish "Equatorial MU (EMU) Radar" just next to the EAR site in Indonesia. The EMU will have an active phased array antenna with the 163 m diameter and 1055 cross-element Yagis. Total output power of the EMU will be more than 500 kW. The EMU is the "MU radar class" facility, and can detect turbulent echoes from the mesosphere (60-80 km). In the ionosphere incoherent-scatter observations of plasma density, drift, and temperature would be possible. Multi-channel receivers will realize radar-imaging observations. Preparation for the EMU progress in many aspect including site survey for the construction, discussion with local government, etc. In March 2019, RISH and LAPAN have 1st Internal School on Equatorial Atmosphere (ISQUAR) 2019 with more than 100 participants at Bandung, Indonesia. The EMU is one of the key element in the project "Study of coupling processes in the solar-terrestrial system" that is one of the important project in the Master Plan 2014, 2017, and 2020 of the Science Council of Japan (SCJ). In the presentation we also touch recent status of the EAR as we now proceed recovery from the lightning damage that occurred in September 2019.

Keywords: Atmospheric radar, Equatorial atmosphere, Low-latitude ionosphere, Indonesia

Development of instruments for dual-band beacon (DBB) experiment of total electron content (TEC)

*Mamoru Yamamoto¹

1. Research Institute for Sustainable Humanosphere, Kyoto University

Measurement of total electron content (TEC). We are measuring the TEC by using dual-band beacon (DBB) technique. It is to transfer two radio signals at coherent but different frequencies. In the ionospheric plasma, the radio wave's propagation velocity is related to the frequency. By detecting the phase variation between two signals, we can estimate TEC through the radio propagation path. Conventional DBB experiments were carried out using the DBB transmitter on the low Earth orbit (LEO) satellites and receivers on the ground. The most commonly used frequencies are 150MHz and 400MHz. We developed GNU Radio Beacon Receiver (GRBR), the digital receiver, based on the software-defined radio technology. Our new development is the digital receiver GRBR-2, which measures the new beacon signal (401MHz/966MHz) from FORMOSAT-7/COSMIC-2 satellites launched in 2019. Observations with GRBR-2 have already been continued in Indonesia, Thailand, and Vietnam since September 2019. The DBB experiment were also conducted from sounding rockets to the ground. For the new rocket experiment planned in 2022, we are now developing a DBB transmitter and antennas on board of the rocket. On the other hand, recently, TEC observations using Global Navigation Satellite System (GNSS) signals become very popular. While the deployment of GNSS by USA, China, Russia, and the EU progress, the price of receivers have dropped dramatically. This situation helps us to develop a new GNSS-TEC receiver system for multiple-point measurements of the ionospheric. In the lecture we will discuss the current status of our developments.

Keywords: Digital radio technology, Total electron density, Sounding rocket, Dual-band beacon

Development of multi-scale numerical simulation model for the study on ionospheric disturbances

*Tatsuhiko Yokoyama¹, Taichi Komoto¹

1. Research Institute for Sustainable Humanosphere, Kyoto University

The ionospheric disturbance called plasma bubbles that occurs in the equatorial ionosphere has an irregular plasma density structure, so it degrades radio wave propagation from various satellites. Although plasma bubbles have been observed for more than 80 years, the generation mechanism has not been clarified and the prediction of plasma bubble occurrence is quite difficult. In this study, we have developed a new simulation model for studying plasma bubbles. Models that simulate the ionosphere can be roughly categorized into two types: the global ionosphere model and the local ionosphere model. There is a trade-off between computational domain and resolution. The High-Resolution Bubble (HIRB) model, which is one of the local ionospheric models, can reproduce plasma bubbles in 1 km resolution, but the simulation domain is limited to a narrow wedge region. The model developed in this study is a multi-scale numerical model which covers the whole longitude with a high resolution domain in the dusk region. The new model has the advantages of both global and local models and compensates both disadvantages. In the multi-scale simulation model, plasma bubbles are generated in the high-resolution domain and penetrate into the topside ionosphere. Although the resolution is not as high as the HIRB model, the generated plasma bubbles contain irregular plasma density structures. Plasma drift velocity simulated in the new model are consistent with observations in the all local time region. It indicates that the global simulation is well performed as well as the plasma bubble generation. In this study, the new simulation model has been developed to simulate the plasma bubble generation and global plasma drift velocity in the whole longitude with a multi-scale grid system. Since it is possible to express the plasma bubble more delicately by increasing spatial resolution, the performance of the new simulation will be greatly improved by parallel computing.

Keywords: plasma bubble, ionosphere, simulation

Study on adaptive clutter rejection system using external receiving antennas for the MU radar

*Ryo Yabuki¹, Hiroyuki Hashiguchi¹, Issei Terada¹, Mamoru Yamamoto¹

1. Research Institute for Sustainable Humanosphere, Kyoto University

Strong clutter echoes from a hard target such as a mountain or building sometimes cause problems of observations with atmospheric radars. In order to reject or suppress ground clutter echoes, it is effective to use NC-DCMP (Norm Constrained- Directionally Constrained Minimum Power) method, which makes null toward the direction of the clutter, if we can receive signals independently from plural antennas [Nishimura et al., JTech., 2012]. It has been demonstrated that the NC-DCMP method is effective to real observation data with the MU (Middle and Upper atmosphere) radar [Hashiguchi et al., Radio Sci., 2018]. Although NC-DCMP method suppresses clutter echoes with almost maintaining the shape of main lobe to add pseudo-noise compared with the conventional DCMP method, the signal-to-noise ratio (S/N) of atmospheric echoes is somewhat degraded. We studied the clutter suppression method with little S/N degradation by using external antennas.

In the NC-DCMP method, the following constrained optimization problem is solved :

$$\text{minimize } P = 1/2 w^H R_{xx} w$$

$$\text{subject to } C^T w^* = N \text{ and } |w^H w| \leq \delta N$$

P is the signal power, w is the weight vector, R_{xx} is the covariance matrix, C is the direction vector of the desired direction, N is the number of array antenna, δ is the norm constraint value, H is a Hermitian operator (complex conjugate transposition), T is a transposition operator, and $*$ denotes a complex conjugate. The gain is different for each sub-array or antenna, the magnitude of the direction vector may be as $C_i = \sqrt{G_i / \|G\|}$. For the special case of $G_1 \gg G_2, G_3, \dots$, $C = [1, 0, 0, \dots]^T$.

Four turnstile antennas were installed in the MU radar site. The signal from the antenna is sent to the MU radar observation room through the coaxial cable after amplified by the LNA with the limiter and BPF. It is further amplified by the LNA in the observation room, and then down-converted to intermediate frequency (5 MHz) signal to input to the multi-channel receiving system of the MU radar.

We compared the NC-DCMP method using the each received data of 25 channels, which is a conventional clutter suppression method, and the NC-DCMP method using the simple combination of 25 channels and 4 channels of external antennas. In the former case, the S/N of the atmospheric echoes is somewhat degraded, but in the latter case the main lobe shape is guaranteed by 25 channel simple synthesis, so the S/N degradation is not observed. In the latter case, the clutter suppression is sometimes insufficient. One cause is considered to be that the range mistakes happen between main and external antennas depending on the external antenna position and the clutter direction. The clutter suppression was improved by optimizing the range in the NC-DCMP processing. Another cause is considered to be that the current positions of external antennas are biased to the north side. Antenna positions should be optimized in the future.

We can apply the achievement of this study to the Equatorial MU radar (EMU), which is proposed to be constructed at West Sumatera, Indonesia. The EMU system is the similar as the MU radar, but its antenna consists of 1045 Yagi antennas with 55 groups and it has 64 receiver channels.

Keywords: Atmospheric radar, Clutter rejection, NC-DCMP method, MU radar

Volume Scatter Simulation for 3D Wind Vector Estimation using Radar Inversion

*Ryosuke Tamura¹, Koji Nishimura¹, Hiroyuki Hashiguchi¹

1. Research Institute for Sustainable Humanosphere

To estimate accurate 3-dimensional wind velocity and its dispersion by an atmospheric radar, Nishimura et al. [1] proposed Spectral Observation Theory (SOT). In this theory, we only postulate that the temporal function of each turbulence scattering obeys ergodic hypothesis. Then, the correlation function (CF) of the received signal is equal to the multiplication of scattering CF, two-way beam pattern CF and window CF; these CFs are determined by wind velocity, its dispersion, and observation time window, respectively. This implies that we can estimate those parameters by implicit inversion based on SOT, which we refer to as radar inversion technique (RI).

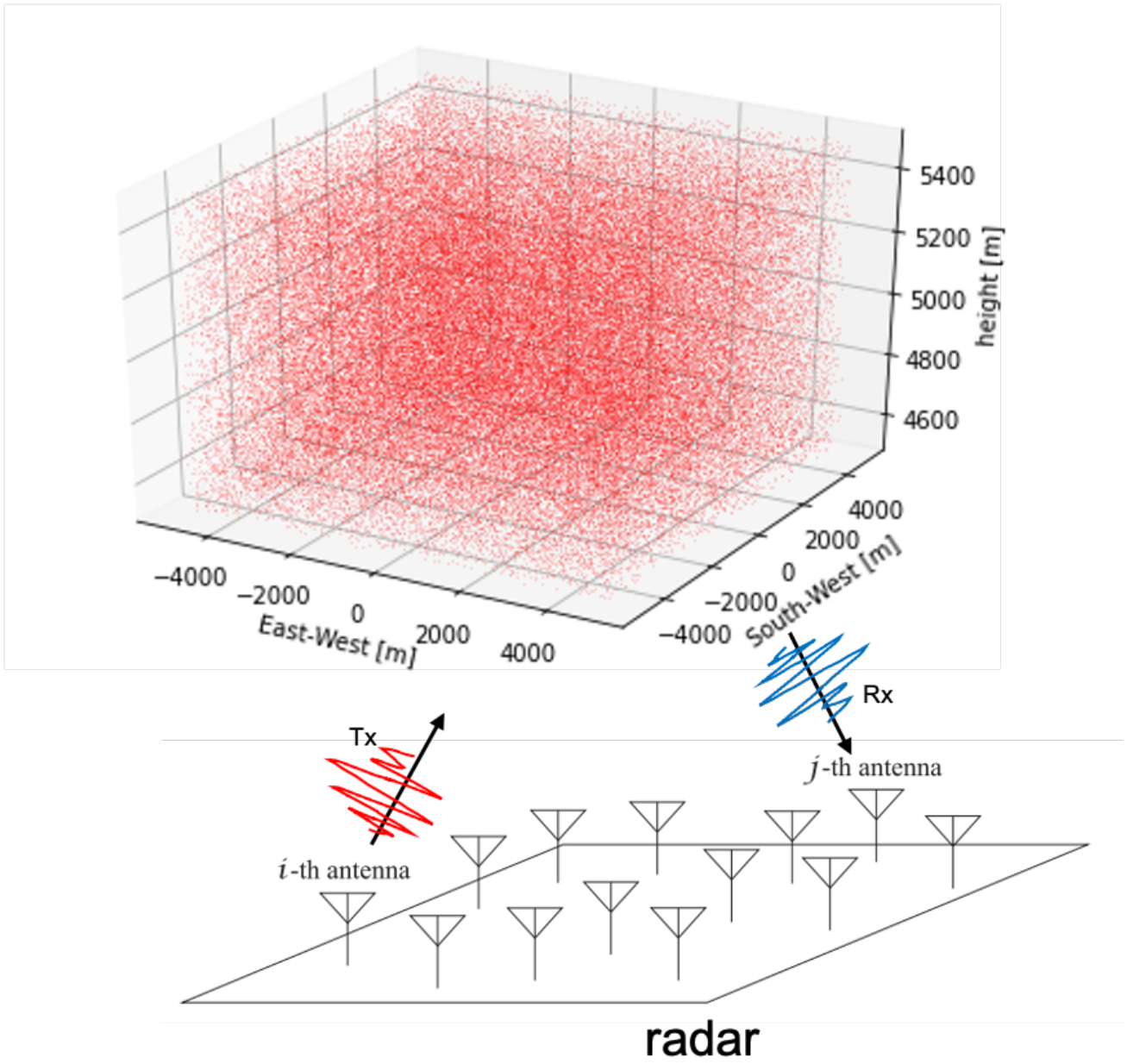
This new analysis technique is characterized in that using multi-received channels radar we are able to estimate the parameters from a single radar beam. By default, however, SOT does not consider aspect sensitivity [2] which is caused by specular reflection from the atmospheric stratified structure. As received signal is in many cases affected by aspect sensitivities and we do not know the true parameters, it is difficult to evaluate the validity of RI. For that reason, we conduct a 3-dimensional volume scatter simulation which assumes that a large number of moving point scatterers that model the atmospheric turbulence. The velocity of the points are random following the normal distribution having a given mean wind velocity and variance.

By this simulation, we can get idealized radar echoes from the atmospheric turbulence, which does and does not affected by the aspect sensitivity. Using the results of the simulations, we evaluate the accuracy of our proposed techniques.

[1] K. Nishimura, M. Kohma, K. Sato and T. Sato, " Spectral Observation Theory and Beam Debroadening Algorithm for Atmospheric Radar, " in IEEE Transactions on Geoscience and Remote Sensing, doi: 10.1109/TGRS.2020.2970200.

[2] Briggs, B. H. "Radar measurements of aspect sensitivity of atmospheric scatterers using spaced-antenna correlation techniques." Journal of atmospheric and terrestrial physics 54.2 (1992): 153-165.

Keywords: atmospheric remote sensing , atmospheric radar



Multiple equatorial ionospheric observation project based on FMCW radar combining MAGDAS/SDR-based scintillation detector

*Akiko Fujimoto¹, Shuji Abe², Toru Mikura¹, Akihiro Ikeda³, Akimasa Yoshikawa²

1. Kyushu Institute of Technology, 2. Kyushu University, 3. National Institute of Technology, Kagoshima College

In recent years, numerical experiments have advanced the understanding of the local generation mechanism of equatorial plasma bubbles (EPBs) that cause radio wave propagation abnormalities, but the relationship with the environmental field that controls the generation and suppression of EPBs has not yet been clarified. We focus on the global formation process of equatorial jet currents (EEJ), which is the electromagnetic drive sources of the environmental field that trigger the local generation mechanism of EPBs. This study aims to reveal the structure and generation mechanism of environmental fields in inner-magnetosphere and ionosphere that is linked to the development of EPBs.

We propose a three-dimensional coupling system of ionospheric E-F regions controlling EEJ as a model that connects the pre-sunset EEJ, PRE at near sunset, and EPBs after sunset. In order to detect this coupling system, we have planned a multi-ionospheric observation project with FM-CW (Frequency Modulated Continuous Wave) radar, MAGDAS (MAGnetic Data Acquisition System) magnetometer network and SDR-based scintillation detector. The FM-CW radar has two kinds of observation modes: one is Ionosonde mode and the other is Doppler mode. FM-CW radar enables continuous multi-mode ionospheric observation by switching between the detection of time evolution from PRE to plasma bubble by Ionosonde mode and the observation of F region electric field by Doppler mode. We have developed a new "autonomous FM-CW control system" without the manual concrete operation schedule. The new FM-CW system consists the supervised machine learning and reinforcement learning by using several ionospheric disturbance triggers. In the presentation, we will introduce the overview of the observation project and explain the new FM-CW control system.

Development of an Autonomous Method for Equatorial Spread-F (ESF) Detection of SEALION Ionosonde Data

*Septi Perwitasari¹, Kornyanat Hozumi¹

1. National Institute of Information and Communications Technology

Equatorial spread-F (ESF) is one of the most important features in space weather because of its significant effect on communication and navigation. Therefore, real-time information on the ESF occurrence will be useful to detect the degradation of radio propagation conditions. SEALION is an ionospheric observation network in the South East Asia that has been on operation since 2003. SEALION has 5 FMWC ionosondes installed in various locations; Chiang Mai (18.76°N, 98.93°E), Chumphon(10.72°N, 99.37°E), Phuket (7.90°N, 98.39°E), Bac Liu (9.30°N, 105.71°E), Cebu (10.35°N, 123.91°E) and Kototabang (0.20°S, 100.32°E). SEALION ionograms are often contaminated with various noises, such as stripes and random noises. Thus, a noise removal step is crucial before applying any detection algorithm. To remove the noises, we applied 4th degree polynomial fit to remove the stripes and 3x3 median filter to reduce the random noise. Following *Bhaneja et al., 2009*' method, the $h' F$ and $foF2$ trace are determined using an edge detection algorithm. Thresholds of non-spread F ionogram are determined by calculating the number of pixel within 100x100 pixel box from the edge of the $h' F$ and $foF2$. The thresholds were calculated from ~1000 nighttime ionograms from different seasons. We identified the range type ESF when the pixel counts within the $h' F$ box exceeded the threshold. The frequency type was identified when the pixel counts within the $foF2$ box exceeded the threshold. The mixed type are identified when the pixel counts in both $h' F$ and $foF2$ boxes were exceeding the threshold. We have applied this method to 2013 Chiang Mai ionograms. The preliminary result shows ~88 % matching with the manual scaling. The application of this method to the data from other ionosonde stations is underway. The details of the method, result, possible improvement of the current method and the design for a real-time warning system will be discussed during the presentation.

Keywords: Equatorial Spread-F, Ionogram, Autonomous detection

Progress of atmospheric coupling studies with the EISCAT_3D radar system

*Hitoshi Fujiwara¹, Satonori Nozawa², Yasunobu Ogawa³, Yasunobu Miyoshi⁴

1. Education and Research Center for Sustainable Development/Faculty of Science and Technology, Seikei University, 2. Institute for Space-Earth Environmental Research, Nagoya University, 3. National Institute of Polar Research, 4. Department of Earth and Planetary Sciences, Faculty of Sciences, Kyushu University

EISCAT_3D is a new research radar system for studies of the upper atmosphere and Geospace. This system consists of multipoint radars which will enable us to monitor spatio-temporal variations (3D structures) of atmospheric and plasma environments. In particular, EISCAT_3D will be a powerful tool for studies of the coupling between the lower and upper atmospheres. For example, it is pointed out that the eddy diffusion process in the mesosphere-lower thermosphere would be important to cause semi-annual mass density variations in the upper thermosphere. In order to understand the phenomena and obtain experimental proof, monitoring of the eddy/turbulent activities in the mesosphere-lower thermosphere is necessary. Furthermore, we should investigate dynamical, chemical, and radiation processes in the mesosphere-lower thermosphere to understand recovery of enhanced mass density in the upper thermosphere after a geomagnetic storm. Observations with the EISCAT_3D system will also contribute to understand the after-storm phenomena.

We point out some outstanding issues which will be research targets for the EISCAT_3D observations. Some examples of numerical simulations will be shown to collaborate with the EISCAT_3D system.

Keywords: EISCAT_3D, multipoint radars, atmospheric coupling, thermosphere, simulation, mesosphere

Optical calibration system of NIPR for aurora and airglow observations

*Yasunobu Ogawa^{1,2,3}, Akira Kadokura^{1,2,3}, Mitsumu K. Ejiri^{1,2}

1. National Institute of Polar Research, 2. The Graduate University for Advanced Studies, SOKENDAI, 3. Joint Support-Center for Data Science Research, Research Organization of Information and Systems

Calibration of optical instruments is important for accurate measurement of the absolute emission intensity of aurora and airglow. The National Institute of Polar Research (NIPR), Japan, has been operating a facility for the optical calibration which consists of three independent calibration systems to share with collaborating researchers. This paper introduces an outline of the facility and specifications of each system, calibration procedures, and examples of calibration results. With this facility, we can obtain the calibration data for the absolute sensitivity of optical instruments with an accuracy of about 2% within a wavelength range between 420 and 1050 nm. In addition, it is possible to calibrate transmission of optical filters and also relative sensitivity of optical instruments as a function of wavelengths. Current facility, upgraded in 2012, has been used by many researchers to calibrate their various optical instruments.

Reference:

Ogawa, Y., A. Kadokura, M. K. Ejiri, Optical calibration system of NIPR for aurora and airglow observations, *Polar Science*, doi:10.1016/j.polar.2020.100570, 2020.

Keywords: Aurora, Airglow, Calibration

Spectroscopic and imaging observations for short-wavelength infrared aurora and airglow at Longyearbyen (78.2°N, 15.6°E) coordinated with EISCAT Svalbard radar and VLF/LF radio wave receivers.

*Takanori Nishiyama^{1,2}, Masato Kagitani³, Yasunobu Ogawa^{1,2,4}, Fuminori Tsuchiya³, Keisuke Hosokawa⁵, Takeshi Sakanoi³

1. National Institute of Polar Research, 2. Department of Polar Science, The Graduate University for Advanced Studies, SOKENDAI, 3. Planetary Plasma and Atmospheric Research Center, Tohoku University, 4. Joint Support-Center for Data Science Research, Research Organization of Information and Systems, 5. The University of Electro- Communications

We are currently developing and testing a 2-D imaging spectrograph to evaluate spatial and temporal characteristics of dayside aurora. It is designed for short-wavelength infrared (SWIR) wavelength ranging from 1.1 to 1.3 microns covering strong auroral emissions in N_2^+ Meinel band (0-0) and N_2 1st Positive bands (1-2 and 0-1) as well as airglow emissions in OH Meinel bands (5-2, 6-3, and 7-4) and O_2 IR band. Its field-of-view (FOV) and angular resolution are 55 degrees and 0.11 degrees per pixel, respectively. If a 30-microns slit is used, wavelength resolutions are 2230 and 5070, with two different gratings (950 lpmm and 1500 lpmm). A signal-to-noise ratio for 1 kR emissions is expected to be larger than 1.0 in a few seconds exposure time. Therefore, we can investigate temporal variability of dayside reconnection and pulsating auroras with sufficient sampling rates of a few seconds. In a test observation, we successfully measured airglow spectrum for OH (7-4) band and O_2 IR band in a twilight condition (solar zenith angle, SZA, is about 96°).

The spectrograph will be installed at The Kjell Henriksen Observatory/The University Centre in Svalbard (KHO/UNIS), Longyearbyen (78.2°N, 15.6°E) by the end of 2021. Taking advantage of its location, 24-hours continuous observations can be expected (SZA larger than 96°) near the winter solstice. Coordinated studies with active/passive radio remote sensing, such as EISCAT Svalbard radar and VLF/LF radio wave receivers, are planned. In addition, we start to consider a brand-new SWIR imager or echelle spectrograph that will be introduced at KHO/UNIS after 2022. A detailed specification of the instrument is presented as well.

Keywords: Aurora and airglow, Short-wavelength infrared, EISCAT Svalbard radar, VLF/LF radio wave receivers, M-I coupling, Mesosphere and Lower Thermosphere

Study of 8 hr and 6 hr atmospheric waves in the polar upper mesosphere and lower thermosphere by using sodium LIDAR data

*Chiaki Morikawa¹, Satonori Nozawa¹, Takuo T. Tsuda², Takuya Kawahara³, Norihito Saito⁴, Satoshi Wada⁴, Toru Takahashi⁵, Tetsuya Kawabata¹, Chris Hall⁶

1. ISEE, Nagoya University, 2. Department of Communication Engineering and Informatics, The University of Electro-Communications, 3. Faculty of Engineering, Shinshu University, 4. RIKEN Center for Advanced Photonics, RIKEN, 5. Electronic Navigation Research Institute, 6. UiT The Arctic University of Norway

Characteristics of 8 hr and 6 hr atmospheric waves in the polar upper Mesosphere and Lower Thermosphere (MLT) region over 7 years between 2012 and 2019 will be presented. Wind velocity and temperature data obtained by the solid state sodium lidar located at Tromsø (69.6 deg N, 19.2 deg E), Norway have been used to analyze these waves. Short periodic tidal waves are poorly known in comparison with 12 hr and 24 hr tidal waves even though an amplitude of the 8 hr tide becomes sometimes comparable to that of 24 hr tidal wave in the polar MLT region [Thayaparan, 1997; Younger et al., 2002]. Previous studies based on observations [Thayaparan, 1997; Akmaev, 2001; Younger et al., 2002; Moudden et al., 2013] and a model [Smith, 2001] indicated that solar heating and nonlinear interactions of 12 hr and 24 hr tides can be considered to generate the 8 h tide. Moudden and Forbes [2013] using TIMED/SABER observations showed that the 8 hr tide achieved maximum amplitudes of order of 5 K (10 K) at 90 km (110 km) at the equatorial region. Pancheva et al. [2021] using wind data by meteor radar at Tromsø over 16 years (2003-2018) showed that, in general, the 8 hr and 6 hr tides had inter annual variability with a quasi-2-year-period, and vertical upward propagating of these waves had different wavelength according to season.

By utilizing both temperature and wind velocity data, we have investigated the characteristics of 8 hr and 6 hr atmospheric waves between 80 and 105 km in terms of altitude variations and day-to-day variations above Tromsø. We have analyzed the data of about 1400 hours (85 nights) for 8 hr wave, and about 1700 hours (138 nights) for 6 hr wave. We will report relationships between these waves and the 12 hr wave in order to discuss generations of these waves, and possible contributions to a temperature structure and atmospheric static and dynamic instabilities between 80 and 105 km. These results are expected to help better understanding of roles of 8 hr and 6 hr waves in the polar MLT region.

REFERENCES:

Akmaev, R. A., Seasonal variations of the terdiurnal tide in the mesosphere and lower thermosphere: A model study, *Geophysical Research Letters*, 28, 3817–3820, <https://doi.org/10.1029/2001GL013002>, 2001.

Moudden, Y., and J. M. Forbes, A decade-long climatology of terdiurnal tides using TIMED/SABER

observations, *Journal of Geophysical Research: Space Physics*, 118, 4534–4550, <https://doi.org/10.1002/jgra.50273>, 2013

Pancheva, D., P. Mukhtarov, C. Hall, A.K. Smith, M.Tsumi, Climatology of the short-period (8-h and 6-h) tides observed by meteor radars at Tromsø and Svalbard, *Journal of Atmospheric and Solar Terrestrial Physics*, 212, 105513, <https://doi.org/10.1016/j.jastp.2020.105513>, 2021

Smith, A.K., and D. A. Ortland, Modelling and analysis of the structure and generation of the terdiurnal tide, *Journal of the Atmosphere Sciences*, 5, 3116–3134, 2001.

Thayaparan, T., The terdiurnal tide in the mesosphere and lower thermosphere over London, Canada (43 deg N, 81 deg W), *Journal of Geophysical Research*, 102, 21,695–21,708, 1997.

Younger, P.T., D. Pancheva, D. Middleton, H. R., and Mitchell, N. J, The 8-hour tide in the Arctic mesosphere and lower thermosphere. *Journal of Geophysical Research*, 107(A12), 1420. <https://doi.org/10.1029/2001JA005086>, 2002.

Keywords: atmospheric waves, polar MLT region, sodium lidar, Tidal wave, Tromsø

Research on the Analysis of Nitric Oxide Molecular Spectral Data with Millimeter-wave Spectroscopic Observations in Tromsø, Norway

*Hirofumi Goto¹, Akira Mizuno¹, Tomoo Nagahama¹, Tac Nakajima¹, Satonori Nozawa¹, Yasusuke Kojima¹, Tetsuya Kawabata¹, Ryuji Fujimori¹, Kazuji Suzuki¹, Yasunobu Ogawa²

1. Institute for Space Earth Environmental Research, Nagoya University, 2. National Institute of Polar Research

In the polar regions, it is known that ozone in the stratosphere and mesosphere is destroyed by the downward transport of odd nitrogen (NO_x), which increase in the upper layers caused by energetic particle precipitation (EPP). Our research group has been observing variation of ozone and NO at Syowa Station in Antarctica since 2011, using molecular emission in the millimeter band due to the rotational transition of atmospheric molecules. As a result, it was found that photochemical reactions due to the sunlight and energetic electron precipitation (EEP) affect the variability of NO (Isono et al., JGR, 2014). However, in the summer season, when daylight hours are long, it became clear that it was not possible to separate the effect of photochemical reactions and that of EEP. Therefore, we are now aiming to solve this problem by installing a new instrument in the Arctic region (Tromsø, Norway), where the seasons are reversed, and conducting simultaneous monitoring at both the North and South polar regions. Because it was for the first time for millimeter-wave ground-based observations in Tromsø, the surrounding radio environment and the characteristics of the new observation equipment are not clear, and it is necessary to confirm what kind of quality data can be obtained. The purpose of this research is to obtain weak NO spectra with sufficient accuracy by the following three steps: 1) establishing a method to examine all acquired NO spectrum data and screen out those of poor quality that cannot be used for analysis; 2) examining optical depth data acquired to correct for the effects of the lower atmosphere and confirming whether it can be used for appropriate correction; and 3) performing appropriate baseline corrections to remove the continuum component in the NO spectral data.

First, NO spectral data from December 26, 2018 to March 10, 2019, when observations were conducted in Tromsø, were all scrutinized to determine the conditions for screening and removal of data containing large noise over all frequencies and spike-like noise in some specific frequencies. The possible origins of the overall noise and the spike-like noise are the contribution of the lower atmosphere due to bad weather and the interference of EISCAT UHF/VHF radar waves operating at close range, respectively.

Next, for the optical depth data, it was judged that a proper correction to the NO spectrum could not be made if there was a large temporal variation and the NO spectrum data for such a period was excluded from the analysis. The criterion for this was defined as the variance of the optical depth values measured during a day being larger than 0.04. On the other hand, we found a period when the calculated optical depth values were negative, which is not possible in principle. The reason of this was found to be the effect of the ice pillars hanging from the eaves at the outer side of the observation window. It was confirmed that the optical depth values could be calculated correctly by removing only the data that seemed to be affected by the ice pillars.

Finally, the baseline correction was performed on the remaining NO spectrum data from the screening. We succeeded in significantly detecting the weak NO spectrum. In addition, the column density of NO was determined from the spectrum. In the future, we are going to compare the results with data from the Syowa Station in Antarctica.

Keywords: Atmospheric Minor Molecules, Ozone, Nitric Oxide, Millimeter-Wave Spectrometer, Middle Atmosphere, Tromsø Norway

Aurora and airglow observations by an optical spectrograph at Tromsø, Norway

*Takuo T. Tsuda¹, Keisuke Hosokawa¹, Satonori Nozawa², Tetsuya Kawabata², Akira Mizuno², Shin-ichiro Oyama², Junichi Kurihara³, Kim Nielsen⁴

1. University of Electro-Communications, 2. Nagoya University, 3. Hokkaido University, 4. Utah Valley University

We have been operating an optical spectrograph for aurora and airglow observations at Tromsø, Norway (69.6°N, 19.2°E) since October 2016. The aperture of the spectrograph, i.e. F-number, is 4. The field-of-view (FOV) is 0.03°x2°, which is pointed at the local magnetic field-aligned direction. As an advantage, this spectrograph is capable to change its resolution and range in the observation wavelength by switching between multiple diffraction gratings.

One of research targets is the pulsating aurora (PsA). The PsA is a diffuse-type aurora, which is characterized by a repetition of brighter (ON) and darker (OFF) auroral emissions with periods of a few to a few tens of seconds. For PsA observation, the spectrograph is mainly tuned for visible range from 480 to 880 nm with a resolution of 1.6 nm and an interval of 0.4 nm. The time resolution is 1 second, and thus it can observe PsAs, which have periods of a few seconds or longer. We performed the data analysis of multiple PsA events, and revealed the PsA spectra for the first time. As the results, the OI 630.0-nm emissions and the N₂ 1PG emissions were found in the both spectra during ON and OFF in the PsA events. The spectra of pulsations were derived as difference spectra between the ON and OFF spectra. From the obtained spectra of pulsations, it is found that dominant pulsations at 630.0 nm were coming from the N₂ 1PG (10,7) band, and there were less or minor contributions of the OI 630.0 nm to pulsations at 630.0 nm.

Another target is the sodium (Na) nightglow from Na D₁ (589.756 nm) and D₂ (589.158 nm) transitions, which are chemically produced emissions in the sodium layer in the mesosphere and lower thermosphere (MLT). The chemical process in the Na D₁ and D₂ emissions have been explained by the Chapman mechanism for many years. The Chapman mechanism expects that the ratio between Na D₁ and D₂ emissions should be constant. On the other hand, some recent observations indicate the D₁/D₂ ratio can be variable, and propose a modification to the Chapman mechanism. To contribute this issue, we have been making spectral observations in the Na D₁ and D₂ lines. By switching to the 4x higher resolution diffraction grating in the spectrograph, the observation wavelength can be tuned for 540-640 nm with 0.4-nm resolution and 0.1-nm interval. Such high wavelength resolution enables that the Na D₁ and D₂ lines can be measured separately.

In the presentation, we will introduce some recent results obtained from such spectral observations in aurora and airglow above Tromsø.

Keywords: Optical spectrograph, Aurora, Airglow, Tromsø

Statistical investigation on thermospheric Na based on Na lidar observations at Tromsø

*Hatsumi Hyodo¹, Takuo T. Tsuda¹, Satonori Nozawa², Takuya Kawahara³, Norihito Saito⁴, Tetsuya Kawabata²

1. The University of Electro-Communications, 2. Nagoya University, 3. Shinshu University, 4. RIKEN

A number of observations of atmospheric metal layers, such as Na, Fe, and K layers, have been widely carried out by using resonance scattering lidars. These metal layers are normally distributed at 80-110 km altitudes, and it can be called normal layers or main layers. By contrast, metals extending from main layers to higher altitudes (above 110 km) are so-called thermospheric metals, which are one of the interesting subjects in the recent lidar studies. While its densities of metallic atoms/ions are quite low compared with those of main layers, such thermospheric metals have potentially an importance in the extension of height coverage by the lidar observations.

It is considered that the thermospheric metals appear intermittently to some extent (not always present). Concerning to Na, there are several reports in the thermospheric Na events at low-, mid-, and high-latitudes. In addition to such event studies, statistical investigation is needed for more comprehensive understanding in the thermospheric Na. Therefore, in this study, we have investigated statistical characteristics in the thermospheric Na (up to 140 km), based on Na lidar observations at Tromsø, Norway (69.6°N, 19.2°E). We have accumulated 274-nights of Na lidar data from 2015 to 2019, and have calculated Na density data with 4-km/60-min integration. After the calculations, we have examined significance in the Na density data based on evaluations of its observational uncertainty. Then, we have defined the significant Na density data above 110 km as the thermospheric Na. Finally, we have derived a probability of occurrence in the thermospheric Na from the number of events of the significant thermospheric Na data. From this data analysis, we have found that the thermospheric Na probabilities were ~95% at 113 km, ~78% at 121 km, and ~44% at 128 km. The results would indicate that the thermospheric Na is not so rare at 110-130 km. In the presentation, we will show these results, and discuss relationship between the thermospheric Na probabilities and the formation mechanism in the thermospheric Na.

Keywords: Thermospheric Na, Resonance scattering lidar, Tromsø

Automated detection system of aurora using deep learning: real-time operation in Tromsø, Norway

*Sota Nanjo¹, Keisuke Hosokawa¹, Satonori Nozawa²

1. The University of Electro-Communications, 2. Nagoya University

With the increase of the ability of computers, we can use the deep learning technique easily for various tasks. Such a technique has also been applied to the auroral physics in recent years. Most of optical observations of aurora store all the data overnight regardless of the appearance of aurora. Consequently, the obtained data contain a massive amount of non-auroral data which are basically useless for auroral physics. Classification of these data is important especially for the statistical analysis of aurora. Clausen and Nichisch (2018) classified the optical data taken from Time History of Events and Macroscale Interactions During Substorms (THEMIS) All-Sky Imager (ASI), the ASI network over North America, using the deep neural network technique. They classified optical images into 7 classes: arc, discrete, diffuse, cloudy, moon, and clear. Their result showed that the classifier has an accuracy of 82% for the validation data. The optical images from THEMIS ASI have no color information (i.e., panchromatic); thus, the result may change if we use optical observations performed by the digital single-lens reflex cameras having three color channels. Kvammen et al. (2020) classified the digital-auroral images into 7 classes. They used the model of ResNet-50 (He et al., 2016) and the result had a precision of 92%; however, their classifier does not cover the non-auroral images. For this reason, we are still not able to analyze a massive number of digital images including the non-auroral images (for example, cloudy, moony conditions) statistically. In this study, therefore, we created a classifier, which can handle all digital camera images including the non-auroral images, using ResNet-50. The classes are arc, discrete, diffuse, aurora+moon, aurora+cloud, clear, cloudy, and dusk/dawn. The training result has a precision of 92%. We published the training data and analysis results on the website. The website also notifies the appearance of aurora in real-time. In the presentation, we will introduce how to use the website and the results of the statistical analysis for the 10 seasons from 2009 to 2020.

Keywords: Machine Learning, Aurora, Digital camera observation, Statistical analysis

Observational evaluation of temperature/wind perturbations associated with small-scale AGWs : Parameterisation and validation of wave structures

*Shin Suzuki¹, Satonori Nozawa², Shin-ichiro Oyama², Kazuo Shiokawa²

1. Faculty of Regional Policy, Aichi University, 2. Institute for Space-Earth Environmental Research, Nagoya University

The Tromsø Na lidar operated by the Institute for Space-Earth Environmental Research, Nagoya University has monitored wind and temperature structures associated with auroral activity in the high latitude upper atmosphere since 2010. Although the observations are limited during the winter night, the lidar detected atmospheric wave signatures with period of a few hours and temperature change related to the wave propagation with high precision (less than 1K). Furthermore, this lidar started five-direction observation from 2012: horizontal distance between the beam positions are 58 km or 22 km at a height of 100 km and the observational setup can detect smaller-scale perturbations.

In this study, we tried to identify small-scale (less than 100 km) and short-period (less than 1 h) gravity waves by using the Tromsø Na lidar. Gravity waves contribute significantly to the wind field and thermal balance in the mesosphere and lower thermosphere (MLT) region because they vertically transport horizontal momentum from the lower atmosphere. It is also pointed that, in particular, smaller-scale and shorter-period waves tend to transport larger momentum. Small-scale gravity waves in the MLT region are mainly studied with airglow imaging measurements. The airglow measurements, however, cannot observe temperature and wind perturbations directly, which are necessary for the estimation of wave's momentum flux. Based on temperature and wind perturbations with the five-direction lidar, we evaluate dynamical effect of small-scale gravity waves propagating in the upper atmosphere quantitatively.

In this presentation, we will report some initial results derived from simultaneous measurements of the lidar and airglow imaging in 2013-2016.

Keywords: Na lidar, atmospheric gravity waves

[E] Poster | P (Space and Planetary Sciences) : P-CG Complex & General

📅 Fri. Jun 4, 2021 5:15 PM - 6:30 PM JST | Fri. Jun 4, 2021 8:15 AM - 9:30 AM UTC | 🏠 Ch.06_1

[P-CG17] Future missions and instrumentation for space and planetary science

convener: Kazunori Ogawa (Japan Aerospace Exploration Agency), Mitsunori Ozaki (Faculty of Electrical and Computer Engineering, Institute of Science and Engineering, Kanazawa University), Naoya Sakatani (Department of Physics, Rikkyo University), Kazuo Yoshioka (Graduate School of Frontier Science, The University of Tokyo)

Not only national space agencies but some universities and even companies in the world are now leading a number of space science and exploration missions and also energetically initiating new research activities for satellite and rocket developments and international collaborations in these days because the Earth observations from the space and the space explorations could be achieved much easier than a few decades ago (e.g. ultra-small satellite). The deployment to the space, which itself is not purely a scientific purpose but one of methods for better sciences, is vigorously motivating the technical innovation and the educational development. For successful space missions, it is also crucial to research and develop aim-oriented on-board instruments, and the fundamental research and development of observational instrumentation with future perspectives could totally lead space missions in some case. Detailed investigation and evaluation on various on-board instruments are needed during their proposals, selections, and fabrications in order to promote the missions, and inevitably we have to make multi-sided arrangements and evolution at every process and aspect of any type of space missions, independently of their mission sizes. In this session, we focus on these comprehensive research activities in the space and astronomy missions, including the mission integrations and the individual instrumental developments, and we also call many presentations showing the uniqueness and renovation regarding the mission strategy and methodology, and the status and latest results in the related state-of-the-art researches and developments, which would provide all of researchers and developers with invaluable opportunities for active discussion, information sharing, and collaboration toward the realization of more missions for more fruitful space sciences and explorations in nearer future.

[PCG17-P01] Challenges for ion measurements in a comet mission

*Satoshi Kasahara¹, Shoichiro Yokota², Kazushi Asamura³, Yoshifumi Saito³, Masafumi Hirahara⁴ (1.The University of Tokyo, 2.Osaka University, 3.ISAS, 4.Nagoya University)

[PCG17-P02] Miniaturization of energetic electron sensor for future planetary explorations using ASIC

*Shin Sugo¹, Satoshi Kasahara¹, Ikeda Hirokazu², Hirotsugu Kojima³, Motoyuki Kikukawa³, Takahiro Zushi⁴ (1.The University of Tokyo, 2.Institute of Space and Astronautical Science, 3.Research Institute for Sustainable Humanosphere, Kyoto University, 4.National Institute of Technology, Nara College)

[PCG17-P03] Development of a miniature ion-trap Fourier-transform mass spectrometer for future space missions

*Oya Kawashima¹, Satoshi Kasahara¹, Yoshifumi Saito², Shoichiro Yokota³, Masafumi Hirahara⁴, Seiji Sugita¹ (1.The university of tokyo, 2.ISAS/JAXA, 3.Osaka univ., 4.Nagoya Univ.)

[PCG17-P04] Development of the bread board model of the Life-signature Detection Microscope (LDM)

*Yoshitaka Yoshimura¹, Akihiko Yamagishi², Atsuo Miyakawa², Eiichi Imai³, Satoshi Sasaki⁴, Mita Hajime⁵, Kensei Kobayashi⁶, Yoko Kebukawa⁶, Naoto Sato⁷, Takehiko Satoh⁸, Keigo Enya⁸, Kazuhisa Fujita⁸, Tomohiro Usui⁸ (1.Tamagawa University, 2.Tokyo University of Pharmacy and Life Science, 3.Nagaoka University of Technology, 4.Tokyo University of Technology, 5.Fukuoka Institute of Technology, 6.Yokohama National University, 7.Meiji University, 8.Japan Aerospace Exploration Agency)

[PCG17-P05] Investigation of the response of an all-sky electrostatic analyzer

Tzu-Fang Chang¹, *SHENG-CHENG TSAI¹, Chih-Yu Johnson Chiang¹ (1.Institute of Space and Plasma Sciences, National Cheng Kung University, tainan, taiwan)

[PCG17-P06] Radar experiments for sounding internal structures of the asteroids using scale-down model

*Atsushi Kumamoto¹, Hideaki Miyamoto², Toshiyuki Nishibori³, Fuminori Tsuchiya¹, Ken Ishiyama⁴ (1.Graduate School of Science, Tohoku University, 2.Graduate School of Engineering, The University of Tokyo, 3.Japan Aerospace Exploration Agency, 4.National Institute of Technology, Tsuruoka College)

[PCG17-P07] **Development and Integration of the High-Speed Current Detection Circuits in Particle Sensors**

*Motoyuki Kikukawa¹, Hirotsugu Kojima¹, Yoshifumi Saito², Kazushi Asamura² (1.Research Institute for Sustainable Humanosphere, Kyoto University, 2.Institute of Space and Astronautical Science)

[PCG17-P08] The new type of plasma wave instruments capable of both waveform and spectrum observation

*Takahiro Zushi¹, Hirotsugu Kojima² (1.National Institute of Technology, Nara College, 2.Research Institute for Sustainable Humanosphere, Kyoto University)

[PCG17-P09] S Band and UHF Band Communication Systems for Kanazawa-SAT3 Microsatellite

*Mayuko Tachiyama¹, Sota Yamamoto¹, Koyo Ina¹, Tomohiko Imachi¹, Satoshi Yagitani¹, Daisuke Yonetoku¹, Yoshiya Kasahara¹, Tatsuya Sawano¹, Makoto Arimoto¹ (1.Kanazawa University)

[PCG17-P10] Attitude Control System for Kanazawa-SAT3 Microsatellite

*Kohei Fujiki¹, Shinsaku Suzukawa¹, Yuki Yasuda¹, Tomohiko Imachi¹, Satoshi Yagitani¹, Yoshiya Kasahara¹, Daisuke Yonetoku¹, Tatsuya Sawano¹, Makoto Arimoto¹ (1.Kanazawa University)

[PCG17-P11] Developing software for Kanazawa-SAT3

*Yuta Inoue¹, Akane Sasaoka¹, Yasuhiro Kishino¹, Tomohiko Imachi¹, Yoshiya Kasahara¹, Tatsuya Sawano¹, Satoshi Yagitani¹, Daisuke Yonetoku¹, Makoto Arimoto¹ (1.Kanazawa University Graduate School)

[PCG17-P12] Development of mid-IR heterodyne spectrometer with hollow optical fiber for solar system exploration

*Satoki Tsukada¹, Hiromu Nakagawa¹, Isao Murata¹, Yasuhiro Hirahara², Yasumasa Kasaba¹, Takashi Katagiri³, Yuji Matsuura⁴, Akiho Miyamoto¹, Atsushi Yamazaki⁵ (1.Science, Tohoku Univ., 2.Environmental Studies, Nagoya Univ., 3.Science and Engineering for Education, Toyama Univ., 4.Biomedical Engineering, Tohoku Univ., 5.Institute of Space and Astronautical Science, Japan Aerospace Exploration Agency)

[PCG17-P13] Investigation of potential candidates for a sample return mission

*Yuri Shimaki¹, Shigeru Wakita^{2,3}, Seitaro Urakawa⁴, Peng Hong⁵, Fumihiko Usui¹, Moe Matsuoka¹, Naoya Sakatani⁶, Satoshi Tanaka¹, Sunao Hasegawa¹, Daisuke Kuroda⁷ (1.Institute of Space and Astronautical Science, Japan Aerospace Exploration Agency, 2.Massachusetts Institute of Technology, 3.Purdue University, 4.Japan Spaceguard Association, 5.Planetary Exploration Research Center, Chiba Institute of Technology, 6.Rikkyo University, 7.Kyoto University)

[PCG17-P14] Observation Plans and Development Status of MIRS: MMX Infrared Spectrometer on the MMX Spacecraft

*Takahiro Iwata¹, Hiromu Nakagawa², Fuminori Tsuchiya², Tomoki Nakamura², Maria Antonietta Barucci³, Jean-Michel Reess³, Pernelle Bernardi³, Alain Doressoundiram³, Sonia Fornasier³, Michel Le

Du⁴, Eric Sawyer⁴ (1.Institute of Space and Astronautical Science, Japan Aerospace Exploration Agency, 2.Tohoku University, 3.LESIA, Observatoire de Paris, 4.CNES)

Challenges for ion measurements in a comet mission

*Satoshi Kasahara¹, Shoichiro Yokota², Kazushi Asamura³, Yoshifumi Saito³, Masafumi Hirahara⁴

1. The University of Tokyo, 2. Osaka University, 3. ISAS, 4. Nagoya University

The Comet Interceptor mission, led by ESA, aims at a long period comet or an interstellar object. JAXA will provide an ultra-small (24 U) daughter spacecraft, whose closest approach will be less than 1,000 km, allowing the first-ever multi-spacecraft fly-by observations of a comet. The small gravity and high gas production rate of comets set neutral-plasma environments that are unique in the solar system, which provides insights into plasma universe. Here we present three challenges for ion measurements in Comet Interceptor: (1) harsh dust environment, (2) necessity of a large field of view, and (3) low-resource instrumentation.

Keywords: Cometary plasma, in-situ mass spectrometry

Miniaturization of energetic electron sensor for future planetary explorations using ASIC

*Shin Sugo¹, Satoshi Kasahara¹, Ikeda Hirokazu², Hirotsugu Kojima³, Motoyuki Kikukawa³, Takahiro Zushi⁴

1. The University of Tokyo, 2. Institute of Space and Astronautical Science, 3. Research Institute for Sustainable Humanosphere, Kyoto University, 4. National Institute of Technology, Nara College

In our solar system, the outer space is filled with plasma, a gas made up of charged particles. The origins of plasma in our solar system are the Sun and the ionized atmosphere of planets and satellites, and their energy is typically less than 10 eV. Nevertheless, high energy electrons (> keV) are observed in all planetary magnetospheres in our solar system. Some of these electrons precipitate into the atmosphere and deposit their energy. To clarify the acceleration mechanism of high energy electrons and to evaluate the effects of energetic electrons on the planetary environment are the important issues in planetary science. ~10-100 keV is key energy range because this is transition energy from thermal to non-thermal distributions of energy spectrum. Recently, APDs (Avalanche PhotoDiodes), which are detectors with high detection efficiency for ~10-100 keV electrons, have been applied to an energetic electron sensor. In this research, we aim to apply APDs to an energetic electron sensor for future planetary explorations. For planetary explorations, which place stringent limitation on payload mass, we aim to miniaturize the sensor by applying the ASIC (Application Specific Integrated Circuit) technology to analog signal processing circuits for APDs. It is composed of preamplifiers, shaping amplifiers, peak holders, and Analog-to-digital converters. We optimized ASIC to process signals from APDs and designed an ASIC so that its dynamic range and the wave form peaking time to be $\sim 10^6 e^-$ and $\sim 1 \mu s$, respectively, in consideration of the gain and the noise characteristics of the assumed detector (APD). The performance was confirmed in the simulation. We conducted layout design of the circuit to fit 5 mm×5 mm chip, which is about 100 times smaller than analog circuit board before ASIC. Furthermore, we developed the circuit to control the ASIC chip and confirmed its operation in simulation.

Development of a miniature ion-trap Fourier-transform mass spectrometer for future space missions

*Oya Kawashima¹, Satoshi Kasahara¹, Yoshifumi Saito², Shoichiro Yokota³, Masafumi Hirahara⁴, Seiji Sugita¹

1. The university of tokyo, 2. ISAS/JAXA, 3. Osaka univ., 4. Nagoya Univ.

In recent solar system exploration missions, high-resolution mass spectrometry has played an important role. In Rosetta mission, for example, carried a double focusing mass spectrometer with high resolving power ($m/\Delta m \sim 3,000$). This mass spectrometer conducted a variety of new chemical/isotopic measurements that greatly improved our understanding of the Jupiter-family comets. Such examples show that high-resolution mass spectrometry is a powerful technique for understanding the evolution of planetary bodies. However, most of the conventional high-resolution mass spectrometers (MSs) are large (~ 1 m in linear dimension) and heavy. This limits the opportunity of high-resolution mass spectrometry despite their high performance. The aim of this study is to develop a compact high-resolution MS. Our design is based on OrbitrapTM, which has recently been used in ground facilities. We have previously showed high mass resolution ($m/\Delta m \sim 10,000$) can be achieved with a small size (~ 10 s cm in linear dimension), using numerical simulations. Then, we have been examining the performance of our new MS with test model experiments. In particular, we are currently working on the improvement of an ion resonator part, which directly determines the sensitivity/power consumption of the instrument. In this presentation, we will discuss the details of experimental tests and most recent results.

Keywords: Mass spectrometer

Development of the bread board model of the Life-signature Detection Microscope (LDM)

*Yoshitaka Yoshimura¹, Akihiko Yamagishi², Atsuo Miyakawa², Eiichi Imai³, Satoshi Sasaki⁴, Mita Hajime⁵, Kensei Kobayashi⁶, Yoko Kebukawa⁶, Naoto Sato⁷, Takehiko Satoh⁸, Keigo Enya⁸, Kazuhisa Fujita⁸, Tomohiro Usui⁸

1. Tamagawa University, 2. Tokyo University of Pharmacy and Life Science, 3. Nagaoka University of Technology, 4. Tokyo University of Technology, 5. Fukuoka Institute of Technology, 6. Yokohama National University, 7. Meiji University, 8. Japan Aerospace Exploration Agency

Present Mars is hostile to life, but recent findings tend to support the possible presence of microbes near the Mars surface. MSL Curiosity has found organic compounds [1], the temporal increase of methane concentration in the Martian atmosphere [2], and reduced sulfur compounds such as pyrite in Martian soil [3]. Methane and reduced sulfur compounds can be energy sources to support the growth of chemoautotrophic microbes [4]. The detection of hydrated salts at Recurring Slope Lineae suggested the possible presence of liquid water [5]. Since UV radiation, which is harmful to life, would be shielded by thin layers (less than a millimeter) of dust or regolith [6], microbes could survive under a depth of several centimeters from the surface. Although the Viking mission in the 1970s did not find evidence for life on the Mars surface [7], the sensitivity of the GC-MS (mass spectrometer) was found not to be very high. It was not able to detect 10^6 microbial cells in 1 gram soil [8, 9], indicating that another life detection program is necessary.

The Life-signature Detection Microscope (LDM), which we have proposed [10], has the potential sensitivity much higher than the Viking instrument. The LDM is based on fluorescent microscopy and detects organic compounds, membrane structures, and catalytic activities stained by fluorescent pigments. This technique is especially useful for the detection of living microbes. It has the potential to visualize a single cell in micron scale. LDM scans about 1 mm^3 and detects less than 10^4 cells in 1 gram regolith, which is comparable to the least populated area of the terrestrial environment, such as the Atacama desert in Chile. If microbes are not detected, we can determine the upper limit of the microbial density, which is useful information to evaluate the risk of human contact with Martian microbes in future manned explorations.

We have developed the bread board model (BBM) of LDM which is composed of 4 parts: a sample chamber, a light source, a microscope, and a CMOS image sensor. The sample chamber has a sample unit which has a sample holder, 2 pigment solution tanks, a filter unit for concentrating cells. By moving the sample chamber, 1 mm^3 of the bottom of the sample holder and a filter unit are photographed by the image sensor through the microscope. The BBM successfully detected and visualized bacteria added in a Mars simulant, MGS-1, at a density of 10^4 cells g^{-1} .

References

- [1] Eigenbrode, J. L., et al., *Science*, 360 (2018) 1096-1101.
- [2] Webster, C. R., et al., *Science*, 360 (2018) 1093-1096.
- [3] Ming, D., et al., *Science*, 343 (2014) 1245267.
- [4] Yamagishi, A., et al., *Biological Sciences in Space*, 24 (2010) 67-82.
- [5] Ojha, L., et al., *Nature Geosci*, 8 (2015) 829-832.
- [6] Mancinelli, R. L., et al., *Planetary and Space Science*, 48 (2000) 1093-1097.
- [7] Margulis, L., et al., *J. Mol. Evol.*, 14 (1979) 223-232.
- [8] Glavin, D. P., et al., *Earth and Planetary Science Letters*, 185 (2001) 1-5.

- [9] Navarro-Gonzalez, R., et al., *Proc Natl Acad Sci U S A*, 103 (2006) 16089-16094.
[10] Yamagishi, A., et al., *Trans. JSASS, Aerospace Technology Japan*, 16 (2018) 299-305.

Keywords: Fluorescence microscope, Astrobiology, Life exploration

Investigation of the response of an all-sky electrostatic analyzer

Tzu-Fang Chang¹, *SHENG-CHENG TSAI¹, Chih-Yu Johnson Chiang¹

1. Institute of Space and Plasma Sciences, National Cheng Kung University, tainan, taiwan

Electrostatic analyzers are often used in spinning satellites to achieve the purpose of three-dimensional plasma measurement. Top hat electrostatic analyzers have been widely used to measure ion and electron fluxes variation in space. It has been widely used in satellite missions for space plasma measurement in the past two decades, and the observational data are of good quality. In recent years, more satellites are designed for multi-task observations, so satellites need to be designed for three-axis stabilization.

Therefore, this study will design a set of all-sky electrostatic analyzers to achieve the same purpose of three-dimensional plasma measurement. The measurement energy range is ~ 20 eV - 20 keV, and the total volume is within 3U, so as to be able to be carried on various scientific satellites as much as possible. In the study, we use Geant4 to investigate the response function of all-sky electrostatic analyzers, and the results will show the best design presented under different specifications.

Keywords: all-sky, electrostatic analyzer, Geant4, plasma

Radar experiments for sounding internal structures of the asteroids using scale-down model

*Atsushi Kumamoto¹, Hideaki Miyamoto², Toshiyuki Nishibori³, Fuminori Tsuchiya¹, Ken Ishiyama⁴

1. Graduate School of Science, Tohoku University, 2. Graduate School of Engineering, The University of Tokyo, 3. Japan Aerospace Exploration Agency, 4. National Institute of Technology, Tsuruoka College

For the preparation of sounding internal structures of the asteroids in future missions, radar experiments have been performed using a scale-down model. The internal structure of an asteroid tells us its history of accretion, metamorphism, differentiation impacts, disruption, and reassembly. Wilkison et al. (2002) compared several models of formation and internal structure models for 433 Eros. Based on the bulk porosity estimated from the mass and volume, and comparison of the sizes of the boulders and craters on the surface, 25143 Itokawa was suggested to be a rubble pile asteroid (Abe et al., 2006; Fujiwara et al., 2006). Imaging of the asteroid internal structure by radar was proposed in several studies. Simulations of radio wave propagation and internal structure imaging were performed by applying seismic migration technique and suggested that bistatic radar was more effective than monostatic radar (Sava et al., 2015; Grimm et al., 2015). Several simulations of radio wave propagation and radar tomography were also performed based on the concept of a bistatic radar system installed on multiple cube satellites (Pursiainen and Kaasalainen, 2016; Takala, 2016; Sousa et al., 2019). The purpose of this study is to perform the radar experiments of the radar sounding of the asteroid internal structures by using a scale-down model. In the radar experiments, 1 m scale-down asteroid model is measured by a bread-board model (BBM) of chirp radar operated in a frequency range from 1 to 3 GHz for demonstration of radar sounding 20-m asteroid in a frequency range from 50 to 150 MHz. In order to obtain reference data for the radar experiment, Finite-Difference Time-Domain (FDTD) simulation was performed. In two dimensional 400×400 grids, the internal permittivity structure of the asteroid model was defined. The permittivity of boulders (rocks) was in a range from 3 to 7 and that of regolith (sand) was 2. In the simulation box, the evolution of the electric field of radar pulse was calculated with changing the locations of transmitter installed on the main orbiter and receiver installed on the sub orbiter. The synthetic echo data can be obtained by sampling the calculated electric field at the receiver on the sub orbiter. In the synthetic radargram, we can find several echo profiles: (1) Diffracted pulses propagating outside of the asteroid, (2) pulses propagating inside of the asteroid, which is severely overlapped with (1) since the bulk permittivity range of the asteroid is ~2, (3) pulses propagating inside the asteroid and reflected at permittivity contrasts in the asteroid, which is not much overlapped with (1) and (2). We, therefore, use the echo profiles (3) for inversion analyses of the internal structures. For the initial trial, we applied Kirchhoff migration to radargram with an assumption of bulk permittivity of 2, and obtain the distribution of the reflectance in the asteroid, which shows good correspondence with the permittivity structure defined in the FDTD simulation.

Keywords: Internal structure of the asteroids, Bistatic radar, radio tomography, Finite-difference Time-domain (FDTD) method, Scale model experiment

Development and Integration of the High-Speed Current Detection Circuits in Particle Sensors

*Motoyuki Kikukawa¹, Hirotsugu Kojima¹, Yoshifumi Saito², Kazushi Asamura²

1. Research Institute for Sustainable Humanosphere, Kyoto University, 2. Institute of Space and Astronautical Science

In outer space near the earth, many high-energy electrons are captured in the radiation band. Since these electrons cause charging of satellites and interfere with their operations, it is important to predict a fluctuation of electron flux in the radiation band. When a geomagnetic storm occurs, electron flux in the radiation band decreases greatly, but after a while, the flux recovers to an original level. We assume that there are some kinds of accelerating mechanisms that produce relativistic energy electrons in space. One of the accelerating mechanisms is “wave-particle interaction.” In this theory, ions and electrons in the intermediate energy band (5-200 keV) are thought to excite plasma waves that produce relativistic energy electrons. However, particle observation techniques in this energy band are not yet sufficiently developed, and there are few examples of observations on wave-particle interactions. The Medium-Energy Particle Experiments (MEPs) are developed to observe particles in the intermediate energy band, and have electrodes in the shape of a spherical shell with an electric field applied to measure the velocity vector of particles coming inside.

To observe the wave-particle interaction, we need the phase difference information between the plasma wave vector and the particle velocity vector. In other words, the information on the time when the particle is arrived in the MEP is important. In order to obtain the time information, the satellite is equipped with a circuit that amplifies and detects the weak current pulses generated at the moment of particle arrival in the MEP. This is called the particle detection circuits, and these conventional circuits are composed of discrete electronic components. These discrete components lead to an increase in volume and weight. This is why they place a heavy burden on the satellite. We integrate the particle detection circuits using ASIC (Application Specific Integrated Circuit) technology. The developed chip is highly small and light-weight. Since the developed chip is expected to be mounted on micro-satellites, simultaneous multipoint observation of wave-particle interactions can be realized at low cost.

Our developed chip consists of two stages. The first stage is the current-voltage conversion circuit. It picks up each current pulse and converts into voltage signals with enough amplitude to drive the second stage. The second stage contains a comparator and a peak-hold circuit. They ensure picking up real signals by setting a threshold level.

In this study, we develop the circuit which can output detection signals within 30ns after the arrival of particles and can be reset within 12ns on inputting the reset command. The size of one channel of the developed circuit is 210 μm×570 μm. Since the conventional circuit was several centimeters in size, we have reduced the area of this circuit by more than one tenth in this study.

In this session, we show the details of the chip designed for the particle detection circuits including experimental results.

Keywords: Wave-particle interaction, MEP, Particle detection circuits, ASIC

The new type of plasma wave instruments capable of both waveform and spectrum observation

*Takahiro Zushi¹, Hirotsugu Kojima²

1. National Institute of Technology, Nara College, 2. Research Institute for Sustainable Humanosphere, Kyoto University

Recently, the miniaturization of the instruments onboard scientific satellites is required because of the diversification of observation targets and the use of microsatellites. In this study, we propose a miniaturized plasma wave instruments for both waveforms and spectrum using an ASIC with variable frequency characteristics to further reduce the size of the plasma wave instruments.

Plasma wave instrument is classified into two types: waveform type and spectrum type. Since these two types of instruments play complementary roles, it is common to have both types of instruments in recent scientific missions. These two types of instruments required different analog circuits, which led to the increase in size of the instruments. The analog circuits of the waveform type are required to have a wide bandwidth to cover the entire frequency coverage, while the spectral receiver is required to have a narrow bandwidth. The dedicated integrated circuit for the new instruments is designed to select from several cutoff frequencies of the band-limiting filter. This makes it possible to measure waveforms with a wide bandwidth when using as waveform type and with a narrow bandwidth when using as spectrum type. The new plasma wave instruments will be realized by combining such externally controllable analog circuits and digital circuits that perform the signal processing required for both the waveform and spectrum type instruments.

In the presentation, we will describe the detail design of the new plasma wave instruments and analog circuit. In addition, we will report the performance of the new receiver based on the simulation using system model.

Keywords: Plasma wave instruments, Plasma wave, Application specific integrated circuit

S Band and UHF Band Communication Systems for Kanazawa-SAT3 Microsatellite

*Mayuko Tachiya¹, Sota Yamamoto¹, Koyo Ina¹, Tomohiko Imachi¹, Satoshi Yagitani¹, Daisuke Yonetoku¹, Yoshiya Kasahara¹, Tatsuya Sawano¹, Makoto Arimoto¹

1. Kanazawa University

Kanazawa University is developing the first Kanazawa University's microsatellite, named as Kanazawa-SAT3(Study and Training in Space and Technology for Kanazawa Cube-Satellite). Kanazawa University satellite's mission object is to identify the source of gravitational waves by detecting the occurrence time and arrival direction of X-rays and gamma rays observed simultaneously with gravitational waves.

In this research, we are developing communication system for Kanazawa University satellite. Kanazawa University satellite has three communication systems, S band communication, UHF band communication and Iridium communication. These systems are composed of each antennas and transceivers. In this paper, we summarize S band communication system and UHF communication system in detail as the following.

S band system is a main communication system between the satellite and the ground station, and plays a role of high speed data communication and beacon transmission. This system, Kanazawa University satellite is equipped with two types of antennas: S band patch antennas and S beacon antennas. On the satellite, the S band patch antennas for both transmission and reception are mounted on the front panel and the rear panel of the satellite. The S beacon antennas for transmission are also mounted on both panels of the satellite. At the ground station, we use a parabolic antenna of 2.4 m in diameter at Kanazawa University. Currently, we have evaluated the characteristics of S-band patch antennas and S beacon antennas by computer simulations and direct measurements. As future work, we have to test wireless communication system using the S band antenna. And also, it is necessary to develop the communication software for transceiver.

About the UHF communication system, it is planed to use about 400 MHz for uplink and 460 MHz for downlink. This system plays a role of transmitting commands from the ground to the satellite and transmitting telemetry information from the satellite to the ground station. On the satellite, the antennas are mounted for receiving and transmitting separately on the front panel and the rear panel of the satellite. We adopt PIFA(planar inverted-F antenna) as UHF band antennas on the satellite. In this antenna, a dielectric medium is inserted between the patch plane and the ground plane to shorten the wavelength to miniaturize the size of the antenna. The plane plates are made of copper, and the dielectric is made of polycarbonate. We have evaluated the characteristics of PIFA by computer simulations and direct measurements. At the ground station, we use a Yagi antenna with 13 crossed elements at Kanazawa University. We designed a BPF to be installed in a ground station and evaluated the characteristics. As future work, we test wireless communication system using the PIFA and the Yagi antenna. Also, it is necessary to develop the communication software for transceiver.

Keywords: Microsatellite, Communication System, Kanazawa SAT3

Attitude Control System for Kanazawa-SAT3 Microsatellite

*Kohei Fujiki¹, Shinsaku Suzukawa¹, Yuki Yasuda¹, Tomohiko Imachi¹, Satoshi Yagitani¹, Yoshiya Kasahara¹, Daisuke Yonetoku¹, Tatsuya Sawano¹, Makoto Arimoto¹

1. Kanazawa University

Kanazawa University has been developing a micro satellite, Kanazawa- SAT3. The observation mission is estimation of the direction of gravitational wave arrival by X-rays. This mission aims to clarify the mechanism of black hole formation. The Kanazawa University satellite is equipped with RW(Reaction Wheel) and MTQ (Magnetic Torquer) as actuators, and STT (Star Tracker), GAS (Geomagnetic Aspect Sensor), GYR (Gyro Sensor), FSS (Fine Sun Sensor), CSS (Coarse Sun Sensor) and GPS (Global Positioning System) as sensors, and these devices are used to attitude control. In the Kanazawa University satellite, the SAPs(Solar Array Panels) are expanded after separation from the rocket, and stops the rotation of the satellite by detumbling control. After that, FSS and STT are used to determine whether day side or night side of the earth. If day side of the earth, sun supplement by using FSS. If night side of the earth, attitude determination by using STT. In stationary operation, the attitude control is conducted to keep the mission equipment facing the deep space direction. In this presentation, we report 1) A Study of Attitude Control System Using MTQ and GAS, 2) A Study on Attitude Control of RW and STT, and 3) Performance comparison and accuracy correction of angular velocity detection for GYR and STT.

MTQs are the device that generates a magnetic moment when current flows through its internal coil. The torque is generated by the interference between this magnetic moment and the earth's magnetic field, the satellite has 3 MTQs placed orthogonal tri-axially, and the direction of total magnetic moment is controlled by the balance of them. GAS is an instrument that detects geomagnetic vectors. MTQ and GAS are connected to a sub processing system named MC (Media Converter), and MC is connected to OBC (Onboard Computer) via UART communication. MC reads the strength of the geomagnetic field from GAS and send it to OBC, and also controls the electric current of each MTQ by PWM control, according to the command which is sent from OBC. We designed the system that performs control in 2-second cycles. When MTQ is activated, GAS detect the magnetic field including the one generated by MTQ, so that the processing routine should be adjusted to prevent this.

RWs are the device that control the attitude of satellite by rotating the internal rotor to generate reaction torque. To study the attitude control method using the RW, we placed a RW on air bearing and rotated, and measured the rotational speed by RE (Rotary Encoder) attached to the air bearing. In this way, we performed angular velocity control by P-control and angular control by PID-control.

STT is the device that observes position of stars in its view and outputs its quaternion and Euler angle of the STT cameras direction. Calculating the declination from the quaternions, the stellar determination accuracy of the STT at stationary conditions is determined to be of the order of 10^{-3} . And also, the STT has a MEMS gyro, and calculating the accuracy, it is on the order of 10^{-2} . The Kanazawa University satellite also has a gyro sensor on MC, and its accuracy is on the order of 10^{-1} , so STT is better in accuracy. However, since the MC is equipped with a microcontroller board, it has advantages in terms of time resolution and the ability to perform signal processing such as digital filtering.

The devices described in this presentation are currently tested for communication with OBC without any problems. In the future, it is necessary to develop OBC software that follows the control laws of the

satellite.

Keywords: Microsatellite, ACS, Kanazawa SAT3

Developing software for Kanazawa-SAT3

*Yuta Inoue¹, Akane Sasaoka¹, Yasuhiro Kishino¹, Tomohiko Imachi¹, Yoshiya Kasahara¹, Tatsuya Sawano¹, Satoshi Yagitani¹, Daisuke Yonetoku¹, Makoto Arimoto¹

1. Kanazawa University Graduate School

Kanazawa University is developing the first Kanazawa University's microsatellite, named as Kanazawa-SAT3. The mission is to detect the occurrence time and arrival direction of gamma rays and X-rays observed simultaneously with gravity waves.

In this research, we are developing software of OBC (Onboard Computer) for Kanazawa-SAT3. OBC controls all components aboard the satellite and edits the telemetry data to transmit the house keeping (HK) data and observation data to send to the earth. OBC is powered by Toppers, a real-time operating system. Toppers is developed in the ITRON specification and connected with OBC via RS 422 and GPIO interfaces.

The application part of onboard software consists of a Main function and eight tasks. OBC operates by periodically calling eight tasks.

Each task waits to be started in hibernation, and executes a process defined as being invoked by the Main function, and then repeats the loop that goes into hibernation again. Task1 performs management of commands. Task2 executes commands. Task3 sends telemetry data to the earth, collects data edits HK. Task4 controls and constantly processes bus components that require communication in a fast cycle. Task 5 controls other bus components. Task 6 performs recording and reading of the data recorder. Task 7 controls mission equipment. Task 8 is a reserve.

Related to developing the software, we held functional tests for components of FSS, GPS and BAT. Each test is composed unit and engagement with OBC. We confirmed the operation and output data of each component in the unit test, and confirmed that component control from the OBC and data reading by the OBC were possible in the engagement test with the OBC.

As a future work, we have to test other component and whole combination will be conducted on FM models, Also, it is necessary to develop an attitude control system needs to be implemented.

Development of mid-IR heterodyne spectrometer with hollow optical fiber for solar system exploration

*Satoki Tsukada¹, Hiromu Nakagawa¹, Isao Murata¹, Yasuhiro Hirahara², Yasumasa Kasaba¹, Takashi Katagiri³, Yuji Matsuura⁴, Akiho Miyamoto¹, Atsushi Yamazaki⁵

1. Science, Tohoku Univ., 2. Environmental Studies, Nagoya Univ., 3. Science and Engineering for Education, Toyama Univ., 4. Biomedical Engineering, Tohoku Univ., 5. Institute of Space and Astronautical Science, Japan Aerospace Exploration Agency

The mid-IR laser heterodyne spectroscopy provides high spectral resolution $> 10^6$, which is much greater than other direct spectroscopic measurements. This technique combines an IR source signal from the observing target and an IR laser (a quantum cascade laser (QCL) and/or a CO₂ gas laser) as the local oscillator (LO). We have developed the mid-infrared laser heterodyne spectrometer MILAHI (Mid Infrared LAsER Heterodyne Instrument) mounted on our dedicated Tohoku 60 cm telescope (T60) at the summit of Mt. Haleakala, Hawaii. This instrument has successfully operated for the measurements of Venusian and Martian atmosphere (Nakagawa et al., 2016; Takami et al., 2020).

In the current system, two beams are combined at a ZnSe beam splitter and then focused onto a HgCdTe photomixer. In this scheme, a precise optical alignment is highly required to combine two beams. Since the wavelength of a single feedback (FB) QCL is restricted within the range of several cm⁻¹, switching LOs is needed for wider wavelength coverage. A CO₂ gas laser covers some parts of the wavelength ranges of 9-12 μm and four QCLs provide the wavelength ranges of 7.43-7.44 μm, 7.71-7.73 μm, 9.54-9.59 μm, 10.28-10.33 μm are installed in MILAHI as LOs. However, smooth switching mechanism of those LOs enhances the complexity of this system. We tried to simplify those optics with mid-IR transmissive hollow fibers.

There is few optical fiber which has a high transmittance at the wavelengths longer than 2 μm. Recently mid-IR (5-20 μm) transmissive hollow fibers has been developed by Tohoku University (e.g., Matsuura et al., 1995). The fibers are made of glass tubing whose inner diameter are 1 mm. Inner surface is covered by a conductive Ag layer covered by a dielectric AgI layer. With this fiber, we have tested the transmittance, heterodyne capability, and coupling/division of light.

(1) Transmittance of 0.5dB/m at 10.6 μm was reported in previous studies (e.g. Matsuura et al., 1995). At the moment, we have achieved about 70% transmittance with a 300 mm hollow fiber at 10.3 μm from our laboratory measurements. Since the transmittance strongly depends on the incident angle of the light, better transmittance might be possible by improving the alignment.

(2) We also confirmed the applicability of hollow fibers to mid-IR heterodyne system. The heterodyne spectroscopy with hollow optical fiber resolved the spectral feature of the narrow laser emission line. Achieved system noise temperature was less than 3,000 K, which was only twice the quantum limit and almost the same as that in the system without hollow fibers.

(3) We have developed the technology of the fiber coupler and divider, which enables coupling or splitting lights by combining fibers directly for the hollow fibers (Tamura et al., 2017). Now, we are testing the efficiency of the heterodyne signal using the fiber coupler. When it is succeeded, the fiber coupler can provide downsizing, weight saving, and high stabilization of the instrument. Those are essential progresses

for this instrument optimizing to space-born missions.

Keywords: Hollow Optical Fiber, mid-IR heterodyne spectrometer

Investigation of potential candidates for a sample return mission

*Yuri Shimaki¹, Shigeru Wakita^{2,3}, Seitaro Urakawa⁴, Peng Hong⁵, Fumihiko Usui¹, Moe Matsuoka¹, Naoya Sakatani⁶, Satoshi Tanaka¹, Sunao Hasegawa¹, Daisuke Kuroda⁷

1. Institute of Space and Astronautical Science, Japan Aerospace Exploration Agency, 2. Massachusetts Institute of Technology, 3. Purdue University, 4. Japan Spaceguard Association, 5. Planetary Exploration Research Center, Chiba Institute of Technology, 6. Rikkyo University, 7. Kyoto University

The Hayabusa2 brought back samples from the C-type asteroid Ryugu to the Earth in December 2020. Since the returned samples have not struggled from thermal alterations during the Earth entry, it is expected that they preserve fragile materials, volatiles, and organic matters. This information is a clue to material evolutions in the early Solar System. Thus, we believe that sample return (SR) missions are keys to understand the planetary formation process. Here we report the evaluation of potential small bodies for a future sample return mission in the 2030s, as a descendant of the Hayabusa2.

To minimize fuel consumption during the cruising phase of a mission, we extracted small bodies with a perihelion of 0.9–1.1 AU and an inclination of <10 degrees from the JPL small body database as the SR candidates. We preferred targets with a diameter >0.3 km and a rotation period >2 hr for the SR feasibility. To evaluate the science value of a target, we examined asteroid spectrum types in the literature (e.g., Binzel et al., 2019) and specific features, such as cometary activity (active asteroid) and satellites (binary/trinary asteroids).

We selected E-type, D-type, active asteroids, and comets as potential candidates for future SR missions. The E-type asteroids are believed to relate to enstatite chondrite and be a remnant of building blocks of the Earth. The D-type asteroids are abundant in Jupiter Trojan and are thought to be enriched in volatiles and organics. Since the active asteroids can be comet-asteroid transition objects, they might preserve volatiles beneath their surface. Comets are composed of silicate dust, ices, and organics which have never been thermally altered materials. We confirmed that some near-Earth objects with these properties could satisfy the mission schedule, such as launch in the early 2030s and return in the early 2040s.

Keywords: Planetary exploration, Asteroids, Comets

Observation Plans and Development Status of MIRS: MMX Infrared Spectrometer on the MMX Spacecraft

*Takahiro Iwata¹, Hiromu Nakagawa², Fuminori Tsuchiya², Tomoki Nakamura², Maria Antonietta Barucci³, Jean-Michel Reess³, Pernelle Bernardi³, Alain Doressoundiram³, Sonia Fornasier³, Michel Le Du⁴, Eric Sawyer⁴

1. Institute of Space and Astronautical Science, Japan Aerospace Exploration Agency, 2. Tohoku University, 3. LESIA, Observatoire de Paris, 4. CNES

The Martian Moons Exploration (MMX) is a probe which will be launched by the Japanese launch vehicle H-III, and it will navigate the quasi satellite orbit of Phobos and will make a fly-by of Deimos. MIRS (MMX InfraRed Spectrometer) is a push-broom imaging spectrometer in the wavelength range of 0.9 to 3.6 micrometers which is one of the candidate instruments to be installed on the MMX spacecraft. It has a field-of-view (FOV) of 3.3 deg width with instantaneous-FOV (IFOV) of 0.35 mrad, which can be scanned by inner along track scan mirror in the range of ± 20 deg.

MMX aims to elucidate the evolution of our solar system by investigating the migration process of primitive bodies in the early stage. MIRS will observe absorptions of hydroxide or hydrated minerals on Phobos and Deimos in the wavelength range of 2.7-3.2 micrometers. By analyzing the behavior of the spectra, we will distinguish between structural water in hydrous silicate minerals, and water ice particles. MIRS will also try to detect the absorption of organic matters in the wavelength range of 3.3-3.5 micrometers. These results will be crucial evidence to answer the question of the origin of the Martian satellites and identify whether they are satellites formed by a giant impact or primitive asteroids captured by Mars gravitational field. MIRS will observe Phobos to survey the sampling site candidates, to investigate the sampling site precisely at the touch-down mode, and to make global mapping. The global mapping of Phobos to select prior areas and landing sites will be performed on the quasi satellite orbit. Precise mapping for candidate landing sites will be followed on the lower altitude. Observations for Deimos will be basically executed from the fly-by orbit. MIRS will also monitor the Martian atmosphere with particular attention to spatial and temporal changes as clouds, dust and water vapor. We will report and discuss on the observation plans and the development status of the MIRS instrument.

Keywords: MMX, Phobos, Deimos, infrared spectrometer, hydrated mineral, Martian atmosphere

[E] Poster | A (Atmospheric and Hydrospheric Sciences) : A-AS Atmospheric Sciences, Meteorology & Atmospheric Environment

📅 Fri. Jun 4, 2021 5:15 PM - 6:30 PM JST | Fri. Jun 4, 2021 8:15 AM - 9:30 AM UTC | 🏠 Ch.07_1

[A-AS01] Large-scale moisture and organized cloud systems

convener: Satoru Yokoi (Japan Agency for Marine-Earth Science and Technology), Hiroaki Miura (The University of Tokyo), Atsushi Hamada (University of Toyama), Masaki Satoh (Atmosphere and Ocean Research Institute, The University of Tokyo)

Water vapor plays a significant role in regulating the global atmospheric circulation, especially in the troposphere. The overturning circulation is directly driven by the longwave radiative cooling of water vapor and the latent heating/cooling through microphysical processes to balance it. This global circulation is composed of diverse atmospheric phenomena with various spatial and temporal scales. Developments of some significant turbulent motions such as 3D isotropic turbulence in clouds, stratocumulus and cumulus convection, squall lines and tropical cyclones, and the Madden-Julian oscillation, are essentially associated with moisture anomaly in each scale. Moisture is accumulated relatively slowly in larger horizontal scales, but is consumed relatively quickly in smaller ones. This significant scale gaps between the accumulation and consumption may be one of the causes of the long-lasting difficulty in developing the theory of the moist atmosphere. The aim of this session is to share recent research results about the relationships between moisture and organized cloud systems in wider ranges of spatial and temporal scales to enhance collaborations between modeling, observational, and theoretical approaches in tackling this challenging task. Research results relating to the Years of the Maritime Continent (YMC), Radiative-Convective Equilibrium Model Intercomparison Project (RCEMIP), mesoscale simulations of severe weather, and global cloud-resolving climate simulations are particularly welcome.

[AAS01-P01] Intraseasonal variability in the initialization of a seasonal prediction system simulated by a new convection scheme

★Invited Papers

*Yuya Baba¹ (1. JAMSTEC Japan Agency for Marine-Earth Science and Technology)

[AAS01-P02] The Different Pathways to self-aggregation between SCALE and WM

★Invited Papers

*Ching-Shu Hung¹, Hiroaki Miura¹, Jin-De Huang², Chien-Ming Wu² (1. The University of Tokyo, 2. National Taiwan University)

[AAS01-P03] A Numerical Study on the Diurnal Variation of Precipitation Bands Observed around the West Coast of Sumatra Island

*Mamiko Terada¹, Hiroaki Miura¹, Satoru Yokoi² (1. The University of Tokyo Department of Earth and Planetary Science, 2. Japan Agency for Marine-Earth Science and Technology)

[AAS01-P04] A conservative and consistent remapping of moisture on the icosahedral mesh

*Hiroaki Miura¹ (1. The University of Tokyo)

[AAS01-P05] Observational study on boundary-layer moist static energy budget over the tropical Indo-Pacific warm pool domain

*Satoru Yokoi¹ (1. Japan Agency for Marine-Earth Science and Technology)

Intraseasonal variability in the initialization of a seasonal prediction system simulated by a new convection scheme

*Yuya Baba¹

1. JAMSTEC Japan Agency for Marine-Earth Science and Technology

Capturing interannual variability originating from coupled-mode phenomena such as El Niño Southern oscillation is important for seasonal prediction system, since the variability has great impact on seasonal variability. To obtain better prediction skill, recent prediction systems employ various assimilation techniques, but not only the assimilation but also improvements of physical parameterization is necessary, because the fidelity of the simulated variability significantly depends on model's physical performance. Large uncertainty is known to exist in the atmospheric component of the system, especially in the representation of clouds. Therefore, improving the parameterization of clouds is considered a key to improve model's performance, and also further improve the prediction skill. We implemented a new convection scheme in a seasonal prediction system (SINTEX-F2), and evaluated the impact of convection scheme in the initialization of the system which was done by SST nudging. In this study, we especially focused on the fidelity of the simulated intraseasonal variability (i.e., MJO) which can be influential to the formation of interannual variability. The first evaluation revealed that the model using different convection schemes simulated similar climatology and atmospheric response to interannual variability, with acceptable small climatological error difference. Qualitative analyses on MJO were conducted using the MJO diagnostics, and the analyses revealed that the new scheme outperformed the original scheme of the system. By using a composite analysis on the organized convection, it was found that the new scheme simulated moisture increase originating from shallow clouds in the advance of the organized convection, which indicated the original superiority of the new scheme (which has been already revealed in preceding studies) was obtained even in the present model. Statistical and quantitative evaluations were finally performed, indicating that the new scheme captured statistical behaviors of MJO better than the original scheme. In conclusion, the new convection scheme outperformed the original convection scheme of the system in terms of intraseasonal variability from various perspectives. The new scheme is therefore expected to improve the seasonal prediction skill, in particular, for the interannual variability which may be affected by the intraseasonal variability. The influence of the convection scheme in practical seasonal prediction should be studied and will be presented in our future study.

Keywords: Intraseasonal variability, Convection scheme, Seasonal prediction system

The Different Pathways to self-aggregation between SCALE and VVM

*Ching-Shu Hung¹, Hiroaki Miura¹, Jin-De Huang², Chien-Ming Wu²

1. The University of Tokyo, 2. National Taiwan University

In this study, self-aggregation simulations following Wing et al. (2018) are conducted focusing on the development toward self-aggregation by two cloud-resolving models (SCALE and VVM). Even though the two models reach self-aggregation state after 40 days of simulations, the pathways toward aggregation are very different given the same sea surface temperature. The dry area expansion through radiative cooling is evident in SCALE which effectively shrinks the moist region while VVM takes a different route through the convection development in the moist region. The subsidence induced by the convection organization further enhances the expansion of the dry region leading to the self-aggregation. The isentropic analyses show that the aggregation in SCALE is through the development of strong shallow circulation while it is through the subsidence warming from aloft in VVM. The time evolution of convective core clouds distribution can be a precursor of the different pathway.

Keywords: self-aggregation

A Numerical Study on the Diurnal Variation of Precipitation Bands Observed around the West Coast of Sumatra Island

*Mamiko Terada¹, Hiroaki Miura¹, Satoru Yokoi²

1. The University of Tokyo Department of Earth and Planetary Science, 2. Japan Agency for Marine-Earth Science and Technology

It is known that the diurnal cycles of precipitation near the Maritime continents have different features between the land and the ocean. One example is near the west coast of Sumatra, Indonesia. After taking the precipitation maximum in the afternoon, the precipitating region keeps moving toward offshore during the nighttime. Although several mechanisms have been proposed about this phenomenon, their validities have not been evaluated sufficiently yet.

The Japan Agency for Marine-Earth Science and Technology (JAMSTEC) had conducted an intensive observation campaign around the west coast of Sumatra from December 2017 to January 2018. This campaign was operated as a part of the Year of the Maritime Continents (YMC) international campaign from July 2017 to February 2020. Prior to the YMC, JAMSTEC also operated a preliminary observation campaign called as Pre-YMC almost in the same geological region as YMC from November to December 2015. In both campaigns, the diurnal cycle of the precipitation was observed, but the observed features were different. While the system developed in most of the days in the first half of the Pre-YMC period, it developed only in some limited days in the YMC.

In this study, we examine the diurnal cycle of the precipitation during the Pre-YMC period. To investigate the mechanism of the offshore propagation of the precipitation, numerical simulations through the Pre-YMC period have been performed a cloud-resolving model, Scalable Computing for Advanced Library and Environment (SCALE). Several sensitivity experiments have also been conducted. The domain-mean fields of zonal wind and relative humidity reasonably followed the time evolution of the large-scale environment. But, in some days, the behaviors of the diurnal cycle of the precipitation system in the observation and the simulation was different.

The sensitivity experiments were conducted in terms of the cloud- radiation interaction, the difference in the cloud microphysics schemes, and the impacts of the large-scale horizontal wind. An interesting result was found when the standard 6-class 1-moment cloud microphysics scheme of SCALE was replaced with the 3-class 1-moment bulk method, which did not represent ice microphysics. Thick clouds prevailed widely in the upper troposphere, and precipitation occurred almost only over the ocean region. The precipitation propagation did not occur. When the clouds were made transparent, being combined with the same 3-class microphysics schemes to both the shortwave and longwave radiations, the precipitation propagation recovered. The result denies the importance of the cloud-radiative interaction as the mechanism of the precipitation propagation. Besides, the heating of the land surface by the shortwave radiation is thought to be essential as the trigger of the precipitation propagation. In the sensitivity experiments that enhanced background westerly winds, the precipitation propagation still occurred, but the frequency of occurrence was reduced, compared to the control experiment. This result indicates that the large-scale westerly makes it difficult for the precipitation propagation to occur. In contrast, under the easterly-enhanced condition, the frequency of the precipitation propagation was raised, showing that the easterly background is favorable for the propagating system.

We also investigate the reasons why the actual observed propagation systems were not reproduced in the simulation on some days. When ERA5 was used for the initial and boundary conditions in place of NCEP-FNL, the improvements of the reproducibility were obvious. In another experiment, the precipitation system could be reproduced well if the simulation period was less than 24 hours. These results commonly indicate that the dry bias, which developed within a day in the SCALE model, set up unfavorable conditions for the occurrence of the propagation events.

Keywords: Diurnal cycle, Precipitation system, Simulation, Pre-YMC

A conservative and consistent remapping of moisture on the icosahedral mesh

*Hiroaki Miura¹

1. The University of Tokyo

A novel remapping scheme is developed as a basis of the seamless integration of a multi-scale atmosphere model on the icosahedral mesh. The remapping scheme enables a conservative, consistent, and third-order accurate two-way remapping between coarser and finer icosahedral meshes. A two-dimensional quadratic profile is reconstructed locally. The scheme can be used for the variables defined for the hexagonal/pentagonal cells such as density and moisture.

Keywords: remapping, reconstruction

Observational study on boundary-layer moist static energy budget over the tropical Indo-Pacific warm pool domain

*Satoru Yokoi¹

1. Japan Agency for Marine-Earth Science and Technology

Over the tropical oceanic regions with vigorous cumulus convection, moist static energy (MSE) in the boundary layer (BL) is considered to be an essential thermodynamic parameter that determines the convective activity. It seems thus important to understand the BL MSE budget processes and their variability. Under the BL quasi equilibrium approximation, the MSE import by surface turbulent fluxes is balanced with its export by entrainment process across the BL top, by convective downdraft process, and by radiative cooling. Among these processes, quantitative estimation of contributions from the entrainment and convective downdraft processes have not been examined intensively so far. Recently, a method of estimating the MSE export by the entrainment process and convective downdraft process separately from surface meteorological observation and upper-air sounding data has been developed. In this study, we analyze observational data collected in several field campaigns by Research Vessel *Mirai* performed over the Indo-Pacific warm pool domain to examine temporal and regional variability in the MSE export by the two processes, and compare results with measures of convective activity around the vessel monitored by a shipborne weather radar. Our results include close quasi-linear relationship between estimated convective downdraft contribution and fractional area with high radar reflectivity, and statistically significant relationship between estimated entrainment contribution and low-cloud coverage.

Keywords: Moist static energy budget, Atmospheric boundary layer, Indo-Pacific warm pool domain, Shipborne observation

[E] Poster | A (Atmospheric and Hydrospheric Sciences) : A-AS Atmospheric Sciences, Meteorology & Atmospheric Environment

📅 Fri. Jun 4, 2021 5:15 PM - 6:30 PM JST | Fri. Jun 4, 2021 8:15 AM - 9:30 AM UTC | 🏠 Ch.07_2

[A-AS04] Machine Learning Techniques in Weather, Climate, Hydrology and Disease Predictions

convener: Venkata Ratnam Jayanthi (Application Laboratory, JAMSTEC), Rajib Maity (Indian Institute of Technology Kharagpur), Swadhin Behera (Application Laboratory, JAMSTEC, 3173-25 Showa-machi, Yokohama 236-0001), Takeshi Doi (JAMSTEC)

The machine learning techniques have found a wide range of applications in weather, climate, Hydrology and Disease predictions. In the recent times, these techniques are being widely used to forecast extreme events such as malaria outbreaks, heat waves, cold waves, flooding and droughts. The techniques are helping the researchers improve the parameterization schemes in the numerical models. The techniques are also being used to improve the numerical model predictions by providing methods to reduce the biases and also to improve the horizontal resolution of the forecasts. The aim of the session is to bring together the researchers working on various techniques of machine learning to enhance the understanding and predictions of weather, climate, Hydrology and Disease predictions for the benefit of the society.

[AAS04-P01] 3D Precipitation Nowcasting: RESNet applied to Highly Dense PAWR Data

*Maha Mdini¹, Takemasa Miyoshi¹, Shigenori Otsuka¹ (1. RIKEN Center for Computational Science)

[AAS04-P02] **A reservoir inflow forecasting model using a Wavelet transformed - deep learning algorithm**

Trung Duc Tran¹, *Jongho Kim¹ (1. University of Ulsan)

[AAS04-P03] Development of an integrated NWP-DA-AI system for 30-second-update 3D precipitation prediction

*Shigenori Otsuka¹, Yasumitsu Maejima¹, Pierre Tandeo², Takemasa Miyoshi¹ (1. RIKEN Center for Computational Science, 2. IMT Atlantique)

3D Precipitation Nowcasting: RESNet applied to Highly Dense PAWR Data

*Maha Mdini¹, Takemasa Miyoshi¹, Shigenori Otsuka¹

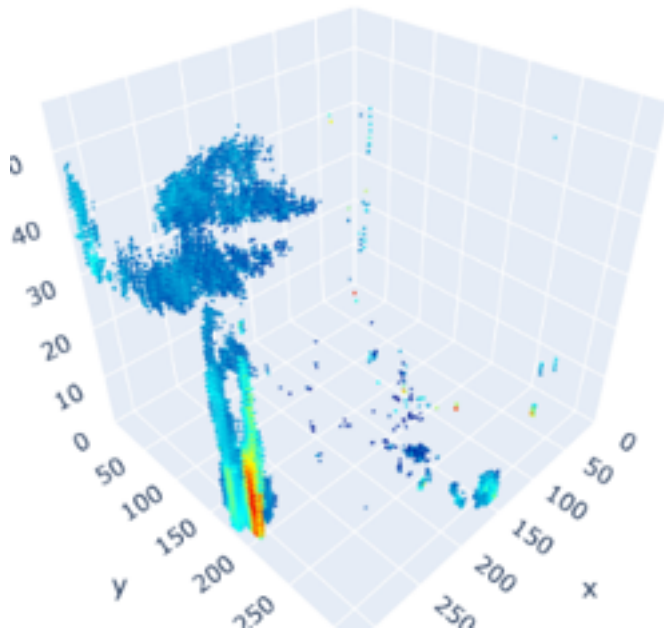
1. RIKEN Center for Computational Science

Sudden heavy rain may lead to disasters like flooding and loss of life and property. To reduce the risk, predicting sudden downpours is of key importance. However, predictability of such events is limited to only for a very short range within an hour or shorter because of their abruptness. In this case nowcasting is an effective approach. Detecting sudden heavy rain even 10 minutes before it occurs can reduce the damage drastically.

Precipitation nowcasting is the process of short-range prediction based on observation data. In the case of sudden rainfalls, this process is difficult due to the fast evolution of the rain and its chaotic nature. Therefore, we need innovative techniques.

The novel Phased-Array Weather Radar (PAWR) offers dense 3D images of reflectivity every 30 seconds. We took advantage of this big data to perform nowcasting using neural networks. We use Residual Neural Networks (RESNet) to compress the images and extract information relevant for the prediction. Next, we use a Convolutional Neural Network (CNN) to make the prediction. Afterwards, we use the same RESNet to map the forecast to the original domain. The RESNet and the CNN are trained jointly for the compression to maximize the prediction accuracy. Our first results show that in most cases we can predict precipitations up to 30 minutes, with an error rate (false positives + false negatives) of 8% . The use of the RESNet allowed to alleviate the memory load and the computational complexity of the prediction. Moreover, training the RESNet and the CNN jointly reduced immensely the prediction noise in non-precipitation regions and improved the accuracy in precipitation regions.

Keywords: Precipitation Nowcasting, Residual Neural Networks, Weather Forecasting



A reservoir inflow forecasting model using a Wavelet transformed - deep learning algorithm

Trung Duc Tran¹, *Jongho Kim¹

1. University of Ulsan

Accurate predictions of inflow would support policy-makers and operators in better performing reservoir operation and management tasks. This study proposed a data-driven model based on deep learning algorithms Long Short-term memory, called SWLSTM, producing accurate daily dam inflow forecasting. SWLSM adopts three main ideas to improve the model's accuracy: (i) it selects an appropriate input variable and a sequence length based on the statistical properties (using partial autocorrelation functions (PACF) and cross-correlation functions (CCF)); (ii) it employs the Wavelet transform (WT) to the selected input predictors to decompose them into sub-series; (iii) it optimizes the hyper-parameters of LSTM using K-fold cross-validation and random search method. The effectiveness of SWLSTM was proved by forecasting the five dams' daily inflow in the Han River watershed (South Korea) with historical data. Different evaluation metrics (i.e., R2, NSE, MAE, PE) are used to generator evaluate the model's accuracy. Overall, SWLSTM outperformed the regular LSTM model in all cases (i.e., evaluation metrics show about 30 to 80% better performance). The results indicate that the selection of the right input variable and the sequence length is effective in reducing noise, increasing efficiency during training a model; the WT enhances the results of forecasting extreme values such as flood peaks; K -fold cross-validation, and random search support setting up model's hyper-parameters more efficient and simple. The results reinforce the potential of a data-driven model for efficient and skillful reservoir inflow forecasting in addressing water-disaster-energy security challenges.

Acknowledgment: This work was supported by KOREA HYDRO & NUCLEAR POWER CO., LTD (No.2019-Tech-11) and the National Research Foundation of Korea (NRF) grant funded by the Korea government (MSIT)(NRF-2019R1C1C1004833).

Keywords: Dam inflow prediction, Long short-term memory, Wavelet transform, Input predictor selection, Hyper-parameter optimization

Development of an integrated NWP-DA-AI system for 30-second-update 3D precipitation prediction

*Shigenori Otsuka¹, Yasumitsu Maejima¹, Pierre Tandeo², Takemasa Miyoshi¹

1. RIKEN Center for Computational Science, 2. IMT Atlantique

The Phased-Array Weather Radar (PAWR), developed by the National Institute of Information and Communications Technology, Osaka University, and Toshiba Corporation, has been in operations since 2012 in Japan. The PAWR scans the whole sky in the 60-km range every 30 seconds at 110 elevation angles. Four PAWRs of the same type have been installed in Osaka, Kobe, Okinawa, and Tsukuba, and two similar ones of other types have been installed in Japan. Taking advantage of the PAWRs' frequent and dense three-dimensional volume scans, we developed two systems: a high-resolution regional numerical weather prediction (NWP) system (SCALE-LETKF, Miyoshi et al., 2016a,b, Lien et al., 2017), and a three-dimensional (3D) precipitation nowcasting system (Otsuka et al., 2016).

Our 30-second-update 3D nowcasting system is running in real time since 2017; the system adopts an optical-flow-based algorithm in the 3D space. Because convective clouds evolve rapidly within a 10-minute forecast, sometimes the assumption of Lagrangian persistence is violated, and the prediction skill of the optical-flow-based system drops quickly with the forecast lead time. The SCALE-LETKF system, on the other hand, provides physically based predictions; therefore, we would expect that the NWP outperforms the nowcast for longer forecasts. Therefore, merging NWP and nowcast will provide better predictions compared to each of them.

We have been developing an algorithm to integrate data-driven approaches and process-driven approaches for precipitation nowcasting. Previously, we reported that a convolutional long short-term memory (ConvLSTM, Shi et al. 2015) extended to the 3D PAWR data (3D ConvLSTM) can successfully predict convective rain events in the 3D space. In addition, this neural network is designed to accept future data from NWP or optical flow-based precipitation nowcasts: an integrated NWP-Data Assimilation (DA)-AI system. We demonstrated that the use of future data from NWP/optical flow improved the prediction accuracy compared with the baseline experiment.

Recently, this integrated data-driven and process-driven precipitation nowcasting system was updated. First, the computational domain was extended in the vertical direction so that we can take advantage of upper air radar echoes. For that, pooling-unpooling is used to reduce the memory consumption and computation time. Second, the convolution operation in ConvLSTM was changed from 2D to 3D so that the new system can fully consider three-dimensional structures of radar echoes. Preliminary experiments with the new 3D ConvLSTM demonstrated that these updates improved the prediction accuracy. We will present the latest results in the meeting.

Keywords: precipitation nowcast, machine learning, data assimilation, phased array weather radar

[E] Poster | A (Atmospheric and Hydrospheric Sciences) : A-HW Hydrology & Water Environment

📅 Fri. Jun 4, 2021 5:15 PM - 6:30 PM JST | Fri. Jun 4, 2021 8:15 AM - 9:30 AM UTC | 🏠 Ch.09_1

[A-HW22] Material transportation and cycling in watershed ecosystems; from headwaters to coastal areas

convener: Morihiro Maeda (Okayama University), Tomohisa Irino (Faculty of Environmental Earth Science, Hokkaido University), Shin-ichi Onodera (Graduate School of Advanced Science and Engineering, Hiroshima University), Adina Paytan (University of California Santa Cruz)

This session aims to synthesize watershed sciences in order to understand dynamic processes in transportation and cycling of materials and nutrients in watershed ecosystems from headwaters to coastal areas. The session will integrate various inter-disciplinary researches including limnology, ground water hydrology, coastal oceanography, meteorology, soil science, sedimentology, forestry, agriculture, fishery, ecology, social science and so on. This session calls for ideas on new methods for understanding the watershed ecosystems, such as tracers and molecular techniques, hydrological modeling, paleontological approaches, and chemical analyses, in order to elucidate physical, chemical and biological mechanisms for shedding light on natural phenomena and their spatio-temporal variations in complex and dynamic aquatic systems under human and climate impacts. Both in laboratory and field studies, social-scientific evaluation of ecosystem services and social-ecological systems will be also welcomed. Through this session, we would like to facilitate interdisciplinary collaboration among participants to create new knowledge on watershed sciences.

[AHW22-P01] Distribution of sea ice rafted detritus yielded from the sediments of Okhotsk coast of Hokkaido, northern Japan

*Tomohisa Irino¹, Ryuki Saijo², Koji Suzuki¹, Jun Nishioka³, Tomohiro Nakamura³ (1. Faculty of Environmental Earth Science, Hokkaido University, 2. Graduate School of Environmental Science, Hokkaido University, 3. Institute of Low Temperature Science, Hokkaido University)

[AHW22-P02] Effect of stream water from nitrogen-saturated forests in the Koise River Basin on nitrogen concentrations in the main river

*Masahiro Kobayashi¹, Yuko Itoh¹ (1. Forestry and Forest Products Research Institute)

[AHW22-P03] **Hydro-geographical Study on the Water Environment of Asakawa River in Tamagawa River System**

*Masato ODA¹, Koji KODERA² (1. Under Graduate Student, Hosei Univ., 2. Department of Geography, Hosei Univ.)

[AHW22-P04] Impact of COVID-19 on air pollutants influx into forest ecosystems in Japan

*Yuko Itoh¹, Toru Okamoto¹, Keiji Takase², Sakae Horisawa³ (1. Forestry and Forest Products Research Institute, Japan, 2. Ishikawa Prefectural University, 3. Kochi University of Technology)

[AHW22-P05] Long-term trends in zooplankton production and ecological transfer efficiency over four decades in Lake Biwa, Japan

*Xin Liu¹, Naoshige Goto¹, Syuhei Ban¹ (1. The University of Shiga Prefecture)

[AHW22-P06] High resolution monitoring for subsidiary nutrient loadings and phytoplankton production in north basin of Lake Biwa

*Syuhei Ban¹, Xin Liu¹, Ken'ichi Osaka¹, Naoshige Goto¹, John Wells² (1. The University of Shiga Prefecture, 2. Ritsumeikan University)

[AHW22-P07] Hydrological controls on phosphorus export from diffuse source in Lake Biwa basin, central Japan.

*Ken'ichi Osaka¹, Haruto Tanabe¹, Syuhei Ban¹ (1. Department of ecosystem study, University of Shiga Prefecture)

[AHW22-P08] The influence of vertical water mixing on inter-annual nitrogen dynamics in Lake Biwa

*Takaaki Ishibashi¹, Ken'ichi Osaka², Keisuke Koba³, Kei Nishida⁴, Takashi Nakamura⁴ (1. Graduate School of Environmental Science, University of Shiga Prefecture, 2. Department of ecosystem study, University of Shiga Prefecture, 3. Center for Ecological Research, Kyoto University, 4. Interdisciplinary Centre for River Basin Environment, Interdisciplinary Graduate School, University of Yamanashi)

[AHW22-P09] Detection of Dissolved Methylphosphonate in Freshwater of Lake Biwa by pre-concentration with Iron(III) hydroxide coprecipitation

Tomoki Yamamoto¹, Kazuma Tsuji³, Yuki Yamanaka³, *Masahiro Maruo¹, Hajime Obata² (1. Department of Ecosystem Studies, School of Environmental Science, The University of Shiga Prefecture, 2. Atmosphere and Ocean Research Institute, The University of Tokyo, 3. Graduate School of Environmental Science, The University of Shiga Prefecture)

[AHW22-P10] Estimation of groundwater and lake water interaction in the deeper zone of Lake Biwa, using ¹⁸O and D in pore water and groundwater

*Shin-ichi Onodera¹, Mitsuyo Saito², Yusuke Tomozawa¹, Takuya Ishida¹, Syuhei Ban³, Noboru Okuda⁴ (1. Graduate School of Advanced Science and Engineering, Hiroshima University, 2. Okayama University, 3. The University of Shiga Prefecture, 4. Kobe University)

[AHW22-P11] Identification of enriched phosphate in groundwater: insights from distribution of phosphate oxygen isotope ratio in aquifer sediments

*Takuya Ishida¹, Yusuke Tomozawa¹, Xin Liu², Mitsuyo Saito³, Shin-ichi Onodera¹, Noboru Okuda⁴, Syuhei Ban² (1. Hiroshima University, 2. The University of Shiga Prefecture, 3. Okayama University, 4. Kobe University)

[AHW22-P12] Long-term Estimation on Phosphorus flux in a Coastal Catchment Influenced by the Anthropogenic Land Use Change

*Kunyang Wang¹, Shin-ichi Onodera¹, Mitsuyo Saito², Yuta Shimizu³ (1. Graduate School of Integrated Arts and Science, Hiroshima University, 2. Faculty of Environmental Science and Technology, Okayama University, 3. National Agriculture and Food Research Organization)

[AHW22-P13] Analysis for the characteristics of water and nutrient discharge in a sub-basin of Osaka Bay catchment

*Shuta Ishihara¹, Kunyang Wang², Mitsuyo Saito³, Shin-ichi Onodera⁴ (1. Faculty of Environmental Science and Technology, Okayama University, 2. Graduate School of Integrated Arts and Sciences, Hiroshima University, 3. Graduate School of Environmental and Life Science, Okayama University, 4. Graduate School of Advanced Science and Engineering, Hiroshima University)

[AHW22-P14] Estimation of groundwater flow and a river water contribution to it in an alluvial plain of western Japan, using tracer methods

*Yusuke Tomozawa¹, Toru Takeuchi², Shin-ichi Onodera¹, Mitsuyo Saito³, Shotaro Fujioka⁴ (1. Graduate School of Advanced Science and Engineering Hiroshima University, 2. Fujita Geology Co., Ltd., 3. Graduate School of Environmental and Life Science, Okayama University, 4. River fishermen)

[AHW22-P15] Estimation of Landuse Change Impact on Water Budget in Higashihiroshima Catchment using SWAT

*Sharon Bih Kimbi¹, Kunyang Wang¹, Shin-ichi Onodera², Ichirow Kaihotsu¹, Shingo Nozaki², Yusuke Tomozawa² (1. Graduate School of Integrate Arts and Sciences, Hiroshima University, 2. Graduate School of Advanced Science and Engineering, Hiroshima University)

[AHW22-P16] Flood Impact on water quality in a Small Catchment Area: Preliminary Study

*Sharon Bih Kimbi¹, Shin-ichi Onodera², Shingo Nozaki², Yusuke Tomozawa² (1. Graduate School of Integrate Arts and Sciences, Hiroshima University, 2. Graduate School of Advanced Science and Engineering, Hiroshima University)

[AHW22-P17] Process of spatio-temporal variation in seagrass-seaweed meadows in intertidal areas of Seto Inland Sea, western Japan

*Mitsuyo Saito¹, Shin-ichi Onodera², Natsushi Soga³, Yuto Ideishi³, Shingo Nozaki², Yusuke Tomozawa² (1. Graduate School of Environmental and Life Science, Okayama University, 2. Graduate School of Advanced Science and Engineering, Hiroshima University, 3. Faculty of Environmental Science and Technology, Okayama University)

[AHW22-P18] Analysis of coastal seagrass bed distribution using UAV and near-infrared camera data

*Toru Iwata¹, Akimitsu Shiraishi¹, Mitsuyo Saito¹, Shin-ichi Onodera² (1. Graduate School of Environmental and Life Science, Okayama University, 2. Graduate School of Integrated and Arts Sciences, Hiroshima University)

[AHW22-P19] **Physically Based Groundwater Flow Simulation using Tracer-aided model in Kumamoto Region, Japan**

*A T M Sakiur Rahman¹, Takahiro Hosono^{2,3}, Yasuhiro Tawara⁴, Youichi Fukuoka⁴, Aurelien Hazart, Jun Shimada³ (1. Postdoctoral researcher, Kumamoto University, 2. Faculty of Advanced Science and Technology, Kumamoto University, 3. International Research Organization for Advanced Science and Technology, Kumamoto University, 4. Geosphere Environmental Technology Corporation, NCO Kanda, Awajicho Building 3F, 2-1 Kanda, Awajicho, Chiyoda-ku, Tokyo 101-0063, Japan)

[AHW22-P20] Quantitative evaluation of groundwater pollution at Ryukyu limestone area in southern Okinawa Island: Trial application of boron isotope

*KE-HAN SONG¹, Yumi Moromizato², Ryuichi Shinjo², Jun Yasumoto³, Kazuko Sawada⁴ (1. Graduate School of Engineering and Science, University of the Ryukyus, Senbaru 1, Nishihara, Okinawa 903-0213, Japan, 2. Department of Physics and Earth Sciences, Faculty of Science, University of the Ryukyus, Senbaru 1, Nishihara, Okinawa 903-0213, Japan, 3. Department of Regional Agricultural Engineering, Faculty of Agriculture, University of the Ryukyus, Senbaru 1, Nishihara, Okinawa 903-0213, Japan, 4. Center for Strategic Research Projects, University of the Ryukyus, Senbaru 1, Nishihara, Okinawa 903-0213, Japan)

[AHW22-P21] **Metagenomic analysis on the groundwater in the Ryukyu Limestone area**

*Maruyama Rio¹, Nanami Mizusawa¹, Jun Yasumoto², Mariko Iijima³, Yasumoto Ko¹, Mina Hirose⁴, Akira Iguchi³, Mitsuru Jimbo¹, Shugo Watabe¹ (1. School of Marine Biosciences, Kitasto University, 2. Faculty of Agriculture, University of the Ryukyus, 3. National Institute of Advanced Industrial Science and Technology, 4. Tropical Technology Plus)

[AHW22-P22] **The effects of groundwater runoff on the coastal bacterial communities near the Ryukyu Limestone area**

*Nanami Mizusawa¹, Akira Iguchi², Mariko Iijima², Rio Maruyama¹, Jun Yasumoto³, Ko Yasumoto¹, Mina Hirose⁴, Shugo Watabe¹ (1. Kitasato University School of Marine Biosciences, 2. National Institute of Advanced Industrial Science and Technology, 3. Faculty of Agriculture, University of the Ryukyus, 4. Tropical Technology Plus)

[AHW22-P23] Water environment issues in Chinese megacity delta-Sewage impacts on Peral river coastal area

*Guangzhe Jin¹, Shin-ichi Onodera², Mitsuyo Saito³, Yuta Shimizu⁴, Jianyao Chen⁵ (1. College of Ocean and Meteorology, Guangdong Ocean University, 2. Graduate School of Integrated and Arts Sciences, Hiroshima University, 3. Graduate school of Environmental and Life Science, Okayama University,

4. Western Region Agricultural Research Center, National Agriculture and Food Research Organization.,
5. The School of Geography and Planning, Sun Yat-sen University)

[AHW22-P24] Assessment of drought trends in the Dakbla watershed, Vietnam

*Tram Ngoc Quynh Vo¹, Hiroaki Somura¹ (1. Graduate School of Environmental and Life Science, Okayama University)

[AHW22-P25] Hydrogeochemical evolution mechanisms of groundwater in the Semarang Coastal Zone, Java Island, Indonesia

*Rizka Maria Maria^{1,6}, Anna Fadliah Rusydi^{2,6}, Shin-ichi Onodera³, Mitsuyo Saito⁴, Seiichiro Ioka⁵, Robert Muhammad Delinom⁶, Wahyu Purwoko⁶, Dadi Sukmayadi⁶, Hendarmawan Hendarmawan¹ (1. Faculty of Geological Engineering, Padjadjaran University, Indonesia, 2. Graduate School of Integrated Arts and Sciences, Hiroshima University, Japan, 3. Graduate School of Advance Science and Engineering, Hiroshima University, Japan, 4. Graduate School of Environmental and Life Science, Okayama University, Japan, 5. Research Institute for Sustainable Energy, Hirosaki University, Japan, 6. Research Center for Geotechnology, Indonesian Institute of Sciences, Indonesia)

[AHW22-P26] A comparative analysis in modeling surface runoff under climate and land use change in two catchments in Iran and Indonesia

*Sharif Joorabian Shooshtari¹, Shin-ichi Onodera², Yuta Shimizu³ (1. Department of Nature Engineering, Agricultural Sciences and Natural Resources University of Khuzestan, Mollasani, Iran, 2. Graduate School of Advanced Science and Engineering, Hiroshima University, 3. Western Region Agricultural Research Center, National Agriculture and Food Research Organization)

[AHW22-P27] Effects of different NH₄⁺-N contents on N₂O and CO₂ emissions from manure compost-amended soil

*Thanuja Deepani Panangala Liyanage¹, Morihiro Maeda¹, Hiroaki Somura¹ (1. Okayama University)

Distribution of sea ice rafted detritus yielded from the sediments of Okhotsk coast of Hokkaido, northern Japan

*Tomohisa Irino¹, Ryuki Saijo², Koji Suzuki¹, Jun Nishioka³, Tomohiro Nakamura³

1. Faculty of Environmental Earth Science, Hokkaido University, 2. Graduate School of Environmental Science, Hokkaido University, 3. Institute of Low Temperature Science, Hokkaido University

The Sea of Okhotsk is a southern limit of seasonal sea ice distribution in the northern hemisphere. Okhotsk coast of Hokkaido, northern Japan, is located at exactly the southern limit and extent of the cold East Sakhalin Coastal Current here might permit an expansion of sea ice distribution to this region in winter. Spring melting of sea ice in this region drops sands and gravels into the sediment in this area and may trigger phytoplankton bloom, which forms hemipelagic diatom-rich sediments associated with abnormally coarse detrital material as ice rafted detritus (IRD). Since the sea ice extent is controlled by severeness of winter monsoon characterized by cold air mass over the Sea of Okhotsk and strong northwesterly blowing sea ice to the southeast, IRD bearing diatom-rich sediments in Hokkaido coastal area could be a suitable archive of past east Asian winter monsoon variability.

In order to examine the location of IRD deposition in the Hokkaido coastal area in the Okhotsk Sea, we collected 10 short sediment core samples using a multiple corer during the R/V *Hakuho-maru* KH20-12 expedition from December 8 to 25, 2020. The sediments consisted of sandy silt or diatomaceous silt at shallower (<200 m water depth) sites and of diatomaceous silt or clay to clayey diatomite at deeper sites (>200 m water depth). Large gravels considered as IRD were found only at 3 sites located ~70 km offshore during our sediment core description and subsampling.

Distribution of potential IRD in this area was also investigated by Geological Survey of Japan in 2000 and 2001 using the R/V *Hakurei-maru II*, and they also reported that the occurrence of gravels in surface sediments was restricted to the sites located ~70 km offshore except the area around shallow and rocky Kitami-Yamato Rise. Gravel deposition during the sea ice melting season has been well known in the further offshore area, therefore the sediments collected were utilized for paleoenvironmental reconstruction. Recently, IRD has rarely deposited in the area closer to the Hokkaido coast, suggesting that sea ice containing IRD usually melted at >70 km offshore regions and the limit of sea ice distribution does not necessarily indicate the location of its melting. In order to utilize the spatial-temporal variation of IRD and diatom-rich sediments as sea ice distribution proxies, mechanisms for connecting the spring sea ice melting with location of IRD deposition need to be further investigated.

Keywords: Okhotsk Sea, sea ice, ice rafted detritus, R/V *Hakuho-maru* KH20-12 expedition

Effect of stream water from nitrogen-saturated forests in the Koise River Basin on nitrogen concentrations in the main river

*Masahiro Kobayashi¹, Yuko Itoh¹

1. Forestry and Forest Products Research Institute

Around metropolitan Tokyo, high nitrate concentrations can occur in water from forest streams, which are nitrogen-saturated due to chronic excessive nitrogen deposition. Stream water from forests in hilly and mountainous areas should reduce nitrogen input to agricultural areas. However, this dilution effect is thought to be smaller in nitrogen-saturated forests. To test this in the Koise River Basin, where the forests are nitrogen-saturated, we periodically sampled water from the main river and a forest stream and compared the nitrate concentrations.

The average nitrate concentration in forest stream water for 2018–2019 was 8.5 mg/L. There was no significant seasonality, although temporal increases were observed during rainfall events. The average nitrate concentration in the main river water during the same period was 9.0 mg/L, and showed marked seasonal fluctuation; moreover, this was substantially lower than that in stream water from the forest in summer.

Denitrification in paddy fields in the basin is thought to be responsible for the summer decrease in nitrate concentrations in the main river. In the Koise River Basin, where forests are commonly nitrogen-saturated, the high nitrogen concentrations in forest stream water are thought to be reduced in paddy fields in the summer. It has been suggested that the stream water in this area is not reducing the nitrogen load to Lake Kasumigaura during the summer, and the forest may be a non-point source.

The Koise River Basin, located just outside metropolitan Tokyo, has been subjected to a large influx of anthropogenic nitrogen emitted by human activities over the years, causing the forest to become nitrogen-saturated. During this period, few coniferous plantations in the area have been thinned, which may have amplified the negative effects of nitrogen saturation in the region's forests by maintaining the high dry deposition capture effect of a crowded canopy.

The paddy fields in the area are thought to purify the nitrogen from the forests during the summer via denitrification. However, as the number of abandoned paddy fields in the area increases, there are concerns about the reduced ability of paddy fields to control eutrophication in Lake Kasumigaura.

Keywords: Forest, nitrogen saturation, paddy field

Hydro-geographical Study on the Water Environment of Asakawa River in Tamagawa River System

*Masato ODA¹, Koji KODERA²

1. Under Graduate Student, Hosei Univ., 2. Department of Geography, Hosei Univ.

I .Introduction

In the Asakawa River, a part of the Tamagawa River system, the deterioration of water quality due to domestic wastewater inflow had been advanced, and to solve this problem, various studies have been carried out(Ogura, 1980). However, most of the studies have conducted on the Minami-Asakawa River, the largest tributary of this river, and there were few comprehensive studies on the entire Asakawa River system. In this study, we will clarify the water environment characteristics of the whole Asakawa River system and examine the influence of the Minami-Asakawa River on the mainstream.

II .Regional Summary

The source of this river is located at the Mt.Jimba in Hachioji City, Tokyo, and flows through Hachioji City before joining the Tamagawa River in Hino City. It has the Minami-Asakawa River, Kawaguchi River, Yudono River, Shiroyama River, Yamada River and other tributaries. The basin is surrounded by mountains and hills, such as the Kanto Mountains to the west, the Kasumi Hills to the north, and the Tama Hills to the south. The upstream area is mainly coniferous forest with low population density. The downstream area is relatively flat, with urban development and a high population density.

III.Reserch Methods

After reviewing the results of previous studies, we started the field survey on May 3, 2020, and have been conducting continuous monthly observations at 34 sites in Asakawa river system. The items to be measured in the field are air temperature, water temperature, electrical conductivity(EC), pH, RpH, COD, and flow rate. The sampled river water was brought to the laboratory for analysis of major dissolved components using TOC and ion chromatography.

IV.Results and Discussion

The EC of the mainstream of the Asakawa River averages around 74-84 $\mu\text{S}/\text{cm}$ in the upper reaches. It increases from the point where the river passes through the mountainous area and enters the city, reaching an average of 132 $\mu\text{S}/\text{cm}$ at Matsue Bridge. In the upstream of the Minami-Asakawa River, the values were higher than those in the upper reaches of the mainstream, averaging 109-115 $\mu\text{S}/\text{cm}$. There was a difference of about 15 $\mu\text{S}/\text{cm}$ in the average EC between the value at the Matsue Bridge before convergence and at the Asakawa Bridge after the confluence of the Minami-Asakawa River, indicating that the mainstream EC increased with the confluence of it. In the lower reaches of the mainstream, the average EC was higher than 190 $\mu\text{S}/\text{cm}$, and values of 240 $\mu\text{S}/\text{cm}$ or higher were observed in November and December. The pH values tended to decrease in the upper reaches of the mainstream, and was 7.2 in the uppermost reaches. The coefficient of variation was small in the upstream and large in the downstream, especially at the Arai Bridge at the downstream end, where the maximum value is 8.7 and the minimum is 7.6, a value gap of more than 1. The maximum values were observed in August at most of the sites, and this is because the low carbon dioxide concentration caused by the increased photosynthesis of algae due to the retention of water and high temperature. In November and December, when there was little precipitation, the values were lowest at many sites, indicating the influence of groundwater inflow and hence the RpH-pH values were mostly high.

V. Conclusion

In the Asakawa River basin, water quality is different between urban and mountainous areas, and the spatial distribution of EC and pH values are also different. The seasonal changes in values of water quality index are influenced by the amount of precipitation, the level of algae photosynthesis, the presence of groundwater inflow and other factors. Along with confluence of Minami-Asakawa River to mainstream, the values are change many time, therefore it has significant effect on mainstream water quality. Hereafter, it will be necessary to clarify the characteristics of these changes through further observations and analyses.

Keywords: Asakawa River, Domestic Wastewater, Precipitation, Algae, Groundwater

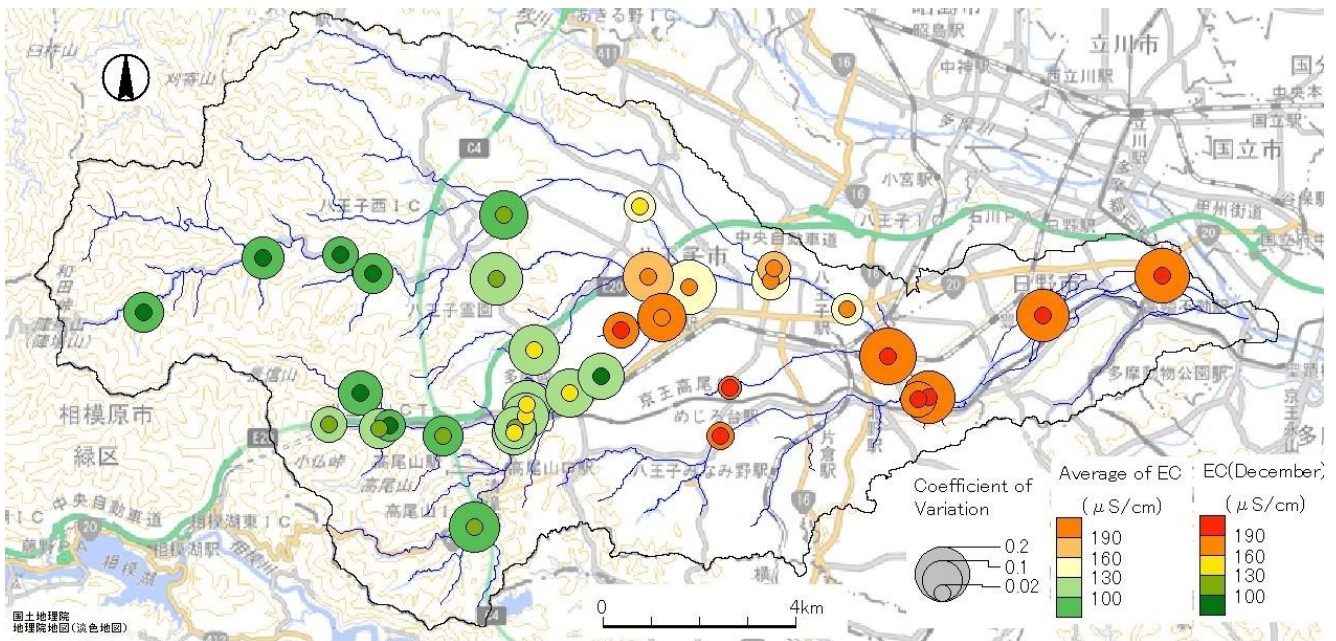


Fig.1 Spatial Distribution of EC

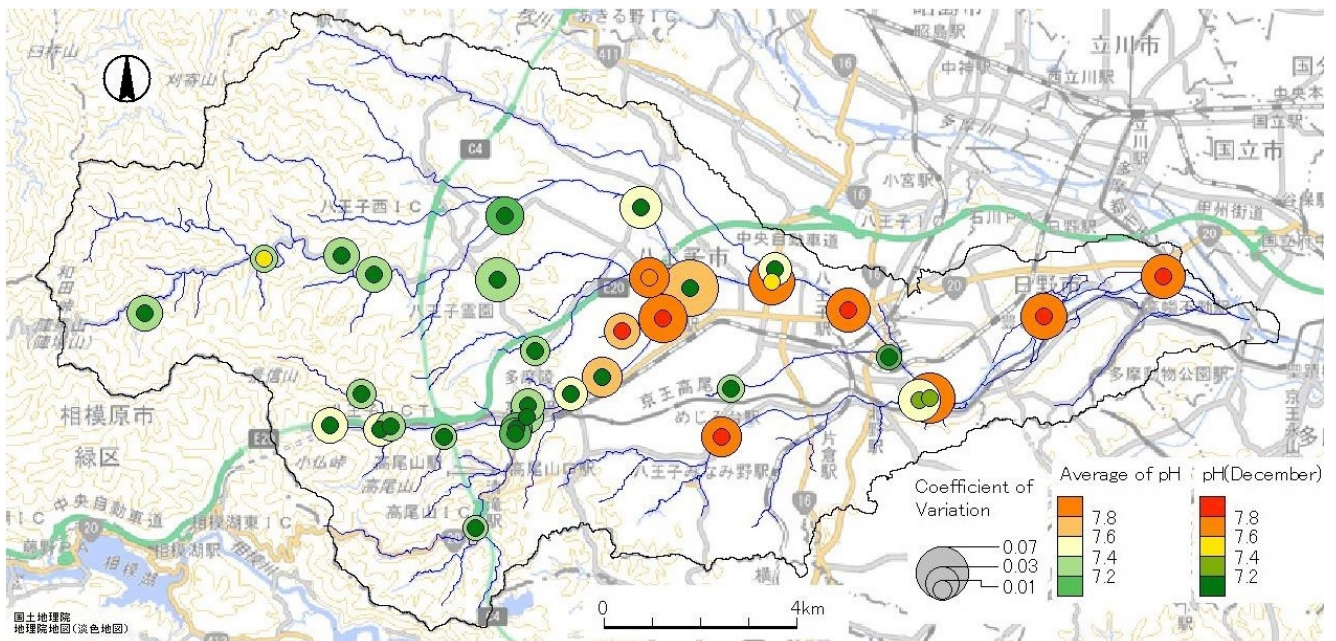


Fig.2 Spatial Distribution of pH

Impact of COVID-19 on air pollutants influx into forest ecosystems in Japan

*Yuko Itoh¹, Toru Okamoto¹, Keiji Takase², Sakae Horisawa³

1. Forestry and Forest Products Research Institute, Japan, 2. Ishikawa Prefectural University, 3. Kochi University of Technology

Atmospheric pollution is one of the most important environmental issues both of the industrialized developed and developing countries. The lockdown of cities and the reduction of economic activity as a countermeasure to the spread of COVID-19 led to a rapid improvement in air pollution in many countries. Clarifying the impact of the changes in atmospheric conditions brought about by the COVID-19 pandemic on the local and global environment is important as data for reconstructing the relationship between developing of human activities and global environmental conservation in the future.

We have been monitoring element cycles in several forest watersheds to determine the effects of human activities in the Tokyo metropolitan area and transboundary air pollutants on forest ecosystems. Therefore, we aimed to clarify the effects of decline human activity due to COVID-19 on forest ecosystems using the long-term monitoring data obtained in Ibaraki, Ishikawa, and Nagano prefectures.

Long-term trends in zooplankton production and ecological transfer efficiency over four decades in Lake Biwa, Japan

*Xin Liu¹, Naoshige Goto¹, Syuhei Ban¹

1. The University of Shiga Prefecture

Lake Biwa is the largest and the oldest lake in Japan. Cladoceran *Daphnia* spp., and copepod *Eodiaptomus japonicus* and Cyclopoida spp. were always dominant zooplankton in this lake over the past half century, contributing >90% of total zooplankton biomass. In this study, we tried to make prediction equations for estimating population growth rates of the three dominant zooplankton species from several abiotic and biotic variables, i.e. temperature, food conditions and individual density, for calculating the zooplankton production. Finally, we calculate ecological transfer efficiency between phytoplankton and dominant zooplankton productions, and discuss about the long-term trends over the four decades (1971-2010) in a large temperate lake.

Zooplankton assemblages were collected at pelagic stations (60-70 m deep) from June 2018 to July 2020, and used for incubation experiments to determine the somatic growth rates (g) in different temperature, food and density conditions. Each 10–15 L lake water with zooplankton assemblages was collected using a 20-L Schindler-Patalas zooplankton trap from 0–20 m with 5 m interval, combined in a 130-L plastic tank, and concentrated with a 100- or 200- μ m-mesh to 1 L. The lake water with concentrated zooplankton was poured to each of six 3-L or four 5-L transparent plastic bottles, filled with the filtered lake water with a 100- μ m mesh. Zooplankton densities (D) were arranged at 1-5 fold higher than those in situ to make broader range of density. Remained zooplankton assemblages were used to determine the initial zooplankton body size.

In 2018 and 2019, zooplankton assemblages were incubated in an incubator for 4 days at average in situ water temperature (T) and light intensity in 0–20 m of water column and photoperiod when the zooplankton was collected. In 2020, the incubation experiments were made with almost similar procedure but included additional higher temperatures. Total phosphorus (TP) and chlorophyll a (Chl. a) concentrations were measured as a proxy of food condition (F). After incubation, zooplankton number were counted, and the body sizes were measured. The g was calculated using equation: $g = (\ln W_4 - \ln W_0) / 4$, where W_0 and W_4 were the mean body weights in zooplankton before and after incubation, respectively. Body weights were estimated from body size using the length-weight equations. To estimate the g from multiple environmental parameters, the g was fitted with a multiple linear regression model, $g = aT + bF + cD + d$ using RStudio software; each of TP and Chl. a as F was fitted in the model 1 and model 2, respectively. The g was transformed to population growth rate (G) using equation: $G = e^g - 1$.

Zooplankton production (P) was calculated using equation: $P = B \times G \times 0.447$. The ecological transfer efficiency (E) was calculated from total zooplankton production divided by primary production of phytoplankton (P_p). Parameters of T , F , D , B and P_p referred to previous studies.

The g in *Daphnia* spp., *E. japonicus* and Cyclopoida spp. showed positive correlation with T and F but negative with D , largely varied 0.01–0.19, 0.01–0.08, 0.01–0.13 day⁻¹, respectively, due to seasonal variation. R^2 of the fitted multiple regression models for the g was 0.6–0.7 in *Daphnia* spp., whereas it was only 0.1–0.2 and 0.3 in *E. japonicus* and Cyclopoida spp. respectively, indicated that multiple regression model estimated in this study can well describe somatic growth in *Daphnia* spp. but not in copepods. In *Daphnia* spp., the model 1 is more suitable to estimate g in *Daphnia* spp. due to the smaller AIC.

Therefore, we estimated g of *Daphnia* spp. in Lake Biwa using model 1 and projected the P from 1971 to 2010. Over the four decades, annual P of *Daphnia* spp. varied 0.5–4.8 gC m⁻² y⁻¹, 2.8 gC m⁻² y⁻¹ on average. It showed similar trend as the biomass, decreased from 1970s until 1993 and exhibited an

increasing trend after 1993. Productions of *E. japonicus* in Lake Biwa were calculated using another method of length-based food model in our previous study. Since sum of *Daphnia* spp. and *E. japonicus* biomasses accounts for >80% of total zooplankton biomass in this lake, secondary production can be calculated from these two taxa. The calculated production varied 5.7–56.4 gC m⁻² y⁻¹, on average 20.9 gC m⁻² y⁻¹, whereas the *E* showed a relative constant trend over four decades, averaging in 9.2%. It also showed 2-fold high value, ca. 20% in late 2000s might be due to the low primary production. P_p in Lake Biwa were measured by different methods and locations. Variance of *E* might be partially regulated by estimating accuracy of P_p .

Keywords: zooplankton, long-term production dynamics, ecological transfer efficiency, lake

High resolution monitoring for subsidiary nutrient loadings and phytoplankton production in north basin of Lake Biwa

*Syuhei Ban¹, Xin Liu¹, Ken'ichi Osaka¹, Naoshige Goto¹, John Wells²

1. The University of Shiga Prefecture, 2. Ritsumeikan University

In Lake Biwa, nutrient loading from non-point source is considered to be an one of the reasons why total phosphorus (TP) concentration did not decline to the level before eutrophication period. Our previous studies suggested that horizontal transportation of nutrients from littoral slope may enhance phytoplankton growth at a pelagic site in north basin of Lake Biwa around rice planting season. It implies that drainages from rice paddies may enhance phytoplankton production and prevent to make further reduction of TP concentration in the lake; that is, particulate phosphorus (PP) from the rice paddies may be deposited to littoral slope, resuspended from the bottom, transported to offshore through internal wave driven by wind, and finally enhance phytoplankton growth. We still do not have enough evidence to confirm this hypothesis, because such wind-driven events occur sporadically. In this study, we simultaneously monitored nutrient concentrations, phytoplankton production, and water movements with high resolution, i.e. minutes to daily, to detect such sporadic events.

A mooring system for monitoring phytoplankton production and lake water movement was situated nearby a buoy of Japan Water Agency (35°18.69'N, 136°08.68'E) from 28 April to 27 July 2020. Water temperatures were measured at 10 min interval at 1 and 5 m, and at 2-m interval from 10 to 30 m with a thermistor chain. *In situ* phytoplankton production was measured using light intensity and chlorophyll *a* (chl. *a*) concentration monitored by sensors attached at 5 m, 10 m, and 15 m and monthly obtained photosynthesis - light intensity curve. Water movements was measured at 10 min interval with an acoustic doppler current profiler (ADCP). Lake waters at 5 and 20 m were collected daily at noon for measuring nutrient concentrations, NO₃-N, NH₄-N, and PO₄-P, with a water pump from 28 April to 17 June 2020. Apart from them, we weekly investigated vertical profiles of water temperature, chl. *a* and nutrient concentrations.

Water temperature gradually increased above 20 m from early May, being >15°C at surface, and then distinct thermocline developed in 10-20 m in late May. Chl. *a* concentration increased above 20 m to exceed 5 μg/L, from early May to late June. Daily nutrient monitoring showed that PO₄-P concentrations sporadically increased over 0.05 μmol/L in early May at both 5 and 20 m, but were always low, around 0.02 μmol/L, thereafter. A 0.015 μmol/L of PO₄-P has been shown to be a critical concentration for phytoplankton growth. NH₄-N concentrations varied 0.03 -4.57 μmol/L at 5 and 20 m from late April to late June. NO₃-N concentrations at 5 m gradually decreased from 6.12 to 2.14 μmol/L by mid-May, further declining to < 1.00 μmol/L thereafter, while those at 20 m were always 4.52-10.49 μmol/L throughout the study period. This decline of NO₃-N at 5 m in May might be caused by phytoplankton growth, implying subsidiary supply of PO₄-P.

Phytoplankton productions were relatively high, 0.5-1.0 gC/m²/d, during May, and gradually decreased in June. Almost 80% of variation of the daily phytoplankton productions could be explained by fluctuation of light intensity. Residuals from ones predicted from a regression equation between the production and light intensity were positive during May but almost zero after June, meaning that some factors other than light, e.g. nutrient supply, might enhance the production during May, when sestonic C:P ratios were quite low, < 100, which indicates that phytoplankton may be relaxed from P limitation. Additional microscopic

observations showed that large phytoplankton dominated in May, implying that there was large-scale pulsed nutrient supply.

These high resolution monitoring of nutrients and production suggested that subsidiary nutrient supply enhanced phytoplankton production in May. We can also show water movement data with an ADCP and a relationship between the production and water movement at the conference presentation.

Keywords: Lake Biwa, Subsidiary nutrient supply, High resolution monitoring, Mooring system, Internal wave, Phytoplankton primary production

Hydrological controls on phosphorus export from diffuse source in Lake Biwa basin, central Japan.

*Ken'ichi Osaka¹, Haruto Tanabe¹, Syuhei Ban¹

1. Department of ecosystem study, University of Shiga Prefecture

Phosphorus is an important nutrient for ecosystems, and its availability is linked to widespread environmental problems, such as eutrophication, hypoxia, and the expansion of harmful algae in aquatic ecosystems (Schindler 1974, 2008; Jones and Bachmann 1976; Correll 1998; Downing et al. 2001). Traditionally, agricultural land has been recognized as major diffuse source of phosphorus exported from watershed (Sims et al., 1998; Brett et al., 2005; Mockler et al., 2017 Sharpley et al., 2008, Schoumans et al., 2014), in recent years, forested watershed has also been recognized as potentially important diffuse source of phosphorus (Ice and Binkley, 2003; Ide et al. 2007, 2008; Loehle et al., 2014).

Many studies tracing phosphorus source from the watersheds have observed the relation between phosphorus export and land use type of watershed, however, these studies were conducted usually in base flow. On the other hand, it have been reported that phosphorus mainly exported during rainfall events from watersheds (Inoue and Ebise 1991; Evans and Johnes, 2004; Ide et al. 2012). Therefor we observed the relation between phosphorus concentrations and land use type of watershed in the different hydrological condition, in order to clarify the contribution of phosphorus export from different land use type watershed.

We collected the river water samples from 20 watersheds in Lake Biwa basin from March 2019 to February 2021. The water samples were collected at once in a month during different hydrological condition. The watersheds consist of several land use: agricultural land, forest, and residential area. We measured total phosphorus (TP), dissolved phosphorus (DP) concentrations with molybdenum blue method, phosphate (PO_4^{3-}) concentrations with ion chromatography. Particulate phosphorus concentrations were calculated as difference between TP and DP.

The averaged TP concentrations in 20 rivers varied largely, ranging from 0.091 to 0.517 mg/L. In base flow condition, the averaged PO_4^{3-} , PP and TP were higher with the increase of part of agricultural land in watershed. In flooded condition, averaged PO_4^{3-} concentrations were also higher with the increase of part of agricultural land in watershed, however, TP and PP concentrations did not relate with part of agricultural land in watershed. In presentation, we will discuss the TP and PP export processes in flooded condition.

Keywords: phosphorus, rainfall event, diffuse source

The influence of vertical water mixing on inter-annual nitrogen dynamics in Lake Biwa

*Takaaki Ishibashi¹, Ken'ichi Osaka², Keisuke Koba³, Kei Nishida⁴, Takashi Nakamura⁴

1. Graduate School of Environmental Science, University of Shiga Prefecture, 2. Department of ecosystem study, University of Shiga Prefecture, 3. Center for Ecological Research, Kyoto University, 4. Interdisciplinary Centre for River Basin Environment, Interdisciplinary Graduate School, University of Yamanashi

Introduction

Nitrogen is a key nutrient in aquatic environments, but an excessive supply of nitrogen leads to deterioration of water quality, so it is important to maintain an appropriate amount of nitrogen compounds in the lake. To control the amount of nitrogen compound in the lake, it is necessary to clarify the dynamics of nitrogen, and for this purpose, it is necessary to measure both external nitrogen inflow and the internal nitrogen cycle. In recent years, the stratification structure of various lakes around the world has been changing due to global warming, and it has been reported that changes in stratification structure also affect nutrient dynamics. In Lake Biwa, the vertical water convection to the bottom has not happened in recent years. So we need to monitor the whole layer data and inter-annual data to clarify the effects of differences in water mixing conditions on nitrogen dynamics. Although many studies have measured the seasonal variation of nitrogen dynamics, a few studies have measured the medium to long-term variation, and there are very few studies on nitrogen dynamics in all layers. Therefore, we aimed to clarify nitrogen dynamics in Lake Biwa using the middle to long-term monitoring data and to elucidate how it is affected by water mixing conditions in this study.

Material and method

In this study, lake water samples were collected every 1-2 months from 2015 to 2020 at 14 depths in the basin of Lake Biwa's North Lake (Depth is about 90 m), and water temperature, dissolved oxygen, and chl.a were measured by CTD probe. We measured the concentrations of nitrogen compounds, nitrogen stable isotope ratio ($\delta^{15}\text{N}$) of nitrogen compounds ($\delta^{15}\text{N}_{\text{DN}}$, $\delta^{15}\text{N}_{\text{NO}_3^-}$, and $\delta^{15}\text{N}_{\text{PN}}$). From the measured nitrogen compound concentrations, $\delta^{15}\text{N}$, and the area of Lake Biwa by depth calculated from the map, the amount of nitrogen compound and $\delta^{15}\text{N}$ in the whole lake water were calculated.

Results and discussion

The amount of dissolved nitrogen (DN) was shown to be decreasing in the long term. Since nitrate-nitrogen (NO_3^-) and dissolved organic nitrogen (DON) account for most of the DN content, it is important to examine the fluctuations of NO_3^- and DON. NO_3^- increased from autumn to winter and decreased from spring to autumn, while DON decreased from autumn to winter and increased from spring to autumn.

The factors that increase or decrease DN is considered to be the inflow from rivers as an external inflow process and the exchanging from the lake bottom as an internal load. Both factors increase the nitrogen compound amount in the lake. Since this cannot be explained by the fact that NO_3^- and DON are fluctuating at the same time, we will discuss the effect of the internal nitrogen cycle. The increase of NO_3^- and decrease of DON from autumn to winter can be attributed to nitrification.

The autumn to winter nitrification event started times vary from year to year. The timing of this nitrification event happened was fast in 2018, slow in 2016, 2020 and no nitrification event has happened in 2017, 2019. Vertical water convection was late in 2016, and no vertical water convection of bottom was in 2019, 2020. Thus we conclude the difference in the timing of this event might be due to the strength of the stratification and timing of vertical water convection.

Keywords: Lake Biwa, Nitrogen dynamics, Inter-annual changes, Nitrogen stable isotope ratio

Detection of Dissolved Methylphosphonate in Freshwater of Lake Biwa by pre-concentration with Iron(III) hydroxide coprecipitation

Tomoki Yamamoto¹, Kazuma Tsuji³, Yuki Yamanaka³, *Masahiro Maruo¹, Hajime Obata²

1. Department of Ecosystem Studies, School of Environmental Science, The University of Shiga Prefecture, 2. Atmosphere and Ocean Research Institute, The University of Tokyo, 3. Graduate School of Environmental Science, The University of Shiga Prefecture

Introduction

Bacteria possibly utilizes P(III) species such as organophosphonates as P resources in freshwater lakes. At the subsurface layer of Lake Saiko (P-limited lake: Yamanashi, Japan), maximum methane concentration is observed under stratified condition in summer. This subsurface methane maximum (SMM) is considered to be formed by metabolism of methylphosphonate (MPn) by cyanobacterium *Synechococcus* to ingest phosphorus [Khatun et al., 2019]. In Lake Biwa (Shiga, the largest in Japan), mesotrophic lake, methane maximum layer is also formed in the epilimnion during summer stratification, but it is not sure this layer is formed by the same reason. We examined the existence of MPn in both lakes but it was not detected as dissolved form yet. However, MPn extracted from particulate matter was detected in Lake Saiko and eutrophic Lake Fukami-Ike (Nagano, Japan) [Tsuji et al., 2020].

We applied the ion chromatographic determination methods to detect dissolved MPn in water of Lake Biwa in combination with pre-concentration method of MPn with iron(III) hydroxide co-precipitation to enhance detection limit and remove matrix in water.

Methods

Analytical condition for the determination of MPn in water was already established by ion chromatography with high volume injection [Tsuji et al., 2019; Maruo et al., 2016]. Condition of MPn co-precipitation with iron(III) hydroxide was investigated by varying pH and amount of iron(III) hydroxide and MPn concentration. In fundamental investigation, MPn in 500 mL sample solution was concentrated by addition of freshly prepared iron(III)hydroxide from iron(II) chloride in the solution. Iron(III)hydroxide was collected on Nuclepore membrane filter (pore size; 0.4 micrometer), and MPn was released by immersing the filter in 25 mL ammonia solution (pH 10). Released MPn was analyzed by ion chromatography.

This method was applied to the determination of dissolved MPn in water samples of Lake Biwa (Shiga, Japan). Waters were sampled by Niskin-X sampler by Research Vessel "Hassaka", The University of Shiga Prefecture, on Sep. 10, 2020, at St. T4 (close to Takeshima Island, max. depth 43 m).

Results and Discussion

pH ranges preferable to the preconcentration of MPn was investigated from pH 4 –10. Finally, pH around 6 was preferable, and recovery of MPn in the concentration range 0.05 –5 nM in the standard solution

was stable (49 - 53%) independent of MPn concentration. Recovery of 5 nM MPn in 5 replicates was constant at the value of 50% (CV 1.6%). MPn was concentrated by 10 folds. Application of this method enabled the detection of MPn up to 0.03 nM in water. From the concentrated sample, dissolved MPn was detected in the concentration around 0.1 nM at the depth 0 -30 m. At the bottom (43 m), 0.2 nM of MPn was detected probably because of bacterial activity in lake sediment.

References

Khatun S, Iwata T, Kojima H, Fukui M, Aoki T, Mochizuki S, Naito A, Kobayashi A, Uzawa R (2019) Aerobic methane production by planktonic microbes in lakes. *Science of the Total Environment* 696: 133916.

Maruo M, Ishimaru M, Azumi Y, Kawasumi Y, Nagafuchi O, Obata H (2016) Comparison of soluble reactive phosphorous and orthophosphate concentrations in river waters. *Limnology* 7: 7-12.

Tsuji K, Maruo M, Obata H (2019) Determination of trace methylphosphonate in natural waters by ion chromatography. *Bunseki Kagaku* 68: 275-278. (Japanese with English abstract)

Maruo M, Tsuji K, Iwata T, Oyagi M, Obata H (2020) Detection of organophosphonates and phosphite in suspended matter of P-limited lakes. Abstract of JpGU2020 session #A-HW32.

Keywords: dissolved methylphosphonate, coprecipitation, P-limited lake, Lake Biwa, ion chromatography

Estimation of groundwater and lake water interaction in the deeper zone of Lake Biwa, using ^{18}O and D in pore water and groundwater

*Shin-ichi Onodera¹, Mitsuyo Saito², Yusuke Tomozawa¹, Takuya Ishida¹, Syuhei Ban³, Noboru Okuda⁴

1. Graduate School of Advanced Science and Engineering, , Hiroshima University, 2. Okayama University, 3. The University of Shiga Prefecture, 4. Kobe University

We examined to estimate groundwater and lake water interaction in the deeper zone of Lake Biwa, using ^{18}O and D in pore water and groundwater to confirm groundwater discharge and nutrient flux. We collected groundwater samples at production and observation boreholes several depths on the eastern coastal area of the lake and the pore water samples in bottom sediment cores at the sites of an eastern and western slopes with the depths of 5m, 10m, 20m, 60m in a northern lake, respectively. The water isotopic ratios in groundwater were lower than those in lake water, and those in deep groundwater were lower than those in shallow groundwater, respectively. The d-values which is a y-intercept on the ^{18}O and D plot with the slope of 8 were larger in groundwater and deep, respectively. The isotopic ratios in spring water of headwater indicated the altitude effect which isotopic ratios in the spring with the higher altitude has lower, and d-values in summer precipitation has smaller than those in winter. These indicated the deeper groundwater came from the mountain slope with the higher altitude. The pore water at the site with the depth of 20m had the larger d-values than those at the site with the shallower depth. This suggested the deeper groundwater contributes to the groundwater discharge at the deep zone of the lake.

* This research was supported by JSPS project (PI Ban,S).

Keywords: groundwater discharge, deep zone, isotope

Identification of enriched phosphate in groundwater: insights from distribution of phosphate oxygen isotope ratio in aquifer sediments

*Takuya Ishida¹, Yusuke Tomozawa¹, Xin Liu², Mitsuyo Saito³, Shin-ichi Onodera¹, Noboru Okuda⁴, Syuhei Ban²

1. Hiroshima University, 2. The University of Shiga Prefecture, 3. Okayama University, 4. Kobe University

1. Introduction

Phosphorus (P) input through groundwater discharge plays a significant role in nutrient cycling and primary productivity in the coastal area (Slomp and Van Cappellen, 2004). Therefore, its biogeochemical cycling in underground environment is important in proper land management and understanding of natural systems.

Recently, phosphate oxygen isotope ratio ($\delta^{18}\text{O}_{\text{PO}_4}$) has been used as a promising tool to elucidate the P cycling (Paytan and McLaughlin, 2012). Previous studies showed the possibility to evaluate P sources, metabolism by organism in some ecosystems. However, it is not clear whether $\delta^{18}\text{O}_{\text{PO}_4}$ is useful for evaluating the P cycling of in underground environment, because few research has applied the $\delta^{18}\text{O}_{\text{PO}_4}$ analysis for underground P cycling (Neidhardt *et al.*, 2018). Determination of $\delta^{18}\text{O}_{\text{PO}_4}$ values in groundwater and lithological sediments would allow us to clarify the P biogeochemistry in underground environment and to predict $\delta^{18}\text{O}_{\text{PO}_4}$ values in groundwater.

In the present study, we aimed to clarify the biogeochemical P cycling in underground environment by comparing $\delta^{18}\text{O}_{\text{PO}_4}$ values in groundwater and lithological sediment from a boring core.

2. Material and method

Our study was conducted on the eastern shore of Lake Biwa in central Japan. The study area is covered by forest in upstream and rice field and built-up in downstream. To monitor shallow (1.8~10.0 m) and deep (24.7~27.5 m) aquifers, two monitoring wells were excavated by rotary drilling at The University of Shiga Prefecture.

The recovered 28 m-long sediment core was divided by 1 m and air-dried. The top 10 cm of each core were ground to powder using a multi-bead shocker (Yasui Kikai) with tungsten carbide beads to homogenize the samples and to enhance the reaction between extraction solution and the sample. The powdered sediment samples were stored at room temperature until analysis. The shallow and deep groundwater samples were collected in May 2019 by siphon technic with a silicon tube. Samples of the lake water and river water were collected near the monitoring wells.

To extract labile P, iron-bound P, authigenic P and detrital P in the sediment sample, the sequential extraction method (SEDEX) was applied (Ruttenberg, 1992). To extract inorganic P in the PP of groundwater, the filter samples were immersed in 1 M HCl for 16 h. The P concentrations in the extractions and soluble reactive P (SRP) in the water samples were measured using the molybdenum-blue method.

The $\delta^{18}\text{O}_{\text{PO}_4}$ analysis was conducted on the groundwater, PP and sediment samples corresponding to shallow and deep aquifers using SEDEX extractions. DIP in the samples were converted to Ag_3PO_4 according to Tamburini *et al.* (2010). The $\delta^{18}\text{O}_{\text{PO}_4}$ values were measured using a TC/EA-IRMS at the Research Institute for Humanity and Nature.

3. Result and discussion

The groundwater, especially in the deep aquifer, was characterized by high SRP concentration (0.74~6.78

$\mu\text{mol L}^{-1}$) and low ORP value (-80~66 mV). The SRP concentration in groundwater was higher than those in the river water (0.33~0.73 $\mu\text{mol L}^{-1}$) and in the lake water (<0.45 $\mu\text{mol L}^{-1}$), indicating groundwater discharge is additional P source to the oligotrophic lake.

The $\delta^{18}\text{O}_{\text{PO}_4}$ values of DIP in shallow (15.1‰) was close to biological equilibrium value based on latest formula (Chang and Blake, 2015). Therefore, DIP in shallow groundwater may be heavily recycled by organisms. Also, PP in shallow groundwater, which had the similar $\delta^{18}\text{O}_{\text{PO}_4}$ value to DIP (15.9‰), was likely affected by biological recycling. In contrast, for deep groundwater, the $\delta^{18}\text{O}_{\text{PO}_4}$ values of DIP (17.4‰) and PP (11.8‰) differed from biological equilibrium value, which suggests the influence of other biological processes and/or P sources. In our poster, we will show the result of $\delta^{18}\text{O}_{\text{PO}_4}$ in sediment samples and discuss the P cycling in groundwater.

Reference

Chang, S. J. and Blake, R. E. (2015), *Geochimica et Cosmochimica Acta*. 150, pp. 314–329. doi:

10.1016/j.gca.2014.10.030.

Neidhardt, H. *et al.* (2018), *Science of the Total Environment*. 644, pp. 1357–1370. doi:

10.1016/j.scitotenv.2018.07.056.

Paytan, A. and McLaughlin, K. (2012), *Handbook of Environmental Isotope Geochemistry*. pp. 419–436.

doi: 10.1007/978-3-642-10637-8.

Slomp, C. P. and Van Cappellen, P. (2004), *Journal of Hydrology*, 295(1–4), pp. 64–86. doi:

10.1016/j.jhydrol.2004.02.018.

Keywords: Phosphorus, Groundwater

Long-term Estimation on Phosphorus flux in a Coastal Catchment Influenced by the Anthropogenic Land Use Change

*Kunyang Wang¹, Shin-ichi Onodera¹, Mitsuyo Saito², Yuta Shimizu³

1. Graduate School of Integrated Arts and Science, Hiroshima University, 2. Faculty of Environmental Science and Technology, Okayama University, 3. National Agriculture and Food Research Organization

Phosphorus is a non-renewable resource and is an important element of the natural material cycle. Phosphorus discharge in coastal catchments not only cause the loss of phosphorus resources, but also cause eutrophication. The quantification of the phosphorus discharge in water were most important indicators of the water environment in coastal area because these processes are related to the transport of large nutrient loads. The phosphorus pollution sources of the surface water environment are divided into point source pollution and non-point source pollution according to the different spatial distribution. Nonpoint source phosphorus pollution from agricultural land is a leading contributor to world water quality impairments.

The Yamato River catchment covers 1077 km² and has been an important crop production base in Western Japan since the 1600s. The region's rich groundwater resources were a major factor in its agricultural development. In recent decades, however, agricultural land has gradually given way cities in the course of rapid urbanization and increasing population. There are 5 sewage treatment plant in the watershed, 3 of them are located in Osaka Prefecture and others are in Nara Prefecture. As of 2010s, the overall sewage treatment pipeline in the basin covers more than 90% of buildings.

SWAT model could meet this need and has proven to be an effective tool for assessing nonpoint source pollution for a wide range of scales and environmental conditions, and it supports inputting point source data according to monthly data. This study used the SWAT model to simulate phosphorus fluxes in the Yamato river catchment for more than 50 years, to study anthropogenic impact on phosphorus discharge into the ocean.

Keywords: Phosphorus discharge, sewerage treatment, non-point source, agriculture impact

Analysis for the characteristics of water and nutrient discharge in a sub-basin of Osaka Bay catchment

*Shuta Ishihara¹, Kunyang Wang², Mitsuyo Saito³, Shin-ichi Onodera⁴

1. Faculty of Environmental Science and Technology, Okayama University, 2. Graduate School of Integrated Arts and Sciences, Hiroshima University, 3. Graduate School of Environmental and Life Science, Okayama University, 4. Graduate School of Advanced Science and Engineering, Hiroshima University

Quantitative evaluation of nutrient discharge in watersheds is important for taking measures of environmental management of enclosed coastal seas. The hydrological model approach is a powerful tool for the evaluation of the impacts of climate change (e.g. extreme rainfall) and human activities (e.g. land-use change) on water and nutrient discharge in watersheds. We aimed to analyze the characteristics of water and nutrient discharge in the Saho River which is a sub-basin of Yamato River catchment inflowing Osaka Bay, western Japan.

The results are as follows;

(1) We applied SWAT (Soil & Water Assessment Tool) to Saho River catchment and succeeded in the model construction for estimating water discharge on an hourly basis considered the effects of flooding.

(2) We also constructed a daily basis nutrient discharge model that considered the water discharge fluctuations during floods with high reproducibility.

(3) We simulated how the catchment water balance will change assuming that all of the current paddy fields and farmland will change to residential areas due to urbanization by the developed hourly basis discharge model. In this simulation, the baseflow will decrease by 0.1 m³/s on average, while the peak flow rate during floods will increase by 1.7 m³/s at maximum. The results suggest the increased risk during floods.

(4) Simulated nitrate-nitrogen inflow from Saho River to Yamato River by the developed daily basis nutrient discharge model was 261 kg/day on average during baseflow periods, 1.5 tons/day at the maximum during floods, and 94.7 tons/day in the annual, respectively.

*This work is supported by the research grants of “Environmental Rehabilitation and Creation of the Osaka Bay Area, 010005, 020004, 2019-2020, PI: Mitsuyo SAITO” and “Asia-Pacific Network for Global Change Research, CRRP2019-09MY-Onodera, 2019-2022, PI: Shin-ichi ONODERA” .

Keywords: urbanized catchment, water and nutrient discharge

Estimation of groundwater flow and a river water contribution to it in an alluvial plain of western Japan, using tracer methods

*Yusuke Tomozawa¹, Toru Takeuchi², Shin-ichi Onodera¹, Mitsuyo Saito³, Shotaro Fujioka⁴

1. Graduate School of Advanced Science and Engineering Hiroshima University, 2. Fujita Geology Co., Ltd., 3. Graduate School of Environmental and Life Science, Okayama University, 4. River fishermen

The purpose of this study was to confirm groundwater flow and a river water contribution to it in an alluvial plain of western Japan, using tracer methods. The research area is located on the Kurashiki alluvial plain, the downstream area of Takahashi River, Okayama Prefecture, Japan. We monitored the water level and water temperature at the 30minutes interval, and collected water samples weekly at Sakazu intake weir station of Takahashi River and at one borehole since May 2017. The observation borehole has the depth of about 11 m. The water samples were analyzed the main anion and cation by the ion chromatography, and hydrogen and oxygen stable isotope ratios by PICARO.

The water temperature in the Takahashi River showed a similar trend to the air temperature in Kurashiki weather station, on the other hand the water temperature in the observation boreholes showed a maximum in the seasonal variation with the delay of 6 months at the depth of 10 m and of 3 months at the depth of 3 m below the ground, respectively. The isotope ratios of hydrogen and oxygen in the river water and groundwater showed some variation. These results suggested groundwater recharge from the river to the underground on the alluvial plain, and the groundwater flow velocity was extremely large. In addition, the hydrogen and oxygen isotope ratios of the river water were significantly decreased in July 2018 and September 2018 during the large outflow. These water was good tracer to detect the influence of river water on groundwater

Keywords: Coastal alluvial plain, groundwater flow, stable oxygen and hydrogen isotope

Estimation of Landuse Change Impact on Water Budget in Higashihiroshima Catchment using SWAT

*Sharon Bih Kimbi¹, Kunyang Wang¹, Shin-ichi Onodera², Ichirow Kaihotsu¹, Shingo Nozaki², Yusuke Tomozawa²

1. Graduate School of Integrate Arts and Sciences, Hiroshima University, 2. Graduate School of Advanced Science and Engineering, Hiroshima University

Increasing population growth with rapid changes in social and economic standards have led to increasing demand in settlements or agriculture areas. To use water resources sustainably, it's important to understand the quantity of water resource both Spatially and temporally. The Soil and Water Assessment Tool (SWAT) model was used to analyse watershed hydrology and variability of streamflow in the Higashihiroshima catchment area. The statistical model performance, which measures the coefficient of determination (R^2) and Nash-Sutcliffe Efficiency (NSE) were used to evaluate the correlation between the observed and simulated daily streamflow. The preliminary result shows a good agreement between the observed and simulated flow. Both NSE and R^2 were found to be greater than 0.7 for the calibration and validation period. The analysis was performed on two different land-use maps (1987 and 2009) to determine the effect of urbanization on the hydrology of the watershed specifically water budget. Landuse change has a profound impact on runoff hydrographs. Increased impervious surfaces are a common cause of increased peak-runoff volumes. This condition will increase erosion, sedimentation on the water body, decreasing water resources, increase agricultural pollutant, landslide and decrease agricultural production.

This study is supported by JSPS (Japan Society for the promotion of Science)

Keywords: Landuse , Water Budget, Hydrology, SWAT

Flood Impact on water quality in a Small Catchment Area: Preliminary Study

*Sharon Bih Kimbi¹, Shin-ichi Onodera², Shingo Nozaki², Yusuke Tomozawa²

1. Graduate School of Integrate Arts and Sciences, Hiroshima University, 2. Graduate School of Advanced Science and Engineering, Hiroshima University

Water quality monitoring of streams and river has been conducted in many regions across the globe, with the goal of protecting human health and the environment. However, particular concern has been on the concentration of sediments and nutrients in water flowing through rivers, given the potentially detrimental effects these constituents have on river health and receiving systems downstream. Sedimentation and turbidity are equally important contributors to declines in riverine fauna and the overall decrease in environmental aesthetic. In this study, Water quality parameters were examined for the Saijo river during the flood period for physicochemical properties such as pH, alkalinity, conductivity, turbidity, Solids and dissolved oxygen (DO). These results are meant to help water resource managers assess and predict local effects of such contaminants on the environment.

Keywords: Flood, Water Quality, Dissolved Oxygen, Solids, Turbidity

Process of spatio-temporal variation in seagrass-seaweed meadows in intertidal areas of Seto Inland Sea, western Japan

*Mitsuyo Saito¹, Shin-ichi Onodera², Natsushi Soga³, Yuto Ideishi³, Shingo Nozaki², Yusuke Tomozawa²

1. Graduate School of Environmental and Life Science, Okayama University, 2. Graduate School of Advanced Science and Engineering, Hiroshima University, 3. Faculty of Environmental Science and Technology, Okayama University

Seagrass-seaweed meadows are regarded as an important coastal ecosystem with several ecosystem services such as global carbon sink, maintenance of coastal food webs, and producing biodiversity. However, the process of these spatial distributions and temporal changes are not well studied for intertidal areas. In the present research, we aimed to examine the process of spatio-temporal variation in seagrass-seaweed meadows in intertidal areas of Seto Inland Sea, western Japan.

Our target area is located on coastal areas of the island in Seto Inland Sea. Distributions of seagrass, seaweed, and bottom materials were investigated at several tens of points from 2014 to 2020. From these results, it was found that the biomass of seagrass and seaweed had decreased significantly between 2014 and 2018, and then has been recovering in recent years. The factors that influenced this result were considered to be the decrease in water depth due to long-term sedimentation, changes in the type of bottom materials, and the supply of nutrients due to the extreme rainfall event in western Japan in 2018.

The results of principal component analysis (PCA) suggests that the distribution of seagrass and seaweed were greatly affected by the type of bottom materials: green algae tended to distribute in gravel-rich area, while eelgrass in the muddy and sandy area. The analysis also suggests that submarine groundwater discharge (SGD) influences the biomass of green algae. Besides, the results of nitrogen stable isotope ratio ($\delta^{15}\text{N}$) analysis revealed that seagrass and seaweed in the target area are strongly affected by the nitrogen supply from the terrestrial area through SGD.

*This work is supported by the research grant of “Grant-in-Aid for Scientific Research (B), 18H03411, 2018-2021, PI: Mitsuyo SAITO” .

Keywords: seagrass-seaweed meadows, spatio-temporal variation, intertidal area, submarine groundwater discharge (SGD)

Analysis of coastal seagrass bed distribution using UAV and near-infrared camera data

*Toru Iwata¹, Akimitsu Shiraishi¹, Mitsuyo Saito¹, Shin-ichi Onodera²

1. Graduate School of Environmental and Life Science, Okayama University, 2. Graduate School of Integrated and Arts Sciences, Hiroshima University

In this study, we analyzed a combination of visible and near-infrared image data obtained using an unmanned aerial vehicle (UAV) with the aim of understanding the distribution of seagrass beds in coastal shallow waters. Algal beds that thrive on dried-up beaches (hereafter referred to as dried-up beds ; DUB) were identified using NDVI, one of the commonly used vegetation indices. In addition, algal beds thriving in seawater (hereafter referred to as submerged beds ; SMB) were identified using the newly developed index NSWI (Normalized Seaweed Index). These results were compared to the results of a ground survey conducted at the same time.

The distribution of NDVI calculated from the data during the lowest tide in July 2020 was generally consistent with the distribution of DUBs. NSWI was able to identify most of the DUBs under conditions where the tidal depth was less than 40 cm.

However, under conditions where the tidal depth exceeded 40 cm, the SMB could not be successfully identified by NSWI using the obtained raw data because of the large attenuation of the reflection from the seafloor as it travels through the long underwater optical path. For this reason, the attenuation of light at each wavelength was corrected using the Lambert-Beer law, and the NSWI was recalculated using the corrected data for improved analysis. The results show that the improved NSWI can identify SMBs under the conditions of tidal depths between 40 and 170 cm.

Using the data from eight flights in July 2020 in the specific area analyzed in this study, we calculated the combined area of DUB and SMB, and found that the area was almost constant regardless of the water depth under the condition of a tidal depth of 140 cm or less. The average of eight data runs showed an area value of 3104 m², with a variance of 462 m². This suggests that the area of seagrass beds in the shallow water can be estimated with a random error of about $\pm 14.9\%$ using the method in this study.

Keywords: Coastal sea grass, UAV, Remote sensing

Physically Based Groundwater Flow Simulation using Tracer-aided model in Kumamoto Region, Japan

*A T M Sakiur Rahman¹, Takahiro Hosono^{2,3}, Yasuhiro Tawara⁴, Youichi Fukuoka⁴, Aurelien Hazart, Jun Shimada³

1. Postdoctoral researcher, Kumamoto University, 2. Faculty of Advanced Science and Technology, Kumamoto University, 3. International Research Organization for Advanced Science and Technology, Kumamoto University, 4. Geosphere Environmental Technology Corporation, NCO Kanda, Awajicho Building 3F, 2-1 Kanda, Awajicho, Chiyoda-ku, Tokyo 101-0063, Japan

Integrated watershed modeling techniques are being applied to examine the surface and subsurface water interactions in recent years. Generally, modeling approaches heavily rely on the best fit of the hydrograph which cannot alone describe entire catchment water dynamics. For holistic understanding of hydrological processes, it is necessary to incorporate and simultaneously simulate tracers which can provide important inferences about water ages, flow paths and origin. Hence, this study incorporated multiple tracers like tritium (^3H), Krypton-85 (^{85}Kr), and groundwater temperature in model and seamlessly simulated tracers coupled with surface and subsurface flows using a fully distributed physically based modeling approach (GETFLOWS) for detailed characterizations of Kumamoto water regimes in southern Japan. The first model developed using the regular hydrometric parameters could not characterize isotopic compositions and groundwater temperature, though it showed acceptable model performance for simulating surface water and groundwater hydrographs for several observation stations located in the area. The second model calibrated by integrating tracers with regular parameters well characterized hydrographs (surface water, groundwater), isotopic compositions and groundwater temperature. Hence, the tracer-aided model was used for simulating groundwater storage, flow paths and groundwater age which showed a close agreement with estimation of water ages using isotopic approaches. The findings of this study clearly indicated that multiple tracers aided can better visualize the subsurface water dynamics than hydrometric model. It is expected that the learning framework presented in this study will be beneficial for field hydrologists and modelers to make joint efforts to build robust models for hydrological processes.

Keywords: Water Modeling, Kumamoto, Tracer aided model

Quantitative evaluation of groundwater pollution at Ryukyu limestone area in southern Okinawa Island: Trial application of boron isotope

*KE-HAN SONG¹, Yumi Moromizato², Ryuichi Shinjo², Jun Yasumoto³, Kazuko Sawada⁴

1. Graduate School of Engineering and Science, University of the Ryukyus, Senbaru 1, Nishihara, Okinawa 903-0213, Japan, 2. Department of Physics and Earth Sciences, Faculty of Science, University of the Ryukyus, Senbaru 1, Nishihara, Okinawa 903-0213, Japan, 3. Department of Regional Agricultural Engineering, Faculty of Agriculture, University of the Ryukyus, Senbaru 1, Nishihara, Okinawa 903-0213, Japan, 4. Center for Strategic Research Projects, University of the Ryukyus, Senbaru 1, Nishihara, Okinawa 903-0213, Japan

Boron concentration and its isotopic composition can be potential tracers for the evaluation of groundwater contamination. We developed a simple method to separate boron (B) from groundwater by utilizing a mini-column of 0.1 mL cation-exchange resin (AG® 50W-X12), which is modified from Nakamura et al. (1992) and Tanimizu et al. (2018). B isotopic composition is analyzed by multi-collector inductively coupled plasma mass spectrometry (MC-ICP-MS). To validate our analytical method, determination of $\delta^{11}\text{B}$ values was performed for seawater reference standards (NASS-5 and NASS-7); our results were in the range of recommended values.

This study focused on two realms of Komesu and Giza Subsurface Dams in southern Okinawa Island. We collected 21 groundwater samples, a spring sample and a river sample from Aug. 19th to 23rd, 2020, and a groundwater sample on Sep. 4th, 2020. After the first investigation, we selected 7 observation well sites in southern Okinawa Island for monthly monitoring of water quality. Besides, two rainwater samples were collected on Aug. 24th, 2020, and Jan. 22nd, 2021. We measured boron concentrations of samples by Q-ICP-MS and analyzed $\delta^{11}\text{B}$ by MC-ICP-MS.

Using these data for the southern Okinawa Island, we characterize and evaluate relative contributions of pollutant sources. The water samples have wide variability in B concentrations (from 18.11 ppb to 168.40 ppb) and B isotopic compositions (from 19.49 ‰ to 38.10 ‰). $\text{NO}_3\text{-N}$ contents are positively correlated with B concentrations and B isotopic compositions. When we assume analyzed rainwaters (having the lowest B and $\text{NO}_3\text{-N}$ contents) as one endmember, these trends can be explained by mixing with possible contaminants (e.g., chemical fertilizer and manure). Although quantitative examination still awaits, our results demonstrate that boron isotopic composition can be utilized as a tracer for groundwater contamination processes.

Keywords: boron isotope, contamination, column separation, MC-ICP-MS

Metagenomic analysis on the groundwater in the Ryukyu Limestone area

*Maruyama Rio¹, Nanami Mizusawa¹, Jun Yasumoto², Mariko Iijima³, Yasumoto Ko¹, Mina Hirose⁴, Akira Iguchi³, Mitsuru Jimbo¹, Shugo Watabe¹

1. School of Marine Biosciences, Kitasto University, 2. Faculty of Agriculture, University of the Ryukyus, 3. National Institute of Advanced Industrial Science and Technology, 4. Tropical Technology Plus

While the microbial community has been considered to play an important role in organic matter decomposition and nutrient cycling in various ecosystems, our current understanding of the microbial community involved in groundwater ecosystem is strikingly insufficient. As a first step to evaluate the effect of the groundwater on coastal ecosystem, we performed metagenomic analysis on the groundwater of the Okinawajima in the southernmost region of Japan, along with measurement of environmental factors. Groundwater samples were collected from the Yaese Town characterized by high agricultural activities. Samples were filtered through 0.2 μ m pore size filter and DNA were extracted from these filters using DNeasy PowerWater Kit (QIAGEN) for shotgun metagenomic analysis. The shotgun data of the groundwater showed that bacteria accounted for 93-98% of the total bacteria at the domain level for all the sampling locations, and Proteobacteria was most dominant at the phylum level, followed by Actinobacteria. Metagenomic analysis revealed the environmental parameters including Oxidation-reduction potential (ORP), Na, Fe and Pb were significantly correlated with certain microbial communities in the groundwater. Further studies are needed to elucidate how the bacterial communities are associated with organic matter decomposition and nutrient cycling in the groundwater and subsequent effects of its submarine discharge on coastal ecosystem.

Keywords: metagenomic analysis, groundwater, okinawajima, Limestone area, Bacteria

The effects of groundwater runoff on the coastal bacterial communities near the Ryukyu Limestone area

*Nanami Mizusawa¹, Akira Iguchi², Mariko Iijima², Rio Maruyama¹, Jun Yasumoto³, Ko Yasumoto¹, Mina Hirose⁴, Shugo Watabe¹

1. Kitasato University School of Marine Biosciences, 2. National Institute of Advanced Industrial Science and Technology, 3. Faculty of Agriculture, University of the Ryukyus, 4. Tropical Technology Plus

Corals are exposed to various stressors such as high water temperature and anthropogenic activities. For example, those inhabiting the coastal area are thought to be strongly affected by terrestrial runoff rich in nutrients and other anthropogenic contaminants. Groundwater is believed to act as a carrier for terrestrial materials running into coastal waters in the southern part of Okinawa Jima Island. However, its lineage to the damage of corals has not been well understood. Because the microbial community plays key roles in biogeochemical cycles, we performed as a first step metagenomic analysis on the coastal seawater as well as on the groundwater in the southern part of Okinawa Jima Island to evaluate the effect of the groundwater runoff on the coastal ecosystem including coral reefs. Coastal water and groundwater samples were collected from Yaese Town and filtered through 0.2 μm pore size filters. Amplicon libraries were constructed using Pro341F/Pro805R primers targeting the V3-V4 region of the bacterial 16S rRNA gene and analyzed by an Illumina MiSeq system, then obtained fastq files were processed by QIIME2. As a result, four prokaryotic phyla, Proteobacteria, Bacteroidetes, Cyanobacteria and Actinobacteria, were found to be dominant in both the coastal water and groundwater samples. Cluster analysis revealed that the samples were divided into 2 groups; one included 16 samples from the coastal waters, and another included 8 samples from the coastal water and 7 samples from the groundwater. Clustering of the latter group comprised of both the coastal water and groundwater samples suggest that the groundwater from certain areas in this study affects the coastal ecosystem at the bacterial community level. We are currently surveying environmental factors in the groundwater which may affect the coastal bacterial communities.

Water environment issues in Chinese megacity delta-Sewage impacts on Peral river coastal area

*Guangzhe Jin¹, Shin-ichi Onodera², Mitsuyo Saito³, Yuta Shimizu⁴, Jianyao Chen⁵

1. College of Ocean and Meteorology, Guangdong Ocean University, 2. Graduate School of Integrated and Arts Sciences, Hiroshima University, 3. Graduate school of Environmental and Life Science, Okayama University, 4. Western Region Agricultural Research Center, National Agriculture and Food Research Organization., 5. The School of Geography and Planning, Sun Yat-sen University

The Pearl River Delta (PRD) is one of the most developed regions in China. It contains seven major cities and will grow into a single mega metropolitan area. The PRD includes a population of over 140 million within an area of 39,380 km². As a result, estuaries in PRD often suffer from water pollution due to growing populations, urbanization, and industrialization.

The main water environment problem in PRD is a rapid increase in water resources demand with relatively low water efficiency, increasing saltwater intrusion, coastal environment problems due to water pollution. The water resource demand type has changed from agriculture to industry with an annual rate of 2.39% until 2015, but with much higher water consumption per unit of GDP than Japan. Estuaries in PRD suffer from multiple contaminants with high nutrient discharging fluxes due to extensive water discharging quantities of the Peral river. With efforts regulating the water quality in PRD, Sever water (Classification higher than 3 of the environmental quality standards) still comprise over 1/3 of the whole water bodies. Results of a field survey in 2017 show high nutrient contents in water and high phosphorus(P) contents (highest of 4000ug/g.DW), and high releasing potential(approx. 50% is mobile P) in the Peral river, indicating a larger sediment P pool with higher mobility than in the Osaka Bay. Our results based on nitrate isotope analysis showed local cities and diluted Peral River water influenced the nitrate dynamics in the coastal area from western Guangdong province, nitrate isotope analysis the dominant nitrate sources is originating from manure and sewage.

Keywords: Sewage, Peral River Delta, Megacity, Sediment, Nutrient

Assessment of drought trends in the Dakbla watershed, Vietnam

*Tram Ngoc Quynh Vo¹, Hiroaki Somura¹

1. Graduate School of Environmental and Life Science, Okayama University

Drought is one of the complex disasters among various natural hazards, especially in mountainous regions. Dakbla watershed is located in the Central Highland of Vietnam, where the extreme events have a significant impact on water resources management. The anomaly of extreme events is one of the main reasons for water scarcity, especially in the dry season. Agriculture can be impaired within a very short period, depending upon the duration of droughts. Farmers still struggle to choose suitable crops under harsh climatic conditions. The situation strongly affects on food security in the area. Therefore, assessment of drought trends was conducted in the target watershed by using various drought indices. The simulation results of the Soil and Water Assessment Tool (SWAT) were utilized for evaluating drought trends during the year 2000 to 2018. The drought tendency was illustrated based on a spatial distribution of sub-watershed level in the target area. In general, understanding the drought trends could support for local authorities and farmers from the aspect of water resources management in the watershed scale and propose a strategy in the future.

Keywords: Water scarcity, Agricultural activities, Water allocation, Mountainous watershed

Hydrogeochemical evolution mechanisms of groundwater in the Semarang Coastal Zone, Java Island, Indonesia

*Rizka Maria Maria^{1,6}, Anna Fadliah Rusydi^{2,6}, Shin-ichi Onodera³, Mitsuyo Saito⁴, Seiichiro Ioka⁵, Robert Muhammad Delinom⁶, Wahyu Purwoko⁶, Dadi Sukmayadi⁶, Hendarmawan Hendarmawan¹

1. Faculty of Geological Engineering, Padjadjaran University, Indonesia, 2. Graduate School of Integrated Arts and Sciences, Hiroshima University, Japan, 3. Graduate School of Advance Science and Engineering, Hiroshima University, Japan, 4. Graduate School of Environmental and Life Science, Okayama University, Japan, 5. Research Institute for Sustainable Energy, Hirosaki University, Japan, 6. Research Center for Geotechnology, Indonesian Institute of Sciences, Indonesia

Semarang city, the capital of Central Java Province is the coastal area in the Java island has the problem of saline groundwater in the coastal region and the high land subsidence rate that influence groundwater condition. Groundwater vulnerabilities in Semarang are influenced by internal factors such as geological type of marine clay and anthropogenic. Based on the problems, it is necessary to conduct a study on hydrogeochemical evolution mechanisms of the groundwater quality. Sixteen dug wells samples, nine bore wells samples, one spring sample and two surface water samples were collected during a field investigation. The Methods including ionic ratios, statistics, Piper diagram, bivariate ion analyses and Gibbs diagrams were used to analyses the hydrogeochemical characteristics and evolution mechanisms. The spatial distribution of key parameters was assessed using a GIS-based simple natural neighbour technique. Results showed that dendrogram statistics of the major hydrogeochemical parameters, including conductivity, Na^+ , Cl^- , Ca^{2+} and Mg^{2+} displayed similar trend distributions, increasing gradually from the southern to northern regions of the study zone; HCO_3^- and SO_4^{2-} have a similar trend. High NO_3^- -N and NH_4^+ -N concentration comes from the influence of settlements and agriculture. The hydrochemistry of the groundwater consists of Na-Cl type, Na-Cl- HCO_3 type, Na- HCO_3 type, Ca- HCO_3 type and Ca-Mg- HCO_3 type. The coastal aquifers are influenced by seawater intrusion, mineral dissolution and ion exchange processes, impacting groundwater evolution.

This studio is supported by the Asia-Pacific Network for Global Change Research (APN) under Grant No. CRRP2019-09 MY-Onodera (funder ID: <http://dx.doi.org/10.13039/100005536>).

Keywords: hydrogeochemical, saline groundwater, anthropogenic, groundwater evolution mechanisms, coastal aquifers

A comparative analysis in modeling surface runoff under climate and land use change in two catchments in Iran and Indonesia

*Sharif Joorabian Shooshtari¹, Shin-ichi Onodera², Yuta Shimizu³

1. Department of Nature Engineering, Agricultural Sciences and Natural Resources University of Khuzestan, Mollasani, Iran, 2. Graduate School of Advanced Science and Engineering, Hiroshima University, 3. Western Region Agricultural Research Center, National Agriculture and Food Research Organization

The specific objective of this study includes comparative analysis of the impact of climate and land use change on the surface runoff for two watersheds viz. Neka River basin (Iran) and Cimanuk watershed (Indonesia) using a SWAT hydrological model. The catchment in Iran is close to Caspian Sea and the Cimanuk catchment located in a coastal area, near to Java Sea. Land Change Modeler developed by IDRISI Selva applied to identify the trends in land use changes in the Neka River basin from 2010 to 2050. Three multispectral remote sensing dataset were used from the database of the US Geological Survey for the years 2002, 2011, and 2017 for the analysis of land use change in the Cimanuk watershed. Moderate (RCP4.5) and intensive (RCP8.5) emissions climate change scenarios were simulated using projections based on 17 CMIP5 climate models to assess changes in precipitation in the Neka River basin. Rainfall projection for long term (2075–2099) was analyzed using an Atmospheric General Circulation Model in Cimanuk catchment. The results revealed the reduction of the forest area by the increases in agricultural area and residential in two basins. Analysis of predicted surface runoff under land use change indicated an increase of 5.1% in the Cimanuk watershed from 2002 to 2017, and an annual increase of 5.5% in the Neka River basin. Changes in surface runoff due to climatic changes leads to increase by +6.1% (12.5%) under RCP4.5 (RCP8.5) scenarios in the lower part of the Neka River basin based on the inter-model average while a slight increase of 0.3% appeared in another basin. Land use change has greater impact than does climate change on variation surface runoff in the Cimanuk watershed, while climate change had more effects than those of land use change in the Neka River basin.

Effects of different NH_4^+ -N contents on N_2O and CO_2 emissions from manure compost-amended soil

*Thanuja Deepani Panangala Liyanage¹, Morihiko Maeda¹, Hiroaki Somura¹

1. Okayama University

Nitrous oxide (N_2O) is a major greenhouse gas that causes global warming and stratospheric ozone depletion. Ammonium nitrogen (NH_4^+ -N) content is considered as a key factor affecting N_2O emissions because ammonium oxidation by nitrifying microorganisms is a major process of N_2O emissions. Exact effects of NH_4^+ -N on N_2O emissions are less examined and even available findings are contradictory. Some studies found strong positive linear correlations between N_2O emissions and NH_4^+ -N content, while others stated reductions in N_2O emissions with increasing NH_4^+ -N content. Therefore, the present study aimed at investigating effects of different NH_4^+ -N contents on N_2O and carbon dioxide (CO_2) emissions from manure compost amended soil.

Greenhouse soil was amended with two types of manure composts (cattle compost, CC and mixed compost was of cattle, poultry, and swine manure, MC) on 3% weight basis. The initial NH_4^+ -N contents were adjusted at three levels of 160, 200, and 400 mg kg^{-1} . The samples were aerobically incubated at 70% water holding capacity at 25°C for 42 days. Emissions of N_2O and CO_2 (gas chromatography) and ammonium and nitrate N contents of soil were measured on days 0, 3, 7, 14, 21, 28, and 42.

The highest cumulative emissions of N_2O (200-420 mg kg^{-1}) and CO_2 (7-11 g kg^{-1}) were observed in MC amended soils at each NH_4^+ -N level. This is probably due to high total N, low C/N, and high mineral N of MC. The MC amended treatments with 160 mg kg^{-1} NH_4^+ -N content showed peak emissions on day 7. In all other treatments, N_2O emissions peaked on day 3, indicating that the nitrification process was enhanced by the addition of NH_4^+ -N. The cumulative N_2O and CO_2 emissions in 400 mg kg^{-1} NH_4^+ -N treatments were lower than those in 200 mg kg^{-1} NH_4^+ -N treatments despite the addition of compost. Higher NH_4^+ -N content would have suppressed the microbial activity probably due to enhanced osmotic effects. In both control and CC amended treatments, cumulative N_2O and CO_2 emissions increased with NH_4^+ -N contents from 160 to 200 mg kg^{-1} , whereas they decreased in 400 mg kg^{-1} NH_4^+ -N treatments. The variation of NO_3^- -N content suggested that the MC amended treatment with 160 mg kg^{-1} NH_4^+ -N content was subjected to a high denitrifying activity compared to the other treatments. With increasing NH_4^+ -N content, the denitrifying activity seemed to decrease due to high osmotic potential. In conclusion, compost with high total and mineral N and low C/N enhanced N_2O and CO_2 emissions at each NH_4^+ -N content. More NH_4^+ -N suppressed microbial activities due to osmotic stress, and therefore lower N_2O and CO_2 emissions were recorded. Soil content of NH_4^+ -N is a key factor in determination of N_2O emissions.

Keywords: Nitrous oxide, Carbon dioxide, Manure compost, Ammonium nitrogen, Microbial activity

[E] Poster | A (Atmospheric and Hydrospheric Sciences) : A-CG Complex & General

📅 Fri. Jun 4, 2021 5:15 PM - 6:30 PM JST | Fri. Jun 4, 2021 8:15 AM - 9:30 AM UTC | 🏠 Ch.10_1

[A-CG29] Extratropical oceans and atmosphere

convener: Toyama Katsuya (Meteorological Research Institute), Youichi Kamae (Faculty of Life and Environmental Sciences, University of Tsukuba), Shoichiro Kido (JAMSTEC Application Lab), Shion Sekizawa (Research Center for Advanced Science and Technology, University of Tokyo)

The extratropical ocean had been considered passive to atmospheric variability. Recent studies, however, revealed active roles of the extratropical ocean in modulating the atmosphere. The goal of this session is to deepen our understanding of the air-sea interaction in the extratropics. A wide variety of researches whose topics range from meso-scale to basin-scale interactions, and from daily to global warming timescales are welcomed. Researches on topics related to extratropical air-sea interaction, including cloud, aerosol, and ecosystem, are also welcomed.

[ACG29-P01] East-Asian atmospheric rivers bring more frequent and intense extreme rainfall under global warming

*Youichi Kamae¹, Yukiko Imada², Hiroaki Kawase², Wei Mei³ (1. Faculty of Life and Environmental Sciences, University of Tsukuba, 2. Meteorological Research Institute, Japan Meteorological Agency, 3. University of North Carolina at Chapel Hill)

[ACG29-P02] AGCM experiments for winters of 2017/18 and 2019/20

*Kazuaki Nishii¹, Bunmei Taguchi², Hisashi Nakamura³ (1. Graduate School of Bioresources, Mie University, 2. Faculty of Sustainable Design, University of Toyama, 3. RCAST, The University of Tokyo)

[ACG29-P03] A breakdown of the diabatic genesis/loss of polar cold air masses and its relationship with air-sea interactions

*Yuki Kanno¹, Toshiki Iwasaki² (1. Central Research Institute of Electric Power Industry, 2. Department of Geophysics, Graduate School of Science, Tohoku University)

[ACG29-P04] Year-to-year variations of the extratropical direct circulation associated with the Aleutian-Icelandic lows

*Masaya Kuramochi¹, Hiroaki Ueda² (1. Graduate School of Science and Technology, University of Tsukuba, 2. Faculty of Life and Environmental Sciences, University of Tsukuba)

[ACG29-P05] Impact of recent warming in East Asian marginal seas on the torrential rainfall event occurred in Kyushu Island, Japan in July 2017

*ATSUYOSHI MANDA¹ (1. Mie University)

[ACG29-P06] **Mechanism of the warming of the North Pacific subtropical mode water from 1901 to 2010 in a regional ocean model**

*Yoshi N Sasaki¹, Tomoya Nakamura¹ (1. Hokkaido University)

[ACG29-P07] Interannual and decadal surface velocity variations in the Kuroshio and Kuroshio Extension System

*YUXIANG QIAO¹, Hirohiko Nakamura¹, Shinichiro Kako¹, Ayako Nishina¹, Tomohiko Tomita² (1. Kagoshima University, 2. Kumamoto University)

[ACG29-P08] Late-winter glider observation of upper ocean responses to weather disturbances in the western subtropical North Pacific

*Toyama Katsuya¹ (1. Meteorological Research Institute)

East-Asian atmospheric rivers bring more frequent and intense extreme rainfall under global warming

*Youichi Kamae¹, Yukiko Imada², Hiroaki Kawase², Wei Mei³

1. Faculty of Life and Environmental Sciences, University of Tsukuba, 2. Meteorological Research Institute, Japan Meteorological Agency, 3. University of North Carolina at Chapel Hill

In July 2018 and July 2020, East Asia experienced extreme heavy rain events. The heavy rainfall were observed over wide area because of contributions from organized water vapor flow called atmospheric river (AR). ARs, filamentary-shaped moisture transport bands, often bring heavy rainfall when they make landfall over the Northern and Southern Hemisphere middle latitudes. Recently, ARs have received increasing attention due to large social damages accompanied by such AR-related hazardous events. Under global warming, AR frequency should be increased because atmospheric moisture content is increased. In addition to such thermodynamic effect, dynamic effect related to atmospheric circulation should also be evaluated through global climate model tests. For evaluation of local extreme rainfall, fine-resolution regional climate models should be used because AR-related extreme rainfall is strongly influenced by orographic effect.

In this study, we use a set of high-resolution global and regional climate simulations called d4PDF to evaluate AR-related extreme rainfall and its change under global warming. Using d4PDF AGCM and RCM simulations, we identified great importance of ARs in extreme rain events in the future climate simulations. In the warming simulations, ARs are accompanied with more water vapor and sometimes bring record-breaking extreme rainfall when they make landfall over China, the Korean Peninsula and Japan. ARs account for 77% and 46% of increased occurrence of extreme rainfall in March-to-May and June-to-August, respectively. In this study, we only focus on role of ARs over East Asia. However, such great importance of ARs in future climate may also be found over western North America and Europe.

Keywords: atmospheric river, heavy rainfall, global warming

AGCM experiments for winters of 2017/18 and 2019/20

*Kazuaki Nishii¹, Bunmei Taguchi², Hisashi Nakamura³

1. Graduate School of Bioresources, Mie University, 2. Faculty of Sustainable Design, University of Toyama , 3. RCAST, The University of Tokyo

We conducted AGCM experiments for 2017/18 winter when Japan suffered from a cold surge, as well as for 2019/20 winter when Japan experienced unusually warmth. Our AGCM cannot reproduce the 2017/18 cold winter in Japan. This may be because convective activity over the eastern Indian Ocean is suppressed too much in response to cool SST anomalies there. The extratropical SST anomalies also contributed to the warmth. While in the 2019/20 winter, our AGCM can successfully simulate the warmth around Japan. This is associated with well simulation of convective activity over the Indian Ocean, and the maritime continent. The extratropical SST anomalies also contributed to the formation of the anticyclonic anomalies and warming over Japan.

Keywords: midlatitude ocean, atmospheric general circulation model

A breakdown of the diabatic genesis/loss of polar cold air masses and its relationship with air-sea interactions

*Yuki Kanno¹, Toshiki Iwasaki²

1. Central Research Institute of Electric Power Industry, 2. Department of Geophysics, Graduate School of Science, Tohoku University

In winter, polar cold air masses generated in high-latitudes outflow into the mid-latitudes intermittently and then lose its coldness due to diabatic heating. However, it is not clear which diabatic processes contribute to the genesis and loss of polar cold air masses. This study quantitatively clarifies which diabatic processes contribute to the genesis and loss of polar cold air masses in the boreal winter and the relationship between diabatic loss of polar cold air masses and surface heat fluxes. We utilize the Negative Heat Content (NHC), proposed by Iwasaki et al. (2014), below potential temperature of 280 K as an indicator of polar cold air masses. Because only diabatic heating and cooling within NHC contribute to its genesis and loss, NHC facilitates the quantitative understanding of the thermal aspect of polar cold air masses. Over the mid- and high latitudes, the NHC is generated by the long-wave radiation. Over the mid- and high latitude Oceans, on the other hand, the NHC is lost primary by the vertical diffusion in the mixing layers and secondary by moist processes. This indicates that polar cold air masses are lost through the air-sea heat exchanges. As the air-sea heat exchanges contribute to lose NHC, we have studied the relationship between the loss of NHC and surface heat fluxes. Over most of the mid- and high latitude Oceans, the loss of NHC have a linear relation with surface heat fluxes. A composite analysis for large NHC loss and large surface heat flux events shows that cold air outbreaks are triggers for the air-sea heat exchanges in these events. However, deviations from the linear relation are found over the Kuroshio Extension region. A composite analysis for these deviations shows that, although the NHC almost the same with winter climatological mean values, strong surface wind is the main driver of strong air-sea heat exchange. These findings suggest that the Kuroshio Extension region has a different air-sea interaction process among the mid- and high latitude Oceans.

Keywords: polar cold air mass, surface heat fluxes, diabatic heating

Year-to-year variations of the extratropical direct circulation associated with the Aleutian-Icelandic lows

*Masaya Kuramochi¹, Hiroaki Ueda²

1. Graduate School of Science and Technology, University of Tsukuba, 2. Faculty of Life and Environmental Sciences, University of Tsukuba

The mass-weighted isentropic zonal mean (MIM) describes the Lagrangian mean meridional circulation, which has an advantage in expressing the lower boundary condition in comparison with those in the Transformed Eulerian-Mean (TEM) method. The extratropical direct (ETD) circulation, in the diagnosis of MIM scheme, is mostly ascribed to the divergence of the Eliassen–Palm (E-P) flux based on the MIM. In this study, the spatiotemporal variations of atmospheric circulation corresponding to the interannual variations of the ETD circulation are examined in the context of wave–mean flow interactions associated with the E-P flux divergence. The results clearly show that the enhanced ETD circulation is closely connected with deepening of the Aleutian low (AL) and weakening of the Icelandic low (IL), and vice versa. Although the AL and IL exhibit the opposite fluctuations, the upward wave-activity flux intensifies both over the eastern North Pacific and the North Atlantic during the strong phase of ETD circulation. The intensified upward flux is concurrent with the enhancements of the meridional heat transport by planetary wave, which is mainly caused by the modulation of circulation in the Aleutian and Icelandic sectors. These results indicate that the variability of ETD circulation can be explained by the coherent fluctuation of the AL and IL accompanied by modulations of planetary wave activity. The physical process involved in the variations of E-P flux will be discussed in terms of the tropical-extratropical linkage associated with the tropical external forcing such as the El Niño–Southern Oscillation (ENSO).

Keywords: Extratropical direct circulation, Aleutian-Icelandic lows, ENSO

Impact of recent warming in East Asian marginal seas on the torrential rainfall event occurred in Kyushu Island, Japan in July 2017

*ATSUYOSHI MANDA¹

1. Mie University

Torrential rainfall events tend to occur more frequently in Japan as well as many parts of the world. Attributing the events to the global warming is, however, a complicated task. Although the majority of the moisture that causes the torrential rainfall comes from the tropics and amount of moisture supply from the ocean surface is not large compared to the horizontal moisture transport from the south, this study has highlighted the importance of atmospheric moistening in the lower troposphere due to recent warming in the mid-latitude oceans. The torrential rainfall event that occurred in Kyushu Island in July, 2017 was selected as a typical test case in the torrential rainfall events during the Baiu rainy season in Japan. Numerical simulations in this study shows that fractional change of the amount of the precipitation due to the oceanic and atmospheric warming since 1980s is 6.8%, corresponding to 10.6 % increase per 1 K of sea surface temperature (SST) rise. It is larger than expected from the Clausius–Clapeyron relationship ($\sim 6\%/K$) and consistent with the previous data analysis study. The SST rise in the east Arian marginal seas plays a fundamental role in intensifying the conditionally unstable conditions in the lower troposphere and in turn increase the amount of precipitation. On the other hand, changes in precipitable water plays a secondary role.

Keywords: convective system, latent heat flux, WRF

Mechanism of the warming of the North Pacific subtropical mode water from 1901 to 2010 in a regional ocean model

*Yoshi N Sasaki¹, Tomoya Nakamura¹

1. Hokkaido University

The present study examines mechanism of warming of the subtropical mode water in the North Pacific from 1901 to 2010 using a regional ocean model. The warming trend of the subtropical mode water in the model was about $+1.2^{\circ}\text{C}/100\text{yr}$, consistent with the previous observational study. In addition, this trend and interannual to decadal variability of the mode water temperature well corresponded to those of the sea surface temperature in the formation region, south of the Kuroshio Extension region. On the other hand, the thickness of the subtropical mode water did not show a significant trend. Consistently, the mixed layer depth in the formation region in winter also did not have a significant trend. It is revealed from two sensitivity experiments of the model that the warming of the subtropical mode water was mainly caused by the warming of atmospheric temperature. However, this warming of atmospheric temperature induced the shallowing of the mixed layer depth in winter in the formation region. Interestingly, this shallowing of the mixed layer depth by the atmospheric warming was canceled out by wind stress forcing, which induced the deepening trend of the mixed layer depth.

Interannual and decadal surface velocity variations in the Kuroshio and Kuroshio Extension System

*YUXIANG QIAO¹, Hirohiko Nakamura¹, Shinichiro Kako¹, Ayako Nishina¹, Tomohiko Tomita²

1. Kagoshima University, 2. Kumamoto University

Interannual and decadal variations of current intensity and current path position are investigated for the entire stream of the Kuroshio and Kuroshio Extension (hereafter, Kuroshio-KE System) in order to clarify how this system is organized with synthesized temporal and spatial features. Our strategy to achieve this purpose is to analyze Hovmöller diagrams of the current intensity and path position, created along an entire stream of this current system using satellite-altimeter derived surface geostrophic velocity data in 1993–2018. The oceanic processes to govern such variations are also examined using satellite-altimetry sea surface height (SSH) data over the North Pacific.

At first, we carried out the study on decadal-scale current variations along the entire stream, and revealed three kinds of coherently organized variations: 1) an out-of-phase current intensity variation between the Kuroshio south of Japan and the KE between 1993–2018; 2) an out-of-phase current intensity variation between the Kuroshio from the east of Taiwan (ETW) to the East China Sea (ECS) and the KE between 2006–2014; and 3) an out-of-phase current path variation between the Kuroshio from the ETW to ECS and the Kuroshio in the Luzon Strait between 1993–2018. These synchronizations were dynamically regulated by the Pacific Decadal Oscillation. The synchronized current intensity variations in 2006–2014, which governed almost the entire current system, were caused by coherent phenomena comprising two kinds of baroclinic Rossby wave propagations along the KE and the subtropical countercurrent, and a regional SSH anomaly advection from the South China Sea (SCS) to the ECS via the Taiwan Strait. However, the synchronized current path variations between 1993–2018 were caused by a long SSH anomaly migration of the Kuroshio from the western North Equatorial Current region to the ECS along with an SSH variation localized in the SCS.

We are now investigating interannual current variations over the Kuroshio-KE System, particularly focusing on those variations in the Kuroshio from the ETW to the ECS, where the interannual variations have strong seasonal dependency probably due to interannual modulations of winter and summer Asian Monsoons. In addition to the above-mentioned decadal features, we will describe the interannual current variations with seasonal dependency over the Kuroshio-KE System in terms of regional syntheses and their underlying mechanisms.

Keywords: air-ocean interaction, western boundary current, interannual–decadal variability, Rossby wave, mesoscale eddy

Late-winter glider observation of upper ocean responses to weather disturbances in the western subtropical North Pacific

*Toyama Katsuya¹

1. Meteorological Research Institute

The ocean glider is a buoyancy driven autonomous underwater vehicle which moves both horizontally and vertically in a sawtooth trajectory through the water toward a specified waypoint. The glider enables us to observe the remote ocean at relatively low cost and at high resolution both in space and time. Using the Slocum glider (manufactured by Teledyne Webb Research), the Meteorological Research Institute (MRI) has conducted hydrographic and biogeochemical observations in the western subtropical North Pacific around the Ogasawara Islands in winter 2020. The glider equipped with CTD, oxygen (RINKO II), and bio-optical (ECO FLBBOD) sensors is capable of monitoring water column down to 1,000m depth. After its deployment on March 3, 2020, the glider swam back and forth for 9 days to do semi-stationary observation at around its deployment location (145E, 30N). During this semi-stationary observation, the glider was set to dive down to 400 m depth to collect high temporal frequency data of the near-surface layer of the ocean. During the 9-day period, total of 150 ascending and descending profiles (more than 15 profiles every day) were obtained. This high temporal frequency data allows us to investigate upper ocean responses to weather disturbances. The observed mixed layer depth and mixed-layer properties as well as near-surface chlorophyll show large temporal variability, which is apparently associated with passages of low-pressure systems and/or weather fronts.

Keywords: ocean glider, mixed layer

[E] Poster | A (Atmospheric and Hydrospheric Sciences) : A-CG Complex & General

📅 Fri. Jun 4, 2021 5:15 PM - 6:30 PM JST | Fri. Jun 4, 2021 8:15 AM - 9:30 AM UTC | 🏠 Ch.10_2

[A-CG32] Land-Atmosphere interactions and Asian monsoon precipitation (LAMos)

convener:G. Hiroshi Takahashi(Department of Geography, Tokyo Metropolitan University), Shiori Sugimoto(JAMSTEC Japan Agency for Marine-Earth Science and Technology), Hatsuki Fujinami(Nagoya University), Hirokazu Endo(Meteorological Research Institute, Japan Meteorological Agency)

This session aims to discuss land-atmosphere interaction over the Asian monsoon region because it is one of the essential components of the Asian monsoon system. Precipitation characteristics and cloud-precipitation processes are closely tied with land-atmosphere interactions, which are also a key target. Over Asia, climates are various, which produces various land-atmosphere-precipitation interactions. The influences of complex topography on precipitation characteristics are also considered. It may be interesting that the interactions can vary with scales in space and in time.

Also, monsoon precipitation variability is a target of this session, which can also be associated with land surface conditions. We want to approach the mechanism behind the precipitation/precipitation characteristics variability. Also, to understand past and future precipitation variability, influences of land-use changes and/or global warming should be considered. A large variety of observations, numerical modeling, and their combined analyses are encouraged.

[ACG32-P01] Links between torrential rainfall and urban land use in Jakarta, Indonesia using Geographically Weighted Regression

*Asteria Satyaning Handayani^{1,2}, Yuzuru Isoda¹ (1.Earth Science Department, Graduate School of Science, Tohoku University, Japan, 2.Agency for Meteorology Climatology and Geophysics (BMKG), Indonesia)

[ACG32-P02] The simulation for the nocturnal precipitation over the Himalayas

*Shiori Sugimoto¹, Kenichi Ueno², Hatsuki Fujinami³, Tomoe Nasuno¹, Tomonori Sato⁴, Hiroshi G. Takahashi⁵ (1.JAMSTEC Japan Agency for Marine-Earth Science and Technology, 2.University of Tsukuba, 3.Nagoya University, 4.Hokkaido University, 5.Tokyo Metropolitan University)

[ACG32-P03] **Simulated precipitation characteristics over the tropical Asian monsoon regions by high-resolution climate models**

*Hiroshi G. Takahashi¹, Rakesh Teja Konduru¹, Nozomi Kamizawa¹, Moeka Yamaji¹ (1.Department of Geography, Tokyo Metropolitan University)

Links between torrential rainfall and urban land use in Jakarta, Indonesia using Geographically Weighted Regression

*Asteria Satyaning Handayani^{1,2}, Yuzuru Isoda¹

1. Earth Science Department, Graduate School of Science, Tohoku University, Japan, 2. Agency for Meteorology Climatology and Geophysics (BMKG), Indonesia

Urban microclimate is an intriguing research topic even after decades of findings. The urban-enhanced precipitation is evident in metropolitan cities of Asian monsoon region, particularly in Japan and China. However, related studies performed in the Southeast Asia region are still rare compared to the latter countries. Therefore, this empirical study of torrential rainfall and urban land use in Jakarta, Indonesia, has been conducted with the aim of investigating the extent of how both are linked there. We used two consecutive years (2018-2019) of high-resolution data from C-band Doppler weather radar in Soekarno-Hatta International Airport, operated by the Indonesian Agency for Meteorology, Climatology, and Geophysics (BMKG), as the main data. Geographically Weighted Regression (GWR) model is adopted to point out the spatially-varying relationships between rainfall and land use variables. The results show that the spatial regression technique analyses strongly indicate the significantly-positive contributions of urban land use parameters to the intensity, spatial, and seasonal characteristics of torrential rainfall in Jakarta. Spatiotemporal analysis of torrential rainfall amount during the selected period reveals distinct characteristics between wet and dry seasons downwind of the urbanized area. Results from this study provide more insights into the effect of urbanization on the precipitation in Jakarta and their predicted locations.

Keywords: Geographically Weighted Regression, torrential rainfall, urban land use, weather radar

The simulation for the nocturnal precipitation over the Himalayas

*Shiori Sugimoto¹, Kenichi Ueno², Hatsuki Fujinami³, Tomoe Nasuno¹, Tomonori Sato⁴, Hiroshi G. Takahashi⁵

1. JAMSTEC Japan Agency for Marine-Earth Science and Technology, 2. University of Tsukuba, 3. Nagoya University, 4. Hokkaido University, 5. Tokyo Metropolitan University

Summer precipitation and clouds developed over the Himalayas and its surrounding region, which is valuable water resource in Asia, have a role in a maintenance of the Asian monsoon circulation. The precipitation dominates between the midnight and early morning over the Himalayan foothills, while it has double peaks during the afternoon-evening and night over the Himalayan slopes. Simulations with a coarse resolution are difficult to simulate this diurnal cycle in precipitation over the Himalayas. In this study, the 2km resolution experiment was conducted using the Weather Research and Forecasting (WRF) model ver. 3.9.1.1 during the mature monsoon season for 8 years from 2003 to 2010 to evaluate the diurnal cycle in precipitation, particularly nocturnal precipitation dominated over the Himalayan slopes and foothills. Then, we diagnose a local-scale physical process for the nocturnal precipitation occurrence.

Comparing with the satellite estimated precipitation from GPM IMERG (V06B), a spatial distribution of the climatological nocturnal precipitation is simulated well in the WRF model although the absolute value of precipitation is underestimated. Diurnal variations in the simulated precipitation averaged over the slopes and foothills are consistent with that in the GPM IMERG and the in-situ observation. When the precipitation dominated over the Himalayan slopes, a monsoon depression over the northwest of the Bay of Bengal contributes to the moisture transport to the slopes. During the daytime, the moisture transported by the synoptic-scale flow causes orographic precipitation at the Himalayan mountain ridges in the model, of which altitude is 2000-2500 m. The simulated precipitation expands widely in the Himalayan slopes from evening until night, and it also occurs a lower-altitude mountain in front of the Himalayas. Meanwhile, the moisture is directly provided from the synoptic-scale monsoon westerlies when the nocturnal precipitation dominated over the Himalayan foothills. In this case, the nocturnal precipitation is formed over the foothills by the convergence between the synoptic-scale monsoon flow and the local-scale downslope wind from the Himalayas. The evaporation cooling near the surface and the spatial heterogeneity of the radiative cooling at the ground would enhance the downslope wind locally. In addition, the cloud convections were likely to be maintained by the latent heating from the cloud and the radiative cooling at the cloud top. The sensitivity experiments suggested that both representation of topography and numbers of vertical layer affected the spatial distribution of the nocturnal precipitation in the model.

Keywords: Asian monsoon, Mountain precipitation, Diurnal cycle in precipitation

Simulated precipitation characteristics over the tropical Asian monsoon regions by high-resolution climate models

*Hiroshi G. Takahashi¹, Rakesh Teja Konduru¹, Nozomi Kamizawa¹, Moeka Yamaji¹

1. Department of Geography, Tokyo Metropolitan University

Over the tropical Asian monsoon regions, precipitation amount varies on the various time-scales. To deeply understand the precipitation variations, precipitation characteristics, such as precipitation frequency, intensity, and extreme, are critical. Over the tropical regions, diurnal precipitation variations are also very essential. Also, these precipitation characteristics may change under global warming conditions. In numerical climate models, how are precipitation characteristics simulated well? This study examines the reproducibility of precipitation characteristics in the numerical climate models. We used CMIP6 (Coupled Model Intercomparison Project Phase 6) climate models, non-hydrostatic global and regional climate models. We evaluate the reproducibility in the simulated precipitation characteristics using the TRMM(Tropical Rainfall Measuring Mission)-GPM(Global Precipitation Measurement) related products. The simulated results by a regional climate model showed a large discrepancy between with and without cumulus parameterization if we use the same model increments. We will show additional results using the CMIP6 climate models.

Keywords: precipitation characteristics, Asian monsoon, seasonal difference

[E] Poster | A (Atmospheric and Hydrospheric Sciences) : A-CG Complex & General

📅 Fri. Jun 4, 2021 5:15 PM - 6:30 PM JST | Fri. Jun 4, 2021 8:15 AM - 9:30 AM UTC | 🏠 Ch.10_3

[A-CG35] Projection and detection of global environmental change

convener: Michio Kawamiya (Japan Agency for Marine-Earth Science and Technology), Kaoru Tachiiri (Japan Agency for Marine-Earth Science and Technology), Hiroaki Tatebe (Japan Agency for Marine-Earth Science and Technology), V Ramaswamy (NOAA GFDL)

Anthropogenic forcings on global environment are expected to cause intensification of extreme events, sea level rise, ocean acidification and deoxygenation, as well as large-scale ecosystem changes. Earth System modeling groups across the world performed simulations and published projection data toward 6th IPCC assessment report due in July, 2021. Various new types of studies, such as event attribution and coupling of socio-economic processes and Earth system dynamics, are emerging in the field of global change projections. In addition, analysis on observational data are becoming increasingly more important for assessing credibility of model projections on the global environment. Interactions and collaborations beyond boundaries of conventional scientific disciplines are desired for dealing with the issue of global changes. This session hosts the latest research findings with a view to model prediction, and interdisciplinary collaborations including those with social sciences.

[ACG35-P01] Future directions of Earth system modeling: outcome of the discussion forum under TOUGOU program

*Michio Kawamiya¹, Kaoru Tachiiri^{1,2}, Tomohiro Hajima¹, Tokuta Yokohata², Junichi Tsutsui³, Takashi Arakawa⁴, Takahiro Inoue^{1,5} (1. Japan Agency for Marine-Earth Science and Technology, 2. National Institute for Environmental Studies, 3. Central Research Institute of Electric Power Industry, 4. Research organization for Information Science and Technology, 5. Remote Sensing Technology Center of Japan)

[ACG35-P02] Development of a coupled Earth and socio-economic system model

*Kaoru Tachiiri^{1,3}, Xuanming Su¹, Ken'ichi Matsumoto^{2,1}, Tomohiro Hajima¹, Tokuta Yokohata³ (1. Japan Agency for Marine-Earth Science and Technology, 2. Nagasaki University, 3. National Institute for Environmental Studies)

[ACG35-P03] **Quantifying committed warming from individual climate forcings based on the Simple Climate Model for Optimization (SCM4OPT)**

*Xuanming Su¹, Katsumasa Tanaka^{2,3}, Kaoru Tachiiri¹, Michio Watanabe¹, Michio Kawamiya¹ (1. Japan Agency for Marine-Earth Science and Technology, 2. Laboratoire des Sciences du Climat et de l'Environnement, 3. National Institute for Environmental Studies)

[ACG35-P04] Simulated impact of the 1815 Tambora eruption on global climate with MIROC-ES2L

*Manabu Abe¹, Tomohiro Hajima¹ (1. Japan Agency for Marine-Earth Science and Technology)

[ACG35-P05] Millennium time-scale experiments with doubled CO₂ concentration by Earth system models

*Tomohiro Hajima¹, Akitomo Yamamoto¹, Michio Kawamiya¹, Xuanming Su¹, Michio Watanabe¹, Rumi Ohgaito¹, Hiroaki Tatebe¹ (1. Japan Agency for Marine-Earth Science and Technology)

[ACG35-P06] Climate impact of reducing CO₂ and other emissions from the COVID-19 pandemic

*Rumi Ohgaito¹, Manabu Abe¹, Tomohiro Hajima¹, Kaoru Tachiiri¹, Michio Kawamiya¹ (1. Japan Agency for Marine-Earth Science and Technology)

Future directions of Earth system modeling: outcome of the discussion forum under TOUGOU program

*Michio Kawamiya¹, Kaoru Tachiiri^{1,2}, Tomohiro Hajima¹, Tokuta Yokohata², Junichi Tsutsui³, Takashi Arakawa⁴, Takahiro Inoue^{1,5}

1. Japan Agency for Marine-Earth Science and Technology, 2. National Institute for Environmental Studies, 3. Central Research Institute of Electric Power Industry, 4. Research organization for Information Science and Technology, 5. Remote Sensing Technology Center of Japan

The TOUGOU program, a research project on climate change funded by MEXT, started in FY2017 and reaches its final year in FY2021. Team MIROC, consisting of major Japanese climate modeling institutions including JAMSTEC, AORI (University of Tokyo), and NIES, has developed an Earth system model MIROC-ES2L under the TOUGOU program. The model has been used to conduct the CMIP6 experiment, and the output data has been distributed through ESGF. Intriguing results have been obtained, such as the improved reproducibility of the ocean sub-surface layer in the equatorial Pacific, which leads to a drastic improvement in the relationship between El Niño and sea surface CO₂ fluxes when temperature and salinity are assimilated. Based on these results, the TOUGOU program scientists are now discussing how they should develop Earth System Science research after the TOUGOU program. One of the important directions is the comprehensive projection of global environmental change that considers factors other than climate change, as suggested by the "Planetary Boundary" concept. Also, to contribute to the Global Stocktake (GST), decadal-scale projection of the carbon cycle should be promoted to clarify the changes in the carbon balance in the recent and future years. A more precise evaluation of the carbon budget required for limiting global warming would also be an essential input to GST. Furthermore, the impact of climate mitigation policies on the global environment through, among others, land-use change can be assessed using a model that combines a socioeconomic model and an Earth system model, considering the interaction between social change and global environmental change.

Keywords: Earth system modeling, Carbon budget, Decadal Prediction, Planetary boundary, IPCC, Climate change

Development of a coupled Earth and socio-economic system model

*Kaoru Tachiiri^{1,3}, Xuanming Su¹, Ken'ichi Matsumoto^{2,1}, Tomohiro Hajima¹, Tokuta Yokohata³

1. Japan Agency for Marine-Earth Science and Technology, 2. Nagasaki University, 3. National Institute for Environmental Studies

In ordinary future projections, link of Earth system model (ESM) and integrated assessment (or socio-economic) model (IAM) is one-way, where the greenhouse gas and land use scenarios developed by IAMs are input to ESM. However, a recent study indicated a possibility for human-carbon cycle feedback to be comparable in size (and opposite in sign) to climate-carbon cycle feedback. Thus, it is indicated that a two-way coupling of ESM and IAM could alter the pathway to meet the given climate (temperature) targets. To consider that, we first carried out a review work on climate-socioeconomic system feedback. By examining around 200 papers for eight sectors/processes (including land productivity (i.e., cropland and pasture), water resources, sea level rise and inundation, natural disasters, other ecosystem services, human health (i.e., labor productivity and disease/health), industry and related economic activities (i.e., energy, infrastructure, tourism and transportation, insurance, and finance), and migration and civil/international conflict), we concluded that land productivity, labor productivity, and energy system play most important roles (although we need to accumulate more studies for each sector to draw solid conclusions). Based on that we are developing a (loosely) coupled ESM-IAM model, by loosely coupling a coupled ESM and integrated land surface model, with a computational general equilibrium model.

Keywords: Earth system model, integrated assessment model, socio-economic model

Quantifying committed warming from individual climate forcings based on the Simple Climate Model for Optimization (SCM4OPT)

*Xuanming Su¹, Katsumasa Tanaka^{2,3}, Kaoru Tachiiri¹, Michio Watanabe¹, Michio Kawamiya¹

1. Japan Agency for Marine-Earth Science and Technology, 2. Laboratoire des Sciences du Climat et de l' Environnement, 3. National Institute for Environmental Studies

We use a simple climate model SCM4OPT v3.0 newly calibrated based on 26 Atmosphere-Ocean General Circulation Models (AOGCMs) from CMIP6. We applied a normalized marginal method to the SCM4OPT v3.0, to quantify the allowable warmings for various sources for the 2 °C and 1.5 °C climate targets. Based on the most up-to-date emission datasets, we calculated 1) temperatures resulting from emissions of the historical period of 1850-2016 (committed warming) and 2) temperatures resulting from emissions of the full period of 1850-2100 (full warming). Then we subtracted the committed warming from the full warming, to obtain the allowable warming. We computed 1) scenario uncertainties by using 161 future pathways considering various socioeconomic development levels (SSP1-5) and radiative forcing targets, and 2) climate uncertainties by emulating the behaviors of 26 AOGCMs.

The preliminary results show that the warming in 2016 is 1.19 ± 0.30 °C. The committed warming in 2100 is 0.88 ± 0.25 °C, which is dominated by CO₂. Specifically, 0.58 °C is caused by historical fossil fuels emissions and 0.14 °C by historical land use change. Historical CH₄, N₂O and fluorinated gas (F-gas) and Montreal Gas emissions are also important contributors to the committed warming, accounting for 0.06 °C, 0.05 °C and 0.09 °C, respectively, due to the relatively large contribution from historical CH₄ emissions and the relative long lifetime for N₂O and F-gas and Montreal Gas emissions. Significant cooling effects also remain, like those from sulfate aerosols and OC emissions, which contribute about -0.03 °C and -0.02 °C, respectively. We will highlight the importance of the committed warming caused by various forcing sources.

Keywords: Simple climate model, Climate change, Committed warming

Simulated impact of the 1815 Tambora eruption on global climate with MIROC-ES2L

*Manabu Abe¹, Tomohiro Hajima¹

1. Japan Agency for Marine-Earth Science and Technology

The volc-long-eq experiment in CMIP6 VolMIP is a climate response experiment to an equatorial volcanic eruption with an initial SO₂ emission of 56.2 Tg, which roughly corresponds to the scale of the 1815 eruption of Tambora volcano on Sumbawa Island, Indonesia (Zanchettin et al. 2016). This eruption is one of the largest volcanic eruptions in the tropics in the last 500 years and is associated with the "Year without Summer" of 1816. The objectives of this experiment are to focus on the atmosphere-ocean interaction and the interannual and decadal-scale response to large-scale volcanic eruptions on global and regional scales, to investigate the differences in response (uncertainties) among models, and to clarify the role of internal variability as a background field in the climate response to volcanic eruptions. In each member, the 20 years simulations were conducted. Except for the input of volcanic eruptions and related forcing data, the background field is assumed to be the situation in 1850 before the industrial revolution. Due to the timing of past volcanic eruptions assumed in each experiment, the vol-long-eq experiment was started on April 1.

In the volc-long-eq experiment, the decline in shortwave radiation associated with volcanic eruptions ends after about eight months, after which the radiation begins to return. On the other hand, the temperature continues to decrease, peaking about four months later and dropping about 1.0 °C on average, then recovering. The difference in the timing of the peak between surface air temperature change and the change in radiation caused by the volcanic eruption was found to be due to the positive feedback related to the snow and sea ice in the high latitudes of the Northern Hemisphere and the slow response of ocean.

Keywords: Earth System model, volcanic impact, climate change

Millennium time-scale experiments with doubled CO₂ concentration by Earth system models

*Tomohiro Hajima¹, Akitomo Yamamoto¹, Michio Kawamiya¹, Xuaming Su¹, Michio Watanabe¹, Rumi Ohgaito¹, Hiroaki Tatebe¹

1. Japan Agency for Marine-Earth Science and Technology

Earth system models (ESMs) are commonly used for simulating the climate-carbon (C) cycle, being applied to century-long climate simulations. Although millennium-long simulations have not been the main target of the models' simulations because of the computational cost, such long-term simulations can provide basic fundamental properties of climate-C cycle models and can be a help to understand the long-term behavior of climate, carbon dioxide (CO₂) concentration, and carbon cycle. This study used two ESMs (MIROC-ESM and MIROC-ES2L) to investigate millennium-scale climate and C cycle adjustment to external forcing. The CO₂ concentration was doubled abruptly at the beginning of the model simulations and kept at that level for the next 1000 or 2000 years. The simulation results were compared with transient simulations of 1% CO₂ increase (1pctCO₂). Unlike the 1pctCO₂ experiment, the change in temperature-cumulative anthropogenic C emission relationship (so called TCRE) was non-linear over the millennium time-scales. The differences in TCRE among existing models suggest large uncertainty in the changes in temperature and cumulative emission in the millennium-long climate-C simulations. Ocean C and heat transport were found to be disconnected over millennium time-scales, leading to a longer time-scale of ocean C accumulation than heat uptake. Although the experimental design used here was highly idealized, this long-lasting C uptake by the ocean should be considered as part of the stabilization of CO₂ concentration and global warming.

Keywords: Earth system model, Carbon cycle, Climate change

Climate impact of reducing CO₂ and other emissions from the COVID-19 pandemic

*Rumi Ohgaito¹, Manabu Abe¹, Tomohiro Hajima¹, Kaoru Tachiiri¹, Michio Kawamiya¹

1. Japan Agency for Marine-Earth Science and Technology

The COVID-19 pandemic had a significant impact on human life around the world, especially in the spring of 2020, when many countries imposed lockdowns and other restrictions. As a result, anthropogenic greenhouse gas emissions, including CO₂, and anthropogenic aerosol emissions fell to unprecedented levels (Le Quere et al. 2020, Liu et al. 2020), with an estimated reduction of about 7% in one year in 2020 (Friedlingstein et al. 2020). A previous study (Forster et al. 2020), which used a simple climate model to estimate the impact of this emissions reduction on global warming, estimated that the direct impact of the emissions reduction in the two years 2020 and 2021 would be negligible and would have little effect on the pace of global warming. However, as the model only calculates global values, it is unable to capture regional changes and their mechanisms. Therefore, the model comparison project CovidMIP (Jones et al. 2021) was launched to simulate the same settings as in the previous study, based on the scenario-MIP SSP2-4.5 of CMIP6, and the Earth system model MIROC-ES2L was also involved. An initial analysis of the results of ensemble simulations using MIROC-ES2L shows that a two-year decrease in emissions results in a decrease in the optical thickness of the Asian region, but there is no significant change in annual mean temperature or precipitation. We will continue with the analysis in shorter timescale and present the results including the multi-model analysis in CovidMIP.

Keywords: COVID-19, greenhouse gas, earth system model

[E] Poster | H (Human Geosciences) : H-TT Technology & Techniques

📅 Fri. Jun 4, 2021 5:15 PM - 6:30 PM JST | Fri. Jun 4, 2021 8:15 AM - 9:30 AM UTC | 🏠 Ch.12_3

[H-TT30] GEOMORPHOLOGICAL APPLICATIONS OF HIGH-DEFINITION TOPOGRAPHY AND GEOPHYSICAL DATA IN THE ANTHROPOCENE

convener: Yuichi S. Hayakawa (Faculty of Environmental Earth Science, Hokkaido University), Tsuyoshi Hattanji (Faculty of Life and Environmental Sciences, University of Tsukuba), Shigekazu Kusumoto (Institute for Geothermal Sciences, Graduate School of Science, Kyoto University), A Christopher Gomez (Kobe University Faculty of Maritime Sciences Volcanic Risk at Sea Research Group), Masayuki Seto (Fukushima Future Center for Regional Revitalization, Fukushima University)

Recent technical developments have enabled us to acquire high-definition topographic and geophysical data for geoscientific research, including geomorphology, land surface processes, subsurface structures, submarine and aerial environments, and geo-ecological interactions. Such high-definition or high-resolution data are particularly useful for studies on relatively short-term, i.e., decadal to millennial time scales, and for future predictions using numerical modelings. In this session, we expect submissions on topics challenging the issues in the Anthropocene, the most recent geological era of the Earth considerably affected by human activities. A range of topics would fit the session framework, such as theoretical works, improvements in the data acquisition, extensive data preservation and archiving, pre- and post-processing, statistical analysis, physical modeling, and numerical simulation for any kind of geoscientific and geomorphological research in the Anthropocene. The methodological approaches may include, but not limited to, laser scanning, SfM-MVS photogrammetry, GNSS precise positioning, SAR interferometry, multi-beam sonar, ground-penetrating radar, geomagnetic and electromagnetic sensors, and multispectral or hyperspectral sensors, based on terrestrial (fixed or mobile) and aerial (UAV or manned airborne) platforms. Geomorphological applications of these methodologies, including geomorphic processes, landform development and its relation to environmental changes, geomorphological hazards and their mitigation, relationships among geomorphic processes, and other natural phenomena and human activities are more than welcome.

[HTT30-P01] Comparison of high resolution multispectral orthoimages with physiological activities of deciduous conifer trees

*Masuto Ebina¹, Wataru Ishizuka¹ (1.Forestry Research Institute, Hokkaido Research Organization)

[HTT30-P02] Subsurface structure of dolines on the Akiyoshi-dai Plateau, Japan: An approach from electrical resistivity tomography

Naoya Hiramoto¹, *Tsuyoshi Hattanji² (1.Graduate School of Life and Environmental Sciences, University of Tsukuba, 2.Faculty of Life and Environmental Sciences, University of Tsukuba)

[HTT30-P03] **Ground-Penetrating-Radar Investigation of drifted wood trapped in river-sand – Laboratory Experiments**

*Christopher A Gomez¹, Norifumi Hotta² (1.Kobe University Faculty of Maritime Sciences Volcanic Risk at Sea Research Group, 2.Graduate School of Agricultural and Life Sciences, The University of Tokyo)

[HTT30-P04] Drainage density and relative relief for the Kitakami Mountains, Japan

*Takashi Oguchi¹ (1.Center for Spatial Information Science, The University of Tokyo)

Comparison of high resolution multispectral orthoimages with physiological activities of deciduous conifer trees

*Masuto Ebina¹, Wataru Ishizuka¹

1. Forestry Research Institute, Hokkaido Research Organization

Recently, much attention has been focused on the study to comprehend the physiological activities of plants using multispectral data taken from UAS and to predict the growth potential or yield of plants effectively on a large scale. In particular, the development of the Phantom4Multispectral (DJI) has made it possible to collect high-resolution multispectral data with simple operations. In this study, Phantom4Multispectral was used to compare the physiological activities measured at the identical and/or post-hoc timing using Mini-PAM (WALZ) and MultispeQ (PhotosynQ) in young deciduous coniferous trees. Studied trees are three larch species; *Larix kaempferi* (Japanese larch), *L. gmelinii*, and their hybrid species. They were the progeny for genetic testing and were three years old after plantation to a site of Hokkaido Research Organization located at Mikasa city, Hokkaido. In this site, planting order was randomly designed. Apparent inter-specific difference was already observed in growth of young trees; superior growth of hybrids and inferior growth of *L. gmelinii*.

In this presentation, we show the results of the comparison between the high resolution multispectral orthoimages acquired by Phantom4Multispectral and the candidate physiological parameters relating the photosynthetic activity and discuss the application of multispectral data.

Keywords: Multispectral, UAS, Physiology

Subsurface structure of dolines on the Akiyoshi-dai Plateau, Japan: An approach from electrical resistivity tomography

Naoya Hiramoto¹, *Tsuyoshi Hattanji²

1. Graduate School of Life and Environmental Sciences, University of Tsukuba, 2. Faculty of Life and Environmental Sciences, University of Tsukuba

Distribution of soil thickness was estimated based on 2-D electrical resistivity tomography (ERT) in more than 10 solution dolines on Akiyoshi-dai plateau in Yamaguchi Prefecture, Japan. The 2-D ERT revealed a transition zone of resistivity values that increase with depth. The upper layer of the transition zone ($< 400 \Omega \cdot m$) was identified as soil on the basis of the result of cone penetration tests. The lower layer immediately below the soil was considered as epikarst, which is composed of fractured limestone with soil. Soil thickness was maximized at the bottom or at the lower slope of dolines. In addition, mean soil thickness at the bottom increases with increasing the size of source area of doline. Soil creep accumulates the larger amount of soil into the bottom of the doline with larger source area. In contrast, soil thickness at the bottom was smaller in dolines with larger ratio of rock exposure (pinnacles) probably due to the limited amount of soil. Although the estimated shape of soil-epikarst boundary was similar to the shape of the ground surface for most slopes, the boundary was not flat for the bottoms of most dolines. The inclined soil-epikarst boundaries below bottom of doline may be a key to solve the development process of dolines in Akiyoshi-dai plateau.

Keywords: karst landform, electrical resistivity imaging, soil thickness

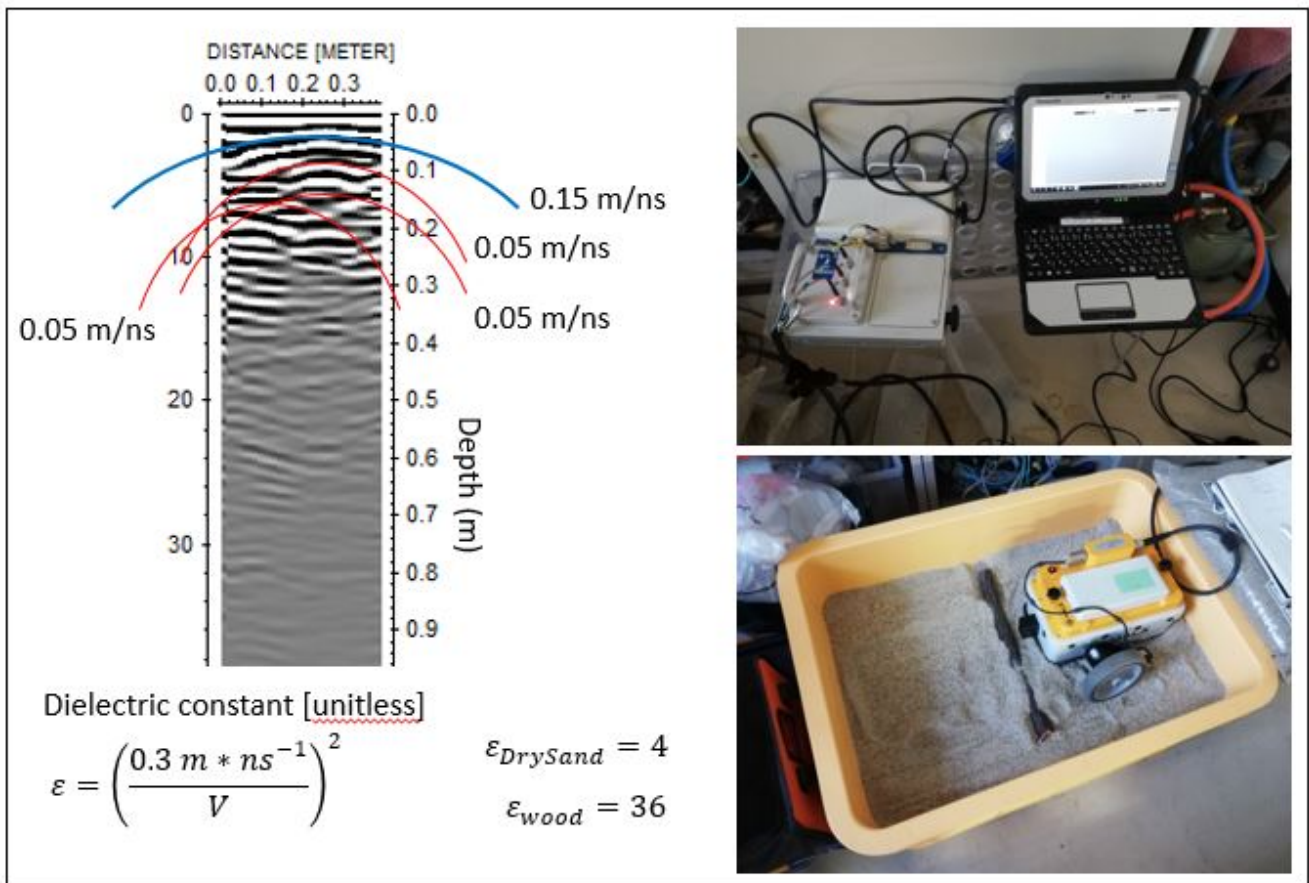
Ground-Penetrating-Radar Investigation of drifted wood trapped in river-sand –Laboratory Experiments

*Christopher A Gomez¹, Norifumi Hotta²

1. Kobe University Faculty of Maritime Sciences Volcanic Risk at Sea Research Group, 2. Graduate School of Agricultural and Life Sciences, The University of Tokyo

The large majority of drifted-wood research has been performed in river corridors, where the recruitment occurs during high flow-stages and from bank erosion. However, there is less work that has been performed on the dynamics of drifted wood during mass-movements and debris-flow recruitment. Empirical evidences from river sediment deposits in Asakura (North Kyushu, Japan) and in the check dams above Kobe City (Kansai Region, Japan) have shown that a portion of the drifted wood could be trapped within sediments. Although the deposition process that traps material with a lower density than water within the sediment is not fully resolved yet, detecting and quantifying this material is a first step in resolving the geometric characteristics of the trapped drifted wood. To reach this overall objective, the present research has turned towards laboratory experiments to solve a first issue: detecting drifted wood inside sediments. Indeed, research investigating tree roots or buried timber (from buried building) all use the geometric characteristics of the buried material to define its nature (for instance tree roots radiating from a known tree), but there are no evidences that the hyperbola being detected are generated by a rock or a root, etc. When the geometric characteristic of the object is not defined, it is then essential to attempt to differentiate the material based on its dielectric properties. For this purpose, the authors have performed laboratory tests with a Mala Ramac GPR 800 MhZ antenna (with an effective pulse of 1.313 ns, and thus a central frequency of 921 MHz, and a λ /wavelength of 32.57 cm) triggered by a coding wheel over a 38 cm strip, recording data once a millimeter. A buried log of 16.5 cm diameter and 19 cm length was buried at 5 cm depth (not the same as on the photograph with the abstract), for a wet mass of 2910 g (density of 194 kg/m³) was used to simulate the buried wood. The radar was dragged over the surface with the buried target, several times with dry to fully saturated conditions. Based on the experiments results, the dry sand provided data within the expected range of dielectric constant for dry sand $\epsilon_{DS}=4$, while the dielectric constant for wood was $\epsilon_{wood}=36$. Saturated sand provided values within the range of 22 –28 (also within the 20 –30 common values). Providing that the common values of the dielectric constant for sandstones is commonly around 6 and the one of shales are of values between 5 and 15, the dielectric constant can be used to determine whether the detected material is made of wood or whether it is a rock, providing that the diameter of the drifted wood is at least (as a rule of thumb) a quarter of the wavelength, i.e. ~ 9 cm diameter, which is enough to detect buried drifted-wood in sediments, and differentiate it from rocks and other blocks.

Keywords: Ground Penetrating Radar, Drifted wood, Geophysics



Drainage density and relative relief for the Kitakami Mountains, Japan

*Takashi Oguchi¹

1. Center for Spatial Information Science, The University of Tokyo

Drainage density has been frequently used as a parameter representing terrain texture. My previous study investigated the relation between drainage density and relative relief for mountains in the Matsumoto region, central Japan, based on geomorphometric work using contour maps and raster digital elevation models. The result indicates that the density of drainage lines along deeply incised channels decreases with relative relief, whereas that of drainage lines along shallow hollows increases with relative relief, and the total drainage density tends to be constant irrespective of relief. These observations were attributed to frequent slope failures leading to the decline of channel banks. The present study applies the same geomorphometric methodology to four mountainous watershed in the Kitakami Mountains, Northeast Japan. The results indicate that the relations between drainage density and relative relief for deep and shallow channels are similar to those for the Matsumoto region, confirming the applicability of previous findings. However, the density of drainage lines along shallow hollows for the Kitakami region tends to be higher than the Matsumoto region for the same relative relief, especially when relative relief is large. This may be ascribed to weaker rainfall intensity in the Kitakami region, which limits the integration of shallow channels by small-scale shallow failures on mountain slopes near ridges.

Keywords: Drainage density, Relief, Channels, Geomorphometry

[E] Poster | S (Solid Earth Sciences) : S-SS Seismology

📅 Fri. Jun 4, 2021 5:15 PM - 6:30 PM JST | Fri. Jun 4, 2021 8:15 AM - 9:30 AM UTC | 🏠 Ch.13_2

[S-SS02] Seismological advances in the ocean

convener: Takeshi Akihara (Earthquake Research Institute, University of Tokyo), Takashi Tonegawa (Research and Development center for Earthquake and Tsunami, Japan Agency for Marine-Earth Science and Technology), Tatsuya Kubota (National Research Institute for Earth Science and Disaster Resilience)

Advances in ocean-bottom seismic observations with seismometers, hydrophones, and pressure gauges have provided us with the opportunity to study seismicity, subsurface structures, and wave phenomena in offshore areas. Permanent (cabled) observatories have enabled long-term monitoring for these targets, and deployments of dense temporary arrays or fiber optic technologies have opened up the possibility of a high-resolution research. Also, such growths of ocean seismology have compelled the community to create/modify data processing techniques. The purpose of this session is to share recent advances in seismology from data obtained in the oceans, including new seismicity and seismic velocity, progress in instrumentation, data processing on active and passive seismic approaches, and characterization of ambient noise. We also welcome presentations by early-career researchers or students who have little experience in international conferences.

[SSS02-P01] Improving the constraint of the 2016 Off-Fukushima shallow normal-faulting earthquake with the high-coverage tsunami data from the S-net wide network: implication on the crustal stress in the overriding plate

*Tatsuya Kubota¹, Hisahiko Kubo¹, Naotaka Yamamoto Chikasada¹, Keisuke Yoshida², Wataru Suzuki¹, Takeshi Nakamura³ (1.National Research Institute for Earth Science and Disaster Resilience, 2.Graduate School of Science, Tohoku University, 3.Central Research Institute of Electric Power Industry)

[SSS02-P02] Receiver function imaging of the amphibious NE Japan subduction zone - effects of low-velocity sediment layer-

*HyeJeong Kim¹, Hitoshi Kawakatsu¹, Takeshi Akihara¹, Masanao Shinohara¹, Hajime Shiobara¹, Hiroko Sugioka², Ryota Takagi³ (1.Earthquake Research Institute, University of Tokyo, 2.Department of Planetology, Kobe University, 3.Research Center for Prediction of Earthquakes and Volcanic Eruptions, Graduate School of Science, Tohoku University)

[SSS02-P03] Transversely isotropic velocity structure of marine sedimentary layers estimated by Rayleigh wave ellipticity of ambient noise

*Shun Fukushima¹, Kiyoshi Yomogida¹ (1.Hokkaido University, Graduate school of Science, Department of Natural History Sciences, Seismology Laboratory)

[SSS02-P04] **Very broadband strain-rate measurements along a submarine fiber-optic cable off Cape Muroto, Nankai subduction zone, Japan**

*Satoshi Ide¹, Eiichiro Araki², Hiroyuki Matsumoto² (1.Department of Earth and Planetary Science, University of Tokyo, 2.Japan Agency for Marine-Earth Science and Technology)

[SSS02-P05] **The lithosphere–asthenosphere boundary beneath the Sea of Japan back-arc basin**

*Takeshi Akihara¹, Kazuo Nakahigashi², Masanao Shinohara¹, Tomoaki Yamada³, Yusuke Yamashita⁴, Hajime Shiobara¹, Kimihiro Mochizuki¹ (1.Earthquake Research Institute, University of Tokyo, 2.Tokyo University of Marine Science and Technology, 3.Japan Meteorological Agency, 4.Disaster Prevention Research Institute, Kyoto University)

[SSS02-P06] **Surface wave envelope fitting for S wave velocity structure of the oceanic upper mantle**

*Haruka Nagai¹, Nozomu Takeuchi¹, Hitoshi Kawakatsu¹, Hajime Shiobara¹, Takehi Isse¹, Hiroko Sugioka², Aki Ito³, Hisashi Utada¹ (1.Earthquake Research Institute, The University of Tokyo, 2.Kobe University, 3.Japan Agency for Marine-Earth Science and Technology)

[SSS02-P07] Application of the wavefield decomposition for the Oldest-1 array data

*Hitoshi Kawakatsu¹, Takehi Isse¹, Nozomu Takeuchi¹, Hajime Shiobara¹, Hiroko Sugioka², YoungHee Kim³, Hisashi Utada¹, Sang-Mook Lee³ (1.Earthquake Research Institute, The University of Tokyo, 2.Kobe University, 3.Seoul National University)

Improving the constraint of the 2016 Off-Fukushima shallow normal-faulting earthquake with the high-coverage tsunami data from the S-net wide network: implication on the crustal stress in the overriding plate

*Tatsuya Kubota¹, Hisahiko Kubo¹, Naotaka Yamamoto Chikasada¹, Keisuke Yoshida², Wataru Suzuki¹, Takeshi Nakamura³

1. National Research Institute for Earth Science and Disaster Resilience, 2. Graduate School of Science, Tohoku University, 3. Central Research Institute of Electric Power Industry

On November 22, 2016, an Mw 6.9 shallow normal-faulting earthquake occurred within the overriding plate off Fukushima Prefecture (12 km, GCMT). Although tsunamis associated with this event have been reported, they are observed only at the landward from the source and thus there might be a difficulty in constraining the tsunami source, in particular for its offshore side. In response to the 2011 Tohoku earthquake, a new offshore observation network, S-net, has been developed off eastern Japan (Aoi et al., 2020), and the S-net ocean-bottom pressure gauges (OBPs) clearly observed the tsunamis. Because the S-net station coverage is significantly high and some of them are located very close to the source, the constraint of the source of the Off-Fukushima earthquake will be significantly improved. We thus analyze the S-net OBP data to estimate the high-resolution fault model of the Off-Fukushima earthquake. After processing the data, pulsive tsunamis with maximum amplitudes up to ~40 cm were recognized. We then estimated the tsunami source, with careful analysis to reduce the influence due to the instrumental noises related to the step and drift signals (Kubota et al., 2020JpGU). We obtained the tsunami source with one large subsidence region, which had narrower spatial extent and larger peak displacement than those previously proposed. We calculated the tsunami waveforms at the NOWPHAS near-coastal GPS buoys and wave gauges, which reproduced the observation very well even though they were not used for the inversion. This indicates that the S-net data dramatically improve the spatial constraint of the source. We also estimated the slip distribution on the fault from the S-net OBP data. The main slip was concentrated in a region of ~30 km × ~20 km with average and maximum slips of ~300 cm and ~600 cm, respectively (Mw 7.1). Based on the shear stress change distribution on the fault from this fault model, we obtained an energy-based, or slip-weighted averaged, stress drop $\Delta \sigma_E$ (Noda et al. 2013) of ~14 MPa on the main slip area.

It has been reported that the normal-faulting seismicity within the overriding plate increased after the Tohoku earthquake, while reverse-faulting seismicity due to the horizontal compression by the subducting plate was dominant before (e.g., Terakawa & Matsu'ura, 2010; Asano et al., 2011), and this change can be attributed to the switch of the stress regime from horizontal compression to extension due to the stress perturbation by the Tohoku earthquake (e.g., Hasegawa et al., 2012). Based on this interpretation, the deviatoric stress around this region is considered to mostly correspond to the static stress change by the Tohoku earthquake. However, the shear stress increase along the fault plane of the Off-Fukushima earthquake, by the Tohoku earthquake (Iinuma et al., 2012) is only ~2 MPa, which is significantly smaller than the stress drop inferred from the fault model. This shortage of the shear stress increase may suggest the deviatoric stress is locally large around the focal area. One probable interpretation is the local extensional stress is fundamentally developed at the shallowest surface of the plate around this region, probably related to its bending due to the force by the subducting oceanic plate (Hashimoto and Matsu'ura, 2006). This horizontal extensional stress may not exceed the crustal strength before the Tohoku earthquake, but the stress perturbation by the Tohoku earthquake enhanced the extensional

stress to provoke the normal-faulting seismicity. This study demonstrated that the use of the higher-coverage S-net OBP data will significantly contribute to improving the constraint of the fault modeling of the offshore earthquakes, which could not be achieved in the past when the S-net was not available. We expect that the S-net wide and dense OBP network will advance our understandings for ocean bottom seismology.

Keywords: S-net, Ocean bottom pressure gauge, Tsunami, The 2016 Fukushima earthquake, Intraplate stress regime

Receiver function imaging of the amphibious NE Japan subduction zone - effects of low-velocity sediment layer-

*HyeJeong Kim¹, Hitoshi Kawakatsu¹, Takeshi Akuhara¹, Masanao Shinohara¹, Hajime Shiobara¹, Hiroko Sugioka², Ryota Takagi³

1. Earthquake Research Institute, University of Tokyo, 2. Department of Planetology, Kobe University, 3. Research Center for Prediction of Earthquakes and Volcanic Eruptions, Graduate School of Science, Tohoku University

We performed receiver function imaging in the northeast Japan subduction zone using an amphibious dataset. To incorporate the ocean bottom seismometers, we identified their significant time delaying and amplifying effects on receiver functions due to low-velocity seafloor sediment. We have corrected those effects to produce a continuous image across ocean and land, and the coherent structures are retrieved. Our images delineate the subducting oceanic Moho and the top of the oceanic crust further to shallower depths than previously reported. The weakening and strengthening signals of the subducting oceanic Moho in the offshore part of images are partially due to the interference with the sediment reverberations. Some of our along-dip structural variations at shallow offshore regions provide structural features that may be related to the dynamics of the NE Japan subduction zone. The sediment effect we discuss in the ocean is also observed in the land part, at places where it is covered with low-velocity sediments (e.g. west part of NE Japan). The difference of continental Moho depths inferred from receiver functions and the active source surveys may be explained by the effect of on-land slow sediments. Our study suggests that the sediments should be taken with caution during teleseismic waveform analysis at both onshore and offshore regions.

Keywords: receiver function imaging, seafloor sediment, ocean bottom seismometers

Transversely isotropic velocity structure of marine sedimentary layers estimated by Rayleigh wave ellipticity of ambient noise

*Shun Fukushima¹, Kiyoshi Yomogida¹

1. Hokkaido University, Graduate school of Science, Department of Natural History Sciences, Seismology Laboratory

Recent development of OBS networks such as S-net and DONET now enables us to measure ambient noise cross-correlations of high-resolution on the sea bottom. Spatiotemporal variations of seismic velocity and vertical transversely isotropy in marine sediment help us to understand dynamic processes associated with plate interaction in a subduction zone such as crack alignment caused by the bending of a subducting plate, fluid migration and dehydration of constituent minerals. The ellipticity of Rayleigh waves (i.e., the ratio of vertical and horizontal amplitudes, V/H) is useful to study seismic velocity of sedimentary layers because V/H is more sensitive to shallow structures than conventional phase or group dispersion data (e.g., Lin et al., 2014).

In this study, we first formulated partial derivatives of V/H for vertical transversely isotropic media including sea water. It is well known that P-wave velocity has little effect on the ellipticity in isotropic media. In the VTI media, however, the effect or distinguishment of PH and PV wave velocities cannot be neglected in comparison to conventional SV wave velocity in media of a certain degree of VTI. This is why, the partial derivative or sensitivity of P wave in isotropic media is the sum of those of PV and PH waves with opposite signs.

Next, since short-period Rayleigh waves have sensitivity for shallow parts, we applied the seismic interferometry to the noise data recorded at S-net stations. The cross-correlations among S3 stations perpendicular to the trench axis clearly show surface wave signals with relatively good symmetry of causal and anti-causal waveforms in the period range from 5 to 12 sec (Fig.1). Their group velocity is very small, about 0.2-0.4 km/s. This signals probably correspond to Scholte waves. Scholte waves propagate parallel to the water-sediment interface, when the shear velocity of the solid is lower than the compressional velocity in the water (1.5 km/s), that is, very loose sediments.

Finally, we estimated V/H spectrum ratios of the extracted Scholte waves at S-net stations and inverted a new velocity model of sedimentary layers. Prior to the V/H inversion, we estimated a velocity model of the basement beneath sediment by the measure phase velocity dispersion. The area in the subarray S3 of deep ocean near the Japan trench axis has small V/H values. This indicates slow velocity regions there, probably very and/or thick soft sediments. The estimated PV and SV wave velocities can explain these low V/H values in the subarray S3. PV and SV wave velocities in shallow sediments are 1.5 ~ 2.0 km/s and 0.50 ~ 1.0 km/s respectively (Fig.2). The estimated SV wave velocity, much is lower than the water P wave velocity can explain the observed low group velocity of Scholte waves.

We expect that the SV and PV wave velocity of the shallow ocean-bottom sediment to vary significantly in space and time. This is why our partial derivatives and the measurement of V/H with ambient noise data of S-net should be useful to retrieve and spatial-temporal variations in the region around the Japan trench.

Keywords: Rayleigh wave ellipticity, seismic interferometry

Fig.1

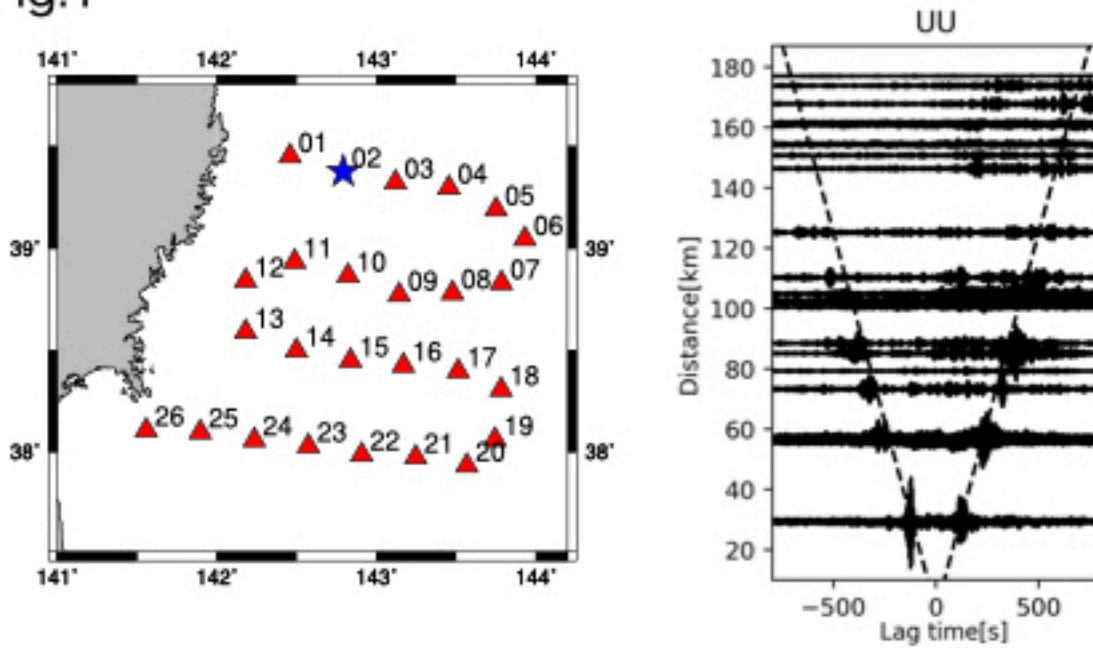


Fig.1 Vertical component cross-correlations at between the N.S3N02 station (blue star) and the others (virtual source) in the subarray NS3 with bandpass filter between 5 and 8 sec. The dashed line indicated group of velocity 0.25 km/s.

Fig.2

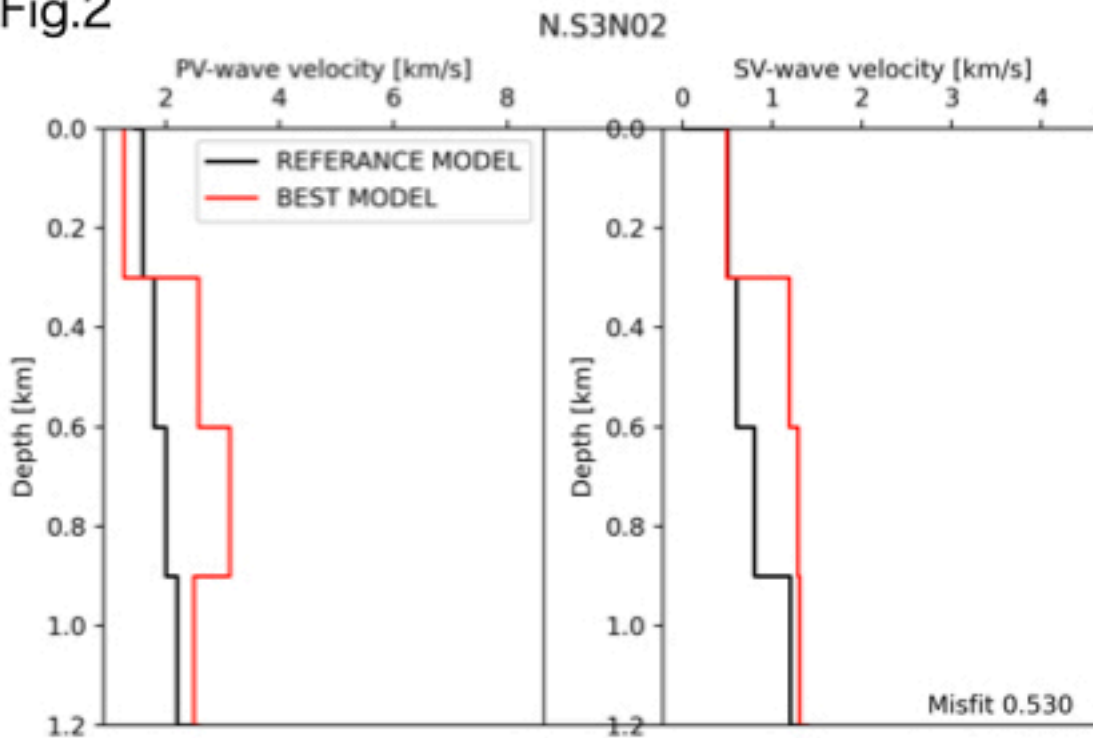


Fig.2 Result model of PV(right) and SV (left) velocity at the station N.S3N02. Black and red lines indicated reference model and best model respectively.

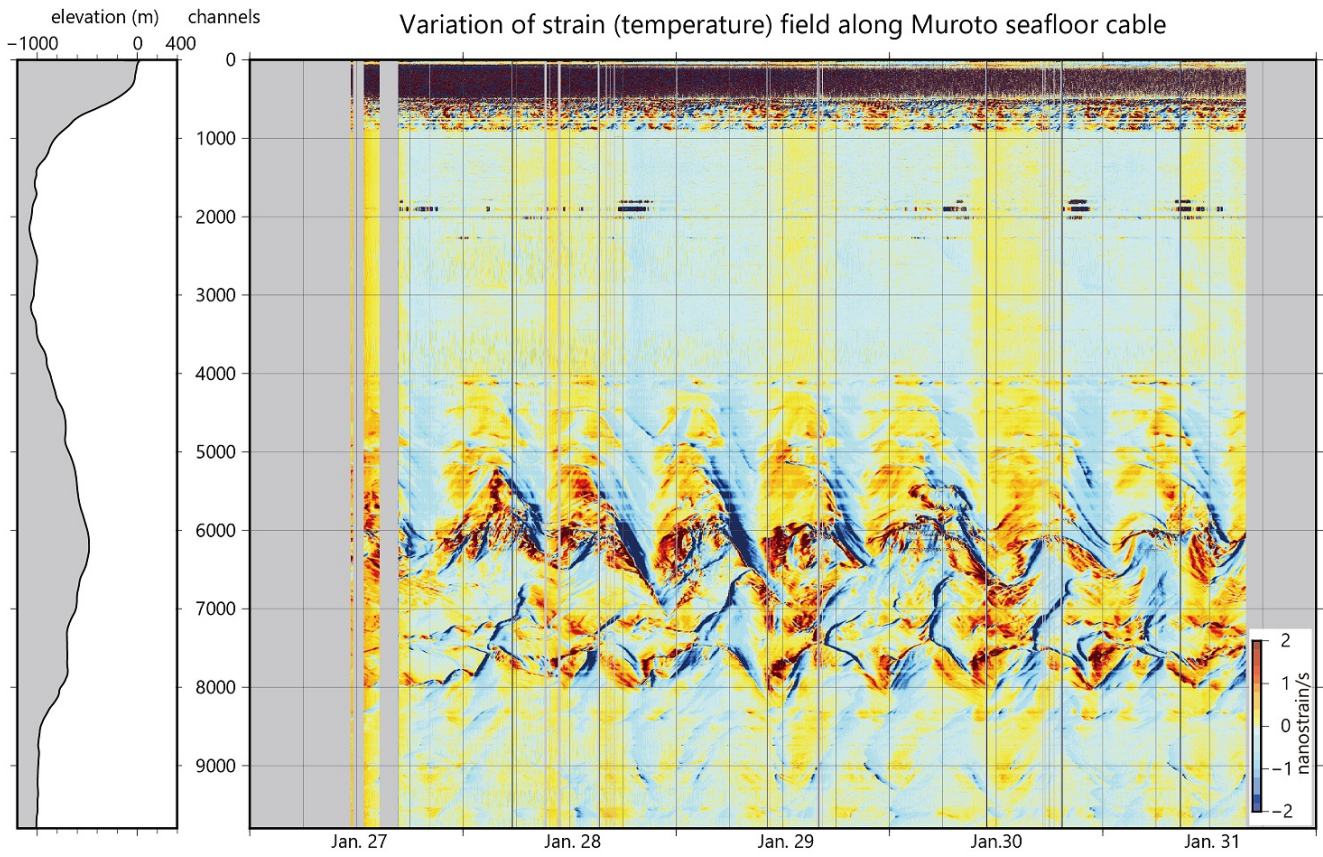
Very broadband strain-rate measurements along a submarine fiber-optic cable off Cape Muroto, Nankai subduction zone, Japan

*Satoshi Ide¹, Eiichiro Araki², Hiroyuki Matsumoto²

1. Department of Earth and Planetary Science, University of Tokyo, 2. Japan Agency for Marine-Earth Science and Technology

Distributed acoustic sensing (DAS) is a new method that measures the strain change along a fiber-optic cable and has emerged as a promising geophysical application across a wide range of research and monitoring. Here we present the results of DAS observations from a submarine cable offshore Cape Muroto, Nankai subduction zone, western Japan. The observed signal amplitude varies widely among the DAS channels, even over short distances of only ~100 m, which is likely attributed to the differences in cable-seafloor coupling due to complex bathymetry along the cable route. Nevertheless, the noise levels at the well-coupled channels of DAS are almost comparable to those observed at nearby permanent ocean-bottom seismometers, suggesting that the cable has the ability to detect nearby micro earthquakes and even tectonic tremors. Many earthquakes were observed during the five-day observation period, with the minimum and maximum detectable events being a local M1.1 event 30–50 km from the cable and a teleseismic Mw7.7 event that occurred in Cuba, respectively. Temperature appears to exert a greater control on the DAS signal than real strain in the quasi-static, sub-seismic range, where we can regard our DAS record as distributed temperature sensing (DTS) record, and detected many rapid temperature change events migrating along the cable: a small number of large migration events (up to 10 km in 6 hours) associated with rapid temperature decreases, and many small-scale events (both rising and falling temperatures). These events may reflect oceanic internal surface waves and deep-ocean water mixing processes that are the result of ocean current–tidal interactions along an irregular seafloor boundary.

Keywords: distributed acoustic sensing (DAS), Muroto submarine cable, broadband seismograms, water mixing process



The lithosphere–asthenosphere boundary beneath the Sea of Japan back-arc basin

*Takeshi Akuhara¹, Kazuo Nakahigashi², Masanao Shinohara¹, Tomoaki Yamada³, Yusuke Yamashita⁴, Hajime Shiobara¹, Kimihiro Mochizuki¹

1. Earthquake Research Institute, University of Tokyo, 2. Tokyo University of Marine Science and Technology, 3. Japan Meteorological Agency, 4. Disaster Prevention Research Institute, Kyoto University

The evolution history of the Sea of Japan back-arc basin remains under debate, involving the opening of sub-basins such as the Japan and Yamato Basins. Detailed knowledge of the lithospheric structure will provide the key to understanding tectonic history. This study identifies the lithosphere-asthenosphere boundary (LAB) beneath the Sea of Japan back-arc basin using S-receiver functions (S-RFs). The study area, including the Japan and Yamato Basins, has been instrumented with broadband ocean-bottom seismometers (OBSs). S-RFs from these OBSs show negative S_p phases preceding the direct S arrivals, suggesting the LAB. The S-RFs also show abnormally reduced amplitudes. For further qualitative interpretation of these findings, we conduct transdimensional Bayesian inversion for S-wave velocity models. This less-subjective Bayesian approach clarifies that low-velocity seafloor sediments and damped deconvolution contribute to the amplitude reduction, illuminating the necessity of such considerations for similar receiver function works. Inverted velocity structures show a sharp velocity decrease at mantle depths, which we consider the LAB. The obtained LAB depths vary among sites: ~45 km beneath the Japan and Yamato Basins and ~70 km beneath the Yamato Rise, a bathymetric high between the two basins. The thick lithosphere beneath the Yamato Rise most likely reflects its continental origin. However, the thickness is still thin compared to that of eastern Asia, suggesting lithosphere extension by rifting. Notably, the Japan and Yamato Basins show a comparable lithospheric thickness. This consistency contrasts with well-documented crustal features: the crust beneath the Yamato Basin is approximately twice thicker than beneath the Japan Basin. Whereas magma injection after the back-arc opening thickens the crust beneath the Yamato Basin, such injection seemingly has little influence on the lithosphere thickness. Lithospheric temperatures still seem to play a role in determining the lithosphere thickness.

Keywords: Sea of Japan, Receiver function, Transdimensional inversion, Ocean-bottom seismometer, Lithosphere-asthenosphere boundary, Seafloor sediment

Surface wave envelope fitting for S wave velocity structure of the oceanic upper mantle

*Haruka Nagai¹, Nozomu Takeuchi¹, Hitoshi Kawakatsu¹, Hajime Shiobara¹, Takehi Isse¹, Hiroko Sugioka², Aki Ito³, Hisashi Utada¹

1. Earthquake Research Institute, The University of Tokyo, 2. Kobe University, 3. Japan Agency for Marine-Earth Science and Technology

Physical characteristics of the oceanic lithosphere and asthenosphere is essential to reveal the mechanism of plate tectonics. The V_p/V_s ratio is one of the most important parameters to constrain chemical composition and temperature. Takeuchi et al. (2020) revealed the depth profile of the P wave velocity beneath the northwestern Pacific plate using waveforms for earthquake events in Northeast Japan observed by broadband ocean bottom seismometers (BBOBSs). The purpose of this study is to infer continuous S wave structure from the crust to the asthenosphere using the same data set. This enables us to reveal the V_p/V_s structure averaged over the event-station path.

Data used in this study is the vertical component of the BBOBSs deployed in the Northwestern Pacific from 2010 to 2014. We collected higher quality waveforms for earthquake events around the Japan trench (Figure 1). We calculated the amplitude of envelope of Rayleigh waves at each period and group velocity and stacked for bin1 (data for events in the continental plate) and bin2 (data for events in the vicinity of the trench). We also calculated synthetic waveforms for the PA5 model (Gaherty et al., 1996) and stacked in the same procedures. We picked the amplitude peak locations for overtone and fundamental mode branch to characterize the shape of envelopes and compared observed peaks and synthetic ones. At periods shorter than 40 s, observation and synthesis for bin 2 are similar with each other, while there are significant discrepancies for bin1 (Figure 2). These results suggest that pure oceanic structure of crust and uppermost mantle in our study region can be well represented by the PA5 model, but raypaths passing through the continental plate are affected by shallower structure of the continent. In the presentation, we plan to also show the measurements for longer period and the S wave velocity structure model obtained from these data.

Keywords: surface wave, lithosphere, asthenosphere

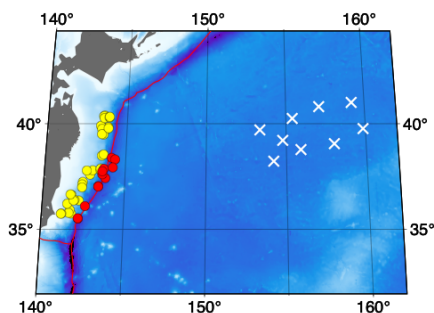


Figure 1. Map of stations (white crosses) and events (bin1: yellow circle, bin2: red circle) used in this study.

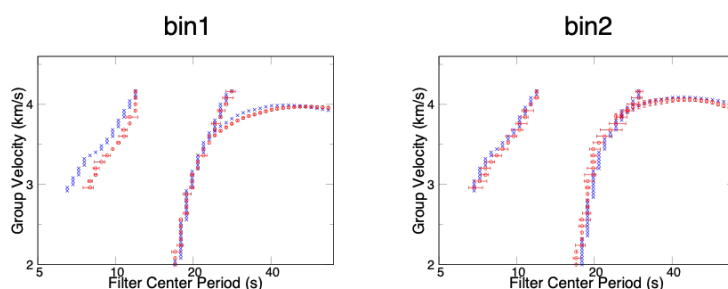


Figure 2. Amplitude peak of surface wave envelope for each bin. The red dots are observed peaks and blue cross are synthetic ones.

Application of the wavefield decomposition for the Oldest-1 array data

*Hitoshi Kawakatsu¹, Takehi Isse¹, Nozomu Takeuchi¹, Hajime Shiobara¹, Hiroko Sugioka², YoungHee Kim³, Hisashi Utada¹, Sang-Mook Lee³

1. Earthquake Research Institute, The University of Tokyo, 2. Kobe University, 3. Seoul National University

We apply the wavefield decomposition method (e.g., Thorwart and Dahm, 2005; Bostock and Trehu, 2012) to the broadband ocean bottom seismic and the differential pressure gage (DPG) data of the Oldest-1 array deployed on the oldest (~170 Ma) seafloor ~1000 km off the Marian trench (e.g., Shiobara et al., 2020, JpGU). We follow the formulation and approach of Bostock and Trehu (2012) and first estimate the thickness of the water layer using DPG data and vertical component seismograms of teleseismic earthquakes and regional deep events. Estimated water depths are consistent with the reported water depths of the 11 seismic stations within few tens of meters and honor the 1D assumption of the local seafloor structure around each station site that allows further analysis assuming 1D structure beneath. We then apply the wavefield decomposition to resolve upgoing P- and S-wave using the vertical and radial component seismograms and DPG data employing both the acoustic and the elastic formulae of Bostock and Trehu (2012). The preliminary analysis indicates that, although both formulae give reasonable results, the acoustic formula gives more stable decomposition. The comparison of decomposed upgoing S-wave and radial component waveforms indicates that the radial component is dominated by S-waves consistent with the presence of the low S-wave velocity sediment at the station sites.

[E] Poster | S (Solid Earth Sciences) : S-IT Science of the Earth's Interior & Tectonophysics

📅 Fri. Jun 4, 2021 5:15 PM - 6:30 PM JST | Fri. Jun 4, 2021 8:15 AM - 9:30 AM UTC | 🏠 Ch.15_2

[S-IT15] Study of the Earth's Deep Interior - Interaction and Coevolution of the Core and Mantle

convener: Kenji Kawai (Department of Earth and Planetary Science, School of Science, University of Tokyo), Tsuyoshi Iizuka (University of Tokyo), Kenji Ohta (Department of Earth and Planetary Sciences, Tokyo Institute of Technology), Taku Tsuchiya (Geodynamics Research Center, Ehime University)

Recent observational and experimental investigations have significantly advanced our understanding of the deep Earth's structure and constituent materials. Yet, even fundamental properties intimately linked with the formation and evolution of the planet, such as details of the chemical heterogeneity in the mantle and light elements dissolved in the core, remain unclear. Seismological observations have suggested vigorous convection in the lower mantle, whereas geochemistry has suggested the presence of stable regions there that hold ancient isotope signatures. The amounts of radioactive isotopes that act as heat sources and drive the deep Earth's dynamic behaviors are also still largely unknown. We provide an opportunity to exchange the achievements and ideas and encourage persons who try to elucidate these unsolved issues of the core-mantle evolution using various methods, including high-pressure and high-temperature experiments, high-precision geochemical and paleomagnetic analyses, high-resolution geophysical observations, geo-neutrino observations, and large-scale numerical simulations. Papers stimulating an interdisciplinary collaboration relating to the establishment of the Japan-SEDI community are also welcomed.

[SIT15-P01] First-principles study on the thermal transport properties of the subducting slab

*Haruhiko Dekura¹ (1. Geodynamics Research Center, Ehime University)

[SIT15-P02] A constraint to thermal conductivity of Earth's core and CMB heat flow by assessment on a stable region of Earth's core

*Takashi Nakagawa^{1,2}, Shin-ichi Takehiro³, Youhei SASAKI⁴ (1. Kobe University, 2. Hiroshima University, 3. Kyoto University, 4. Setsunan University)

[SIT15-P03] Self-diffusion of hcp-iron at high pressure

*Daisuke Yamazaki¹, Naoya Sakamoto², Hisayoshi Yurimoto² (1. Institute for Planetary Materials, Okayama University, 2. Hokkaido University)

[SIT15-P04] Inner core differential rotation inferred from antipodal seismic observations

*Seiji Tsuboi¹, Rhett Butler² (1. JAMSTEC, Center for Earth Information Science and Technology, 2. University of Hawaii at Manoa)

First-principles study on the thermal transport properties of the subducting slab

*Haruhiko Dekura¹

1. Geodynamics Research Center, Ehime University

The temperature structure of the Earth's interior is still one of the most uncertain physical quantities. Since the viscosity is a key parameter controlling the style of the mantle convection and is sensitive to temperature, the temperature profile of the mantle provides a basis for a better understanding of mantle dynamics. The subducting slab is one of the potential sources producing both the temperature and chemical heterogeneities in the deep Earth. The heat transport mechanism by thermal conduction is likely to be dominant in the subducting slab. Therefore, the temperature heterogeneity of the deep mantle induced by the subduction can be better constrained by determining the lattice thermal conductivity (κ) of its constituent minerals. However, precise determinations of the κ under the deep mantle conditions are still challenging, making the heat transport properties of the subducting slab remain unclear. We have recently initiated the first-principles determination of the κ of those minerals based on the density-functional theory for a tighter constraint on the temperature structure. In this presentation, we will report our progress of both harmonic and anharmonic phonon calculations of SiO_2 and CaSiO_3 perovskite necessary to compute κ under the lower mantle conditions.

Keywords: Lower mantle, Thermal transport property, Theory

A constraint to thermal conductivity of Earth's core and CMB heat flow by assessment on a stable region of Earth's core

*Takashi Nakagawa^{1,2}, Shin-ichi Takehiro³, Youhei SASAKI⁴

1. Kobe University, 2. Hiroshima University, 3. Kyoto University, 4. Setsunan University

It is still controversial for an emergence of a stable region at the top of Earth's core in theoretical modeling because both thermal conductivity of Earth's core and heat flow across the core-mantle boundary (CMB) have not been clearly constrained from mineral physics and geophysical observations, ranging 20 to 220 W/m/K for the thermal conductivity (denoted as κ) and 5 to 20 TW for the present-day CMB heat flow (denoted as $Q_{\text{CMB}}^{\text{P}}$). In this study, in order to resolve these uncertainties, we try to constrain the values of thermal conductivity of Earth's core and the present-day CMB heat flow by requiring continuous generation of geomagnetic field in addition to existence of a stable region at the top of present Earth's core using a one-dimensional thermal and compositional evolution model.

Numerical experiments for various values of κ and $Q_{\text{CMB}}^{\text{P}}$ show that the solutions satisfying both long-term magnetic field generation and emergence of a stable region is possible only when κ is larger than 40 W/m/K and $Q_{\text{CMB}}^{\text{P}}$ is less than 18.5 TW. The specific required value of κ depends on $Q_{\text{CMB}}^{\text{P}}$. If the expected CMB heat flow would be as large value as 17.5 TW, which is suggested by the recent studies on the core evolution theory (e.g., Labrosse, 2015), should be a high value such as about 212 W/m/K to satisfy our requirements. The thickness of an expected stable region would be about 30 km in this case. In contrast, when $Q_{\text{CMB}}^{\text{P}}$ is as small as that derived from numerical mantle convection models (e.g., 10 TW; Nakagawa and Tackley, 2010), the required value of κ decreases to 110 W/m/K. In this case, a stable region extends about 75 km thickness below CMB.

If the requirements assumed in this study is confirmed by certain geophysical observations and/or $Q_{\text{CMB}}^{\text{P}}$ can be restricted more precisely with some methods, our assessment scheme would be useful for evaluations of the radial convective structure of Earth's core and for further constraint of the value of thermal conductivity of Earth's core.

Keywords: Earth's core, Stable region, Magnetic field generation, Chemical coupling, Thermal conductivity

Self-diffusion of hcp-iron at high pressure

*Daisuke Yamazaki¹, Naoya Sakamoto², Hisayoshi Yurimoto²

1. Institute for Planetary Materials, Okayama University, 2. Hokkaido University

The size of the earth's inner core of the earth is much smaller than that of mantle and hence geophysical observation of the inner core is difficult, for example, rheological properties of the inner core is poorly understood. The recent observations have suggested that the flow is not only an axial symmetrical component but also the possibility of flow in the horizontal plane. For the interpretation of the anisotropy of seismic waves formed in such a flow geometry, the flow mechanism and mobility of the constituent minerals (the viscosity) are key parameters. Because viscosity is strongly dependent on the diffusion of constituent elements, we determine the diffusion rate experimentally and predict the viscosity and deformation mechanism of the inner core. The inner core is composed of a solid iron alloy with the crystal structure of hcp, hcp-iron. The alloying is mainly done with Ni and other light elements, but primarily the rheological properties of pure iron are thought to represent the inner core properties. Therefore, in this study, we focused on the self-diffusion coefficient of iron in hcp-iron. Since hcp-iron is a stable phase only under high pressure, a diffusion experiment was conducted at a pressure of 45 GPa and a temperature of 1100-1300 by means of high pressure and temperature experiment combined with the isotope diffusion method. In the high-pressure experiments, Kawai-type assemblies composed with "binderless" tungsten carbide material of the second stage anvil to generate a pressure of 45 GPa were compressed in a DIA-type high pressure apparatus at Okayama University. Because the upper limit of temperature for the stability field of hcp-iron at 45 GPa is ~1300K, which is relatively low temperature to observe the thermally activated process, we needed diffusion duration more than 100 hours to obtain reliable diffusion length. The diffusion profile was obtained on the recovered specimen by analysis with the isotope microscope IMS1270 + SCAPS installed at Hokkaido University. In order to calibrate the irregular deformation of the specimen under high pressure and the spatial resolution of the analysis, a 30-minute diffusion sample was used as a reference. At 45 GPa and 1300 K, the diffusion coefficient was determined to be $10^{-17.49}$ m²/s. In order to extrapolate the diffusion coefficient obtained by the experiment to the inner core condition, it is necessary to accurately estimate the model parameters of temperature and pressure dependence. Therefore, we are trying to determine the diffusion coefficient in the pressure range of 15 GPa to 60 GPa.

Inner core differential rotation inferred from antipodal seismic observations

*Seiji Tsuboi¹, Rhett Butler²

1. JAMSTEC, Center for Earth Information Science and Technology, 2. University of Hawaii at Manoa

The Earth's Inner Core may rotate at a different speed than Earth's crust-mantle. We use observations for antipodal earthquake and station pairs to examine the arrival time shift of the whispering-gallery wave which propagates tangentially along the top of the Inner Core. Observations of these waves for earthquakes which occurred at the same location reveal that travel times vary by 0.2 sec over the past 20 years. We propose that these time shifts are caused by the interaction of a zero rigidity patch (lateral heterogeneity) at the Inner Core surface with the Inner Core differential rotation. The simplest interpretation infers a rotation rate of 0.05 degree/year, which is one order of magnitude smaller than those reported by previous studies. Our result may also give constraint to the provenance of a zero rigidity patch at the Inner Core surface. The Fresnel zone coverage of whispering-gallery PKIKP+ antipodal measurements beneath the Inner Core boundary extend over ~60% of the boundary surface, in contrast to PKiKP-PKP paths which individually measure specular reflections (~1 Hz) from the top of the ICB over Fresnel zones each encompassing 0.002% of the Inner-Outer Core boundary.

Keywords: Inner core, Antipodal seismic observation, Differential rotation

[E] Poster | S (Solid Earth Sciences) : S-IT Science of the Earth's Interior & Tectonophysics

📅 Fri. Jun 4, 2021 5:15 PM - 6:30 PM JST | Fri. Jun 4, 2021 8:15 AM - 9:30 AM UTC | 🏢 Ch.15_3

[S-IT16] Structure and Dynamics of Earth and Planetary Mantles

convener: Takashi Nakagawa (University of Leeds), Takashi Yoshino (Institute for Planetary Materials, Okayama University), Dapeng Zhao (Department of Geophysics, Tohoku University)

Interdisciplinary approach can lead to a better understanding of dynamics and evolution of the deep interiors of the Earth and planets. We welcome any submissions of recent results in observational, theoretical and experimental studies on seismology, geomagnetism, mineral physics, dynamics of deep interiors, and any other relevant fields from researchers in many countries. Integration of such results is also welcome. In particular, we encourage any contributions focusing on "plate and mantle dynamics in Earth and terrestrial planets". We also encourage papers stimulating an interdisciplinary collaboration relating to establishment of the Japan-SEDI community.

[SIT16-P01] ***None could explore* Origin of Plate Tectonics and Driving Force.**

***Abduction with Evolution* explained and *verified all of them*, Formation Mechanism of Deep Ocean Floor (Plate), and Cause of Sudden Changes in Plate Movement Direction.**

*Akira Taneko¹ (1. SEED SCIENCE Lab.)

[SIT16-P02] High-temperature deformation properties of Li-doped polycrystalline olivine

*Bunrin Natsui¹, Takehiko Hiraga¹ (1. Earthquake Research Institute, University of Tokyo)

[SIT16-P03] **Lattice preferred orientation of akimotoite and its implication to seismic anisotropy in the Earth's mantle**

*Longli Guan¹, Daisuke Yamazaki¹, Noriyoshi Tsujino¹, Yoshinori Tange², Yuji Higo² (1. Institute for Planetary Materials, Okayama University, Misasa, Japan, 2. Japan Synchrotron Radiation Research Institute, 1-1-1 Kouto, Sayo, Hyogo 679-5198, Japan.)

None could explore Origin of Plate Tectonics and Driving Force.
Abduction with Evolution explained and verified all of them,
Formation Mechanism of Deep Ocean Floor (Plate), and Cause of
Sudden Changes in Plate Movement Direction.

*Akira Taneko¹

1. SEED SCIENCE Lab.

It has been 100 years since Mr. Wegener proposed Theory of Continental Drift. To study only "How Plate Tectonics happened" without thinking "Why Plate Tectonics happened", I think "It is wrong without a correct Basis". I explained all of them, **Formation Mechanism of Deep Ocean Floor (Plate)**, and **Cause of Sudden Change** in Plate Movement Direction and **verified by Abduction with Evolution**.

1. Mechanism of Moon Formation by "Multi-Impact Hypothesis"

A Mars-sized differentiated protoplanet CERRA was formed at Ceres position in Asteroid Belt. A SuperMassive Gas Giant Jupiter was formed on Outside. Orbit of CERRA is flattened **toward Perigee of Jupiter** by Perturbation of Outer Jupiter to Position where Gravitational Force of Sun and Jupiter are balanced. CERRA ruptures in a balanced position and becomes a Train Mantle Asteroid like Comet Shoemaker-Levy Ninth, lining up in a row and orbiting the same Elliptical Orbit. At Intersection of this Orbit and Earth's Orbit, they collided irregularly during Meeting Cycle, which became **Origin of Great Extinction of Species**. Initial collision of a **Moon-sized Mantle Fragment** with Earth ejected Earth's Mantle like a Newton Cradle, and forming Moon.

⇒ Important Point here is that Earth's Mantle is ejected from Earth, and Moon and Earth's Mantle have almost the same Composition. [However, in Simulation of "Giant Impact Hypothesis", Impactor Mantle is ejected as Moon, and Impactor Mantle needs to coincide with Earth Mantle by chance.]

2. Origin of Earth's Deep Ocean Floor

Next, intermittent Collisions of Multiple Train Mantle Asteroids with Earth result in Mantle Defects at different

positions on Earth, Mantle is isostasy and has a depth of about 4 km. It was Origin of **Sea**, which accounts **for 70%**. Mantle Crack due to Collision was Origin of **Plate Boundary, Pressure drop** due to Crack caused Remelting and outflow of Mntle, and **Crust that escaped Collision** became Continental Plate. Uneven Distribution of Rotating Earth's continents becomes a Global Eccentricity, and Deviation between Moment of Inertia and Axis of Rotation becomes a couple to Plate, and Driving Force is generated on Plate.

3. Origin of Driving Force.

Uneven distribution of Rotating Earth's continents becomes a **global eccentricity**, and Deviation between Moment of Inertia and Axis of Rotation becomes a **couple** to Plate, and **Driving Force** is generated on Plate. This provided a fundamental solution to Fact that **Plate did not wrinkle and buckle**, and was driven smoothly even on a transform fault, and **Contradiction in Thermal Convection Drive Theory** was resolved.

4. Collision Hypothesis to Opposite point of Earth, --- Origin of kimberlite pipe ----

Since Earth is a sphere, **Shock wave** of a huge mantle collision with Earth **concentrates** at Opposite point at Same time, and *eruption pressure is generated*, and Lower Mantle Eruption becomes Origin of Kimberlite Pipe.

Subsequent Continental Drift with Mines, Traces of Plume Outflow from underground pipes are Evidence of **Continental Drift**.

5. Origin of **Tilt of Earth's Axis of rotation**

Collision with Equatorial position causes an Increase in Rotation speed, but in Collision to High Latitudes, A Couple is generated by Inertial Force of the center of gravity and Impact Force, and Inclination of Earth's Axis is assumed.

High-Latitude Collision traces include **Mirunui mine** in Saha, Russiawy, Eurasian continent has not moved, and Collision Position is estimated to be Position of **Drake Passage** in South America from Origin Hypothesis of Kimberlite. **Evidence** of obliquity is Traces of Emperor Seamount and Hawaiian Islands plume on Pacific Plate, and Formation of **Titis Sea** due to high-latitude collisions.

Sudden Change in Direction of Pacific Plate' Move are **Evidence** due to Tilt of Earth's Axis.

6. Origin of Pacific Circular Arc Archipelago, Back-arc Basin and Trenches along Arc. Fig Cross Section.

Mantle defects due to Collision of Giant Meteorites and **Depression of Surrounding Crustal Plate** *due to isostasy* were **Origins of Isolated archipelago** and **Back-Arc Basin**, and **Subduction of Ocean Convex Plate** was also **Origin of Arc Trench**. As Evidence of Depression, it can be pointed out that **Dykes of peridotite**, which had been stratified at Depth of about 30 km underground, are lined up at an Angle close to vertical and rise as Ridges of Mountains. Examples of this are **peridotites** in Hidaka Mountains of Hokkaido and ridges of **sawtooth dikes** in Gitingitin Mountains of Philippines.

Important > Cause is Collision at High Latitudes, Titis Sea Formation, **Multi-Impact Hypothesis** as all Causes. Result of Abduction with Evolution, Paradigm that can be Verified Retroactively.

Keywords: Why plate tectonics occurred, origin of PT, peeling of collision plate, moment of inertia , Origin of deep ocean floor , Origin of kimberlite pipe, Origin of plate driving force, Origin of Slope of Earth's Axis , Origin of Pacific Circular Arc Archipelago, Back-arc Concave Basin and Solitary Trench, P-PS06 (3 Thu J). S-IT16 (4 Fri E), M-IS10 (5 Sat E), M-IS24 (6 Sun J)

The Origin of The Moon and The Earth in Multi-Impact Hypothesis with Abduction. SIT25-P01 2020 7-12

2. Orbital transition of Protoplanet CEREA & Tidal Rupture.

● By passing the angular momentum to Jupiter, the far point of CEREA moves to the near point side of Jupiter. ● At Far point where Attractive forces of Jupiter and Sun balance, CEREA ruptures at tide. ◎ CEREA train mantle fracture fragment (like Shoemaker-Levi 9th Comet). ◎ Intermittent collision, Sea deficit

By Multi-Impact Hypothesis We verify all Mystery of Solar System

木星摂動でセラ分裂
破片の地球衝突軌道
マントル破片の衝突
月形成の接線衝突
時間差衝突で大絶滅

セラ誕生時の軌道
地球軌道
セラ分裂マルチ
インパクト説

Moon Formation Hypothesis
M-IS22 P01
M-ZZ56 P01

◎ CEREAの軌道は、 $6.45 \times 10^4 \text{ km}$ 、 $6.72 \times 10^4 \text{ km}$ could be calculated at the intersection of the earth orbit and CEREA mantle fracture fragment elliptical orbit.

The Origin of The Moon and The Earth in Multi-Impact Hypothesis with Abduction. SIT25-P04 2018 5-22

6. Idea of cause of ground magnetic field due to core eccentricity?

Origin of the Arctic Archipelago Back Arcuate Concave Basin in Pacific Rim.

[Current situation] Because the attitude of the Van Allen belt over Brazil has declined, About 10% of the core (500 km / 6400 km Earth radius) eccentricity was presumed.

Pacific uplift is due to Isostasy
Arcuate Islands (Japan)
Plate tectonic arc basins (Japan sea)
CEREA's Mantle fracture elliptical orbit
Near Oceanic Trench
Plate
Plate Back arc basins
Brazilian central position
Magnetic anomaly
The attitude of the Van Allen belt has declined
by T.J. Sherril
Origin of plate tectonics and the Pacific arcuate back-arc basin

Description: A Collision to the Pacific Ocean position caused a mantle defect. An uplift of Darwin took place due to an isostasy. The surrounding concave plate out-spaces due to the mantle substance shortage and it becomes a back arc concave basin. One piece eccentricity of liquid core and solid core was formed. The eccentricity of the rotational axis of the geomagnetic fluid decreases at the Brazilian position of the Van Allen belt. C. The mantle defect is surrounded by an arcuate collapse, and in the Philippine position it is doubly depressed. So it suggests a second collision.

The Origin of The Moon and The Earth in Multi-Impact Hypothesis with Abduction. SIT25-P01 2020 7-12

5.1 Crust formation in the Gondwana continent and the cause and distribution of Kimberlite pipes? Howland position collision => Precambrian Mirok Drake Strait Position Collision => Midland Mine Collision to High Latitude => Origin of the 23.5° of the Earth's spin axis.

Back side Mantle meteorite collision impact shock wave concentration -> pressure

Impact force - pipe forming crack. ● 1.75 million ago

Movement ● Approximately 60 million years ago Shock wave - pipe formation

In case Source: Kenji Suwa "Know the Earth from the African Continent" Iwanami Nikon Newspaper 2003 p103, p108, Plot Seod Akira data: Pastalis et al

Ice-flow direction
Drake Passage (66°W, 63°N)
Pole

● : ダイアモンド産出・キンバーライト噴出有り
■ : ダイアモンド産出・キンバーライト噴出無し
● : ダイアモンド産出無し・キンバーライト噴出有り
○ : ダイアモンド産出無し・キンバーライト噴出無し

図 3 Ice-flow directions, palaeomagnetic pole position and extent of Late Carboniferous glaciations, キンバーライト産出(噴出)位置とダイアモンド産出状況

マルチインパクト仮説 => 創志社雑誌: はよと地球の起源 M-IS10, M-IS24, S-1115, P-PS06, I changed impactor from Differentiated Mars to Moon-sized Mantle.

12. 月の起源論: 成績表

Origin of Moon with Abduction by Evolution. Origin of Plate Tectonics, Ocean floor.

TABLE 3. A "Super Cool". The Author's Opinion of How Well Five Models of Lunar Origin Satisfy Seven Constraints. Wood (1946): 倉本正臣 2009 倉本正臣の論文: 補正版

Hypothesis Model => Evolution result, 1 stars	Impact Capture	Coagcretion	Earth Fusion	Collisional Epoch	Differentiation Capture	Col. Impact Hypothesis by Van der Meer
Lunar Mare, (Chthonic/low viscosity)?	B	B	D	I	B	A ~ A -> eccentricity formation?
Earth-Moon angular momentum	C	B	B	B	Re C	A. Re=5000 Re. Re=49000
Volatic element depletion	C	C	B	B	C	A. Collision and fraction inches
Fe depletion	B	D	B	I	B	A. Impactor is only Mantle.
Oxygen isotopes	B	A	A	B	B	A. Moon/Mantle is Earth's case.
(Stability of mantle trace element patterns)	(C)	(D)	(A)	(C)	(C)	(A). Earth's Mantle has been BIASD INTO MOON
Magma ocean	D	C	A	A	B	None. Irrespective of Moon formation A. Porphyron Gas
Physical plausibility	D	C	B	I	B	
Survivable Mechanism of Collision	F	F	F	F	F	A. Multi-Impact Hypothesis
Moon always faces to Earth	F	F	F	F	F	A. Eccentric Moon rotates with Earth at common center
Origin of the deep ocean floor	F	F	F	F	F	A. Multi-Impact Hypothesis
Origin of plate boundaries	F	F	F	F	F	A. Opposite crack by mantle lamination
Origin of plate tectonics, driving force	F	F	F	F	F	A. Minimalization of Eccentricity
Circular Pacific arc Islands and back-arc basin	F	F	F	F	F	A. Earth deficiency Movement of Inertia
Inclination of the Earth's rotation axis (inclined change in moon's direction)	F	F	F	F	F	A. High latitude collision, Formation of Teth Sea, Initiation of Plate Movement

*For readers unfamiliar with the U.S. educational system: A is the best grade, F (failing) is the worst. F (failing) means all arguments have not been computed and a grade cannot yet be awarded. F: Model is Wrong, Inappropriate.

左側の既記月形成の提案: 深融中, 右端は太陽系初期の超新星爆発説, 今も固存地球への衝突.

High-temperature deformation properties of Li-doped polycrystalline olivine

*Bunrin Natsui¹, Takehiko Hiraga¹

1. Earthquake Research Institute, University of Tokyo

In order to understand the upper mantle flow, it is important to determine high-temperature deformation properties of major constituent minerals of the upper mantle such as olivine. Olivine is considered to contain water (H₂O) up to 0.1 wt.% in the upper mantle. The deformation properties of hydrous olivine have been experimentally investigated, which have revealed that the viscosity is greatly reduced by the presence of water (Mei and Kohlstedt, 2000). At the same time, one study questions the existence of water weakening or proposes very small effect of water on olivine rheology based on Si self-diffusion experiments (Fei et al., 2013). Recently, Yabe and Hiraga (2020) showed significant weakening of polycrystalline olivine due to grain-boundary-disordering which begins from a certain temperature near solidus. They proposed the water weakening as a result of grain-boundary-disordering in which the starting temperature is lowered by the water.

In this study, we compare high-temperature deformation properties of lithium-doped and undoped olivine. We expected Lithium (Li⁺) to behave like water (H⁺), which helps to elucidate the mechanism of water weakening, even under 1 atm creep tests. Li-doped polycrystalline olivine (Mg₂SiO₄) with an average grain size of ~1 μm and porosity of <3.5 vol% was synthesized using vacuum sintering technique. This polycrystalline material was deformed at atmospheric pressure, temperatures of 843~996 °C, and stresses of 5~200 MPa. We found that the material deformed with the same strain rate at the same stress and grain size but nearly 200°C lower temperature for the undoped olivine, which showed a dramatic effect of Li on olivine diffusion creep. We discuss the mechanism of Li effect on olivine rheology, which is expected to provide insight into water weakening.

Keywords: mantle rheology, diffusion creep, upper mantle, olivine, water weakening

Lattice preferred orientation of akimotoite and its implication to seismic anisotropy in the Earth's mantle

*Longli Guan¹, Daisuke Yamazaki¹, Noriyoshi Tsujino¹, Yoshinori Tange², Yuji Higo²

1. Institute for Planetary Materials, Okayama University, Misasa, Japan, 2. Japan Synchrotron Radiation Research Institute, 1-1-1 Kouto, Sayo, Hyogo 679-5198, Japan.

Seismic anisotropy has profound implications for understanding the dynamic process of the Earth's deep interior and it has been observed in the lower mantle transition zone (MTZ). The seismic anisotropy can be often caused by lattice preferred orientation (LPO) of elastically anisotropic minerals. The origin of the observed anisotropy is still unclear and debated as the dominant minerals in the lower MTZ, ringwoodite and majorite, are nearly isotropic. Akimotoite (ilmenite-structured $(\text{Mg, Fe})\text{SiO}_3$) has a strong elastically anisotropic feature and it is one of the main constituting minerals at the cold region of the lower MTZ. Therefore, the LPO of akimotoite plausibly contributes to the seismological observations of anisotropy. To investigate the LPO of akimotoite developed during deformation, the well-controlled uniaxial and shear deformation experiments on the akimotoite aggregates were conducted at 21-23 GPa and 900-1300°C by using D111 Kawai-type multianvil apparatus. Maximum strains of uniaxial and shear deformation experiments are 0.23 and 2.1, respectively. The most dominant slip system of akimotoite would be $\langle 11\text{-}20 \rangle$ (0001) with no change of slip system between 900-1300°C based on LPO patterns of deformed akimotoite aggregate. Our present results indicate that: (i) The observed strong V_{SH} (or V_{SV}) azimuthal anisotropy with azimuthally isotropic V_{SV} (or V_{SH}) can be explained by the horizontal (or vertical) deformation of akimotoite, and (ii) The V_{SH} faster polarization anisotropy observed near the stagnant slabs above the 660 km discontinuity and the slabs penetrating across the 660 km discontinuity with shallow dips (dip angle is no more than 45°) can be explained by the horizontal deformation of akimotoite and the V_{SV} faster polarization anisotropy observed near the slabs steeply penetrating across the 660 km discontinuity (dip angle is larger than 45°), in contrast, can be explained by the vertical deformation of akimotoite.

Keywords: akimotoite, Lattice preferred orientation, seismic anisotropy, subducting slabs, mantle transition zone

[E] Poster | M (Multidisciplinary and Interdisciplinary) : M-GI General Geosciences, Information Geosciences & Simulations

📅 Fri. Jun 4, 2021 5:15 PM - 6:30 PM JST | Fri. Jun 4, 2021 8:15 AM - 9:30 AM UTC | 🏢 Ch.20_2

[M-GI30] Near Surface Investigation and Modeling for Groundwater Resources Assessment and Conservation

convener: Jui-Pin Tsai (National Taiwan University, Taiwan), Makoto Taniguchi (Research Institute for Humanity and Nature), Ping-Yu Chang (National Central University)

Groundwater resources serve as a vital source for regional water supply under the climate change condition. However, improper use of the available groundwater resources leads to serious environmental disasters such as land subsidence or seawater intrusion. Therefore, groundwater management is a key issue for groundwater resource conservation. Before applying any management practice, it is essential to accurately assess the groundwater system in multi-scales. In this session, we focus on the issues associated with the application of near-surface investigation and modeling on groundwater resources assessment. We welcome studies related to numerical modeling, spatiotemporal modeling, data fusion, and field investigation using hydrogeological approaches, geophysical approaches, geochemical approaches, and remote sensing. We also welcome the studies associated with groundwater contamination transport and remediation, geothermal energy exchange, groundwater microorganisms, hot spring, volcanic hydrology, and environmental disasters evaluation and prevention. We especially encourage pilot groundwater management studies that solve multi-scale and interdisciplinary problems.

[MGI30-P01] Multiple-point geostatistics for Simulation of Lithological Classification

*TING-AN LIN¹, Hwa-Lung Yu¹ (1. National Taiwan University)

Multiple-point geostatistics for Simulation of Lithological Classification

*TING-AN LIN¹, Hwa-Lung Yu¹

1. National Taiwan University

In the applications and studies of undergroundwater, it is important to understand the geological lithological composition in the study area. In order to find out the lithological distribution in the study area, many geological spatial statistical methods used to analyze the lithological composition on unknown points. One of the shortcomings in the traditional geostatistical methods like two-point based method(e.g., Kriging) is that they based on variogram, therefore, not able to handle complex and heterogeneous spatial structures. Additionally, their results are too smooth. Multiple-point geostatistics is a general statistical framework to model spatial fields with complex structures. The goal of Multiple-point geostatistics is to overcome the limitations of the variogram. It uses training image(TI) instead of variogram to estimate the conditional probability at interpolation location by the observed data and the already interpolated data. Take advantage of TI helps extracting spatial structure information and precisely describing more complex structures. This study focuses on Choshui river alluvial fan, using multiple-point geostatistics method to do simulation of lithological classification.

Keywords: Multiple-point geostatistics, Lithological Classification, Training Image

[E] Poster | M (Multidisciplinary and Interdisciplinary) : M-SD Space Development & Earth Observation from Space

📅 Fri. Jun 4, 2021 5:15 PM - 6:30 PM JST | Fri. Jun 4, 2021 8:15 AM - 9:30 AM UTC | 🏠 Ch.19_3

[M-SD39] Micro-satellite and its constellation in remote sensing

convener:Yukihiro Takahashi(Department of CosmoSciences, Graduate School of Science, Hokkaido University)

Micro- or nano-satellites are becoming a general tool for the earth remote-sensing. The performance of the spectral camera or thermal infrared camera might be equivalent or even better compared to conventional larger satellites. The target pointing technique enables frequent and 3-D measurements, which are not available with most of the existing satellites. Under the international collaboration, we can share not only the obtained images but also the machine time for the on-demand operation. Here we discuss the present status and future prospect of utilization of micro-satellites and the international cooperation.

[MSD39-P01] Status of International Micro-satellite Consortium

*Yukihiro Takahashi¹ (1.Department of CosmoSciences, Graduate School of Science, Hokkaido University)

[MSD39-P02] Preliminary design and case study of Satellite Operation Management System for constellations and ground station network

*Yuji Sakamoto¹, Shinya Fujita¹, Naoya Shiraishi¹, Toshinori Kuwahara¹, Junichi Kurihara² (1.Department of Aerospace Engineering, Graduate School of Engineering, Tohoku University, 2.Faculty of Science, Hokkaido University)

[MSD39-P03] Development of a Miniature Ku-band RF Transceiver for Airborne Remote Sensing

*VOON CHET KOO¹, How Hsin William Hii², Yee Kit Chan¹ (1.Multimedia University, 2.iRadar Sdn Bhd)

[MSD39-P04] Myanmar Earth Observation Micro-Satellite Development and its Applications

*Hline Htet Win¹, San Lin Phyo¹, Ye Min Htay¹, Junichi Kurihara¹ (1.Hokkaido University)

[MSD39-P05] Extreme weather monitoring in Indonesia using TIS camera onboard on LAPAN A4

*Purwadi Purwadi¹, Yukihiro Takahashi², Findy Renggono¹, Halda Aditya Belgaman¹, Arif Saefudin³ (1.Agency for Assessment and Application for Technology, Jakarta 10340, Indonesia, 2.Faculty of Science, Hokkaido University, Sapporo 0600810, Japan, 3.National Institute of Aeronautics and Space of Indonesia, Jakarta 13220, Indonesia)

[MSD39-P06] Determination of Water Contaminant Concentration using Band Ratio and Statistical Method

*Ahmad Shaqeer Mohamed Thaheer¹, Yukihiro Takahashi¹ (1.Hokkaido University)

[MSD39-P07] Method for improving the exhaust speed and thrust of storage type Regolith Thruster

*Noruji MUTO¹, Necmi Cihan ORGER¹, Jose Rodrigo CORDOVA-ALARCON¹, Kazuhiro TOYODA¹, Mengu CHO¹ (1.Graduate school of Kyushu Institute of Technology)

[MSD39-P08] Lunar Observations with a Multispectral Sensor Onboard RISESAT Microsatellite and its Radiometric Calibration

*Masataka Imai^{1,2}, Junichi Kurihara³, Toru Kouyama^{1,2}, Toshinori Kuwahara⁴, Shinya Fujita⁴, Yuji Sakamoto⁴, Sei-Ichi Saitoh⁵, Takafumi Hirata⁵, Hirokazu YAMAMOTO⁶, Yuji Sato⁴, Yukihiro Takahashi³ (1.Artificial Intelligence Research Center, National Institute of Advanced Industrial Science and Technology (AIST)), 2.AIST-UTokyo Advanced Operand-Measurement Technology Open Innovation Laboratory (OPERAN-DO-OIL), AIST, 3.Faculty of Science, Hokkaido University, 4.Department of Aerospace

Engineering, Tohoku University, 5.Arctic Research Center, Hokkaido University, 6.Geological Survey of Japan, AIST)

Status of International Micro-satellite Consortium

*Yukihiro Takahashi¹

1. Department of CosmoSciences, Graduate School of Science, Hokkaido University

Satellite remote sensing is useful for global monitoring. We are promoting an international organization “Asian Micro-satellite Consortium (AMC)” with a concept of “sharing”, namely, the sharing of satellite technology, data, and applications. If the target pointing is possible, we can take images for any location once or twice a day only with one very small satellite. Therefore, on-demand image acquisition with several tens of micro-satellite under the international agreement provides continuous monitoring. We are developing the request system for disaster and environmental monitoring. They can get frequent imaging opportunities at a very low cost. Now the member institutions have several micro-satellites in space with cutting-edge payloads such as super multi-spectral cameras. This world-first system will provide revolutionary changes in disaster and environmental management. Here we introduce the latest situation of AMC activities.

Keywords: micro-satellite, constellation

Preliminary design and case study of Satellite Operation Management System for constellations and ground station network

*Yuji Sakamoto¹, Shinya Fujita¹, Naoya Shiraishi¹, Toshinori Kuwahara¹, Junichi Kurihara²

1. Department of Aerospace Engineering, Graduate School of Engineering, Tohoku University, 2. Faculty of Science, Hokkaido University

This paper shows the preliminary design of satellite operation management system and initial operation case studies that achieve the reduction of human work time and human error in satellite operation and also quickly reflect the observation request of a data user. An unlimited number of satellites, ground stations, and users (including non-space operators) can be used within the capacity of the database. It is a platform for ground station sharing, satellite operation management support, satellite data archives and distribution. This system will be upgraded into an on-demand spectrum measurement service for non-space operators. Initial operation will start with 4 satellites and 3 ground stations managed by Tohoku University, and the system will be expanded to 10 satellites and 6 ground stations by the end of 2022.

The core Web services are SOM (Satellite Operation Management) and SDM (Satellite Data Management). Depending on operator or data user requests, the Web API automatically generate the tasks for satellites and ground stations. The system provide communication opportunities between ground stations and satellites, imaging opportunities using target point attitude control by satellites, and archiving of communication data and imaging data via the Internet. Full automation of satellites and ground stations is the goal, as immediacy is required from request to data distribution.

The system can greatly reduce the development efforts of especially new satellite operators and organizations. Planning work of satellite operations requires a great deal of time, and a solution to reduce human work time and human error must be required. Since the date and time of the communication task and the imaging task are calculated automatically, the command templates prepared for each task are combined after the task titles and time stamps are automatically modified. Operation planners only have to devote their efforts to final confirmation of each satellite-specific settings (power management, memory management, etc.), and have time to concentrate their efforts, such as developing final confirmation software specific to each satellite.

Keywords: microsatellite, satellite operation, ground station

Development of a Miniature Ku-band RF Transceiver for Airborne Remote Sensing

*VOON CHET KOO¹, How Hsin William Hii², Yee Kit Chan¹

1. Multimedia University, 2. iRadar Sdn Bhd

A new miniature Ku-band RF transceiver has been designed and developed at Multimedia University, Malaysia. This system is a compact radio frequency module operating at 17-18 GHz with built-in digitally tuned oscillator suitable for frequency-modulated continuous wave (FMCW) Synthetic Aperture Radar (SAR) operation. It is a small size, lightweight system that can be mounted on a small unmanned aerial vehicle for remote sensing applications. A series of field measurements has been conducted to verify the performance of the RF transceiver. This paper highlights the design and development of the RF transceiver, as well as its preliminary results.

Keywords: Synthetic Aperture Radar, RF Circuit Design, Radar Transceiver

Myanmar Earth Observation Micro-Satellite Development and its Applications

*Hline Htet Win¹, San Lin Phy¹, Ye Min Htay¹, Junichi Kurihara¹

1. Hokkaido University

The improvement of technology leads to cost-effective microsatellite development which can be compared with industrial large satellites. Due to the advantages of short development time and easily accessible technology demonstration, launching of microsatellites increases every year. Since most of the small satellites are launched in Low Earth Orbit (LEO), it needs implementation of constellation satellites to increase temporal resolution and ground coverage for observation in contrast to high-altitude large satellites. The Asian Micro-satellite Consortium (AMC) was formed from 16 universities and space agencies from emerging Asian countries and aims to implement the constellation of microsatellites. The first Myanmar microsatellite, Lokanat-1 is built with collaboration between Myanmar Aerospace Engineering University, Hokkaido University and Tohoku University. Lokanat-1 is the Earth observation satellite at 420 km with 51.6 degree inclination. To conduct Earth observation, four scientific sensors, namely, high precision telescope (HPT), spaceborne multispectral imager (SMI) with two liquid crystal tunable filters (LCFT), wide field camera (WFC) and middle field camera (MFC) are equipped in it. The HPT with 2.2 m ground sample distance (GSD) and four spectral bands such as red, green, blue and near infrared is used to obtain high spatial resolution images which can be applied in a variety of remote sensing areas. The SMI which has 47m GSD is used for monitoring vegetation and water changes. To observe large-scale cloud patterns and distribution, the WFC which has a fish-eye lens is used. The MFC with 35 m GSD and 58×44 km field of view (FOV) assists to calibrate the attitude determination algorithm. Images captured with these high performance cameras can be applied to monitoring and evaluation of staple food crops in main agricultural regions, water resource monitoring, forestry monitoring and disaster management, urban planning in Myanmar. The success of the Lokanat-1 will achieve the major goals of the program that is to promote the social and economic development of Myanmar through the space technology applications.

Keywords: Microsatellite, Earth observation, Remote sensing, Constellation, High spatial resolution

Extreme weather monitoring in Indonesia using TIS camera onboard on LAPAN A4

*Purwadi Purwadi¹, Yukihiro Takahashi², Findy Renggono¹, Halda Aditya Belgaman¹, Arif Saefudin³

1. Agency for Assessment and Application for Technology, Jakarta 10340, Indonesia, 2. Faculty of Science, Hokkaido University, Sapporo 0600810, Japan, 3. National Institute of Aeronautics and Space of Indonesia, Jakarta 13220, Indonesia

Indonesia is a country that is often struck by floods and forest fires. The El-Nino and La Nina phenomena are natural factors that cause Indonesia to experience two different disasters. During El Nino, most parts of Indonesia experience minimum rainfall, resulting in drought which triggers forest and land fires. Conversely, when La Nina hit, Indonesia experienced quite extreme rainfall which causing floods. LAPAN A4 is prepared to be a part of a microsatellite consortium in Asia that will carry a thermal infrared sensor (TIS) camera designed by Hokkaido University. This TIS camera has a spec measurement range of 100 °C to -60 °C. So, it can be used to detect hotspots during the dry season or cloud growth during the rainy season. TIS cameras have independently conducted several tests to test the resistance of TIS cameras to the environment when stored, launched, and operated. Temperature calibration has also been carried out to get a digital value function as a temperature value. The current status of LAPAN-A4 development is being assembled and tested.

Keywords: hotspot, severe weather, LAPAN A4, TIS Camera

Determination of Water Contaminant Concentration using Band Ratio and Statistical Method

*Ahmad Shaqeer Mohamed Thaheer¹, Yukihiro Takahashi¹

1. Hokkaido University

Understanding pollution of inland waters such as rivers and lakes is an important issue, especially in water security for human life and pollution impact at the outflow, i.e., the ocean. Mainly, pollution in urban areas of Southeast Asia such as Malaysia is a serious issue. However, the in-situ measurement method is not sufficient due to the frequency and the number of observation points. The current trend of using remote sensing tools such as satellites and drones shows a great expectation in the water measurement field. These methods can observe a wide area in a short interval time. Nevertheless, remote sensing in water areas greatly depends on sunlight incidence angle and wave intensity on the water surface. Such a method of isolating and quantitatively estimating pollution due to multiple factors has not been established, especially in field-measurement. A spectral reflectance with polarization at visible and near-infrared wavelengths is obtained to solve these problems. Laboratory experiments, field-measurement, water sampling inherent optical properties observation, and satellite data analysis have been conducted. In the laboratory experiment, a wave generator creates artificial waves on the water surface, along with a combination of chlorophyll (biologically originated) and soil particles. Each concentration is estimated from the mixture reflectance spectrum.

Keywords: Water contaminant, Multispectral, Band ratio

Method for improving the exhaust speed and thrust of storage type Regolith Thruster

*Noruji MUTO¹, Necmi Cihan ORGER¹, Jose Rodrigo CORDOVA-ALARCON¹, Kazuhiro TOYODA¹, Mengu CHO¹

1. Graduate school of Kyushu Institute of Technology

A problem in lunar-orbit missions is the short orbital life of low-orbit spacecraft due to the moon's irregular gravity field. To sustain the orbit, much propellant is required to be loaded, whereby the mission would be costly. In recent years, electric propulsion devices have been applied to small satellites, which are growing in demand because of their short time required for development and the low risk of mission failure. We here suggest the "Regolith Thruster", a new electric propulsion system which collects propellant material during the lunar-orbit flight. The Moon surface is covered with clastic materials derived from the weathered surface rocks called regolith, and its dust particles are of micro-meters in diameter. The dust particles are suspended above the moon surface, as observed by American lunar explorers.

Two types of Regolith Thruster have been considered. The "breathing type" captures lofted dust particles in orbit and accelerates them directly with a voltage applied grid. Our theoretical studies suggest that a grid of several-tens-of-square-meters class will be necessary to obtain sufficient thrust with this type. The "storage type" thruster uses electron source to generate secondary electrons to release the dust particles by micro-cavity charging. Dust particles are released by electrification in micro cavities (microcavities) formed by each other. This is due to the very small size of the microcavities on the lunar surface, so that the patched surface charge causes a strong repulsion against adjacent dust particles, which moves to the grid and is accelerated. When using a regolith simulant with a particle radius of $45 \mu\text{m}$ or less, only a small thrust of about 10^{-9} N can be obtained with the storage type. The volume required for the "particle storage space" of a storage-type regolith propulsion system, assuming that particles of each size fill the storage space, exponentially increases as the particle radius increases. If the particle radius is $5 \mu\text{m}$ or less, each side can be made to fit into a cube of $10 \times 10 \times 10$ cm (= 1U size small satellite).

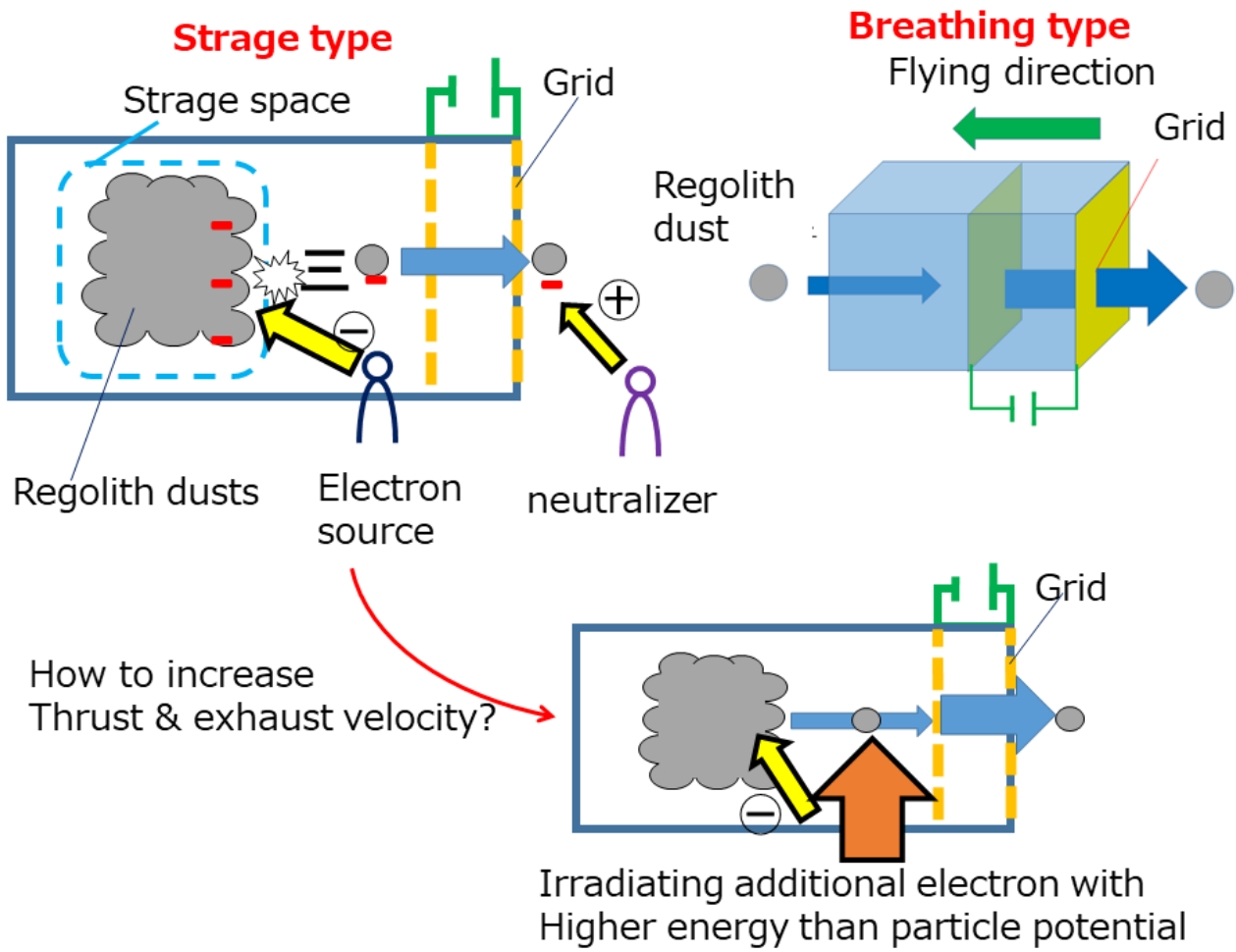
Assuming that the regolith thruster obtains the velocity increment ΔV used in the previous studies, the required propulsion and satellite specifications can be investigated: the weight ratio of propellant and regolith thruster increases as the particle radius increases. This tendency is significant with a large value of ΔV . The propulsion device gains thrust because it shoots mass from the fuselage and propels by reaction. Once the weight ratio required to obtain the ΔV of the launched object (and propellant) and the spacecraft is obtained, the weight ratio will increase as the particle radius increases. The particles are desired to be of $1.0 \mu\text{m}$ or less in radius so that the weight ratio can be easily achieved for a small satellite.

But, required particles total volume overs particle storage space of storage typeat regolith thruster at least 1.01 times for reaching $\Delta V=40$ m/s. We tried to solve this problem by irradiating electron energy to lavitated regolith dust particles, increasing exhaust velocity.

As result, particles can increase its exhaust velocity by our trial. In case of $0.1 \mu\text{m}$ radius particle, It can increase from 300 to 2100 m/s by irradiating 500eV energy electron. In case of $18 \mu\text{m}$ radius, velocity was increased from 6 to 13.5 m/s at same energy irradiation. Specific impulse (I_{sp}) and thrust of storage type Regolith Thruster can satisfy it of Pulsed Plasma Thruster, Vacuum Arc Thruster, and Electropray

Thruster.

Keywords: Moon, Regolith, electric propulsion, lunar exploration



Lunar Observations with a Multispectral Sensor Onboard RISESAT Microsatellite and its Radiometric Calibration

*Masataka Imai^{1,2}, Junichi Kurihara³, Toru Kouyama^{1,2}, Toshinori Kuwahara⁴, Shinya Fujita⁴, Yuji Sakamoto⁴, Sei-Ichi Saitoh⁵, Takafumi Hirata⁵, Hirokazu YAMAMOTO⁶, Yuji Sato⁴, Yukihiro Takahashi³

1. Artificial Intelligence Research Center, National Institute of Advanced Industrial Science and Technology (AIST)), 2. AIST-UTokyo Advanced Operand-Measurement Technology Open Innovation Laboratory (OPERAN-DO-OIL), AIST, 3. Faculty of Science, Hokkaido University, 4. Department of Aerospace Engineering, Tohoku University, 5. Arctic Research Center, Hokkaido University, 6. Geological Survey of Japan, AIST

Lunar calibration is one of the radiometric calibration methods by utilizing the Moon as a standard reflector. It provides sufficient calibration opportunities without requiring any special equipment and is suitable for nano/microsatellites. This study applies lunar calibration to a multispectral sensor, Ocean Observation Camera (OOC), onboard a microsatellite named Rapid International Scientific Experiment Satellite (RISESAT). We used two Moon models of the RObotic Lunar Observatory (ROLO) and SELENE/Spectrum Profiler (SP) and simulated the irradiance of the Moon at each Moon observation. Comparing the observed and simulated Moon irradiance, we proved OOC had experienced negligible sensitivity degradation in any of the four spectral bands during 16 months of our monitoring period from August 2019. However, a bluing trend in the OOC's sensor sensitivity was revealed, which indicating a 15% alternation in the sensitivity at maximum. Also, the sensor performance was changing due to the sensor temperature variation. We derived calibration parameters from the Moon observations and validated them by comparing the top-of-atmosphere reflectance of Railroad Valley Playa with the Radiometric Calibration Network dataset. Although we successfully corrected the bluing trend in the visible range, the lunar and vicarious calibration parameters for the infrared band were unexpectedly inconsistent. Stray light contamination can be a plausible explanation of this inconsistency, and further discussion is introduced in this presentation.

Keywords: Remote sensing, Earth observation, Nano/microsatellite, Lunar calibration